Development of an electrolyte based on ionic liquid for lithium ion batteries

Hassan Srour

Numéro d'ordre : Année 2013

THESE DE L'UNIVERSITE DE LYON

Présentée

devant l'**UNIVERSITE CLAUDE BERNARD – LYON 1**

ECOLE DOCTORALE de CHIMIE

Spécialité **CHIMIE**

Pour l'obtention du

DIPLOME DE DOCTORAT

(arrêté du 7 août 2006)

présentée et soutenue publiquement le

02 Octobre 2013

par

SROUR Hassan

Développement d'un électrolyte à base de liquide ionique pour accumulateur au Lithium

---

Directeur de thèse : *Dr.* Catherine SANTINI *(CNRS)*
Co-encadrant: *Dr.* Hélène ROUAULT*(CEA)*

Jury

Pr. B. ANDRIOLETTI (Univ-Lyon 1)

Pr. M. COSTA GOMES (ICCF)

Mr. Y. CHAUVIN (Nobel 2005)

Rapporteur

Pr. Tom WELTON (Imperial College, UK)

Dr. Karim ZAGHIB (IREQ, Canada)

UNIVERSITE CLAUDE BERNARD - LYON 1

Président de l'Université	**M. François-Noël GILLY**
Vice-président du Conseil d'Administration	M. le Professeur Hamda BEN HADID
Vice-président du Conseil des Etudes et de la Vie Universitaire	M. le Professeur Philippe LALLE
Vice-président du Conseil Scientifique	M. le Professeur Germain GILLET
Directeur Général des Services	M. Alain HELLEU

COMPOSANTES SANTE

Faculté de Médecine Lyon Est – Claude Bernard	Directeur : M. le Professeur J. ETIENNE
Faculté de Médecine et de Maïeutique Lyon Sud – Charles Mérieux	Directeur : Mme la Professeure C. BURILLON
Faculté d'Odontologie	Directeur : M. le Professeur D. BOURGEOIS
Institut des Sciences Pharmaceutiques et Biologiques	Directeur : Mme la Professeure C. VINCIGUERRA
Institut des Sciences et Techniques de la Réadaptation	Directeur : M. le Professeur Y. MATILLON
Département de formation et Centre de Recherche en Biologie Humaine	Directeur : M. le Professeur P. FARGE

COMPOSANTES ET DEPARTEMENTS DE SCIENCES ET TECHNOLOGIE

Faculté des Sciences et Technologies	Directeur : M. le Professeur F. DE MARCHI
Département Biologie	Directeur : M. le Professeur F. FLEURY
Département Chimie Biochimie	Directeur : Mme le Professeur H. PARROT
Département GEP	Directeur : M. N. SIAUVE
Département Informatique	Directeur : M. le Professeur S. AKKOUCHE
Département Mathématiques	Directeur : M. le Professeur A. GOLDMAN
Département Mécanique	Directeur : M. le Professeur H. BEN HADID
Département Physique	Directeur : Mme S. FLECK
Département Sciences de la Terre	Directeur : Mme la Professeure I. DANIEL
UFR Sciences et Techniques des Activités Physiques et Sportives	Directeur : M. C. COLLIGNON
Observatoire des Sciences de l'Univers de Lyon	Directeur : M. B. GUIDERDONI
Polytech Lyon	Directeur : M. P. FOURNIER
Ecole Supérieure de Chimie Physique Electronique	Directeur : M. G. PIGNAULT
Institut Universitaire de Technologie de Lyon 1	Directeur : M. C. VITON
Institut Universitaire de Formation des Maîtres	Directeur : M. A. MOUGNIOTTE
Institut de Science Financière et d'Assurances	Administrateur provisoire : M. N. LEBOISNE

Acknowledgements

The work presented in this thesis was carried out at the C2P2/CPE-Lyon and CEA/Liten/LMB laboratories during 2011-2013.

I am grateful to the thesis jury members for their precious time which they have spent for my thesis. I would like to thank Prof.Tom Welton and Dr. Karim Zaghib for agreeing to be referee of my thesis manuscript and for their suggestions to improve it. I am also thankful to Professors Margarida Costa Gomes, and Bruno Andrioletti to accept to participate to my committee. I am grateful to Mr Yves Chauvin to accept to judge this work, for ideas and advice at critical stages of my research work.

During my doctoral fellowship, I have had a pleasure to work and learn from a number of skilled scientists. First and foremost, I would like to thank my thesis advisor, Dr. Catherine Santini and Dr. Helene Rouault for their guidance throughout my graduate studies. Their encouragement, patience, and assistance have guided me through my research project and have ensured the completion of my degree.

My warm thanks to Dr. Pascale Husson and Bernard Fenet for their fruitful collaboration. I also thank you all, the current and the previous members of both LCOMS and LMB team laboratory for making graduate life stimulating, fun and interesting.

To Ewelina, Léa, Inga, Leila, Yasmine, Walid[2], Cherif, thank you for being there to share with me my brightest days and carry me through my darkest hours. To the Lebanese friends, I thank you for being with me all the time and starting this journey with me.

I thank my father for challenging me to reach greater heights, my mum for always quietly standing by me, and my brother for his support all the time.

Table of Contents

Abbreviations and Acronyms

Units

h: hour	min: minute	S: second	g: gram
C: degree Celsius	K: kelvin	R.T: room temperature	

Techniques

NMR: Nuclear magnetic resonance
HRMS: High resolution mass spectrometry
SEM: Scanning electron microscopy
CV: Cyclic voltammetry
ICP: Inductively coupled plasma

Chemicals

IL: Ionic liquid
Im: Imidazolium
Py: Pyrolidinium
P: Phosphonium
C_1: Methyl, C_2: Ethyl, C_4: Butyl, C_6: Hexyl, C_8: Octyl

$C_1C_4Im^+$: 1-butyl-3-methylimidazolium cation
TFSI or NTf_2^-: Bis(trifluoromethanesulphonyl)imide anion
FSI: Bis(fluorosulfonyl)imide
DCA: Dicyanamide
BF_4: Tetrafluoroborate
PF_6: Hexafluorophosphate
SCN: Thiocyanate
[C_2mim][NTf_2], b) [C_4mim][OTf], c) [C_4mim][BF_4], and d) [C_4mim][PF_6]
Tf : Triflate
DMSO- d_6: Dimethyl sulfoxide

Materials

Cgr: Graphite
LFP: $LiFePO_4$
LTO: $Li_4Ti_5O_{12}$
LCO: $LiCoO_2$
Li-ion: lithium ion
PVDF: polyvinylidene fluoride
SHE: Standard hydrogen electrode

Introduction

Energy requirements increase as the need for energy storage for renewable energy and nomad devices. Among all the existing batteries, lithium ion batteries have been given substantial attention today because of their high energy density, absence of toxic metal such as lead or cadmium, and no memory effect [1-3]. Nowadays, share in the global sales for Ni-Cd is 23%, for Ni-MeH – 14% and for Li-ion portable batteries is 63%. Moreover, the global market for lithium ion (Li-ion) batteries in light duty vehicles will grow from $1.6 billion in 2012 to almost, $22 billion in 2020 (Figure 1).

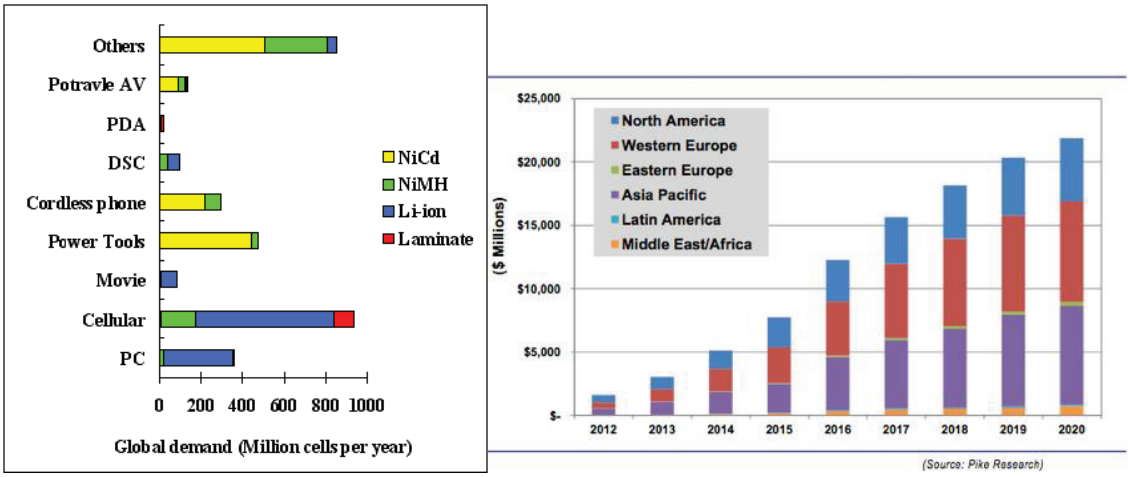

Figure 1: a) Custom made cells for world markets b) Evolution of market for Li-ion batteries

The battery industry is becoming consolidated; Asian suppliers held 95% of the market last year. These companies are gaining ground due to low pricing and improving quality. The price of Li-ion batteries has dropped by 20-50% during the last few years (Figure 2).

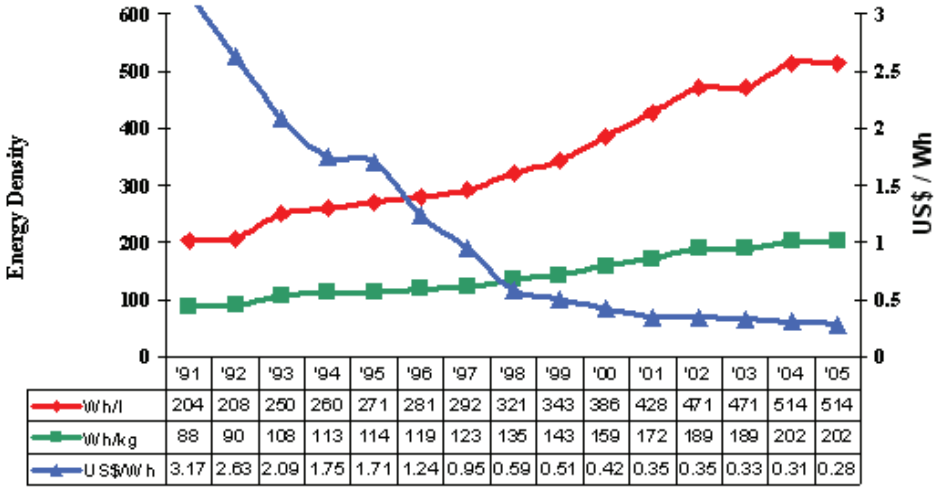

	'91	'92	'93	'94	'95	'96	'97	'98	'99	'00	'01	'02	'03	'04	'05
Wh/l	204	208	250	260	271	281	292	321	343	386	428	471	471	514	514
Wh/kg	88	90	108	113	114	119	123	135	143	159	172	189	189	202	202
US$/Wh	3.17	2.63	2.09	1.75	1.71	1.24	0.95	0.59	0.51	0.42	0.35	0.35	0.33	0.31	0.28

Figure 2: Li-ion price and energy density

The electrolyte is commonly a solution containing an inorganic lithium salt ($LiPF_6$ - lithium hexafluorophosphate, $LiNTf_2$ - lithium bis(trifluoromethane)sulfonylimide, *etc.*) dissolved in a mixture of organic solvents such as propylene carbonate (PC), ethylene carbonate (EC), dimethyl carbonate (DMC), diethyl carbonate (DEC). These solvents have a number of inherent limitations and drawbacks. Conventional electrolytes have some safety concerns, especially due to their flammability and volatility. Under the right circumstances, the electrolyte in a Li-ion battery can ignite or even explode.

Ionic liquids (ILs) are composed of ions, exhibit negligible vapor pressure, similar to solid salts. Unlike most organic solvents, they do not vaporize unless heated to the point of thermal decomposition, typically 200-300°C or more [4]. They have no flash point. They are considered as non-flammable [5].

As a result, IL-based cells are free from the explosion or pressure risks of Li-ion cells using conventional electrolytes. Moreover, they show a broad electrochemical stability window, generally >5 V, which is necessary for the application in Li-ion batteries with high-energy cathodes [6]. Among all available ILs, imidazolium derivatives exhibit the higher thermal stability, as well as high ionic conductivity [7]. ILs may play a role in providing safer, more robust energy storage for the future [8-10].

A challenge for implementation of ILs as Li-ion battery electrolytes is their somewhat limited lithium ion transport properties related to their high viscosity implying low cycling and power delivery for IL-based batteries. Other disadvantages are their cost compared to carbonate, and the lack of specified purity grade which has to be assessed in order to be able to evaluate the reliability of the cycling tests. These drawbacks explain their current limited use at industrial level.

Consequently, the aim of my PhD was to design new synthetic routes reducing wastes and cost, and novel ILs to tune their physico-chemical and electrochemical properties to improve their performances as electrolytes in Li-ion cells.

My PhD Work is at the interface of three domains of ILs:

- Synthesis
- Physico-chemical, electrochemical, and transportation properties
- Applying ILs as electrolyte for Li-ion batteries

To obtain the most accurate results in each part, we focus our work on imidazolium based ILs,

generally associated to the bis(trifluoromethanesulfonyl)amide (NTf_2 or TFSI) anion.

In a first part, the different synthetic procedures for imidazolium based ILs have been reviewed. Then, the description of novel synthetic routes of imidazolium-ILs has been reported.

The second part, focused on Li-ion batteries, a bibliographic chapter on the description of the principle, advantages, and limits of batteries based on organic carbonates electrolytes has been realized, followed by an overview of the literature concerning the data on imidazolium-ILs as electrolyte. Then, the influence of substituting on an imidazolium ring on the cyclic performance in different experimental conditions (temperature, concentration of lithium salt, and organic additives) have been evaluated in coin cells based on graphite or lithiated titanium oxide as negative electrodes and lithiated iron phosphate as positive electrode.

1. Yamaki, J., Encyclopedia of *Electrochem Power Sources* (2009) 183-191.
2. Tarascon, J.M., M. Armand, *Nature* **414** (2001) 359.
3. Park, J.-K., Principles and applications of lithium secondary batteries, *Wiley-VCH, Weinheim*, (2012).
4. Wasserscheid, P., T. Welton, Ionic liquids in synthesis, *Wiley-VCH, Weinheim*, (2008).
5. Diallo, A.O., A.B. Morgan, C. Len, G. Marlair, *Energy Environ. Sci*. **6** (2013) 699-710.
6. Ohno, H., Electrochemical Aspects of Ionic Liquids, Second Edition, *Wiley, N.Y*., (2011).
7. Sato, T., T. Maruo, S. Marukane, K. Takagi, *J. Power Sources,* **138** (2004) 253-261.
8. Armand, M., F. Endres, D.R. MacFarlane, H. Ohno, B. Scrosati, *Nat. Mater*. **8** (2009) 621-629.
9. Passerini, S., W.A. Henderson, Encyclopedia of *Electrochem Power Sources*, (2009) 85–91.
10. Lewandowski, A., A. Swiderska-Mocek, *J. Power Sources* **194** (2009) 601-609.

Chapter 1
Ionic liquids: Synthesis

1. State of the art

The discovery of ILs can be dated back to the work of Paul Walden in 1914. The first low melting salt, was the ethylammonium nitrate, with melting point of 12°C [1]. Since then, studies of ‘’molten salts’’ have seldom been concerned with ILs in particular, until a renaissance of the interest in these kinds of liquids began to be registered in literature. In 1951, Hurley and Wier developed low melting salts with chloroaluminate ions for low-temperature electroplating of aluminium [2]. Wilkes et al. in 1982 developed the use 1-alkyl-3-methylimidazolium as cation [3]. In the mid-1980s, this medium was used as solvents for organic synthesis [4]. In 1990s, an understanding that molten salts having melting point below 100°C created a new unique media for chemical reactions became widespread and the term ‘’room temperature ionic liquids’’ (RTILs) was assigned to them. The number of synthesized RTILs exceeds 500 and research in the area is expanding rapidly. There is virtually no limit in the number of salts with low melting points. Earle and Seddon have estimated this number to be of the order of 1 billion [5].

Published Items in Each Year

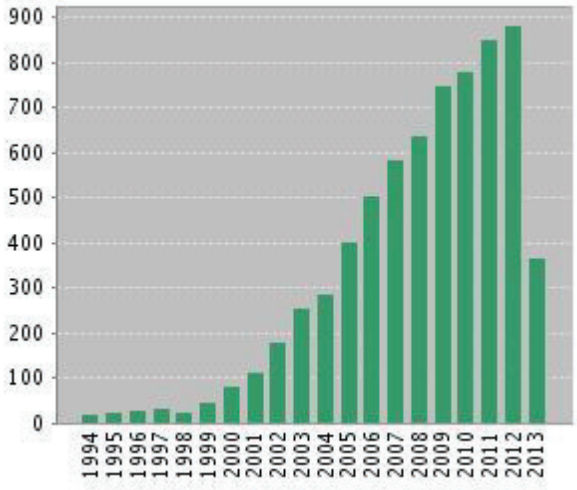

The latest 20 years are displayed.

Citations in Each Year

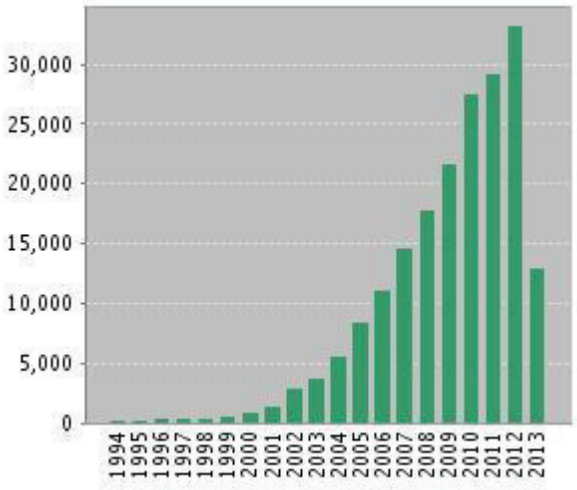

The latest 20 years are displayed.

ILs usually consist of a large unsymmetrical organic cation associated with a polyatomic anion that may be either organic or inorganic (Figure 1). Symmetrical species tend to pack more effectively in the solid state, and so highly symmetrical anions and cations tend to form salts with higher melting points [6].

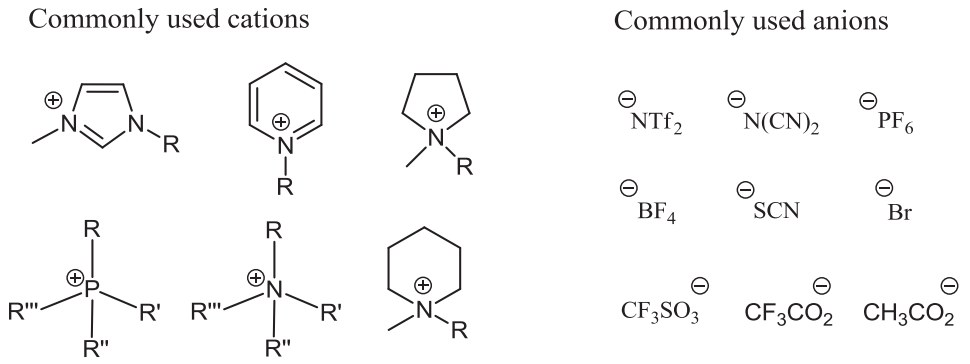

Figure 1: Some common cations and anions used in ILs.

The modular nature of ILs means that structural modifications can either be made to the anion, the cationic core, or substituents on the anion or cation. Hence, a wide diversity in IL structure is possible, and by altering either the cationic or the anionic component of an IL, their physical properties can readily be fine-tuned. Physical properties of the ILs could be tailored following the process requirements such as melting point, viscosity, density, solubility, and hydrophobicity [7].

ILs fulfill all conditions required as green solvents. Prominently, they are not volatile do not leave any hazardous wastes on work-up, and several of them are recyclable.

Keeping in mind the above principles of green chemistry, ILs have attracted much attention in the scientific community (chemists, biologists, and other related workers) during the past two decades or so. Because of these attractive properties, ILs are employed in a broad area of applications Separation technology [8-11]; Catalysis [12-14]; Biomass treatment, [15, 16]; Lubrication [17]; Energy storage [18-21].

1.1 Principles of green chemistry

For the ILs science, they use often these words ‘’green and IL’’ but not all ILs are green. There is conflict in the designer classification of ILs. The green IL synthesis is the ability to prepare the salts to process distinctly with non-green characteristics (toxicity, explosive, etc). What is more, the preparation and purification of the salts are also often extremely dirty, requiring the use of large volumes of harmful organic solvents. Therefore, the green IL synthesis has only occurred if both IL product and its preparation comply with all 12 principles of green chemistry as listed below [22-24]:

The twelve principle of green chemistry

1- It is better to prevent waste than to treat or clean up waste after it has formed.
2- Synthetic methods should be designed to maximize the incorporation of all materials used in the process into the final product.

3- Wherever practicable, synthetic methodologies should be designed to use and generate substances that possess little or no toxicity to human health and the environment.
4- Chemical products should be designed to preserve efficacy of function while reducing toxicity.
5- The use of auxiliary substances (e.g. solvents, separation agents, etc.) should be made unnecessary wherever possible and innocuous when used.
6- Energy requirements should be recognized for their environmental and economic impacts and should be minimized. Synthetic methods should be conducted at ambient temperature and pressure.
7- A raw material of feedstock should be renewable rather than depleting whatever technically and economically practicable.
8- Unnecessary derivation (blocking group, protecting/deprotecting, temporary modification of physical/chemical processes) should be avoided whenever possible.
9- Catalytic reagents (as selective possible) are superior to stoichiometric reagents.
10- Chemical products should be designed so that at the end of their function they do not persist in the environment and break down into innocuous degradation products.
11- Analytical methodologies need to be further developed to allow for real-time, in-process monitoring and control prior to the formation of hazardous substances.
12- Substances and the form of a substance used in chemical process should be chosen so as to minimize the potential for chemical accidents, including releases, explosions and fires.

To date, many reviews have summarized the status of ionic liquid syntheses [6, 25-28]. The greenness of various synthesis and purification methodologies have been reviewed and classified through SWOT (Strengh, Weakness, Opportunities Threats) analysis, % atom economy, and *E*-Factors [26].

In this chapter, concentrated on ILs based on 1-alkyl-3-methylimidazolium $[C_1C_nIm]^+$ cations, we provided an overview of the synthetic approaches currently available. We have also discussed a number of specific purification and characterization of ILs related to the nature of their components.

1.2 Ionic liquid preparations

1.2.1 Typical ionic liquid synthetic routes

The general synthesis of ILs involves a consecutive quaternisation-metathesis reaction procedure as shown in Figure 2. Many ILs are prepared by a metathesis reaction from a halide or similar salt of the desired cation. We also scanned the different routes using differing energy sources to promote IL

syntheses, via conductive (conventional heating), microwave irradiation, ultrasonic irradiation.

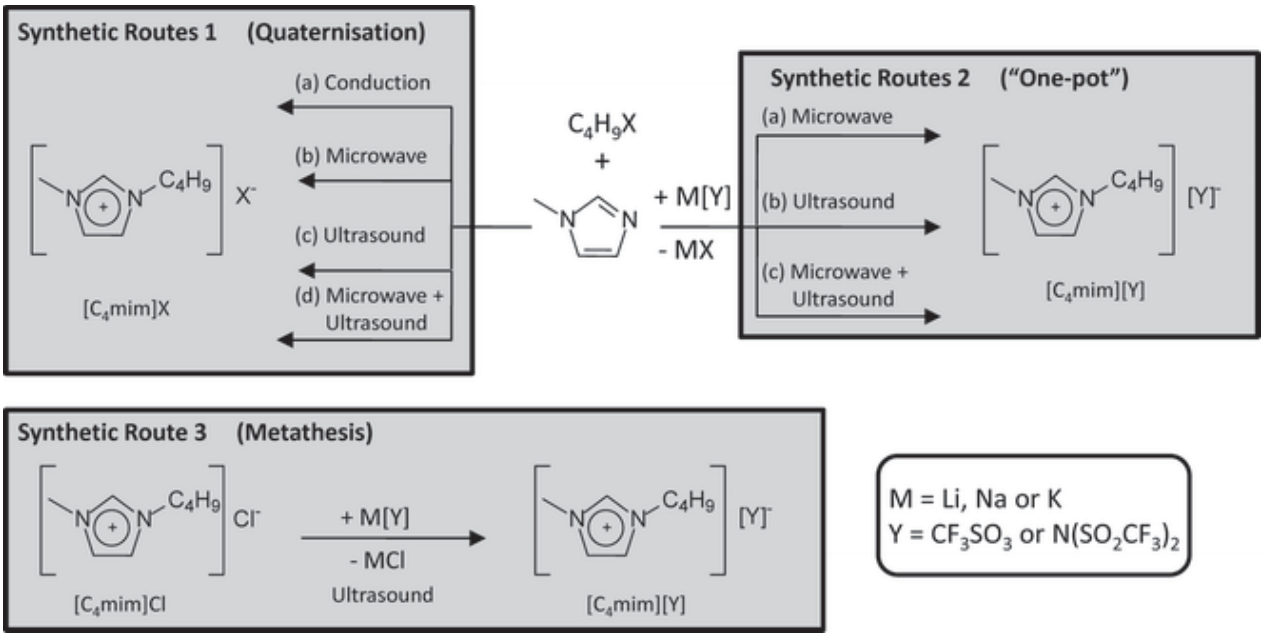

Figure 2: typical ILs synthetic routes [26].

1.2.2 Synthetic route 1 (quaternisation)

Conductive heating preparation of 1-alkyl-3-methylimidazolium halide salts

The literature shows that most of 1-alkyl-3-imidazolium halide salt preparations are executed using traditional heating under reflux, although nowadays an atmosphere of dry nitrogen or argon is sometimes used (Scheme 1). Since, it has been found to promote the production of colorless ILs and prevents the formation of hydrated halide salts from adventitious water [29].

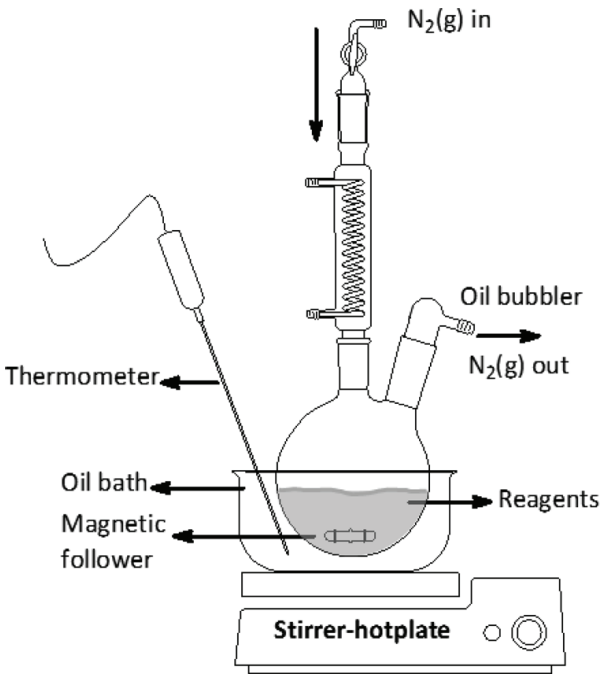

Scheme 1: Traditional synthesis arrangement for preparing 1-butyl-3-methylimidazolium halide salts.

Almost without exception, reported preparations of l-alkyl-3-methylimidazolium halide salts use an excess of 1-haloalkane and long reaction time to achieve good yields (Scheme 2) which means that the reactions are not in line with the 2nd principle of green chemistry, which states: ‘’synthetic methods should be designed to maximize the incorporation of all materials used in the process into the final product’’. It also means that although the preparations of the halide salts are 100% atom efficient, with every atom of the starting materials incorporated into the final product, their E-factors are very poor, since excess 1-haloalkane is required to promote completion of the reactions at a reasonable rate. It also follows that the smaller excess of 1-haloalkane, the lower the E-factor value will be, provided that no organic solvent is used during the preparation.

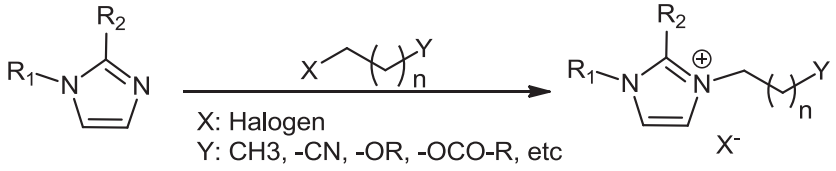

Scheme 2: Synthetic route 1.

Some reported preparations of l-alkyl-3-methylimidazolium halide salts also make use of an organic solvent [30, 31] to reduce the viscosity of the reaction mixture and thus improve mass transfer, but also to control the reaction temperature and prevent product scrambling [32]. However, the molecular solvent employed, and also the excess of 1-haloalkane employed, require removal and subsequent

disposal, which also do not comply with the 1st principle of green chemistry, which states: it is better to prevent waste than to treat or clean up waste after it has formed. Therefore, the practice of employing an organic solvent during the preparation of l-alkyl-3-methylimidazolium halide salts further increases the E-factor and is highly undesirable.

The 5th principle of green chemistry states that: ‘’the use of auxiliary substances (e.g. solvents, separation agents, etc.) should be made unnecessary wherever possible and innocuous when used’’, which means that ideally, no solvent should be used during preparation, but, if a solvent is to be used, it must be green and recycled. In order to align with the 1st, 2nd and 5th principles of green chemistry and have low E-factor values, neither excess 1-haloalkane nor organic solvent should be employed during the synthesis of alkyl-imidazolium halide salts.

The use of conductive heating (usually an oil bath or heating mantle) to prepare l-alkyl-3-methylimidazolium halide salts also does not align with the 6th principle of green chemistry, which states: ‘’energy requirements should be recognized for their environmental and economic impacts and should be minimized. Synthetic methods should be conducted at ambient temperature and pressure’’. Therefore, since conductive heating is slow, it is also energy inefficient because the transfer of heat from the heat source to the reaction mixture depends on the thermal conductivities of all the materials that must be penetrated such as the flask and solvent. In addition, the traditionally heated reactions are kinetically limited by the boiling point of the l-haloalkane employed and can take several days.

Purification of 1-alkyl-3-methylimidazolium halide salts

The purification of 1-alkyl-3-methylimidazolium halide salts (Figure 3) is generally dirty with poor *E-factors*, since the excess 1-haloalkane, unconverted 1-methylimidazole and any solvent used during their preparation require removal and are therefore out of line with the 5th principle of green chemistry (Figure 3). If water-free ionic liquids containing halide ions are desired, their preparation and purification must be conducted under strictly anhydrous conditions from start to finish, for example, using Schlenk techniques. It must be noted, ILs containing halide anions (especially chloride) absorb a lot of water from the atmosphere as they form very stable hydrates [33]. Also needless to say, removing water under reduces pressure and heating require a large energy input and thus contributes further to the green inefficiency (via non-compliance with the 6th principle of green chemistry) of the purification of 1-alkyl-3-methylimidazolium halide salts.

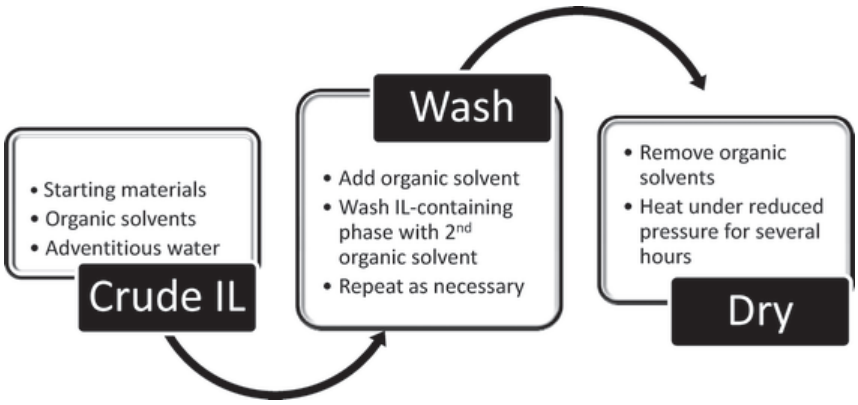

Figure 3: Schematic diagram of the purification of [C_4mim][X] base IL [26].

In our laboratory, we have developed the following process: the starting material mixture was stirred for 48 h at 65°C under argon, then the hot solution was canulated into anhydrous toluene cooled at 0°C, under vigorous mechanical stirring. The white precipitate (ex: [C_1C_4Im][Cl]) formed was filtered and washed repeatedly with toluene and dried overnight *in vacuo*. The main advantages of our procedure compared to the process depicted in Figure 3.

- No additional solvent used in the quaternisation step
- Total removal of the starting material (amine)
- Filtration decreases sharply the solvent quantity for washing

This procedure could consider as an improvement for green synthesis efficiency.

Ionic liquids syntheses promoted by microwave irradiation

It has long been recognized that much more efficient energy sources exist to promote chemical reactions compared with conductive heating. The key advantage of modern scientific microwave equipment is the ability to control reaction conditions very specifically, monitoring temperature, pressure, and reaction time [34].The microwave irradiations have started to attract attention for the preparation of ILs [35-38]. The promotion of 1-alkyl-3-methylimidazolium halide syntheses using microwave irradiation is favored by an ionic conduction heating mechanism since ILs absorb well microwave irradiation (Scheme 3).

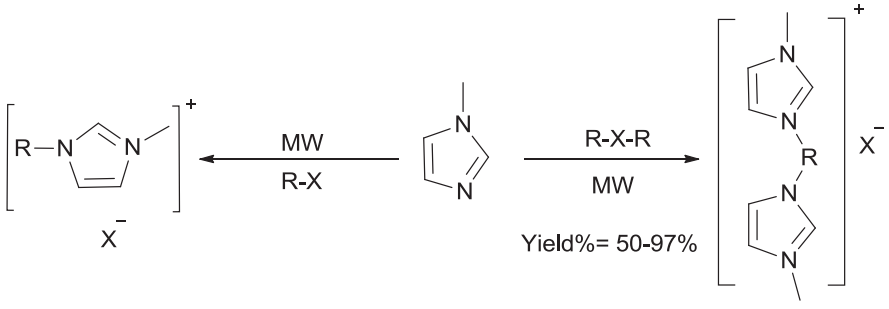

Scheme 3: Microwave- promoted preparation of 1-alkyl-3-methylimidazolium haide.

As in that ILs are formed during the reaction depicted in Scheme 3, the ILs absorb microwave energy and speed up the reaction. In brief, microwave irradiation represents a far more efficient mode of heating to prepare ionic liquids than conductively heated syntheses. In addition, all microwave-assisted ionic liquid preparations align with the 6th principle of green chemistry by virtue of reduced preparation times and vastly reduced energy consumption.

Synthesis of ionic liquids promoted by ultrasonic irradiation

At about the same time, appear ultrasound-promoted preparations of ILs (Scheme 4) [39, 40].

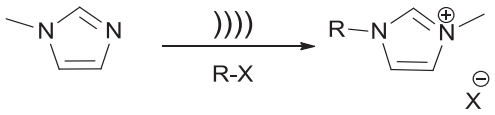

Scheme 4: Ultrasound- promoted preparation of 1-alkyl-3-methylimidazolium halide.

The promotion of chemical reactions with ultrasound is due to a physical phenomenon known as cavitation, which is the formation, growth and implosive collapse of bubbles in a liquid [41]. The collapse or implosion of such bubbles results in some fascinating physical effects, which include the formation of localized hotspots in an elastic liquid and reduction of particle size [42]. In terms of ILs synthesis, the formation of hotspots favors quaternisation (route 1), whereas the reduction of particle size favors both quaternisation and metathesis steps (route 3). Both phenomena improve mass transport overcoming the high viscosity of ILs. Together, hotspot formation, particle size reduction and the reduced preparation times compared with traditional methods all speed up IL syntheses and thus represent a significant green advantage, especially if the preparations are performed solvent free. Despite the apparent green advantages of ultrasound-assisted IL preparations, a phenomenon which renders these preparations inadequate is that, almost without exception, ionic liquids discolor and decompose when exposed to ultrasonic irradiation for the time required to obtain acceptable conversions [43]. Needless to say, this decomposition of ionic liquids is a severe disadvantage to the successful and widespread implementation of the technology and, from a green chemistry perspective, does not align with the 1st principle of green chemistry since very dirty purification and decolorization of the salts are required, which also give very poor E-factors [44]. It seems that the use of water could reduce the impact of cavitation on ionic liquids and so the impact of ultrasound on this hydrophobic ionic liquid [45].

Synthesis of ionic liquids promoted via halide free route

The vast majority of ionic liquids are usually prepared by quaternisation of imidazole's, alkyl amines or phosphine's, often employing alkyl halides as alkylating agents, followed by anion metathesis.

The anion metathesis methods produce a large number of ILs of good quality, but the contamination by residual halide could limit the production of high purity materials. The halide traces in the resulting ILs drastically change the physical and electrochemical properties of the neat ILs [46].

Therefore various synthetic strategies have been devised to synthesize via halide free route [47]. The direct synthesis of 1,3-disubstituted imidazolium tetrafluoroborate ILs achieved in a one-step procedure (Scheme 5) affords a mixture of ILs. This non selectivity implies that this route does not comply with the 1st and 2nd principle of green chemistry.

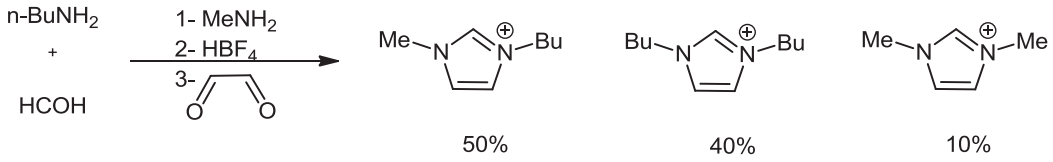

Scheme 5: Halogen free synthesis of ILs.

Other halide free syntheses of ILs have been obtained via a direct alkylation reaction of phosphine, amine, pyridine, or azole yielding ILs based on alkyl sulfates, [48] alkylsulfonate, [49] dialkylphosphate, [50-51] and dialkylphosphonate [51] or alkyl triflates, [52-53], (Scheme 6). This means that the reactions are in line with 1st, 2nd and 5th principle of green chemistry. However, the range of ILs accessible via this route is limited based on the alkylating reagent. Another drawback is the sophisticated purification procedure to separate all products through liquid-liquid extraction.

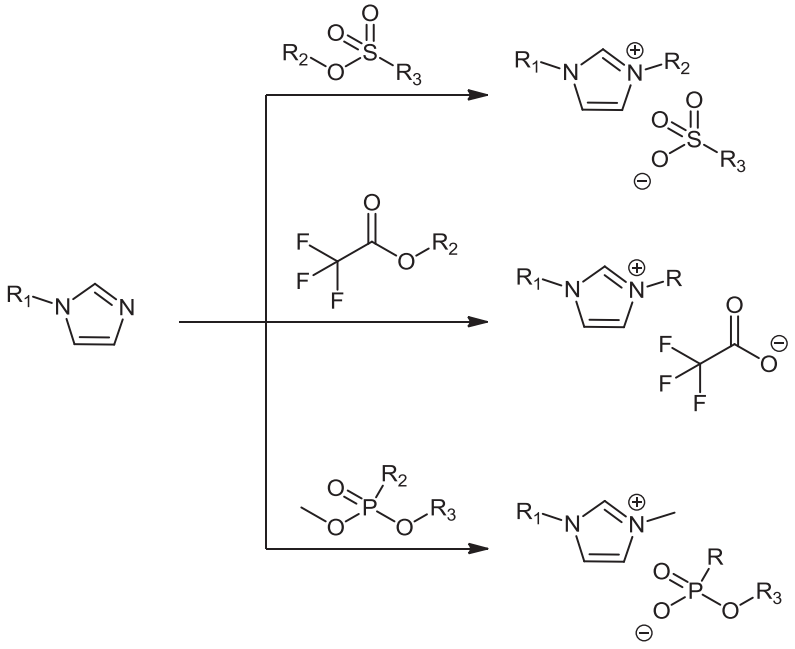

Scheme 6: Halide free synthesis of ILs [48-53].

1.2.3 Metathesis reaction

Most of common ILs are prepared via metathesis with a metal salt or an acid base neutralization reaction producing a stoichiometric amount of waste MX or HX (Scheme 7) [54].

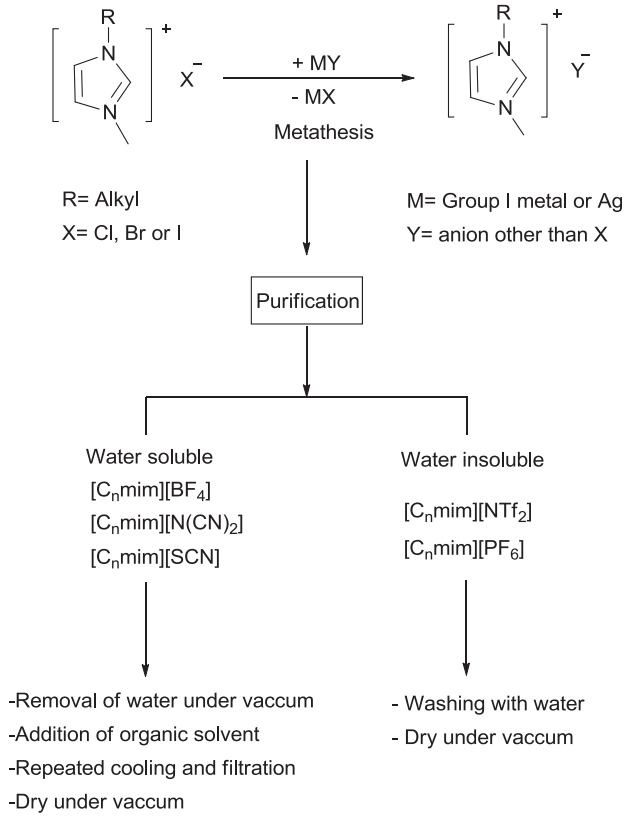

Scheme 7**:** General metathesis routes of ILs.

Hydrophobic ILs are easily separated from reaction media if the metathesis reaction occurs in water. However, the slow decantation and removing water require a large energy input. For the water-miscible ionic liquids the separation of the by-products from the desired IL becomes challenging. To make feasible this separation, the exchange reaction of the halide anion is generally performed in the presence of silver salt associated to numerous anions *e.g.* dicyanamide, thiocyanate, tetrafluoroborate (Scheme 8) [55-59]. This method has proven to be reliable and effective method for small-scale synthesis. Unfortunately, for industrial or large scale quantities this route is expensive and a large amount of silver halide as by-product [60-61].

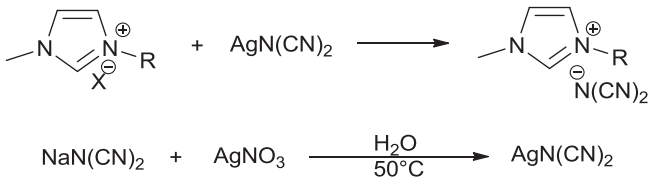

Scheme 8: Metathesis reaction using silver salt.

Complete precipitation of silver halides from organic solvents can also be quite slow, leading to silver-contamination products. Consequently, the metathesis reactions are generally run in aqueous solution with either the free acid of the appropriate anion, or its ammonium or alkali metal salt [62]. The resulting ILs are extracted from the aqueous solution by an organic solvent *i.e.*CH_2Cl_2. However, ILs are contaminated by appreciable amounts of chloride or bromide ions. This lowers the yield of the final product since their elimination requires several aqueous washings. The use of small water volume and lowering the temperature to ~ 0°C can reduce the loss of ILs affording yields in a range of 70–80 %. The use of molecular solvent, of silver salt, and the generated amounts of salts require removal and subsequent disposal, which do not comply with the 1st principle of green chemistry. Therefore, the practice of employing an organic solvent and water during the metathesis reaction further increases the E-factor and is highly undesirable.

The aim of this work is to use ILs as electrolytes for lithium ion batteries. This application requires high quality ILs (low chloride and water content). These impurities are generally introduced during the preparation of the ILs, which commonly involves a halide precursor, mainly a chloride or a bromide salt. Seddon et al. showed that presence of chloride led to a substantial increase of viscosity, even at low concentrations. Moreover, chloride and bromide can be easily oxidized at rather low potentials and interfere with the electrochemical process cause decrease in the electrochemical stability window. In lithium ion battery, as the electrolyte is based on mixture of ILs and lithium salts, traces of residual Li^+ from the synthetic procedure, perturbs their cycling performance. To take into account all these points to reduce the cost of ILs preparation, an alternative synthetic route has been attempted.

II. Results and discussion

In an attempt to reduce the wastes and IL cost. We developed alternative synthetic silver and water free route for ILs. For this purpose, the metathesis reaction was performed at the melting point temperature of the amine halide salts, playing the role of solvent, in the presence of the alkaline salt of the chosen anion [63-64].

2.1 Synthesis procedure

The metathesis reaction was performed using amine halide melt reagent as a solvent, 70°C for imidazolium chloride and 120°C for pyrrolidinium and phosphonium chlorides. In these liquid phases, the appropriate alkaline salt in 1.1 excess was added. In the exchange reaction (1), following

Pearson's principle the cations of Na^+ or Li^+ associated to the anions such as $[A]^- = [N(CN)_2]^-$, $[BF_4]^-$, $[NTf_2]^-$ afforded a total exchange with $[Cl]^-$ associated to imidazolium, pyrrolidinium, phosphonium cations (Table 1) [65].

$$[A]^-[Na]^+ + [Im]^+[Cl]^- \rightarrow [A]^-[Im]^+ + [Na]^+[Cl]^- \quad (1)$$

Then, CH_2Cl_2 (THF is only used for dicyanamide anion) was added to the reaction media to dissolve the resulting IL and to precipitate the resulting metal salt *i.e.* NaCl. For complete salt precipitation several-filtration cycles could be performed, generally two with CH_2Cl_2 and at least three with THF (no additional quantity of solvent is required). After evaporation of solvent, the IL was kept under high vacuum (10^{-5} mbar) at R.T. for 24 h, at this step the yield was *c.a.* 90%. The purity of the ILs can be judged using a variety of spectroscopic techniques.

Table 1: Metathesis reaction of ILs.

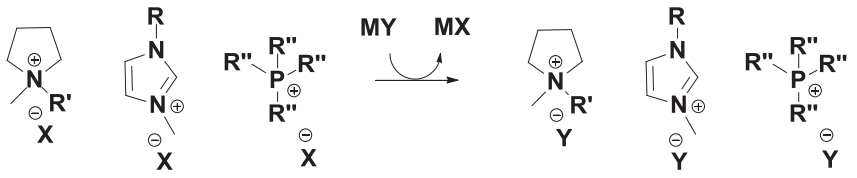

Entry	Ionic Liquids	Conditions	Abreviations	Yield[a] (%)
1	1-butyl-3-methylimidazolium dicyanamide	70°C, 24 h	$[C_1C_4Im][N(CN)_2]$	85
2	1-butyl-3-methylimidazolium thiocyanate	70°C, 24 h	$[C_1C_4Im][SCN]$	90
3	1-butyl-3-methylimidazoliumtetrafluoroborate	70°C, 24 h	$[C_1C_4Im][BF_4]$	90
4	1-butyl-3-methylimidazolium Bis (trifluoromethane)-sulfonimide	70°C, 24 h	$[C_1C_4Im][NTf_2]$	90
5	1-hexyl-3-methylimidazolium dicyanamide	70°C, 24 h	$[C_1C_6Im][N(CN)_2]$	87
6	1-hexyl-3-methylimidazolium thiocyanate	70°C, 24 h	$[C_1C_6Im][SCN]$	90
7	1-hexyl-3-methylimidazoliumtetrafluoroborate	70°C, 24 h	$[C_1C_6Im][BF_4]$	90
8	1-octyl-3-methylimidazolium dicyanamide	70°C, 24 h	$[C_1C_8Im][N(CN)_2]$	90
9	1-octyl-3-methylimidazolium tetrafluoroborate	70°C, 24 h	$[C_1C_8Im][BF_4]$	90
10	N- butyl- N- metylpyrrolidinium dicyanamide	120°C, 24 h	$[Py_{14}][N(CN)_2]$	90
11	N-butyl-N-metylpyrrolidinium bis(trifluoromethanesulfonyl)amide	120°C, 24 h	$[Py_{14}][NTf_2]$	90
12	Tetrabutylphosphonium bis(trifluoromethanesulfonyl)amide	120°C, 24 h	$[P_{4444}][NTf_2]$	90
13	Tetrabutylphosphonium tetrafluoroborate	120°C, 24 h	$[P_{4444}][BF_4]$	90

[a] Isolated yield after purification and dryness.

2.2 Analysis and characterization

Several analytical techniques have been used to determine the purity of our samples:

Water: the water has been determined by Karl Fisher. Generally, keeping ILs under high vacuum (10^{-5} mm) at RT or 60°C overnight leads repetitively to a water contamination of ~ 12 ppm.

Chloride: traces of chloride have been determined by ^{1}H-NMR, HRMS, and cyclic voltammetry.

NMR spectroscopy is the most common method for characterizing of ILs, but it is not an appropriate method for judging purity. In the case of imidazolium ($C_{2\text{-}H}$) based ILs, the impact of traces H_2O, $[Cl]^-$ and organic solvents on the chemical shift values of C_2-H proton in ^{1}H NMR ($\delta_{C2\text{-}H}$) has been reported [46].

For the imidazolium based ILs chloride traces lead to downfield of $\delta_{C2\text{-}H}$, which is attributed to the formation of stronger hydrogen bonds between C_2-H bond and $[Cl]^-$ anion, compared to the bond between C_2-H and anions $[BF_4]^-$ or $[NTf_2^-]$. A correlation between the evolution of δC_2-H and the $[Cl^-]$ concentration has been found, which could be used as a calibration curve to determine the $[Cl^-]$ amount in ILs.

In Figure 4, we compare the ^{1}H spectra of several samples of $[C_1C_6Im][N(CN)_2]$ from different sources. We considered that the commercial one (99.5% pure, (Fig 4c)) and the one synthesized following our procedure (Fig 4b) exhibit the same $\delta_{C2\text{-}H}$ proton (9.1 ppm, external DMSO- d_6), contrarily to the sample (Fig 4a) in which 1 mol.kg^{-1} of $[C_1C_6Im][Cl]$ has been added. In this case the $\delta_{C2\text{-}H}$ is deshielded from 9.1 to 9.4 ppm.

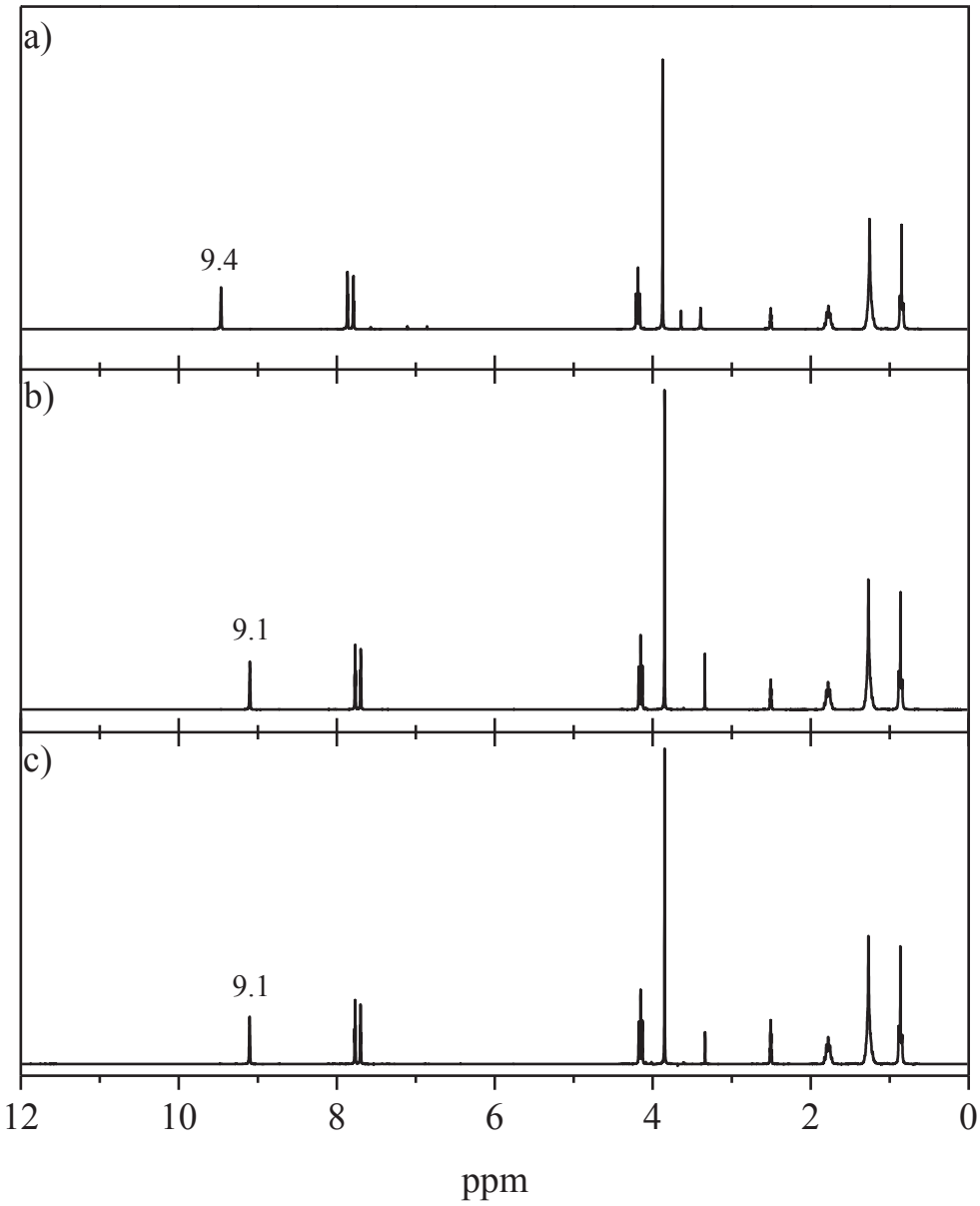

Figure 4: ^{1}H NMR spectra of 1-hexyl-3-methylimidazolium dicyanamide, (a) contaminated with 1-hexyl-3-methylimidazolium chloride (1 mol kg^{-1}) (b) commercial (c) prepared in our laboratory.

High resolution mass spectroscopy (HRMS) delivers both information about the mass and the isotope pattern of a compound and can be used for the structural analysis upon performance of MS/MS experiments. Therefore, it is a valuable tool for identification and characterization of an analyte as well as for the identification of impurities. Unwanted by-products formed during the synthesis or by hydrolysis of components of the ILs can be identified by this method, specifically the chloride contamination. For convenience, it is possible to judge the level of chloride up to 10 ppm using this technique. Figure 5 shows the high resolution mass spectra (HRMS) of the commercial $[C_1C_6Im][N(CN)_2]$ (99.5% pure, Figure 5a) and a sample prepared by our process

$[C_1C_6Im][N(CN)_2]$ (Figure 5b).

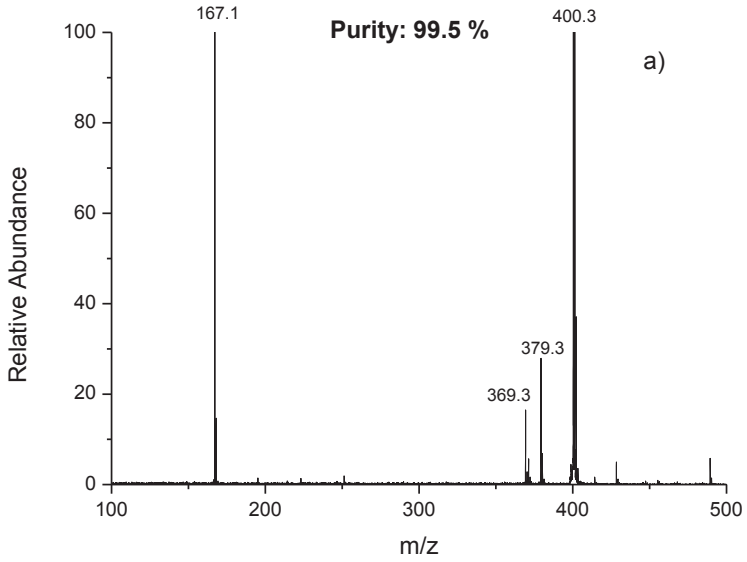

Figure 5a: High resolution mass spectra of commercial 1-hexyl-3-methylimidazolium dicyanamide (99.5% pure).

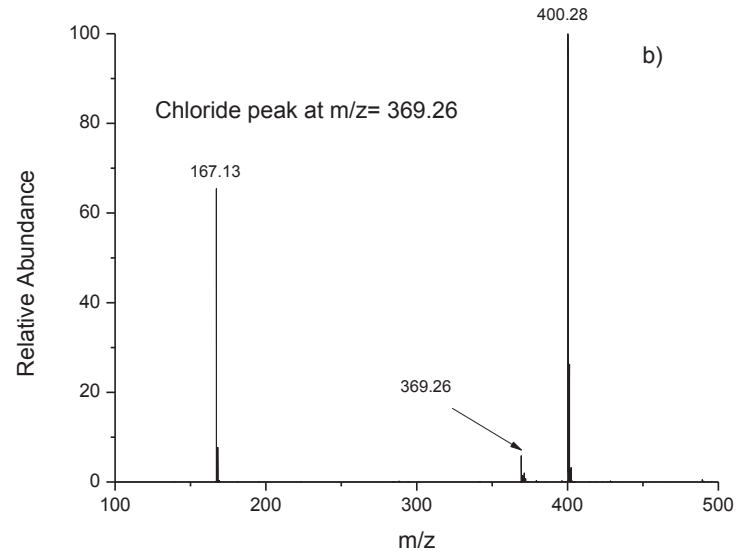

Figure 5b: High resolution mass spectra of 1-hexyl-3-methylimidazolium dicyanamide synthesised in our lab.

In HRMS, besides the peak at 167.1 and 400.3 m/z corresponding to $[C_1C_6Im]^+$ and $[C_1C_6Im]_2[N(CN)_2^-]$ respectively, the peak at 369.26 is due to $[C_1C_6Im]_2[Cl]^-$. The comparison of the HRMS of the two samples (Figures 5a and 5b) allows concluding that the $[Cl]^-$ contamination in our sample is inferior to 0.5% as for all ILs obtained through our chemical procedure see Appendix I page 112.

The cyclic voltammetry of ILs with a platinum working electrode, a platinum counter electrode and a

silver wire as the reference provides a very quick indicator of the general impurity [66]. The effect of the presence of chloride anion in $[C_1C_4Im][NTf_2]$ and in $[C_1C_4Im][N(CN)_2]$ on their cyclic voltammogram was depicted in Figures (6 and 7), respectively. In the presence of $[C_1C_4Im][Cl]$ a broad peak appeares ≈ 0 V in their cyclic voltammogram and a decrease of their electrochemical window is noticed.

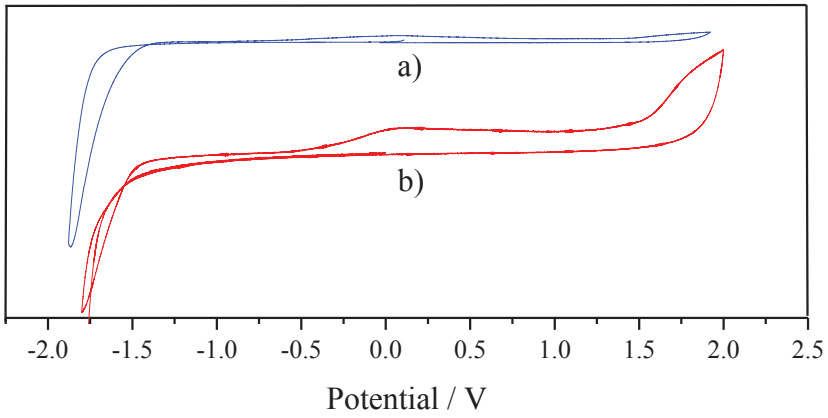

Figure 6: Cyclic voltammogram of 1-butyl-3-methylimidazolium dicyanamide (a) prepared in our lab (b) contaminated with chloride (1 mol kg^{-1}).

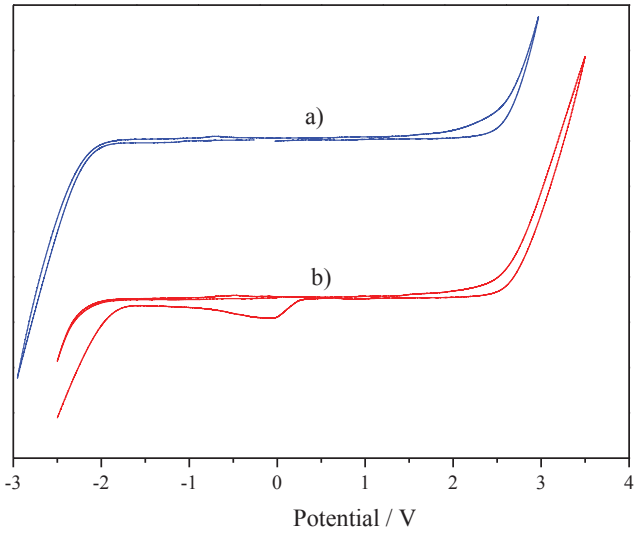

Figure 7: Cyclic voltammogram of 1-butyl-3-methylimidazolium bis(trifluoromethylsulfonyl)imide (a) prepared in our lab (b) contaminated with chloride (1 mol kg^{-1}).

Determination of Na^+ and Li^+ traces is still challenging. ICP analyses need a diluted solution of IL into water or alcohol leading to loss of materials. Currently, in our laboratory we attempt to determine the $[Na]^+$ and $[Li]^+$ concentration by ^{23}Na and ^{7}Li solutions NMR. This approach presents the advantage of use neat IL, but needs to find the optimal NMR parameters to establish accurate calibration curves.

2.3 Experimental Part

See Appendix I page 112.

2.4 Conclusions

The market of Lithium-ion is growing due to the demand in powering portable devices. So the price of lithium-ion batteries has dropped by 20-50% during the last few years. The ILs which is safer than organic carbonates will be potential substitute if their cost and efficiency are improved.

Consequently, one of the goal of my PhD was to design new synthetic routes reducing wastes and cost and novel ILs to tune their physical-chemical and electrochemical properties to improve their performances as electrolytes in Li cells. This approach was always based on the willing to develop standard synthesis procedure yielding to high purity Ils.

For the common ILs, an alternative synthetic silver and water free route has been developed. For this purpose, the metathesis reaction is run at the temperature of the melting point of the amine halide salts, playing the role of solvent, in the presence of Na or Li salt of the chosen anion A, in order to favour the ion exchange following Pearson principle.

$$[A]^-[Na]^+ + [Im]^+[Cl]^- \rightarrow [A]^-[Im]^+ + [Na]^+[Cl]^- \quad (1)$$

Therefore, imidazolium, phosphonium pyrrolidinium based ILs and anions associated with different anions such as dicyanamide, thiocyanate, tetrafluoroborate and Bis(trifluoromethylsulfonyl)imide were obtained in high purity ($\geq$ 99.5%) and high yields. Significant effort has been put into designing experiments and developing methods to detect and analyse all traces of impurities in the ILs.

III References

1. Davis, J.H., Jr., C.M. Gordon, C. Hilgers, P. Wasserscheid, *Wiley-VCH, Weinheim,* Synthesis and purification of ionic liquids, (2003), pp. 7-21.
2. Hurley, F.H., T.P. Wier, Jr., *J. Electrochem. Soc.* **98** (1951) 207-212.
3. Wilkes, J.S., J.A. Levisky, R.A. Wilson, C.L. Hussey, *Inorg. Chem*. **21** (1982) 1263-1264.
4. Fry, S.E., N.J. Pienta, *J. Am. Chem. Soc.* **107** (1985) 6399-6400.
5. Earle, M.J., K.R. Seddon, *Pure Appl. Chem.* **72** (2000) 1391-1398.
6. Welton. T, *Chem Rev*. **99**(8) (1999) 2071-2084.
7. Holbrey, J.D., R.D. Rogers, in, Physicochemical properties: physicochemical properties of ionic liquids: melting points and phase diagrams, *Wiley-VCH,Weinheim,* (2008), pp. 57-72.
8. Zhang, L., X. Yu, Z. Ge, Y. Dong, D. Li, *Appl. Mech. Mater.* **121-126** (2012) 65-69.
9. Meindersma, W., F. Onink, H.A.B. de, Green separation processes with ionic liquids, *Wiley-VCH, Weinheim,* (2010).
10. Han, D., K.H. Row, *Molecules* **15** (2010) 2405-2426.
11. Werner, S., M. Haumann, P. Wasserscheid, *Annu. Rev. Chem. Biomol. Eng.* **1** (2010) 203-230.
12. Olivier-Bourbigou, H., L. Magna, D. Morvan, *Appl. Catal*., A **373** (2010) 1-56.
13. Niedermeyer, H., J. P. Hallett, I. J. V. Garcia., P. A. Hunt, T. Welton, *Chem Soc Rev;* **41**(23) (2012) 7780-7802.
14. Crowhurst, L., Lancaster, N. L, Arlandis, J. M. P, Welton. T, *J. Am. Chem. Soc*, **126** (2004), 11549-11555.
15. Staerk, K., N. Taccardi, A. Boesmann, P. Wasserscheid, *ChemSusChem* **3** (2010) 719-723.
16. Brandt, A., J. Graesvik, J.P. Hallett, T. Welton, *Green Chem*. **15** (2013) 550-583.
17. Uerdingen, M., in: P.T. Anastas (Ed.), Handbook of Green Chemistry *Wiley-VCH, Weiheim*, (2010), pp. 203-219.
18. Ohno, H., Electrochemical Aspects of Ionic Liquids, Second Edition, *Wiley, N.Y.,* (2011).
19. Armand, M., F. Endres, D.R. MacFarlane, H. Ohno, B. Scrosati, *Nat. Mater*. **8** (2009) 621-629.
20. A. Matic, B. Scrosati, *MRS Bulletin*, **39** (2013), 533-537.
21. Passerini. S, Appetecchi. G.B, *MRS Bulletin*, **38** (2013), 540-547.
22. Sheldon, R., *Nature* (London) **399** (1999) 33.
23. Anastas, P., J. Warner, Green Chemistry: Theory and Practice, *Oxford Univ Press*, (1998).

24. Anastas, P.T., M.M. Kirchhoff, *Acc. Chem. Res.* **35** (2002) 686-694.
25. Welton, T., *Chem. Rev*. **99** (1999) 2071-2083.
26. Deetlefs, M., K.R. Seddon, in, The green synthesis of ionic liquids, *Wiley-VCH Verlag GmbH & Co. KGaA, Weinheim*, (2010), pp. 3-38.
27. Zhang, Z., Y. Li, H. Xiao, C. Tu, C. Wang, *Adv. Mater. Res.* (Durnten-Zurich, Switz.) **581-582** (2012) 326-329.
28. Ferguson, J.L., J.D. Holbrey, S. Ng, N.V. Plechkova, K.R. Seddon, A.A. Tomaszowska, D.F. Wassell, *Pure Appl. Chem.* **84** (2012) 723-744.
29. Abdul-Sada, A.a.K., A.E. Elaiwi, A.M. Greenway, K.R. Seddon, *Eur. Mass Spectrom*. **3** (1997) 245-247.
30. Bonhote, P., A.-P. Dias, N. Papageorgiou, K. Kalyanasundaram, M. Graetzel, *Inorg. Chem*. **35** (1996) 1168-1178.
31. Suarez, P.A.Z., J.E.L. Dullius, S. Einloft, R.F. de Souza, J. Dupont, *Inorg. Chim. Acta* **255** (1997) 207-209.
32. Jeapes, A.J., R.C. Thied, K.R. Seddon, W.R. Pitner, D.W. Rooney, J.E. Hatter, T. Welton, *Pat WO2001015175*, Process for recycling ionic liquids, (2001), p. 8 pp.
33. Elaiwi, A., P.B. Hitchcock, K.R. Seddon, N. Srinivasan, Y.-M. Tan, T. Welton, J.A. Zora, J. Chem. Soc., *Dalton Trans*. (1995) 3467-3472.
34. Rogers, R.D., K.R. Seddon, ACS Symp. Ser., (2003); 856.
35. Deetlefs, M., K.R. Seddon, *Green Chem*. **5** (2003) 181-186.
36. Varma, R.S., V.V. Namboodiri, *Pure Appl. Chem.* **73** (2001) 1309-1331.
37. Varma, R.S., V.V. Namboodiri, *Chem. Commun.* (Cambridge, U. K.) (2001) 643-644.
38. Boros, E., K.R. Seddon, C.R. Strauss, *Chim. Oggi* **26** (2008) 28-30.
39. Namboodiri, V.V., R.S. Varma, *Org. Lett.* **4** (2002) 3161-3163.
40. Lévêque, J.-M., J.-L. Luche, C. Pétrier, R. Roux, W. Bonrath, *Green Chem* **4** (2002) 357-360.
41. Oxley, J.D., T. Prozorov, K.S. Suslick, *J. Am. Chem. Soc*. **125** (2003) 11138-11139.
42. Leveque, J.-M., J.-L. Luche, C. Petrier, R. Roux, W. Bonrath, *Green Chem.* 4 (2002) 357-360.
43. Li, X., J. Zhao, Q. Li, L. Wang, S.C. Tsang, *Dalton Trans.* (2007) 1875-1880.
44. Chatel, G., C. Goux-Henry, J. Suptil, N. Kardos, B. Andrioletti, M. Draye, *Ultrason. Sonochem* **19** (2012) 390-394.

45. Chatel, G., R. Pflieger, E. Naffrechoux, S.I. Nikitenko, J. Suptil, C. Goux-Henry, N. Kardos, B. Andrioletti, M. Draye, *ACS Sustainable Chem. Eng*. **1** (2013) 137-143.
46. Seddon, K.R., A. Stark, M.-J. Torres, *Pure Appl. Chem*. **72** (2000) 2275-2287.
47. Dupont, J., S.R.F. de, P.A.Z. Suarez, *Chem. Rev*.**102** (2002) 3667-3691.
48. Himmler, S., S. Hörmann, R. van Hal, A.S. Schulz, P. Wasserscheid, *Green Chem*. **8** (2006) 887.
49. Del Sesto, R.E., C. Corley, A. Robertson, J.S. Wilkes, *J. Organomet. Chem.* **690** (2005) 2536.
50. Kuhlmann, E., S. Himmler, H. Giebelhaus, P. Wasserscheid, *Green Chem*. **9** (2007) 233.
51. Brandt, A., J.P. Hallett, D.J. Leak, R.J. Murphy, T. Welton, *Green Chem*. **12** (2010) 672-679.
52. Sachnov, S.J., P.S. Schulz, P. Wasserscheid, *Chem. Commun*. **47** (2011) 11234-11236.
53. Holbrey, J.D., W.M. Reichert, R.P. Swatloski, G.A. Broker, Pitnern W. R., K.R. Seddon, Rogers R. D., *Green Chem* **4** (2002) 407-413.
54. Rogers, R.D., K.R. Seddon, Ionic liquids IIIB : Fundamentals, Progress, Challenges and Opportunities Transformationds and Processes, *ACS,* Washington, (2005).
55. Wilkes, J.S., M.J. Zaworotko, *Chem. Comm.* (1992) 965-967.
56. Larsen, A.S., J.D. Holbrey, F.S. Tham, C.A. Reed, *J. Am.Chem.Soc* **122** (2000) 7264-7272.
57. MacFarlane, D.R., J. Golding, M. Forsyth, G.B. Deacon, *Chem. Commun*. (2001) 1430-1431.
58. MacFarlane, D.R., S.A. Forsyth, J. Golding, G.B. Deacon, *Green Chem* **4** (2002) 444-448.
59. Pringle, J.M., J. Golding, G.B. Forsyth, G.B. Deacon, M. Forsyth, D.R. MacFarlane, *J. Mat. Chem*. (2002) 3475-3480.
60. Hallett, J.P., T. Welton, *Chem. Rev.* 111 (2011) 3508-3576.
61. Rogers. R. D, Seddon. K. R, Industrial applications for green chemistry, ACS Washington, (2002).
62. Anderson, J.L., J.K. Dixon, E.J. Maginn, J.F. Brennecke, *J. Phys. Chem. B* **110** (2006) 15059-15062.
63. Srour, H., L. Moura, H. Rouault, C.C. Santini, in: CEA-CNRS, Nouveau procédé de synthèse écologique et économique de liquides ioniques, *Pat WO2013037923* (2013).
64. Srour, H., H. Rouault, C.C. Santini, Y. Chauvin, *Green Chem.* **15** (2013) 1341-1347.
65. Gutel, T., P. Campbell, C.C. Santini, F. Lefebvre, C. Lucas, Y. Chauvin, *Chimica Oggi* **27** (2009) 48-50.
66. Burrell, A.K., R.E.D. Sesto, S.N. Baker, T.M. McCleskey, G.A. Baker, *Green Chem*. **9** (2007) 449-454.

Chapter 2

Lithium ion batteries: Imidazolium based ionic liquids as electrolytes

I- General introduction

Demands for advanced storage energy increase with every year. Finite energy source and global warming push the society toward the development of renewable energy (e.g., solar energy and wind energy.). However, the intermittent nature of renewable energy source relies on efficient energy storage systems to manage load leveling. This necessity has been met by the technology of batteries.

Battery is a device consisting one or several electrochemical cells, which can convert stored electrochemical energy into electrical energy. Two types of batteries are distinguished: primary and secondary batteries. Primary batteries are capable of one-time use, the most common are alkaline. These batteries use zinc as the anode and manganese dioxide as the cathode with aqueous solution of potassium hydroxide as the electrolyte – the "alkaline" part of the battery. Secondary batteries also called rechargeable, which designed to be recharged and used, multiply times. Usually assembled in the discharge state they must be charged before used them.

The construction of the battery allows a restoration of the original electrode materials by applying a voltage or a current from an external source. Commonly used types of these batteries are: nickel–cadmium (NiCd), nickel–zinc (NiZn), nickel metal hydride (NiMH), and lithium-ion (Li-ion) cells [1]. The challenge is to use materials, which can be produced on a large scale with high efficiency while still maintain low-enough costs for worldwide adoption.

Among all the existing batteries, Li-ion batteries have been given substantial attention today because of their high energy density, absence of toxic metal such as lead or cadmium, and no memory effect. Nowadays, share in the global sales for Ni-Cd is 23%, for Ni-MH – 14% and for Li-ion portable batteries is 63%. In case of Pb-acid batteries, the use is limited mostly to SLI (starting, lighting, and ignition) in automobiles or standby applications, while Ni–Cd batteries remain the most attractive technologies for high-power applications like power tools (Figure 1) [2].

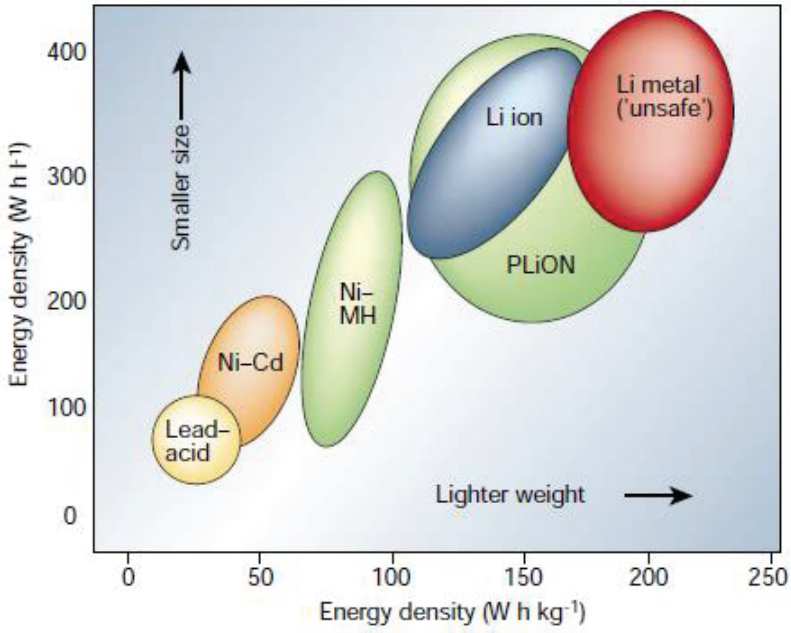

Figure 1: Comparison of the different battery technologies in terms of volumetric and gravimetric energy density [2].

1.1 Li-ion batteries

Li-ion batteries are already used in many applications but the improvement of this technology is still necessary to be strongly introduced on new markets such as electric vehicles, hybrid electric vehicles or photovoltaic solar cells. Because of their design flexibility, Li-based currently become one of the most important and commonly used rechargeable battery systems.

The motivation for using a battery technology based on Li metal as anode is established on its properties. Lithium is the lightest metal (M = 6.94 g mol^{-1}; ρ = 0.53 g cm^{-3}) and has the lowest reduction potential (E_0 = -3.04 V *vs.* SHE). However, the use of pure lithium metal as anode may lead to a constant capacity loss during cycling and unwanted side reactions. During the moderate and fast recharge step, lithium plating in liquid electrolyte occurs simultaneously with some lithium corrosion and passivation. Lithium classically deposits as dendritic, highly reactive metal particles (Figure 2) [2]. The dendrites are covered with surface film and therefore become partially electrochemically inactive, which reduces the cycle life of the cell (Figure 3) [3]. Furthermore, the dendrites may create filaments, which locally cause short circuit in the cell. Due to the low melting point of metallic Li (about 453 K) the local overheat can lead to combustions and production of explosion hazards.

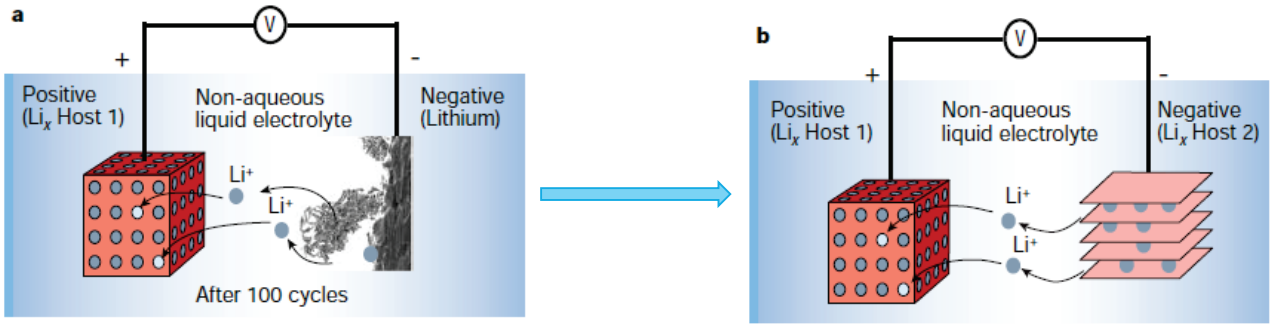

Figure 2: Schematic representation and operating principles of Li batteries. a) Rechargeable Li-metal battery (the picture of the dendrite growth at the Li surface was obtained directly from in situ SEM), b) Rechargeable Li-ion battery [2].

The surface films formed on lithium metal can be easily cracked, and the passivation is broken during both Li deposition and dissolution. This leads to known dendrite formation and to a massive loss of both lithium and solution species due to the surface reactions and the 'repair' of the surface films (on an increasing Li surface area).

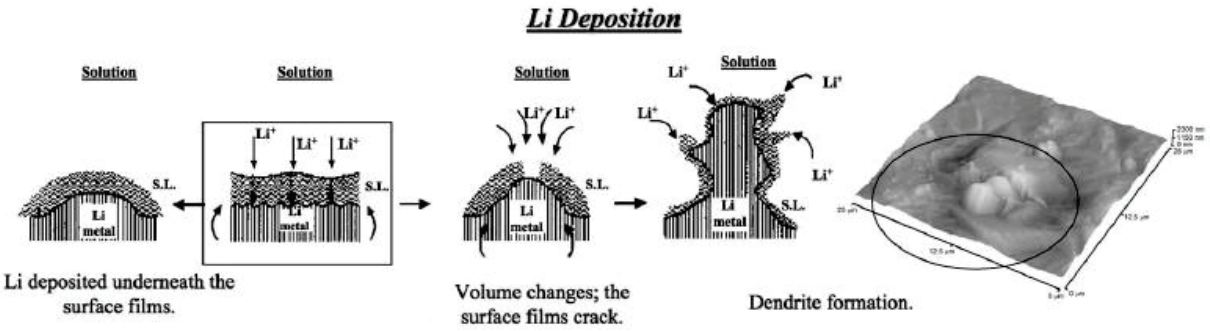

Figure 3: The beginning of the dendrite formation (Li electrodes in an EC-DMC/$LiPF_6$ solution) [3].

Possible changes, like doping the Li surfaces or changing the solvent, did not improve the performance of Li electrodes at fast charging rates as observed in AA secondary batteries containing these modifications [3]. Consequently, the most effective method to overcoming the problems with the metallic lithium electrode was the replacement of the Li metal by insertion electrode materials.

1.2 Electrodes

To circumvent the safety issues surrounding the use of Li metal, several alternative approaches were pursued in which either the electrolyte or electrode was modified. This research was focused on the reaction of Li-ions with insertion materials (carbon-based like graphite, $Li_4Ti_5O_{12}$, TiO_2, etc), conversion materials (iron oxides, cobalt oxides) and alloys (Si, Sn). Today's batteries are dominated by intercalation materials. An ideal battery has a high-energy capacity, fast charging time and a long

cycle time. The capacity and nominal potential are determined by the lithium saturation concentration of the electrode materials (Figure 4).

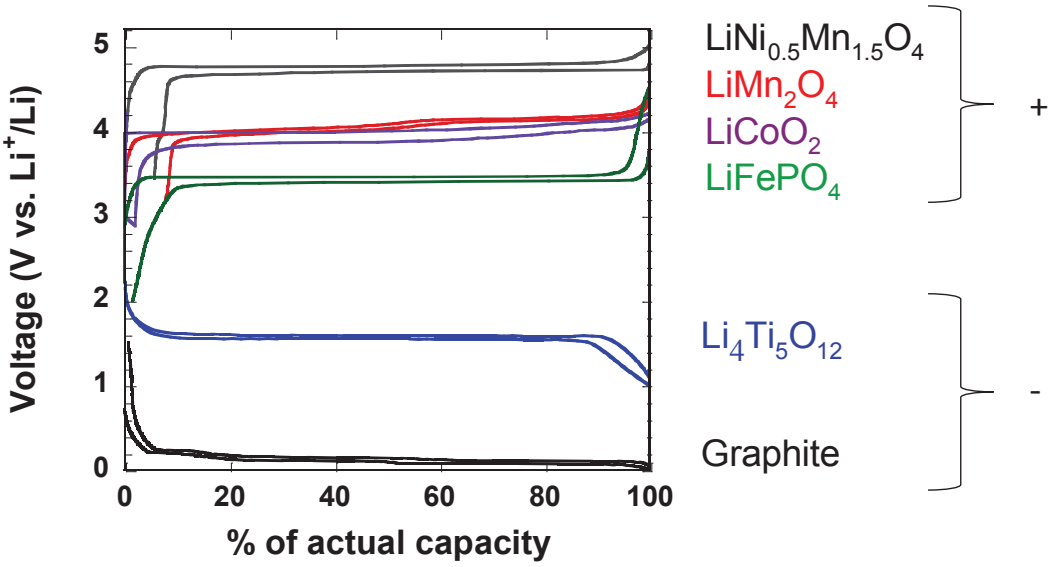

Figure 4: Lithium ion technology: different technology and nominal voltage.

1.2.1 Negative electrodes

Graphite (Cgr)

The use of carbon-based anode materials helps to resolve safety issues at the lithium metal electrode, since Li ions can be inserted within this type of electrode, in a stable state and they exhibit both higher specific charges and more negative redox potentials than most metal oxides, chalcogenides, and polymers.

Nowadays, the most common anode material is Cgr, where one lithium reacts with six carbons. The voltage in comparison to lithium electrode (Li^+/Li) ranges between 0.0 to 0.25 V (Equation 1).

$$Li^+ + xe^- + 6C \leftrightarrow LiC_6$$

$$C_c = 372\ mAh/g$$

Equation 1: Theoretical capacity of Cgr.

Graphite exfoliation & solid electrolyte interface (SEI) formation

During the early stage of lithium intercalation, lithium ions tend to be intercalated together with electrolyte solvents due to the thermodynamic reasons. This route could cause exfoliation and decomposition of graphene sheets [3].

The intercalation of Li^+ and other alkali metal ions from organic donor solvent electrolytes into fairly crystalline graphitic carbons often leads to solvated graphite intercalation compounds, $Li(solv)_yC_n$

(Figure 5). This so-called “solvated intercalation” is linked with great expansion of the graphite matrix (typically ~150%), often leading to deterioration of the graphite and as a result to a drastically decreased charge storage capability [4].

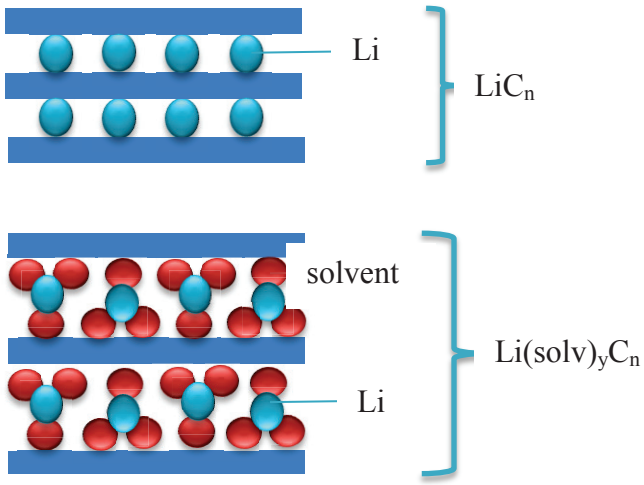

Figure 5: Schematic drawing of binary (LiC_n) and ternary [$Li(solv)_yC_n$] lithium Cgr intercalation compounds [4].

Key factor that determines the stability of graphite electrodes in Li insertion processes is to what extent protective surface films are formed rapidly enough before co-intercalation can take place. To stop this process from occurring, an electrolyte additive is used to create the solid electrolyte interface (SEI) layer on the graphite surface before the simultaneous intercalation of lithium ions and the electrolyte solvent [5] (Figure 6). The composition and morphology of the SEI layers depend on the kind of electrolyte used. There is general agreement that films formed in organic solvent ± based electrolytes comprise: i) thick, porous, electrolyte permeable films of organic (polymeric and oligomeric) decomposition products; and ii) thin, compact, electrolyte impermeable films of inorganic decomposition products [4].

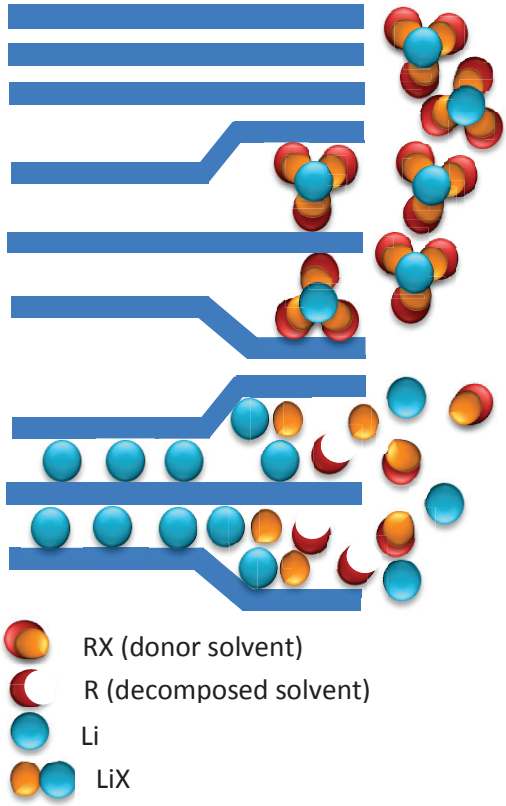

Figure 6: Film formation mechanism on the Cgr [4].

$Li_4Ti_5O_{12}$ (LTO)

Lithium–titanium oxides (LTO) have theoretical capacity of 175 mAh/g with operating voltage of 1.55 V vs. Li^+/Li. In practical, the maximum recovered capacity at low current is in average 165 mAh/g and depends on the synthesis route. Electrode slurry manufacturing based on nano sized particles requires a great amount of solvent and thus lowers the productivity of the electrode. Furthermore, due to the nano size, electrodes are sensitive for level moisture, which can cause impede in manufacturing process and aggravate battery characteristic. LTO with relatively low specific capacity but high rate capability is being studied for use in hybrid electric vehicle (HEV) batteries [5]. LTO has a low capacity density, which is about half that of Cgr. The interest of such material is that there is no dendrite formation at high charging rates thanks to its high potential vs. Li^+/Li. In addition, no passivation film responsible of some over tension at the electrode surface is formed, contrary to the Cgr based electrode.

1.2.2 Positive electrodes

The current state for positive electrodes relies on $LiCoO_2$, $LiNi_{1/3}Mn_{1/3}Co_{1/3}O_2$ or $LiMn_2O_4$ with recently discovered polyanionic compounds like $LiFePO_4$ (Figure 7).

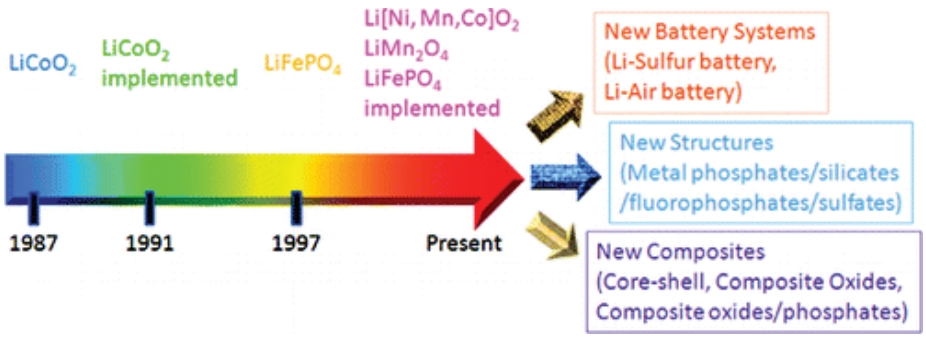

Figure 7: Cathode materials in time scale.

LiFePO$_4$ (LFP)

Olivine LFP has attracted a lot of attention in recent years due to great deal of potential, especially in the area of safe performance. This material has many advantages of low cost, non-toxicity and thermal stability in the fully charged state. In addition, LFP has a large theoretical capacity of 170 mAh/g and good cycle stability [6-9]. These polyanion-containing compounds show reversible electrochemical lithium extraction/insertion in an interesting potential region between 3 V and 3.5 V vs. Li/Li$^+$ as well as high lithium diffusion rates [4].

LFP has an orthorhombic olivine structure which consists of [FeO$_6$] octahedral with oxygen corner-sharing [PO$_4$]$^{3-}$ tetrahedral with a high theoretical capacity (170 mAh/g), LFP is environmentally friendly and occurs naturally as the mineral triphylite (Figure 8).

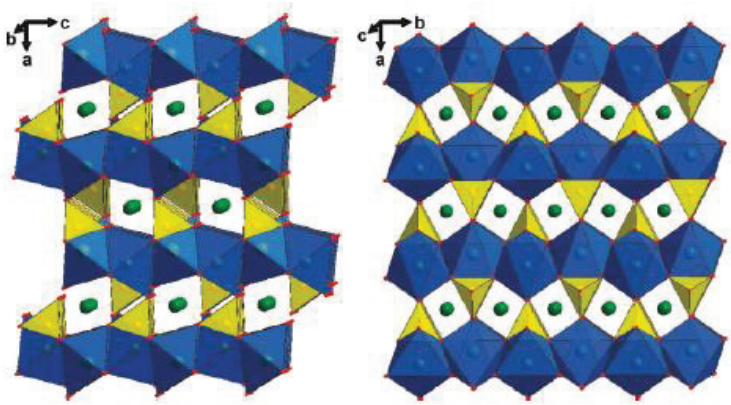

Figure 8: Polyhedral representation of the structure of LFP (space group P*nma*) viewed (a) along the b-axis and (b) along the c-axis. The iron octahedra - blue, the phosphate tetrahedral - yellow, the Li-ions – green [10].

It can be observed that associated with LTO as negative electrode, fast recharge can be obtained, but with low energy density. It can find applications in power batteries. Cell using graphite as negative electrode has higher energy density and it can be used in storage batteries (Figure 9).

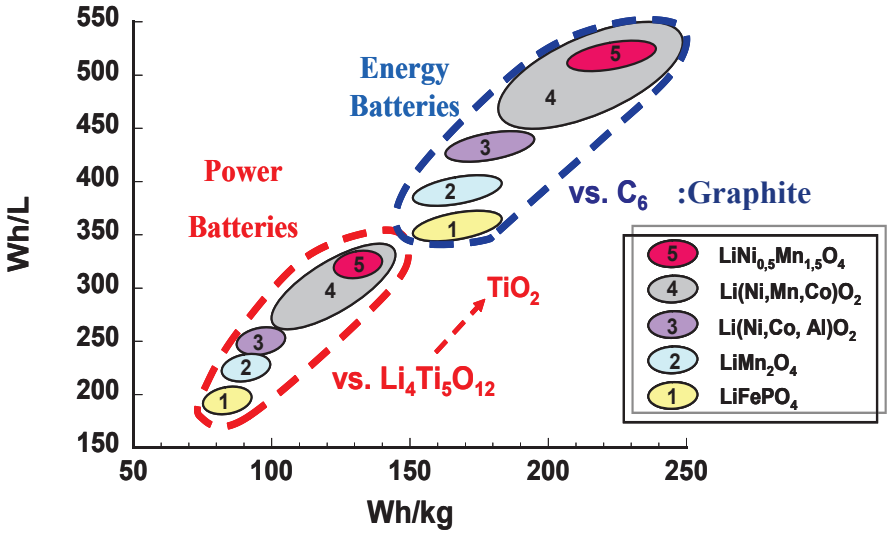

Figure 9: Comparison between cathode materials vs. LTO and Cgr.

1.3. Organic electrolytes

Besides the electrodes, the electrolyte, which commonly refers to a solution comprising the salts and solvents, constitutes the third key component of a battery. Its choice is actually crucial, and is based on criteria that differ depending on whether we are dealing with lithium polymer or liquid-based Li-ion rechargeable batteries.

The electrolyte is commonly a solution containing an inorganic lithium salt ($LiNTf_2$ - lithium bis(trifluoromethane)sulfonylimide, $LiPF_6$ - lithium hexafluorophosphate, *etc.*) dissolved in a mixture of organic solvents such as propylene carbonate (PC), ethylene carbonate (EC), dimethyl carbonate (DMC), diethyl carbonate (DEC) (Figure 10).

a)

Common name	Formula	Mol. wt. (g/mol)
Lithium hexafluorophosphate	$LiPF_6$	151.9
Lithium tetrafluoroborate	$LiBF_4$	93.74
Lithium perchlorate	$LiClO_4$	106.39
Lithium hexafluoroarsenate	$LiAsF_6$	195.85
Lithium triflate	$LiSO_3CF_3$	156.01

b)

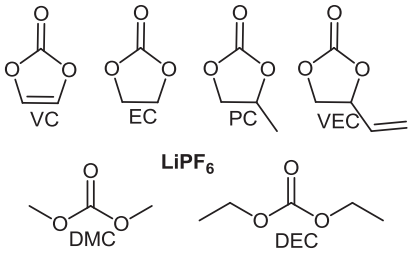

Figure 10: Examples: a) Lithium salts and b) organic solvents.

These solvents have a number of inherent limitations and drawbacks. Conventional electrolytes have some safety concerns, especially in case of their flammability and volatility of the solvents. Under the right circumstances, the electrolyte in Li-ion battery can ignite or even explode. Some of the examples of the accidents with lithium ion batteries are presented in Table 1 [11].

Table 1: Some lithium ion battery fire and explosion accidents in past few years [11].

Some lithium ion battery fire and explosion accidents in the past few years.

No.	Date	Accidents replay	Fire causes
1	18 July, 2011	EV bus catch fire, Shanghai, China	Caused by overheated $LiFePO_4$ batteries
2	11 April, 2011	EV taxi catch fire, Hangzhou, China	Caused by 16 Ah $LiFePO_4$ battery
3	3 September, 2010	A Boeing B747-400F cargo plane catch fire, Dubai	Caused by overheated lithium batteries
4	26 April, 2010	Acer recalled 2700 laptop batteries, as Dell, Apple, Toshiba, Lenovo and Sony done in 2006	Potential overheating and fire hazards
5	March, 2010	Two iPod Nano music player overheating and catching fire, Japan	Caused by overheated lithium batteries
6	January, 2010	Two EV buses catch fire, Urumqi, China	Caused by overheated $LiFePO_4$ batteries
7	July, 2009	Cargo plane catch fire before fly to USA, Shenzhen, China	Caused by spontaneous combustion of lithium ion batteries
8	21 June, 2008	Laptop catch fire in a conference, fire burning 5 min, Japan	Caused by overheated battery
9	June, 2008	Honda HEV catch fire, Japan	Caused by overheated $LiFePO_4$ batteries
10	2006–now	Tens of thousands of mobile phone fires or explosions	Caused by short-circuit, overheating, etc.

Note: all the accident data are from the Internet.

Fire and explosion of the Li-ion battery is related to the flammability of the electrolyte, the rate of charge and/or discharge, and the engineering of the battery pack. It can cause crack, ignition, or explosion when exposed to high temperature or short-circuiting. The adjacent cells may also then heat up and fail, in some cases, causing the entire battery to ignite or rupture [11].

Thermal runaway is one of the failure modes in batteries and it occurs when an exothermic reaction goes out of control. The reaction rate increases due to growth in temperature, which cause escalation in temperature and henceforth a further increase in the reaction rate which possibly resulting in an explosion (Figure 11).

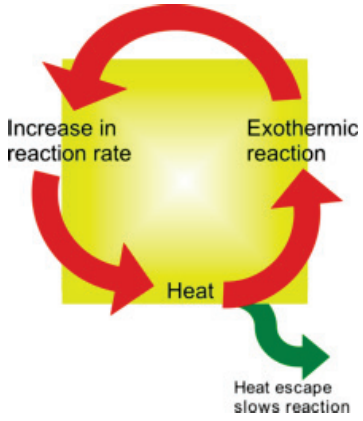

Figure 11: Diagram of thermal runaway.

For the Li-ion battery runaway, it is caused by the exothermic reactions between the electrolyte (alkyl carbonates, particularly the linear carbonates) and the anode and cathode, inducing the temperature and pressure increasing in the battery, in order to lead to the battery rupture at last.

The battery typically undergoes the following reactions: SEI decomposition, reaction between the negative active material and electrolyte, reaction between the positive active material and electrolyte, electrolyte decomposition, and the reaction between the negative active material and binder, etc.

More precisely, the first step of the battery runaway is the break of the thin SEI film on the negative electrode, due to overheating or physical penetration. The SEI layer decays at the relatively low

temperature ~ 342 K, and when this film is broken, the electrolyte reacts with the graphite anode during the formation process but at a higher and uncontrolled, temperature. Heat from SEI decomposition reaction causes the reaction of intercalated lithium with the organic solvents used in the electrolyte releasing flammable hydrocarbon gases (ethane, methane and others). This typically begins around 373 K but with some electrolytes it can be as low as 341 K. The gas generation due to the breakdown of the electrolyte causes pressure to build up inside the cell. At around 403 K the polymer separator melts, causing the short circuits between the electrodes. Finally heat from the electrolyte breakdown causes breakdown of the metal oxide cathode material releasing oxygen which enables burning of both the electrolyte and the gases inside the cell. The breakdown of the cathode is also highly exothermic sending the temperature and pressure even higher. After the deterioration of SEI layer formed on anode, the lithiated anode material decomposes again and reaches to the second exothermic peak about 483 K with the presence of electrolyte. The total heat generation can reaches 2000±300 J g^{-1}, which is dangerous for the battery. All the above reactions contribute heat and pressure in the cell and in return speed up the reactions, which caused safety problems for Li-ion batteries in some consumer electronics and have difficult the deployment of Li-ion batteries for some electric and hybrid cars [11].

Current Li-ion battery electrolytes also suffer from a limited operational temperature range. At temperatures above ~ 333 K, the electrolyte solution used in most commercial Li-ion batteries can deteriorate. The dissolved lithium salts can undergo chemical reactions with the solvents at these elevated temperatures, negatively affecting performance. Because these reactions are irreversible, function is not fully restored even when the temperature is reduced, and the reaction products can pose additional safety issues. Performance also suffers below 253 K as this is approaching the freezing point of the normal electrolyte solutions.

Consequently, there is active research on a variety of approaches to eliminate or mitigate these problems; one such approach is the replacement of conventional battery electrolytes with special solvents known as room temperature ionic liquids (RTILs).

II- Li-ion cells based on ILs electrolytes

2.1 Ionic liquids (ILs)

Ionic liquids (ILs) are defined as molten salts that are liquid over a wide temperature range and are comprised a bulky unsymmetrical organic cation associated with weakly coordinating organic and inorganic anions. Room temperature ionic liquids (ILs) have melting points below 373 K, and may

have melting points as low as 183 K. These low melting points are achieved because of IL structural characteristics:

1. Large size of cations and anions,
2. Charge delocalization in ions,
3. Considerable conformational freedom of cations and anions, and high melting entropy,
4. Asymmetric cation structure.

ILs can be defined as aprotic or protic (depending on the nature of cation), with their liquid character being determined by the judicious choice of ionic structures. Common IL cations include imidazolium, pyridinium, alkylammonium, alkylphosphonium, pyrrolidinium, guanidinium, and alkylpyrrolidinium. IL anions can be selected from a broad range of inorganic anions [e.g. halides ($[Cl]^-$, $[Br]^-$, $[I]^-$), polyatomic inorganics ($[PF_6]^-$, $[NO_3]^-$, $[BF_4]^-$), and polyoxometallates], or more topically from organic anions such as, $[NTf_2]^-$, and $[Tf]^-$. The properties of ILs, in terms of conductivity, hydrophobicity, melting point, viscosity, solubility, etc., can be tuned by altering the substitutive group on the cation, or the combined anion [12-13, 5] (Figure 12).

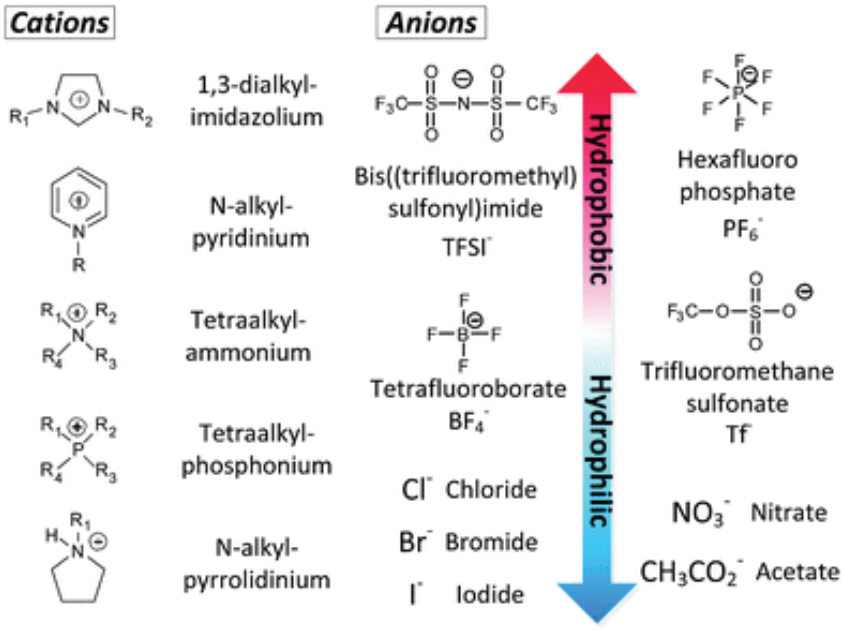

Figure 12: Examples of cations and anions used in the formation of ILs, together with changes in hydrophilic–hydrophobic properties associated with anion type [13].

ILs composed of ions, exhibit negligible vapor pressure, similar to solid salts. Unlike most organic solvents, ILs do not vaporize unless heated to the point of thermal decomposition, typically 473-573 K or more. As a result, IL-based cells lack the explosion or pressure risks of Li-ion cells using conventional electrolytes and it is considered to discard organic electrolytes with ILs system.

Furthermore, ILs have no flash point and due to this fact, they are consider as a non-flammable [2] (Table 2). Among all various ILs, studies have been focused in particular on imidazolium derivatives that have a relatively low viscosity and high ionic conductivity (Table 2) [14].

Table 2: Examples of viscosity (η), density (ρ), ionic conductivity (K) and electrochemical window (EW) of some ILs at ~293 K [15].

Ionic Liquid	η [cP]	ρ [g cm^{-3}]	κ [mS cm^{-1}]	EW[b] [V]
Aprotic				
[C_2mim][NTf_2]	34[1]	1.53[109]	8.8[1]	4.3
[C_4mim][NTf_2]	52[1]	1.44[109]	3.9[1]	4.8
[C_8mim][NTf_2]	74[41]	1.33[109]	–	5.0
[C_4dmim][NTf_2]	105[37]	1.42[109]	2.0[13]	5.2
[C_6mim][FAP]	74[56]	1.56[109]	1.3[56]	5.3
[C_4mpyrr][NTf_2]	89[37]	1.4[109]	2.2[2]	5.2
[C_4mim][OTf]	90[1]	1.3[1]	3.7[1]	4.9
[C_4mim][BF_4]	112[37]	1.21[72]	1.7[148]	4.7
[$N_{6.2.2.2}$][NTf_2]	167[55]	1.27[55]	0.67[45]	5.4
[C_4mim][NO_3]	266[72]	1.16[72]	–	3.7
[C_4mim][PF_6]	371[72]	1.37[72]	1.5[148]	4.7
[$P_{14.6.6.6}$][NTf_2]	450[149]	1.07[109]	–	5.0
[$P_{14.6.6.6}$][FAP]	464[109]	1.18[109]	–	5.6
[C_4mim]I	1110[67]	1.49[109]	–	2.1
[C_6mim]Cl	7453[56]	1.05[109]	–	3.2
Protic				
[DEA][AC]	336[29]	1.22[29]	0.14[29]	2.4
[DPA][[BF]	19[29]	0.97[29]	1.19[29]	2.7
[TEtA][Ac]	11[29]	0.96[29]	1.27[29]	3.4
[DEA][Cl]	305[29]	1.24[29]	0.86[29]	4.0
Distillable				
DIMCARB	77[33]	1.05[33]	1.7[33]	2.0
DIECARB	14[33]	0.91[33]	0.053[33]	2.1
MEETCARB	85[33]	0.98[33]	0.37[33]	1.9
MESACARB	70[33]	0.95[33]	0.18[33]	1.8
Organic				
Acetonitrile	0.34[150]	0.79[150]	7.6[150][a]	5.0[43][a]
Dichloromethane	0.44[150]	1.33[150]	–	3.5[43][a]
N,*N*-Dimethylformamide	0.92[150]	0.94[150]	4.07[150][a]	4.3[43][a]
Dimethylsulfoxide	1.99[150]	1.10[150]	2.7[150][a]	4.4[a]
Propylene carbonate	2.5[150]	1.21		4.7[43][a]

[a] organic solvents containing 0.1 M Bu_4NClO_4 at 295 K. [b] EW data in aprotic RTILs obtained at a 10 μm diameter Pt electrode,[53] data in protic[29] and "distillable"[33] RTILs obtained at a glassy carbon electrode.

The impact of viscosity of ILs on physicochemical properties in particular ionicity has been studied by various teams using different approaches, such as Walden plot, which illustrates qualitative features of ionicity in ILs [13]. By using the deviations from the reference line (0.01 mol.L^{-1} KCl/H_2O solution) in Walden plot, specific ILs have been classified as "good" or "poor" ionic liquids.(Figure 13) [16].

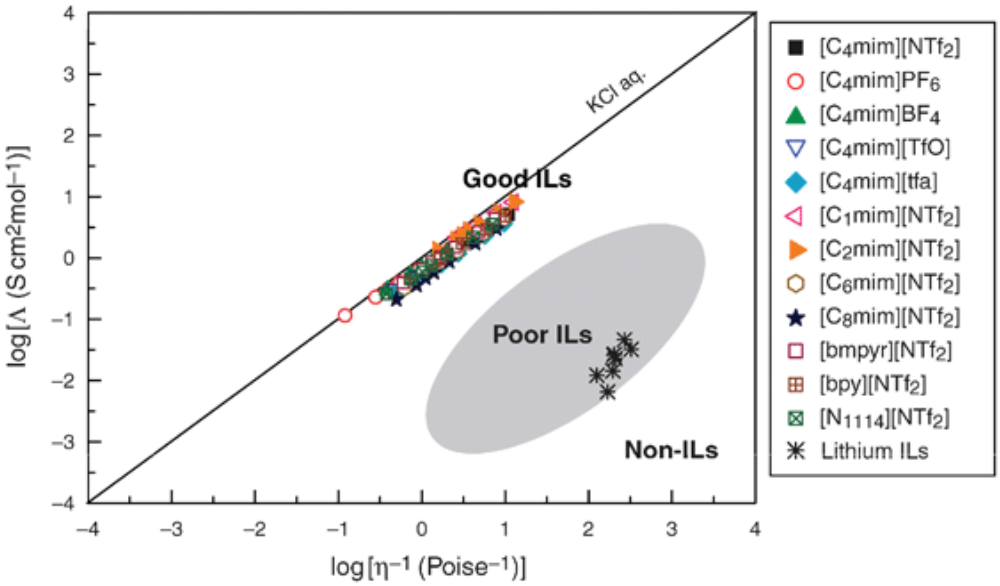

Figure 13: Walden plot of log(molar conductivity, Λ) against log(reciprocal viscosity η^{-1}), which includes the classification for ILs proposed by Angell et al. [16].

It can be observed that the data for the aprotic ILs, $[C_1C_nIm][NTf_2]$ lie slightly below the reference line, which can imply that their molar conductivity is lower than that expected, likely due to ion aggregation [17]. However they could be considered as "good ILs".

The interest in the use of ILs as battery electrolytes is based also on other properties like high conductivity, relatively high electrochemical stability and large electrochemical window (EW). (Table 2) [15, 18, 19].

Electrochemical window (EW) is one of the most important characteristics to be identified for solvents and electrolytes and it is calculated by subtracting the reduction potential (cathodic limit) from the oxidation potential (anodic limit).The development of EW for ILs is one of the main important innovations since this indicate enhancement in the cathodic limiting potential of the ILs. Usually, EW measurements are realized by linear sweep voltammetry (LSV) and cyclic voltammetry (CV). One of the main factors affecting EW is water content narrowing of EW limits at both cathodic and anodic limits: *e.g.* EW decreased when IL has been vacuum-dried > atmospheric > wet at 298 >318 K >338 K (Figure 14) [20]. In general, the presence 1-alkyl functionality in imidazolium RTILs affords larger EW [21].

The electrochemical stability of the Li^+ conducting electrolyte of above 4 V is necessary in practical application to Li-ion batteries. Imidazolium salts stability is above 4 V which is sufficient to be used as electrolytes in Li-ion batteries.

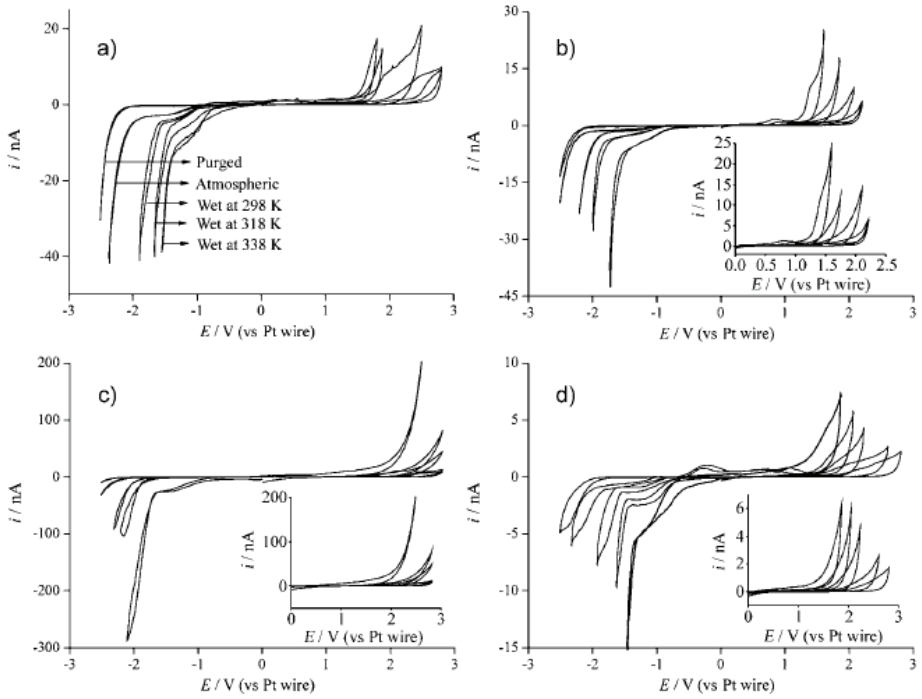

Figure 14: Effect of increasing water concentration on the electrochemical window of a) $[C_1C_2Im][NTf_2]$, b) $[C_1C_4Im][OTf]$, c) $[C_1C_4Im][BF_4]$, and d) $[C_1C_4Im][PF_6]$ as found under vacuum-dried, atmospheric, and wet conditions (at temperatures of 298, 318, and 338 K). Data are reported under conditions of cyclic voltammetry at a scan rate of 100 mVs^{-1} using a 10 mm diameter Pt micro disk electrode [20].

2.2 Electrolytes based on ionic liquids (ILs)

When a lithium salt LiX is dissolved in an IL, (as observed) there is formation of an electrolyte (LiX/IL). Classical solutions of electrolytes for Li-ion batteries are gained by dissolution of Li salts in molecular solvents. This kind of system consists of solvated ions, their charged or neutral combinations and solvent molecules. However, also liquid electrolytes only composed of salts may be used. Salt may be melted down, by providing to the system enough heat to counter balance the salt lattice energy [14]. The solubility of various inorganic Li salts was investigated in ILs. This electrolyte (IL/LiX), whatever is the concentration of lithium salt (C_{Li}), exhibits a higher viscosity and lower conductivity than the pure IL [14].

The binary system with common anion $[NTf_2]^-$ demonstrated the highest solubility among the usual Li-salt e.g. in $[C_1C_2Im][NTf_2]$, $LiNTf_2$ has a solubility of 0.4333±0.0035 in molar fraction of salt (corresponding to 0.3592±0.0033 in mass fraction) [23]. Rosol and al. determined the solubility of the lithium salt $LiClO_4$, LiSCN and $LiNTf_2$ in $[C_1C_2Im][NTf_2]$ by FTIR-ATR. In $[C_1C_2Im][NTf_2]$, the solubility of $LiNTf_2$ (0.4 $mol.L^{-1}$) and $LiClO_4$ (0.3 $mol.L^{-1}$) was reasonable, but it was poor solvent for $LiPF_6$ (0.1 $mol.L^{-1}$) [22].

The dissolution of $LiNTf_2$ is an exothermic process and the value of the dissolution enthalpy is 18.07±4.61 kJ/mol. As solution of $LiNTf_2$ in $[C_1C_4Im][NTf_2]$ share, the same anion, the addition of extra NTf_2 anions will not result in an enthalpy change in the system. Therefore, the high solvation energy should come from the solvation of Li^+ ion by multiple $[NTf_2]^-$ anions. These authors suggested that when Li^+ ion is solvated in the $[C_1C_4Im][NTf_2]$, forming an ion clusters with two to four NTf_2^- anions through strong interaction of Li^+ ion with the O and N atoms of the anion [24]. Experimental measurements performed by Raman spectroscopy [25], and ab-inito calculations [26] and molecular dynamics MD simulation [27] suggest that $Li[NTf_2]_2^-$ is the most probable species with a radius of 0.7 nm, and Li^+ is directly solvated by the oxygen atoms (Scheme 1). In the system $[C_1C_1C_2Im][Li][PF_6]$ when $LiPF_6$ molar ratios ranged from 0.3 to 0.5, the coordination number of $[PF_6]^-$ around $[Li]^+$ is about 4 and tends to increase with $LiPF_6$ concentration [28].

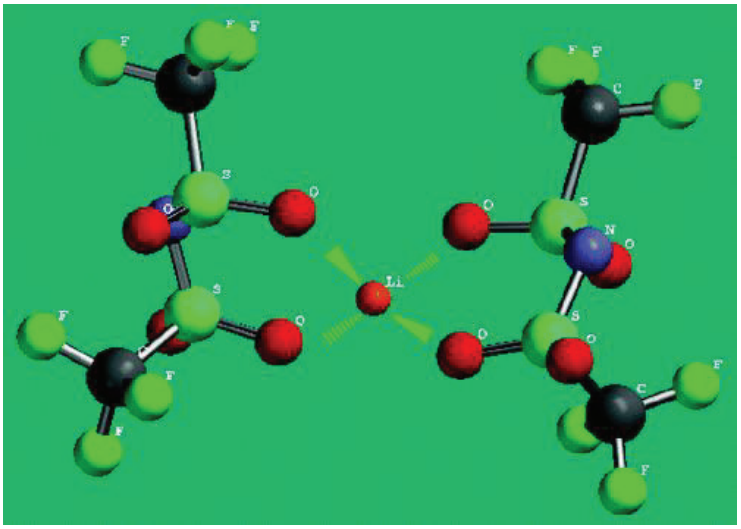

Scheme 1:. Structure of a Li^+ ion solvated with two NTF_2^- ions [24].

By MD simulations it was proved that Li^+ ion transport in $[Pyr_{1,1}][Li][NTf_2]$ and $[C_1C_1C_2Im][Li][PF_6]$ is heavily dependent on Li^+ ion coordination [27, 28]. This $[Li]^+$ transport in $[Pyr_{11}][Li][NTf_2]$ occurs mainly by exchange of $[NTf_2]^-$ (structure diffusion mechanism) and that was the minor contribution of Li^+ diffusion with the whole coordination shell (vehicular mechanism). Consequently, the importance of the stability of the first coordination sphere of Li^+ ion impacts the Li^+ diffusion [27].

In electrolyte $[C_1C_4Im][Li][NTf_2]$ and $[C_1C_1C_4Im][Li][NTf_2]$ the diffusion coefficients of the ions have been measured by pulsed gradient spin echo (PGSE) NMR technique. The diffusion of $[Li]^+$ ion was increased by the dispersion of silica into $[Im][Li][NTf_2]$. Although the viscosity of the media

increased. The authors speculated that the silica species coordinate $[Li]^+$ and release solvating $[NTf_2]^-$ anions [29].

2.3 Literature view of lithium ion batteries based on imidazolium ionic liquids as electrolytes

In this part, through some examples of the literature, we have attempted to highlight the key factors improving the cycling performance of Li-ion cell using imidazolium based IL as solvent of the electrolyte.

Initial investigations in Li-ion batteries with ILs involved in the composition of the electrolyte have been carried by Carlin and Osteryoung 1997 [30]. Currently, many laboratories worldwide are engaged in the investigation of ILs with the aim of establishing their effective potential as Li-ion battery electrolytes [31]. Table 3 summarizes some tested systems based on imidazolium-ILs electrolytes.

Table 3: Summary of tested systems (electrolyte formulation and materials intercalation).

Electrolyte	System	Reference
$C_1C_2ImNTf_2$ + 1.0 mol.L^{-1} $LiNTf_2$	$Li/LiCoO_2$ $Cgr/LiCoO_2$	Garcia 2004 [33], Holzapfel 2004 [34], Holzapfel 2005 [35], Seki 2006 [36]
$C_1C_3ImNTf_2$ + 1.0 mol.L^{-1} $LiNTf_2$	$Li/LiFePO_4$	Kim 2010 [37]
$C_1C_nImNTf_2$ (n=2 and 4) + 1.0 mol.L^{-1} $LiBF_4$	$MoSe/LiNi_{0.5}Mn_{1.5}O_4$	Markevich 2006 [38]
$C_1C_4ImBF_4$ + 1.6 mol.L^{-1} $LiBF_4$	$LiFePO_4/Li_4Ti5O_{12}$	Giroud 2009 [39]

A lithium battery based on LCO and LTO as electrode with $[C_1C_2Im][Li][NTf_2]$ or $[C_1C_2Im][Li][BF_4]$ as electrolyte has been tested at 298 K (Figure 15). The electrolyte $[C_1C_2Im][Li][NTf_2]$ shows good cycling stability at 1C rate. After 200 cycles, the LTO /$[C_1C_2Im][Li][NTf_2]$ /LCO system still delivers up to 106 mAh/g. In this sense, the $[NTf_2]$ based IL outperforms the electrolyte $[C_1C_2Im][Li][BF_4]$ and the organic electrolytes in terms of cycling performance (Figure 15) [33].

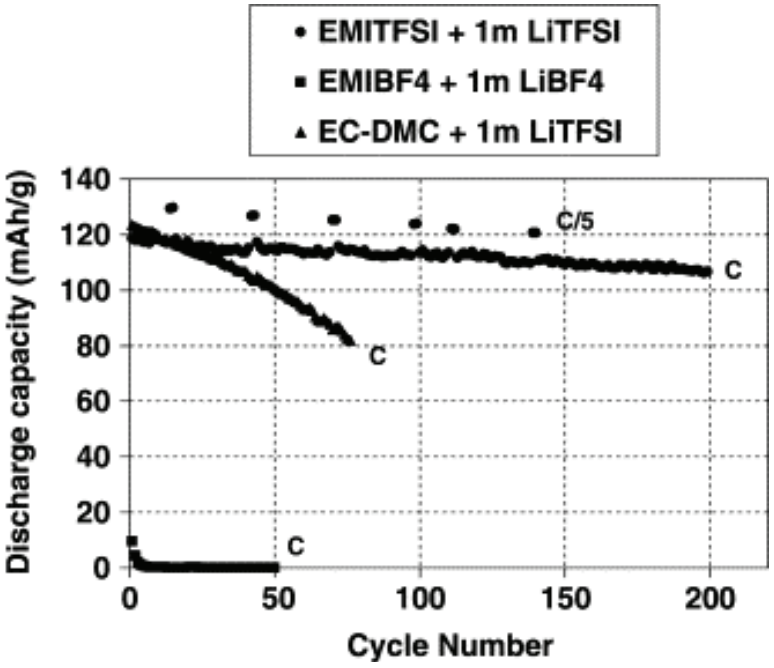

Figure 15: Capacity stability with cycle number obtained at a rate of 1C at 298 K; comparison between the different electrolytes: $[C_1C_2Im][NTf_2]$ at 1 mol.L^{-1} $LiNTf_2$, $[C_1C_4Im][BF_4]$ at 1 mol.L^{-1} $LiBF_4$ and 1 mol.L^{-1} $LiNTf_2$ EC/DMC [33].

Due to the poor cathodic stability of imidazolium-based cations easily reduced by electrochemical deprotonation around 1.5 V vs. Li [32] (Scheme 2).

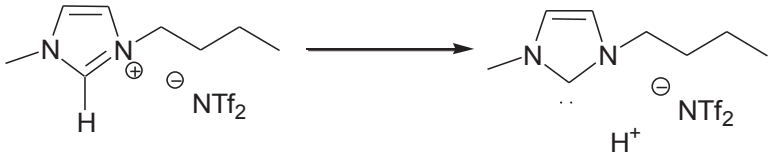

Scheme 2: Electrochemical deprotonation.

Several adjustments in the nature of the electrode, the use of additives and finally in the modification of the imidazolium ring have reported in order to prevent their cathodic degradation on commonly-used anode materials such as Cgr and Li-metal.

2.3.1 Electrodes

The $LiNi_{0.5}Mn_{1.5}O_4$ spinel working with $[C_1C_4Im][Li][BF_4]$ at 1 mol.L^{-1} solution showed reversible charging/decharging characteristic with a high 4.8V potential versus Li/Li$^+$ couple [35]. This is related to the oxidation of Ni^{2+} to Ni^{4+} with Mo_6S_8 Chevrel phase as an anode instead of Li.

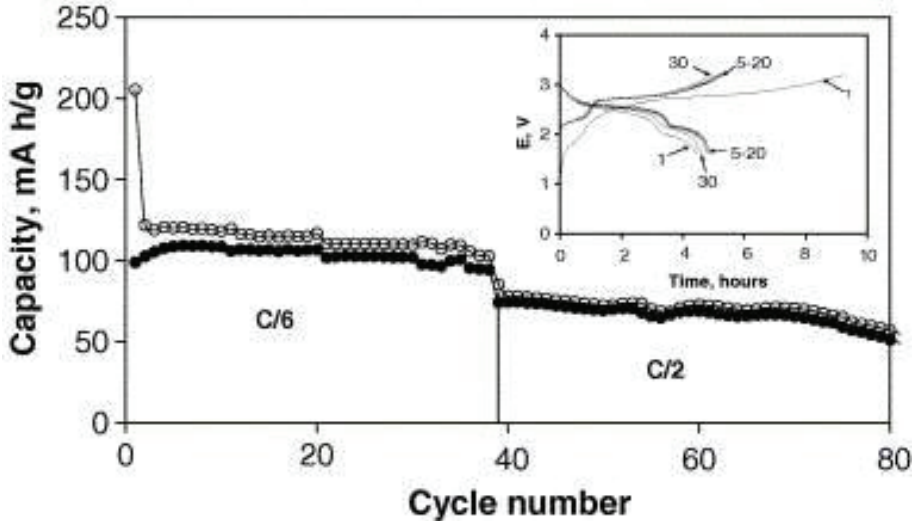

Figure 16: Galvanostatic cycling of $LiNi_{0.5}Mn_{1.5}O_4/Mo_6S_8$ cells at 303 K in 1 mol.L^{-1} $LiBF_4/[C_1C_2Im][BF_4]$ with C/6 and C/2 rates [38].

A stable cycling performance of a $LiNi_{0.5}Mn_{1.5}O_4/Mo_6S_8$ cell at different cycling rates could be obtained (Figure 16), with the charge–discharge potential curves appearing in the insert. The two plateaus on the potential profile are related to the two stages of Mo_6S_8 Chevrel phase lithiation.

Different electrodes, generally under half cell devices have been tested with the electrolyte IL-LiX. One of the first early reports describes a successful $Li/LiMn_2O_4$ cell with $[C_1C_2Im][Li][BF_4]$ or $[C_1C_4Im][Li][BF_4]$ [40]. With Li/LCO and Li/ $LiMn_2O_4$ cells with imidazolium-based ILs mixed with $LiNTf_2$ discharge capacities around 135-110 mAh/g and ~100 mAh/g, were obtained at 303 K respectively [38]. An initial discharge capacity of 152.6 mAh/g was produced with the Li/LFP system with $[C_1C_1C_nIm][Li][NTf_2]$- vinylene carbonate (VC), at temperature 298 K [41].

On ILs based on trialkylimidazolium cation with one or two ether groups and $LiNTf_2$ anion in the Li/LFP systems had a capacity ~128 mAh/g at 1C rate and 108 mAh/g at 2.5C rate [42].

Ishikawa at al focused their studies on the problem of irreversible cationic intercalation into graphene interlayers at ca. 0.5 V vs Li/Li^+ and found out that ionic liquids containing FSI with the Li cation can prevent such an irreversible reaction and provide reversible Li intercalation into graphite interlayers. Electrolyte based on $[C_1C_2Im][Li][FSI]$ with 0.8 mol.L^{-1} $LiNTf_2$ in the Li/C_{gr} cells, gives value of the reversible capacity approximately 360 mAh/g during 30 cycles at 0.2C rate [43].

2.3.2 Additive

Graphitized carbon materials have difficulty in obtaining the practical $[Li]^+$ intercalation/deintercalation capacity in ILs without additives. Side reactions, such as cation

intercalation leading to exfoliation of the graphite layer and ILs decomposition occur during the first reduction. This reaction becomes a source of extremely large irreversible capacity and poor properties [44].

Holzapfel et al presented results of standard graphite electrodes in electrolyte based on $[C_1C_1C_2Im][NTf_2]$ with VC content [18]. This IL shown reversibly permit lithium intercalation into standard graphite when vinylene carbonate is used in small amounts as additive. The best performance was obtained when 5% vol of VC was added to a 1.0 $mol.L^{-1}$ solution of $LiPF_6$ in $[C_1C_1C_2Im][NTf_2]$ (Figure 17).

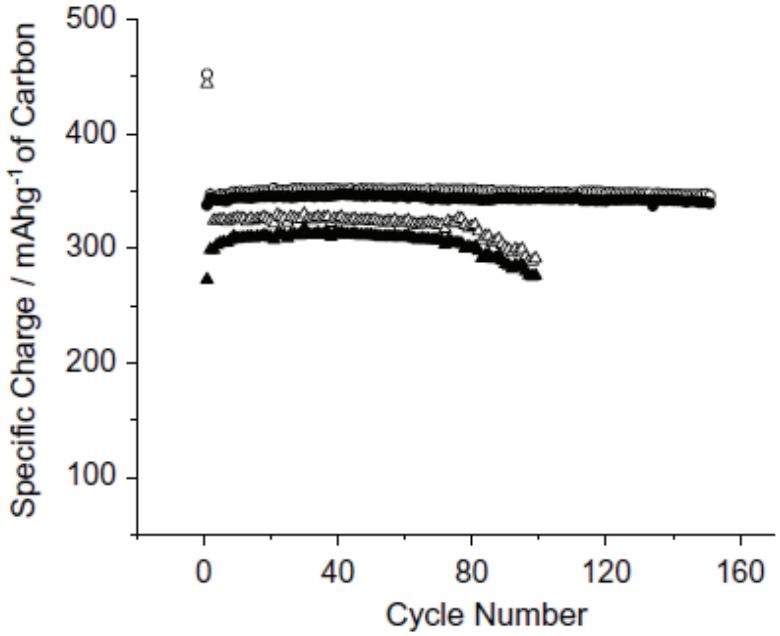

Figure 17: Electrochemical cycling of SFG44 graphite in $[C_1C_1C_2Im][NTf_2]$, 1 $mol.L^{-1}$ $LiPF_6$ and containing as additive 2% or 5% of vinylene carbonate [18].

The cycling behavior of the graphite electrode is analogous to the one of a graphite electrode in a standard electrolyte based on organic carbonates with respect to the reversible charge capacity and very low fading [18].

Yan and et al studied various $[C_1C_1C_nIm][Li][NTf_2]$ ionic liquids; prepared by changing carbon chain lengths and configuration of the alkyl group; and their electrochemical properties and compatibility with Li/LFP battery electrodes. Addition of VC improves the compatibility of electrolytes towards Li-anode and LFP cathode, and enhanced the formation of solid electrolyte interface to protect Li-anode from corrosion (Figure 18) [41].

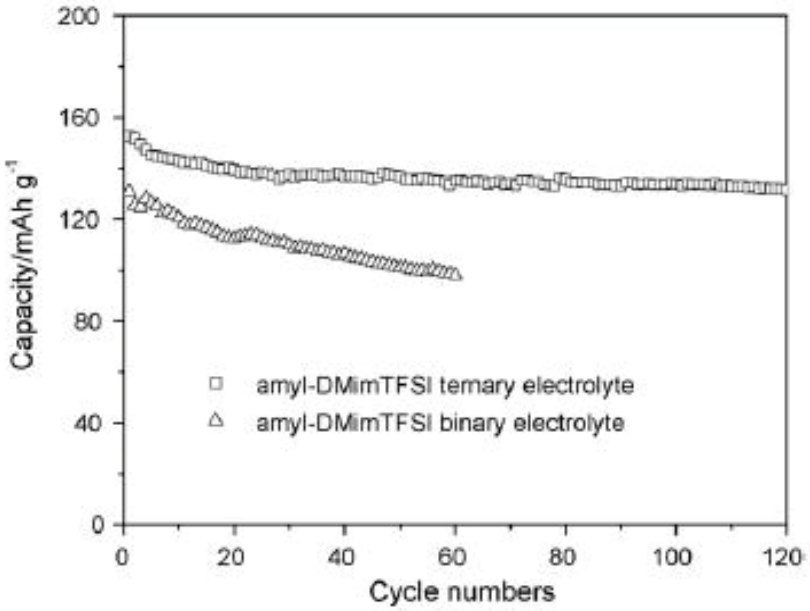

Figure 18: Cycle-life performance for Li/electrolytes/LFP cell with $C_1C_1C_5ImNTf_2$ binary electrolyte [0.2 $mol.L^{-1}$ solution of $LiNTf_2$ in the IL] and ternary electrolyte [addition of 5 wt% VC to the binary electrolyte] at RT [41].

Battery with the electrolyte-based on $[C_1C_1C_5Im][NTf_2]$ shows best charge/discharge capacity and reversibility due to relatively high conductivity and low viscosity, its initial discharge capacity is about 152.6 mAh/g, which the value is near to theoretical specific capacity (170 mAh/g). These results clearly indicates this type of ILs have fine application prospect for Li-ion batteries as highly safety electrolytes in the future [41].

With Li/LFP cells with different electrolytes $[C_1C_4Im][BF_4]$/γ-BL (γ-BL = γ-butyrolactone), the effect of VC addition was even more significant for the cyclic performance. The initial discharge capacity of the cell with VC was 144 mAh/g. However, the initial reversible capacity (104 mAh/g) and columbic efficiency (76%) without VC became smaller. After 10 cycles, the discharge capacity of the cell containing VC electrolyte was 142 mAh/g, and higher than that of the electrolyte without VC (54 mAh/g). Moreover, the capacity loss of the cell containing VC was only 3.5% after 20 cycles (Figure 19).

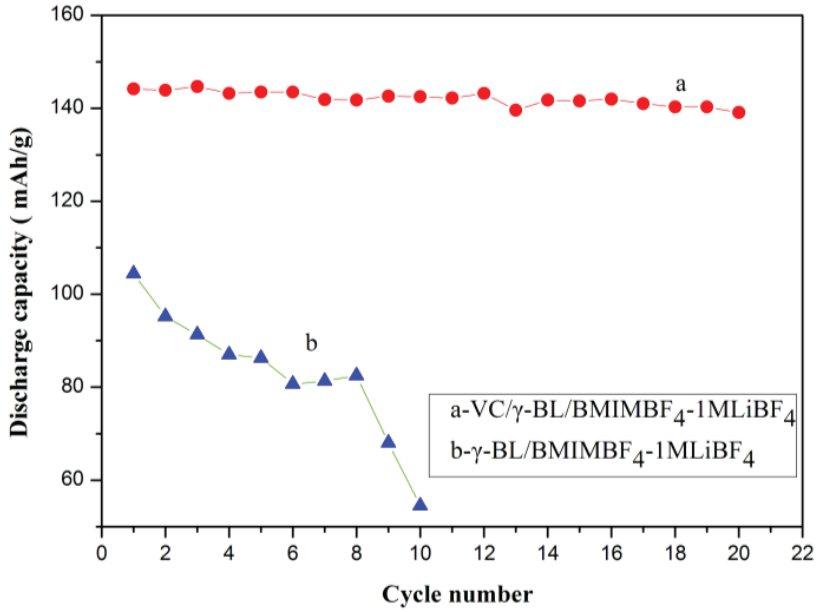

Figure 19: Cyclic performance of Li/LFP cells in different electrolytes [45].

The addition of VC (1.17 V vs. Li/Li^+) with a higher reductive potentials than the electrolyte solvents ($[C_1C_4Im][BF_4]$, 1.0 V vs. Li/Li^+), implies that the additive is preferably reduced to form an insoluble solid product, which subsequently is covered onto the surface of Li foil as a preliminary film to deactivate catalytic activity. Therefore, VC additive provides the better efficient SEI in the mixture electrolyte.

Cycle performance of Li/LFP cell with an IL-gel polymer electrolyte based on $[C_1C_3Im][Li][NTf_2]$ electrolyte incorporated in a polymer gel based poly(vinylidene fluoride-co-hexafluoropropylene) results in excellent charge/discharge capacity and good cycling stability with a conductivity above~10−4 Scm^{-1} at 0°C, a value proposed as a benchmark for large capacity batteries for EV's or HEV's [37].

Other researcher groups have modified the imidazolium ring by either modifying the nature of alkyl groups or replacing the acidic proton at *C2* position by the methyl donating group [36, 46].

2.3.3 Alkyl chain impact

Fundamental understanding of the effect of the alkyl groups on the microscopic ion dynamics is crucial in order of molecular design of ILs. This modifications cause change in the interactive forces, and the properties of the ILs are determined by the cumulative effect of the electrostatic interaction between the ionic species and the induction interactions between the ions, aggregates, and clusters. In this study, Tokuda et al. prepared a series of RTILs with a variety of alkyl chain lengths, e.g., ($[C_1C_nIm][NTf_2]$), where n = 1, 2, 4, 6, 8. For the ILs with relatively shorter hydrocarbon chains, the

transference number decreases almost linearly with increasing temperature. With an increase in the number of carbon atoms, viscosity initially decreases from $[C_1C_1Im][NTf_2]$ to a minimum at $[C_1C_2Im][NTf_2]$ and then increases with further increase in the alkyl chain length [47].

Seki et al investigated the molecular design of various ILs, in particular to endorse charge delocalization in the imidazolium cation ring and to control the three dimensional attack at the second position of the imidazolium cation ring [48]. Five types of ILs: $[C_1C_nIm][NTf_2]$, where n= 1, 2, 4, 6, 8 were investigated. The battery performance was exhibit using Li/LCO cells with IL mixed electrolyte. The initial discharge capacities for all electrolytes (except $[C_1C_1Im]^+$) cation were around 135 mAh/g. The cycle performance was improved with the extension of the alkyl chain length of the imidazolium cation ring, especially when the alkyl chain is longer than butyl (> 4 carbons) (Figure 20).

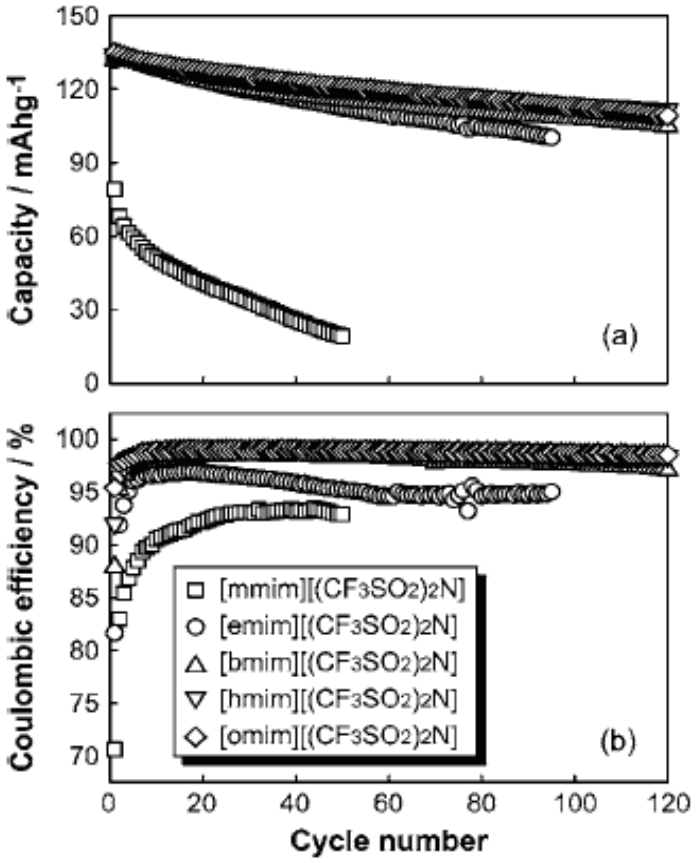

Figure 20: Cycle-life performances Li/LCO cells: a) discharge capacity and b) Coulombic efficiency [48].

In case of $[C_1C_6Im][NTf_2]$ and $[C_1C_8Im][NTf_2]$ cation IL electrolyte systems have high capacity retention (over 110 mAh/g) after 100 charge/discharge cycles. In case of calculated Columbic efficiency, it can be observed that it improved with increasing length of alkyl chain. These results

imply that the side reactions at electrode/electrolyte interfaces (probably reductive decomposition at Li-metal anode) decreased with the extension of the alkyl chain length due to formation of stable interfaces, for example solid electrolyte interface (SEI) [48].

2.3.4 Impact of C_2-H on cycling performance

Seki et al in 2007 also studied the relationship between the stable imidazolium-based IL at RT: $[C_1C_1C_3Im][NTf_2]$ (with introduced stable methyl group at the second position of the imidazolium cation) and the lithium salt ($LiNTf_2$) mixed electrolytes [46]. Electrochemical performance was investigated using Li/LCO cell system and the initial charge and discharge, 143 and 133 mAh/g, were obtained. After 50 cycles, the discharge capacities were at 120 mAh/g and decreased to 113 mAh/g after 100 cycles, high reversibility in all cases was observed (Figure 21).

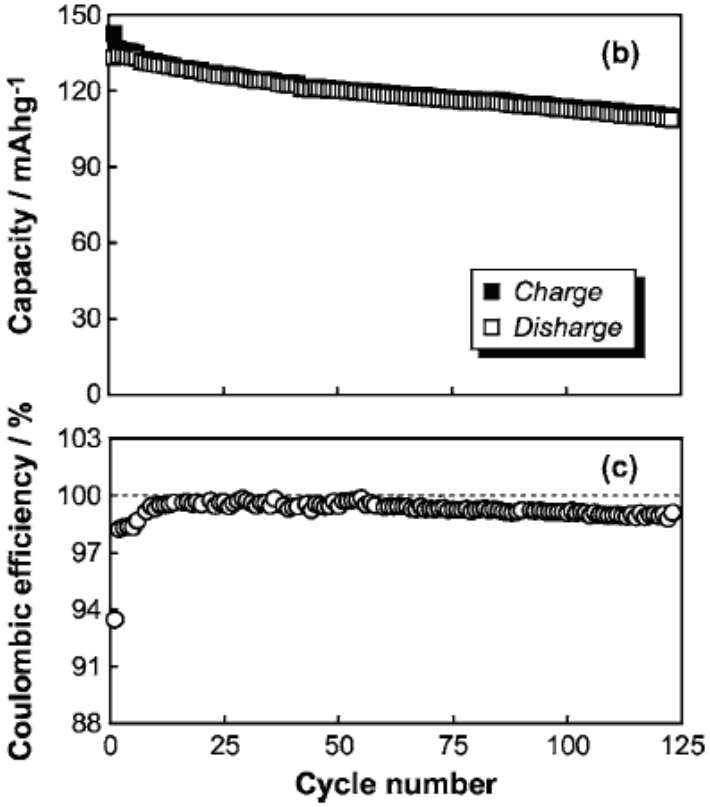

Figure 21: The charge-discharge profiles of the Li/LCO cell: b) the cycle number dependences of charge and discharge capacities, and c) coulombic efficiency of the cells (voltage region 3.0–4.2 V, current density 0.05 mA cm^{-2} = 1/8 C) at RT [46].

2.3.5 Impact of salt concentration on cycling performance

Figure 22 shows that, at lower discharge rates, the discharge capacity is close to the theoretical one, in case of all $LiNTf_2$ concentrations. For higher C rate, e.g. C_{LiX} = 0.3-0.5 $mol.kg^{-1}$, some local maximum can be observed, which suggests that, lower lithium concentration, can be not sufficient for

supplying of lithium ions from electrolyte at each electrode/electrolyte interfaces. However, with bigger concentration, the viscosity is higher and some low discharge capacities might be observed. Li/LCO cell with $[C_1C_1C_3Im][Li][NTf_2]$ electrolyte shows high charge-discharge reversibility for more than 100 cycles, which can imply that an optimal $LiNTf_2$ concentration exists [46].

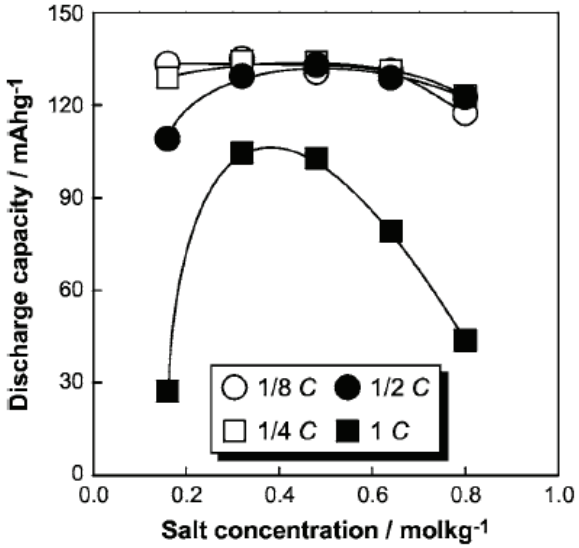

Figure 22: Relationships between the lithium salt concentration and the discharge capacities under various discharge rates (1/8 C, 1/4 C, 1/2 C, and 1 C) for Li/LCO cell at 303 K [46].

Continuation of this work, Seki published in 2012, $[C_1C_1C_3Im][Li][NTf_2]$ electrolyte with different salt concentration was investigated with $Li_{1.10}Al_{0.095}Mn_{1.805}O_4$ positive electrode vs Li metal. High discharge capacity (~ 100 mAh/g) and high capacity retention above concentration 0.32 mol kg^{-1} can be observed. Batteries showed a sufficient reversibility for more than 50 cycles, with the optimal concentration (0.32-0.64 mol kg^{-1}) (Figure 23) [49].

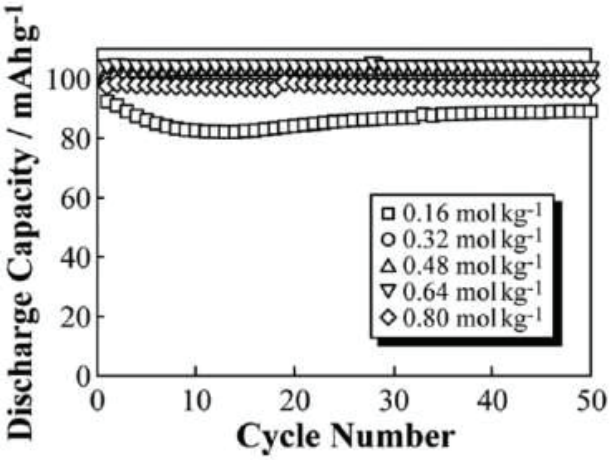

Figure 24: Cycle number dependences of discharge capacities of $[Li_{1.10}Al_{0\text{-}095}Mn_{1.805}O_4$ | $[C_1C_1C_3Im][Li][NTf_2]$ | Li-metal] cells with various lithium salt concentrations [49].

2.4 Conclusions

The results, are in part contradictory especially in defining the electrochemical stability of lithium conducting, with $[C_1C_nIm][Li][NTf_2]$ based electrolytes. Most commonly it is believed that these solutions have a poor cathodic stability limit associated with the tendency of imidazolium-based cations to be reduced by electrochemical deprotonation around 1.5V vs. Li. This apparently prevents the use of IL-based solutions with common low voltage anode materials, such as Li metal, Cgr or even LTO [31]. However some guideline appears, i) most of the results were reporting half Li-ion cell devices, ii) whatever the nature of electrode, addition of VC improves the performance of cycling; iii) When n>4 in $[C_1C_nIm][NTf_2]$ a higher capacity retention was observed. This has been related, but no prove, to a decrease of the side reactions at electrode/ electrolyte interfaces; iv) The substitution of $C_{2\text{-}H}$ by $C_{2\text{-}Me}$, a high reversibility was observed; v) An optimal for the concentration in $LiNTf_2$ of (0.32-0.64 mol kg^{-1}) in the electrolyte has been found.

2.5 CEA results of lithium ion batteries based on ionic liquids as electrolytes

In 2005 CEA-LITEN has developed through Dr. Giroud-PhD a systematic screening of commercial available ILs and lithium salts in order to use their mixture as electrolyte in Cgr/LFP based Li-ion technology.

Firstly, reference electrolyte [19], solutions composed of $C_1C_4ImBF_4$ with $LiBF_4$ as lithium salt in the following contents: C_{Li}= 0.5; 1; 1.2; 1.4 1.6 mol.L^{-1} have been analysed through thermal, physic-chemical and electrochemical characterization [50].

Cycling ability tests $[C_1C_4Im][Li][BF_4]$ (C_{LiBF4} = 0.5; 1; 1.2; 1.4 1.6 mol.L^{-1}) with Li/LTO have been carried out in order to assess the lithium insertion and de-insertion over 20 cycles. The best performance has been obtained with C_{Li}= 1.6 mol.L^{-1} (Figure 24).

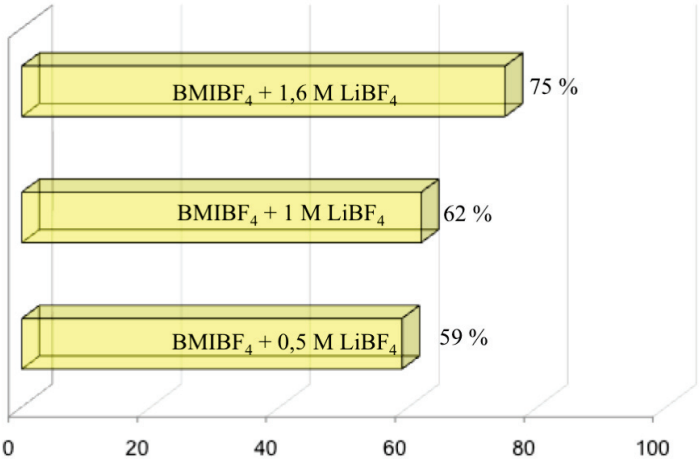

Figure 24: recovered capacity (%).

The cycling capacities determined by galvanostatic chronopotentiometry during 20 cycles at C/20 are reported in Figure 25. It is observed that the charge and discharge capacity are very close. The cycling, capacity reported to the mass of LFP active material and current rates obtained at 298 K. The average potentials for insertion and de-insertion equal to 1.75 V and 2 V independently of the cycle number. Moreover the polarisation of 250 mV shows that $[C_1C_4Im][Li][BF_4]$ (1.6 mol.L^{-1}) was more resistive than conventional organic electrolytes.

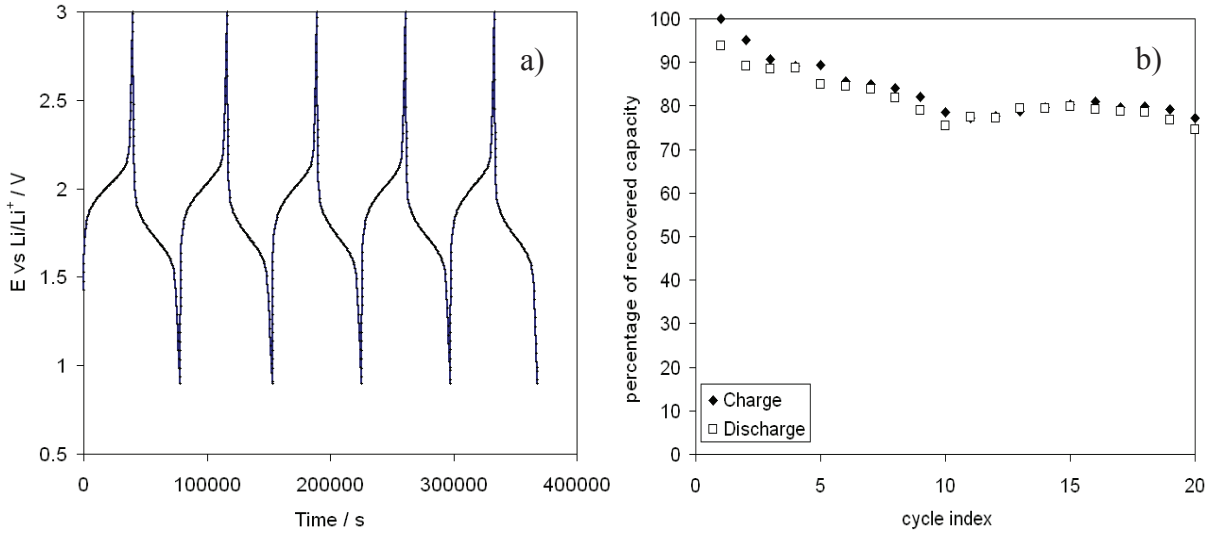

Figure 25: a) voltage time profile and b) recovered capacity versus cycle number at 293 K.

Then, the influence of the nature of the IL (cation and anion) and of lithium salts on physico-chemical and electrochemical characterization and cycling performances has been carried out (Figure 26).

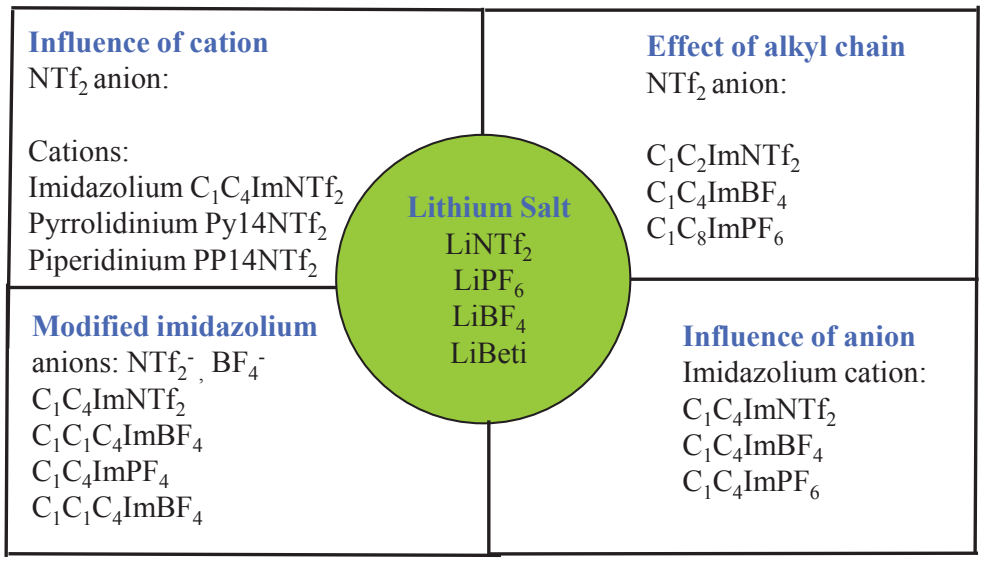

Figure 26: schematic diagram of ILs and lithium salts used to study the effect of structure and salt nature.

Due to their higher thermal and electrochemical stability (EW ~ 6 V), whatever is the anion, the pyrrolidinium and imidazolium based ILs have been selected. The anion NTf_2 has been preferred to BF_4 due to its better stability toward oxidation. The modification of the pyrrolidinium imidazolium cycle {length of the N- alkyl (Py_{1n} and C_1C_nIm n: 2, 3, 4 and 6) and methyl substitution of imidazolium C_2 carbon} gave rise to a complex and opposite variation of their physico-chemical, transport and electrochemical properties. [51] Since ILs based on [Py_{13}] and [C_1C_nIm] cations have accurate physic-chemical, transport and electrochemical properties, they have been retained. Finally two lithium salts $LiPF_6$ and $LiNTf_2$ have been retained.

At this step, the compatibility of reference ([C_1C_4Im][BF_4]) and pre-selected electrolytes ([Py_{13}][NTf_2] and [C_1C_nIm][NTf_2]) have been tested in cycling to determine if Li^+ insertion/ desinsertion mechanism occurs into Cgr and LFP electrodes (Figure 27).

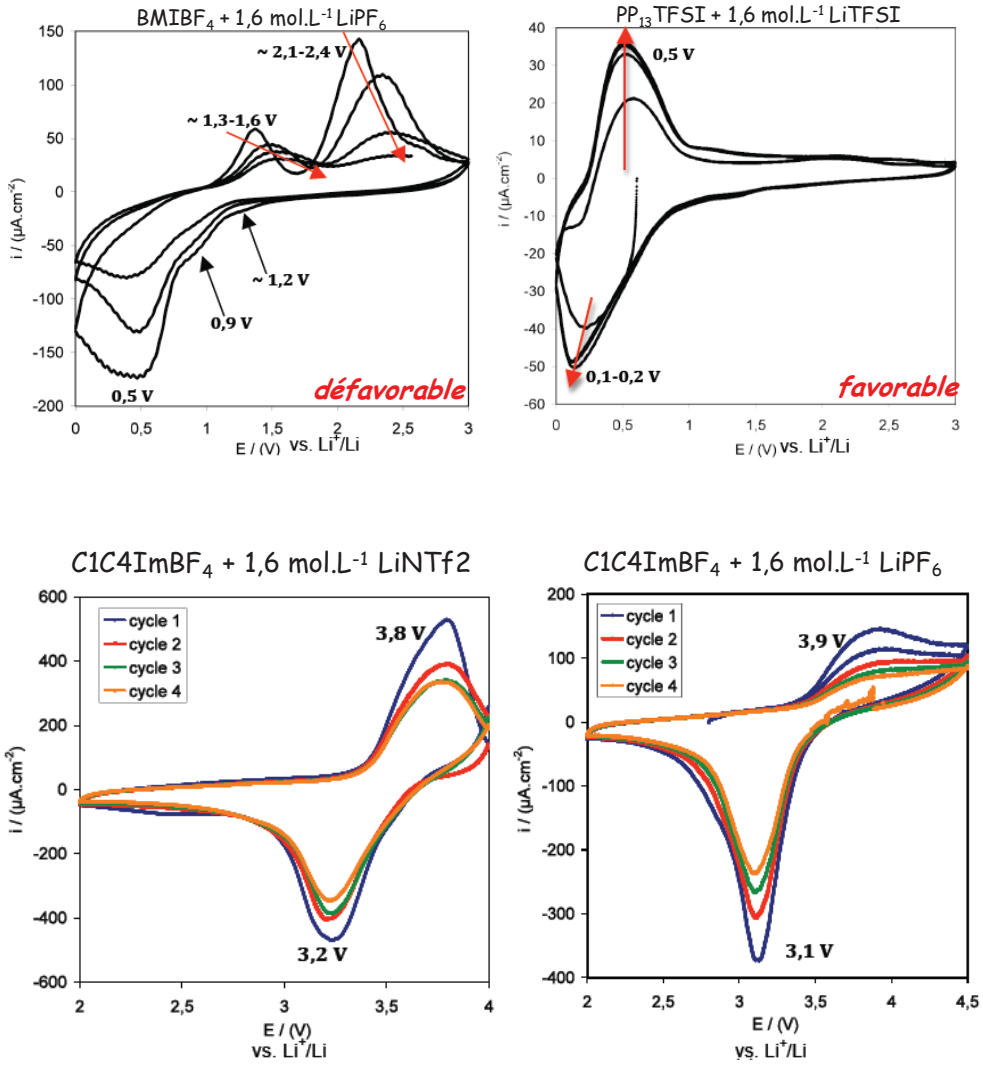

Figure 27: Insertion mechanism: a) Cgr Electrode b) Insertion mechanism into LFP Electrode.

The different attempts are sum up into Table 4.

Table 4: electrolytes/electrodes compatible.

	Cgr	$LiFePO_4$
$C_1C_4ImBF_4$ + 1,6 M $LiPF_6$	NO	NO
$C_1C_4ImBF_4$ + 1,6 M $LiNTf_2$	NO	Yes
C_1C_4Im TFSI + 1,6 M $LiPF_6$	NO	NO
C_1C_4Im TFSI + 1,6 M $LiNTf_2$	NO	Yes
C_1C_6Im TFSI + 1,6 M $LiNTf_2$	Yes	Yes
PP_{13}TFSI + 1,6 M $LiNTf_2$	Yes	Yes

In conclusion two electrolytes are compatible with Cgr and LFP electrodes; $[C_1C_6Im][Li][NTf_2]$ at and $[PP_{13}][NTf_2]$ at 1.6 mol.L^{-1}. A prototype Li-ion battery (pouch cell) has been manufactured with the last one [52].

Starting from these literature view and previous CEA results, and taking into account that our work is focused onto imidazolium based ILs, we have firstly studied the cyclic performance of $[C_1C_6Im][Li][NTf_2]$ at 1.6 mol.L^{-1} in different experimental conditions (temperature 298 and 333 K, concentration of lithium salt, and C_{LiNTf2} = 0.5; 1;1.6 mol.L^{-1}, with and without any organic additives). Then, C_2-substituted and/or functionalized imidazolium cations have been used as solvent of $LiNTf_2$. Each time the performances of these electrolytes were evaluated in coin cells through cycling tests with Cgr or LTO as negative electrodes and LFP as positive electrode.

III Refrences

1 BATTERY BASICS: A primer for battery technology, CECOM LRC . *Power Sources Team*.

2 J.-M. Tarascon, M. Armand, *Nature*, **414** (2001) 359.

3 D. Aurbach, E. Zinigrad, Y. Cohen, H. Teller, *Solid State Ionics*, **148** (2002) 405– 416.

4 M. Winter, J. O. Besenhard, M. E. Spahr, P. Novak, *Adv. Mater.*, **10** (1998) 725.

5 J.-K. Park, *WILEY-VCH*, (2011).

6 B. C. Melot, J.-M. Tarascon, *Acc. Chem. Res*, **46** (2012) 1226–1238.

7 A.S. Andersson, B. Kalska, P. Eyob, D. Aernout, L. Haggstrom, J.O. Thomas, *Solid State Ionics,* **140 (**2001) 63–70.

8 D.D. MacNeil, Z. Lub, Z. Chen, J.R. Dahn, *J. Power Sources*, **108** (2002) 8–14.

9 M. Takahashi, S. Tobishima, K. Takei, Y. Sakurai, *Solid State Ionics*, **148** (2002) 283– 289]

10 B. L. Ellis, K.T. Lee, L. F. Nazar, *Chem. Mater*. **22** (2010) 691–714.

11 Q. Wang, P. Ping, X. Zhao, G. Chub, J. Sun, C. Chen, *J. Power Sources*, **208** (2012) 210–224.

12 P. Wasserscheid, T. Welton, Ionic liquids in synthesis, *WILEY-VCH*, (2003).

13 Y-S. Ye, J. Rick, B.-J. Hwang, *J. Mater. Chem. A*, **1** (2013) 2719.

14 T. Sato, T. Maruo, S. Marukane, K. Takagi, *J. Power Sources*, **138** (2004) 253–261.

15 L. E. Barrosse-Antle, A. M. Bond, R. G. Compton, A. M. O'Mahony, E. I. Rogers, D. S. Silvester, *J.Chem. Asian.*, **5** (2010) 202 – 230.

16 W. Xu, E. I. Cooper, C. A. Angell, *J. Phys. Chem. B,* **107** (2003) 6170-6178.

17 K. Ueno, H. Tokuda, M. Watanabe, *Phys. Chem. Chem. Phys.,* **12** (2010) 1649–1658.

18 M. Holzapfel, C. Jost, A. Prodi-Schwab, F. Krumeich, A. Wursig, H. Buqa, P. Novak, *Carbon*, **43** (2005) 1488–1498.

19 M. Armand, F. Endres, D. R. MacFarlane, H. Ohno, B. Scrosati, *Nature Mat*, **8** (2009) 621.

20 A. M. O'Mahony, D. S. Silvester, L. Aldous, C. Hardacre, R. G. Compton, *J. Chem. Eng. Data* **53 (**2008) 2884–2891.

21 R. K. Donato, M. V. Migliorini, M. A. Benvegnú, J. Dupont, R. S. Gonçalves, H. S. Schrekker, *Solid State Electrochem*, **11** (2007) 1481–1487.

22 Z. P. Rosol, N. J. German, S. M. Gross, *Green Chem.*, **11** (2009) 1453–1457.

23 A. B. Pereiro , J.M.M. Araujo, F.S. Oliveira, J.M.S.S. Esperanca, J.N. Canongia Lopes, I.M. Marrucho, L.P.N. Rebel, *J. Chem. Thermodynamics*, **55** (2012) 29–36.

24 A. Andriola, K. Singh, J. Lewis, L. Yu, *J. Phys. Chem. B*, **114** (2010) 11709–11714.

25 L. J. Hardwick, M. Holzapfel, A. Wokaun, P. Novak*, J. Raman Spectrosc*., **38** (2007) 110–112.

26 S. Tsuzuki, K. Hayamizu, S. Seki, Y. Ohno, Y. Kobayashi, H. Miyashiro, *J. Phys. Chem. B,* **112** (2008) 9914–9920.

27 O. Borodin, G. D. Smith,W. Henderson, *J. Phys. Chem. B,***110** (2006) 16879-16886.

28 S. Niu, Z. Cao, S. Li, and T. Yan *J. Phys. Chem. B* **114** (2010) 877–881.

29 A. Borner, Z. Li, D. A. Levin, *J. Chem. Phys*., **136** (2012) 124507.

30 J. Fuller, R. T. Carlin and R. A. Osteryoung *, J. Electrochem. Soc.* **144** (1997) 3881-3886.

31 B. Scrosati, J. Garche, *J. Power. Sources* (2010) **195**, 2419–2430.

32 P. Hapiot and C. Lagrost, *Chem. Rev*., **108** (2008) 2238-2264.

33 B. Garcia, S. Lavallee, G. Perron, C. Michot, M. Armand, *Electrochimica Acta,* **49** (2004) 4583–4588.

34 M. Holzapfel, C. Jost, P. Novak, *Chem . Commun.*, (2004) 2098.

35 H. Srour**,** H. Rouault, C. Santini, *J. Electrochem Soc*, **160**, (2013) 66-69.

36 S. Seki, Y. Kobayashi, H. Miyashiro, Y. Ohno, A. Usami, Y. Mita, N. Kihira, M. Watanabe, N. Terada, *J. Phys. Chem. B*, **110** (2006) 10229.

37 J.-K. Kim A. Matic, J.-H. Ahn, P. Jacobsson *J. Power Sources* **195** (2010) 7639–7643.

38 E. Markevich, V. Baranchugov, D. Aurbach, *Electrochem Commun*, **8** (2006) 1331.

39 N. Giroud, H. Rouault, E. Chainet, J.-C. Poignet, *ECS Trans***, 16 (35)** (2009) 75-88.

40 T. Tsuda, C. L. Hussey, *Electrochem Soc Interface*, **16** (2007) 42-49.

41 C. Yan, L. Zaijun, Z. Hailang, F. Yinjun, F.Xu, L. Junkang*, Electrochimica Acta.* **55** (2010) 4728–4733.

42 Y. Jin, S. Fang, M. Chai, L. Yang, K. Tachibana, S. Hirano*, J. Power Sources*, **226** (2013) 210-218.

43 M. Ishikawa, T. Sugimoto, M. Kikuta, E. Ishiko, M. Kono, *J. Power Sources*, **162** (2006) 658–662.

44 H. Sakaebe, H. Matsumoto, K. Tatsumi, *Electrochimica Acta*, **53** (2007) 1048–1054.

45 H. Wang, S. Liu, K. Huang, , X. Yin, Y. Liu, S. Peng Int. *J. Electrochem. Sci*., **7** (2012) 1688 – 1698.

46 S. Seki, Y. Ohno, Y. Kobayashi, H. Miyashiro et al, *J. Electrochem Soc*, **154** (2007) A173-A177.

47 H. Tokuda, K. Hayamizu, K. Ishii, A. B. Hasan Susan, M. Watanabe *J. Phys. Chem. B,* **109** (2005)**,** 6103-6110.

48 S. Seki, Y. Mita, H. Tokuda et al, *Electrochem. Solid-State Lett*, **10** (2007) A237-A240.

49 S. Seki, Y. Ohno, Y. Mita, N. Serizawa, K. Takei, H. Miyashiro, *ECS Electrochem Letters,* **1** (2012) A77-A79.

50 Giroud, N., H. Rouault, E. Chainet, J.-C. Poignet, *ECS Trans*. **35** (2009) 75-88.

51 Giroud, N., in, Electrolytes liquides ioniques pour accumulateurs lithium-ion, PhD, *Institut Polytechnique de Grenoble*, Grenoble, (2008).

52 Giroud, N., E. Chainet, H. Rouault, in, Ionic liquids containing electolyte for secondary lithium battery Commissariat à l'Energie Atomique, *Pat. WO* (2010) *10023185*.

IV. Results and discussion

A. Cycling performance of $[C_1C_6Im][Li][NTf_2]$ coupled with Cgr and LFP electordes

B. Li-ion cell based on Cgr/LFP with Im-$LiNTF_2$ electrolyte

C. Battery performance: compatibility of $[C_1C_nIm][NTf_2]$ and $[C_1C_1C_nIm][NTf_2]$ (n=4,6) coupled with LTO/$LiFePO_4$

D. Effect of Lithium Salts on the Transport and Electrochemical Properties of Nitrile-Functionalized Imidazolium-based Ionic Liquids.

IV Results and discusion

In the continuity of the CEA results, we have firstly studied the cyclic performance of $[C_1C_6ImNTf_2][Li][NTf_2]$, at 298 K, with a concentration of lithium salt, C_{LiNTf2} = 1.6 mol.L^{-1}, with and without vinylene carbonate (VC). In this chapter, the electrolyte $[C_1C_6Im][NTf_2]/LiNTf_2$ has been referred as to $[C_1C_6Im][Li][NTf_2]$. The electrolytes have been evaluated in full device coin cells with Cgr or LTO as negative electrodes and LFP as positive electrode.

A. Cycling performance of $[C_1C_6Im][Li][NTf_2]$ coupled with Cgr and LFP

A1 Cyclic voltammetry on graphite electrode

Figure A1 shows the cyclic voltammograms (CV) of Cgr in the $[C_1C_6Im][Li][NTf_2]$ with C_{LiNTf2} = 1.6 mol.L^{-1}, without (a) and with (b) VC co-additive (5% in vol.). The voltammograms were obtained between 0 and 3 V vs. Li/Li$^+$ at a scan rate of 100µV.s^{-1}.

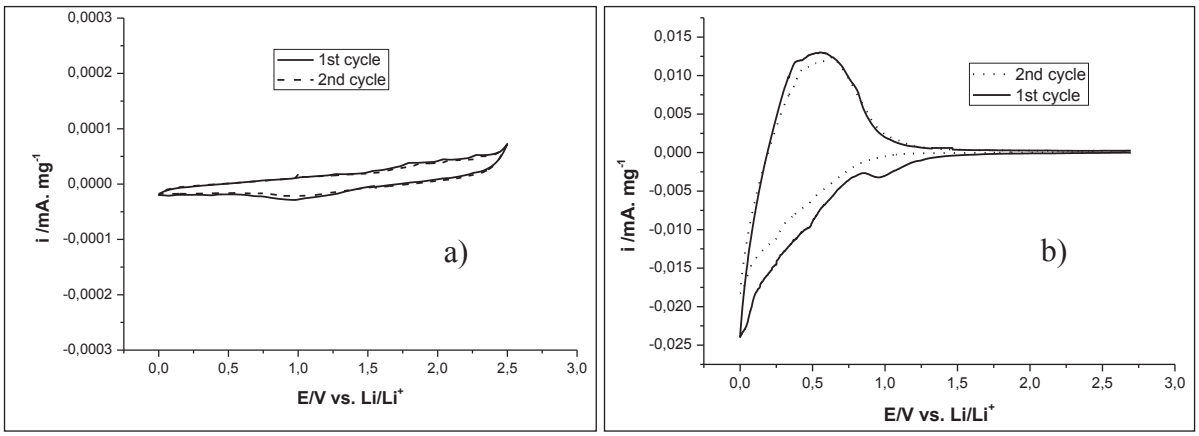

Figure A1: Cyclic voltammograms (first 2 cycles) of Cgr composite electrode in $[C_1C_6Im][Li][NTf_2]$ with C_{LiNTf2} = 1.6 mol.L^{-1} a) without VC additive b) with 5%vol. of VC additive.

As shown in figure A1a, the absence of VC additive, the graphite electrode displayed flat cyclic voltammogram with very low current densities (typically less than 10µA.cm^{-2}) showing no lithium insertion /de-insertion peaks. In the presence of VC, the system exhibits anodic and cathodic peaks respectively between 0.2 and 0.6 V vs Li$^+$/Li, (Figure A1b). These observations suggest that the insertion/de-insertion of lithium cations into the Cgr structure is made possible by the presence of VC additive, even if the mechanism remains low.

Without VC additive, the graphite surface wetted by $[C_1C_6Im][Li][NTf_2]$ is not compatible to sustain reversible lithium insertion/deinsertion [1-3]. The VC agent induces the passivation of the graphite based electrode by forming a Solid Electrolyte Interface (SEI) favouring the reversible lithium insertion/de-insertion [4,5]. However, the electrode passivation by VC additive in the imidazolium

based electrolyte may appear not as efficient as in the organic electrolyte, due to the low kinetics mechanism of lithium insertion/de-insertion demonstrated by the broad peaks with low current densities observed on the cyclic voltammogram.

Nevertheless, VC induces favourable passivation of the Cgr surface allowing reversible lithium insertion/de-insertion it was added as additive to the ionic liquid electrolyte for the cycling tests shown in the following part.

A2 Galvanostatic measurements on Graphite/$LiFePO_4$ cells

The electrochemical performances of the negative Cgr and positive LFP composite electrodes were tested at 298 K in full cell lithium ion configurations with $[C_1C_6Im][Li][NTf_2]$ with C_{LiNTf2} = 1.6 mol.L^{-1} electrolyte and at different ratio of VC (0, 2 and 5%vol) as the electrolyte additive.

Table A1: Charge-discharge capacity for the first three charge-discharge cycles for different electrolyte formulation of $[C_1C_6Im][Li][NTf_2]$ with C_{LiNTf2} = 1.6 mol.L^{-1}at C/20 rate and 298K for Cgr/LFP.

Electrolyte	Charge capacity (mAh/g)			Discharge capacity (mAh/g)		
	1st	2nd	3rd	1st	2nd	3rd
$[C_1C_6Im][Li][NTf_2]$	20.11	1.68	1.03	0.29	0.23	0.22
$[C_1C_6Im][Li][NTf_2]$ + 2% vol. VC	39.21	19.51	11.11	17.98	16.74	7.78
$[C_1C_6Im][Li][NTf_2]$ + 5% vol. VC	119.20	121.281	119.554	119.10	120.11	115.63

The charge-discharge efficiencies of the lithium ion cells achieved at C/20 during the first 3 cycles are summarized in Table A1. No cycling was observed for the test cell without VC additive [5-7]. In contrast, depending on the ratio of additive, the addition of VC into the electrolyte influenced the cycling performances, the better capacities being reached at 5% vol VC [4,5,9].

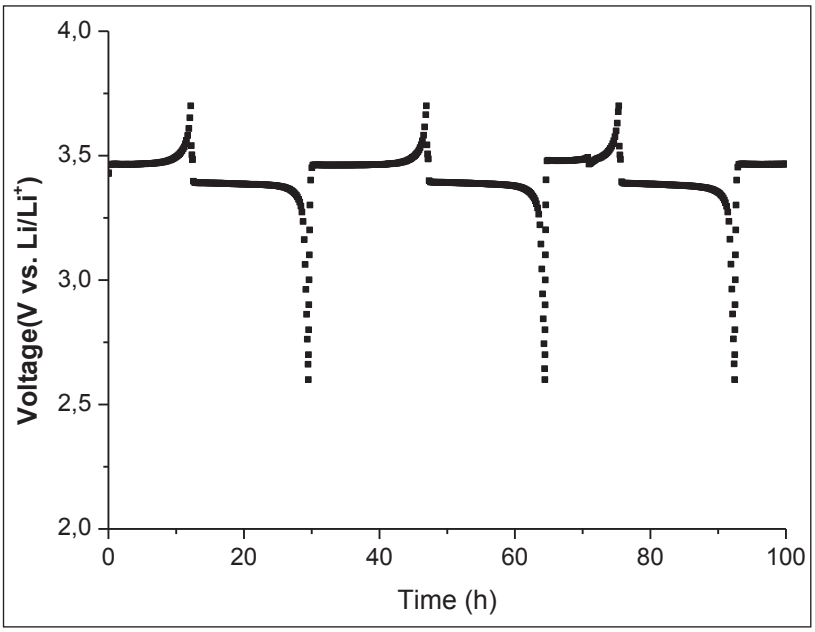

Figure A2: Profile of charge-discharge curves of Cgr/LFP with $[C_1C_6Im][Li][NTf_2]$ with C_{LiNTf2} = 1.6 mol.L^{-1}at 5%vol of VC additive.

Figure A2 shows the profile of the charge-discharge curves of this system, it is completely similar to Cgr/LFP charge-discharge curve obtained in conventional organic electrolyte, exhibiting a flat plateau at around 3.4V. These results confirm the beneficial effect of VC as already observed with all ILs tested on Cgr based Li-ion systems [1] and justified by the formation of a passivation film on the Cgr electrode usually regarded as the solid electrolyte interface (SEI) [8].

Scanning electron microscopy (SEM) was performed. Figure A3a shows a Cgr electrode before cycling; the graphite particles show a rather uniform morphology. Figure A3b shows an electrode after several cycling at 298 K at C/20, the surface is covered by a layer film; these observations could demonstrate the formation of SEI layer.

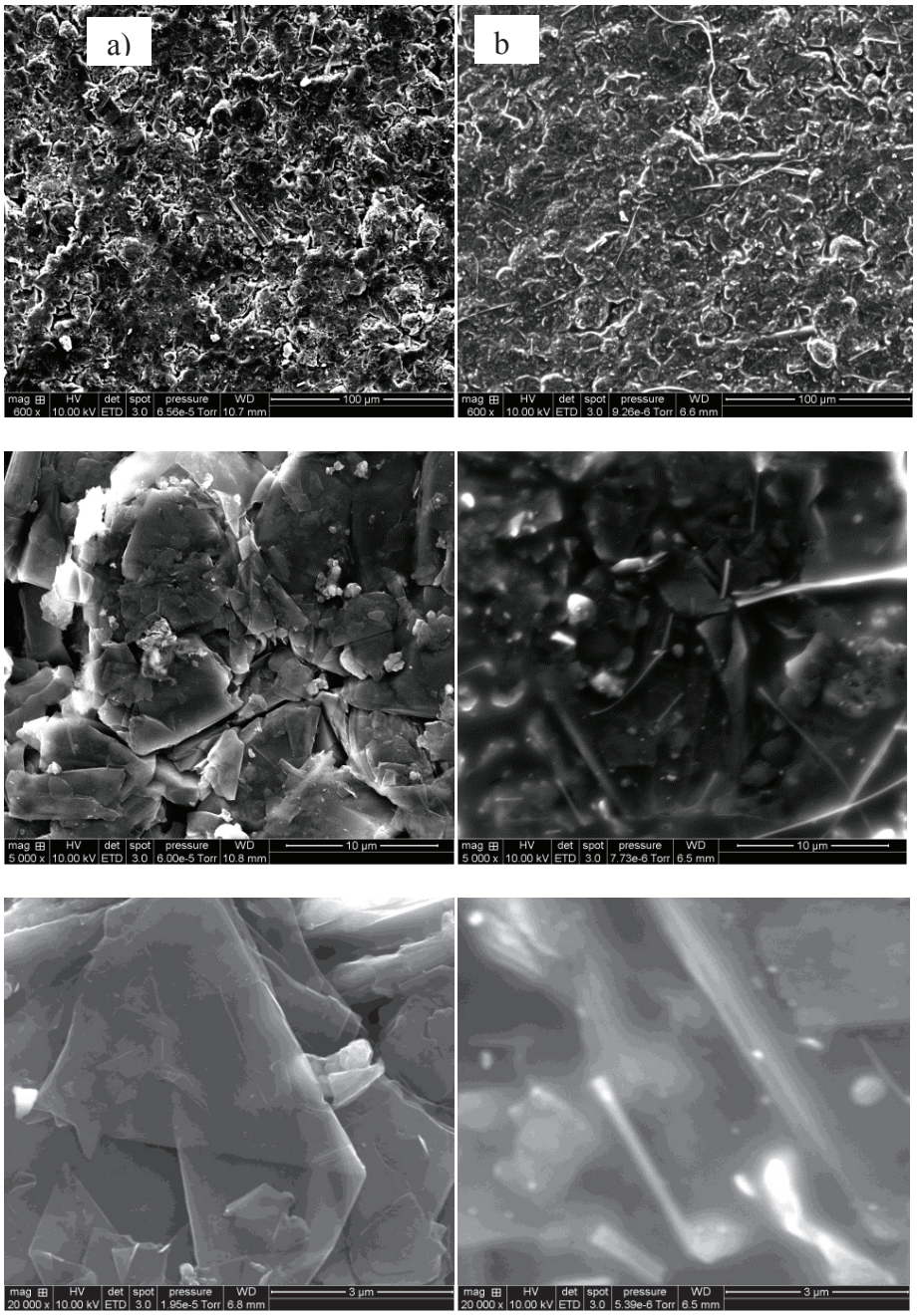

Figure A3: SEM micrographs of cycled Cgr anode (a) original Cgr morphology, (b) post mortem Cgr at the end of cycling at 298 K.

Figure A4 shows the results of cycling test performed at 298 K at C/10 rate on several tens of cycles. The cell displayed an initial capacity of about 120 mAh/g during the first 5 cycles and then slightly decreased to reach 80 mAh/g after 40 cycles (loss of capacity of about 0.7% per cycle up to 20) and 20 mAh/g after 75 cycles.

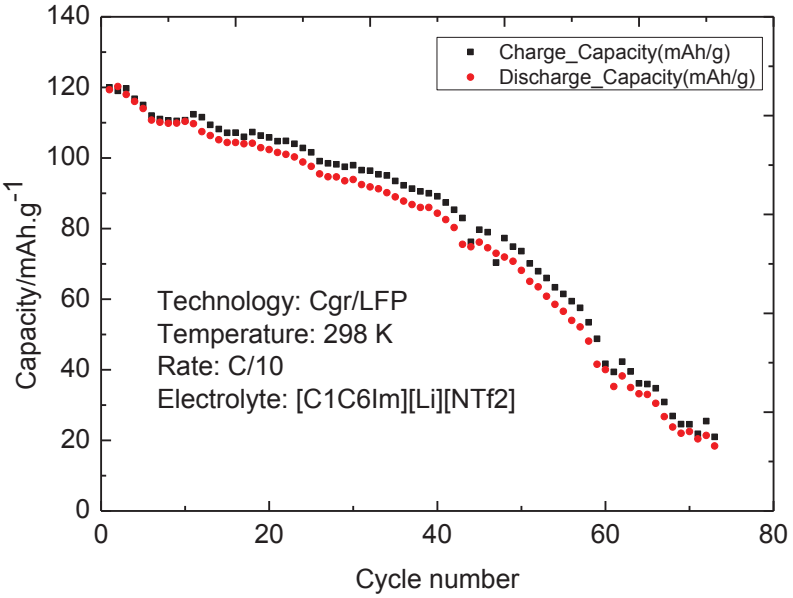

Figure A4: Cycle performance of graphite/LFP cell with $[C_1C_6Im][Li][NTf_2]$ with C_{LiNTf2} = 1.6 mol.$L^{-1}$and 5%vol of VC at C/10 rate (b) 298 K.

Considering the good results at 298 K, the cycling performances of the full system have been evaluated at higher current rates. The test consisted of a sequence of cycles performed successively at C/20, C/10, C/5, C/2, C, 2C and 5C for 5 cycles per rate at 298 K. After this sequence, a second sequence of cycles at C/10 was performed (Figure A5). The aim of the second sequence was to check if the cycling test at high current rates could negatively affect the cell performances.

Up to C/2, the system performances are remarkable with a recovered capacity of 75 mAh/g while the performances at C/10 appear equivalent to the initial ones after the cycling sequence at high rates. Indeed, after a slight decrease of the recovered capacity upon the first five cycles, it remains stable at 110 mAh/g, indicating that the cycling test at high current rate (up to 5C) did not substantially damage the cell.

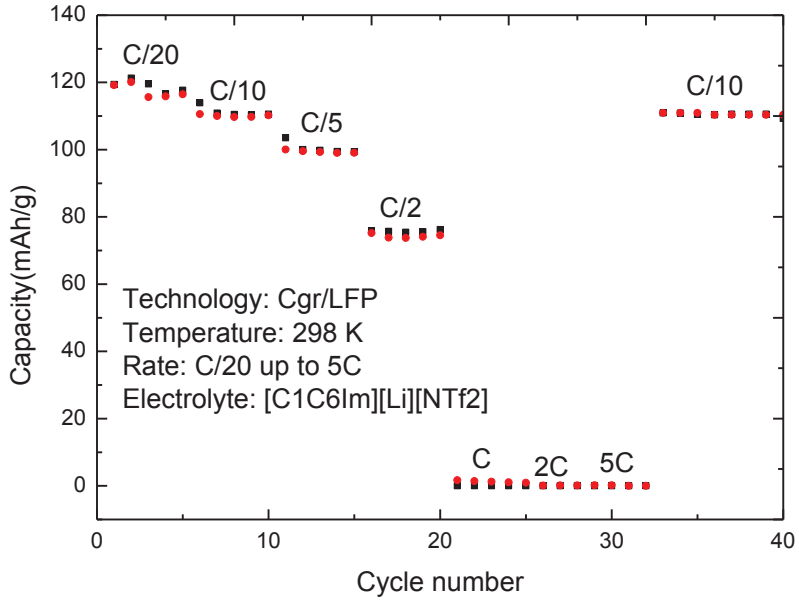

Figure A5: Cycling behavior of Cgr/LFP cell with $[C_1C_6Im][Li][NTf_2]$ with C_{LiNTf2} = 1.6 mol.L^{-1}and 5%vol of VC: Delivered charge-discharge capacity recorded at different rates at 298 K.

Such results have to be emphasized since such performances obtained in full system (using Cgr based electrode instead of Li-metal electrode) with imidazolium based electrolyte at room temperature are not usually presented. It demonstrated that imidazolium cation based ionic liquids may be envisioned as solvent for traditional lithium-ion system (using graphite based negative electrode) in conditions that judicious passivating agent in optimized ratio is added and the imidazolium cation induced larger electrochemical window.

A3 Conclusions

Vinylene carbonate (VC) as additive appears essential for improving the interfacial compatibility between the Cgr electrode and the $[C_1C_6Im][Li][NTf_2]$ with C_{LiNTf2} = 1.6 mol.L^{-1} electrolyte. As promising results, the addition of 5 vol% VC in $[C_1C_6Im][Li][NTf_2]$ with C_{LiNTf2} = 1.6 mol.L^{-1} induces the best charge and discharge performances with a high reversible capacity (120 mAh/g) and good capacity retention (80% for 35th cycle).

These good results allow us to pursuit further investigations on imidazolium based ionic liquid to be used as electrolyte for lithium ion secondary battery with Cgr in the presence of an additive for the SEI forming at the Cgr based electrode

A4 References

1 S. F. Lux, M. Schmuck, G. B. Appetecchi, S. Passerini, M. Winter and A. Balducci, *J. Power Sources,* **192** (2009) 606-611.

2 T. Sugimoto, Y. Atsumi, M. Kikuta, E. Ishiko, M. Kono and M. Ishikawa, *J. Power. Sources*, **189** (2009) 802-805.

3 J. Reiter, M. Nadhern and R. Dominko, *J. Power Sources*, **205** (2012) 402-407.

4 N. Giroud and H. Rouault, *Patent*, US 2011/0206979, (2011).

5 X.-G. Sun and S. Dai, *Electrochimica Acta*, **55** (2010) 4618-4626.

6 A. Lewandowski and A. Aswiderska-Mocek, *J. Power Sources*, **171** (2007) 938-943.

7 M. Holzapfel, C. Jost, A. Prodi-Schwab, F. Krumeich, A. Wursig, H. Buqa and P. Novak, *Carbon*, **43** (2005) 1488-1498.

8 P. B. Balbuena and Y. Wang, Lithium-ion batteries solid-electrolyte interphase, http://site.ebrary.com/id/10106582 .

9 D. Aurbach, Y. Talyosef, B. Markovsky, E. Markevich, E. Zinigrad, L. Asraf, J. S. Gnanaraj, H.-J Kim, *Electrochimica Acta* **50** (2004) 247–254.

B. Li-ion cell based on Cgr/LFP with Im-$LiNTF_2$ electrolyte

B1 Physico-chemical, electrochemical and transportation properties of $[C_1C_4Im][NTf_2]$, $[C_1C_6Im][NTf_2]$ and $[C_1C_4Im][Li][NTf_2]$ and $[C_1C_6Im][Li][NTf_2]$

In this part, the impact of the addition of lithium salt on viscosity, conductivity, translational diffusion, and molecular motion in lithium bis(trifluoromethanesulfonyl)imide ($LiNTf_2$) in two ILs with two different imidazolim cation (1-methyl-3-butylimidazolium $[C_1C_4Im]^+$) and (1-methyl-3-hexyl imidazolium $[C_1C_6Im]^+$) has been evaluated. The ionic conductivity, viscosity, ion self-diffusion coefficients, and electrochemical stability for the neat $[C_1C_4Im][NTf_2]$ and $[C_1C_6Im][NTf_2]$ and for the electrolytes $[C_1C_4Im][Li][NTf_2]$ and $[C_1C_6Im][Li][NTf_2]$ at different $LiNTf_2$ concentration (C_{Li} = 0, 0.5, 1, and, 1.6 $mol.L^{-1}$) and temperature (263, 273, 283, 293, 313, and 333 K). Then $[C_1C_nIm][Li][NTf_2]$ with (C_{Li} = 1.0, and, 1.6 $mol.L^{-1}$) and at temperature (298, and 333 K).have been used as the electrolyte in a Li-ion battery with Cgr and LFP as respectively negative and positive electrode.

Viscosity

Viscosity is an important property of ionic liquids because it strongly influences diffusion of species which are dissolved or dispersed in a media such as an IL. IL viscosity is ordinarily influenced by the interaction of the cation, anion and other interactions such as hydrogen bonding and the symmetry of the ions [1]. Figure B1 compares the measured viscosity of $[C_1C_6Im][NTf_2]$, $[C_1C_4Im][NTf_2]$ and $LiNTf_2$ up to 1.6 $mol.L^{-1}$ at different temperature. $[C_1C_4Im][NTf_2]$ is less viscous than $[C_1C_6Im][NTf_2]$ at different temperatures and different salt concentrations. The addition of the $LiNTf_2$ lithium salt to the ILs significantly increases the viscosity as reported [2,3].

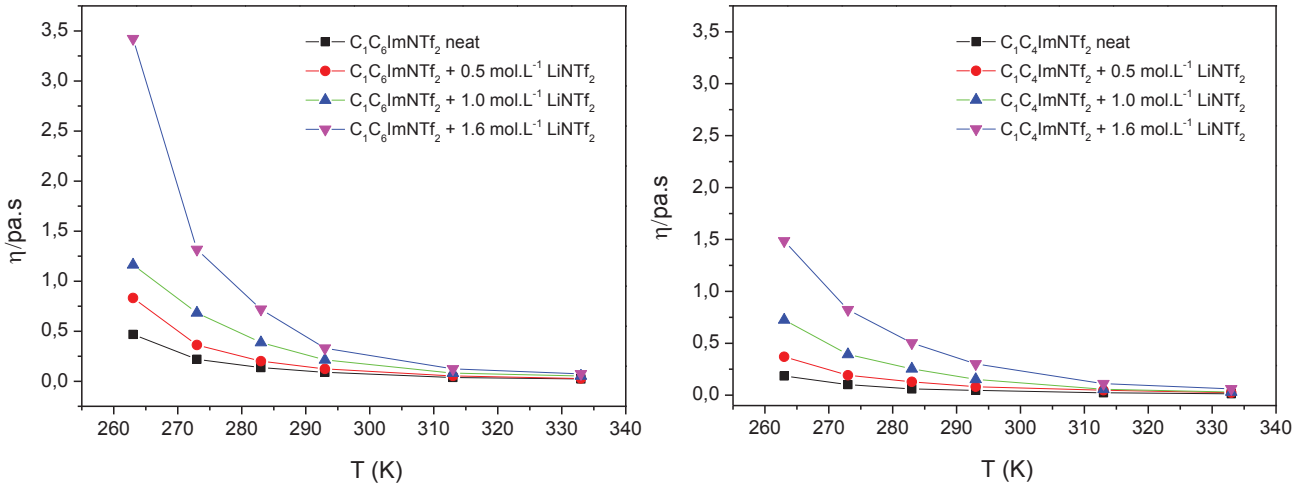

Figure B1: Viscosity of $[C_1C_nIm][NTf_2]$ (n = 4, 6) / $LiNTf_2$ mixtures as a function of $LiNTf_2$ content (C_{Li} = 0, 0.5, 1, and, 1.6 mol.l^{-1}) and temperature (263, 273, 283, 293, 313, and 333 K).

Ionic conductivity

The electrolytic conductivity of a medium is a measure of the number and mobility of available charge carriers. Although ionic liquids are composed entirely of ions, they are in general significantly less conductive than concentrated organic electrolytes [4]. Moreover, likewise the viscosity we studied the dependence of the ionic conductivity on the C_{Li} and on temperature. The neat ionic liquids show moderate ionic conductivity values in the range of 1.788 and 3.392 mS.cm^{-1} at 298 K. For all the temperatures tested and whatever the C_{Li} the ionic conductivity in $C_1C_4ImNTf_2$ ionic liquid was one order of magnitude higher than $[C_1C_6Im][NTf_2]$ as already reported [5,6]. On the other hand, the ionic conductivity decreased significantly with the salt content but not linearly in agreement with the literature [7,8] as shown in Figure B2.

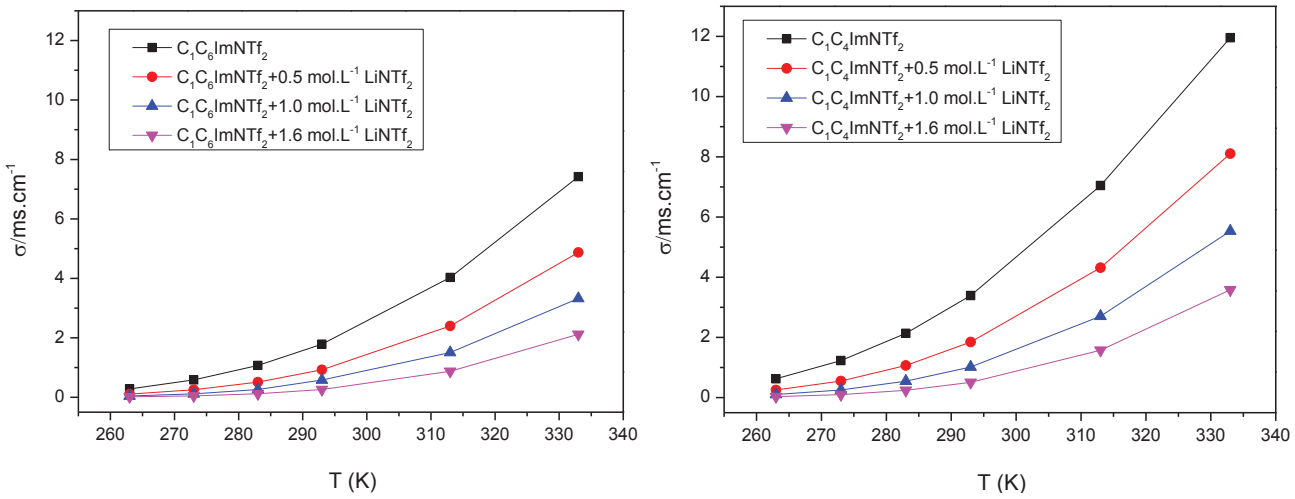

Figure B2: Ionic conductivity of $[C_1C_nIm][NTf_2]$ (n = 4, 6) / $LiNTf_2$ mixtures as a function of $LiNTf_2$ content C_{Li} = 0, 0.5, 1.0, and, 1.6 mol.L^{-1} at the temperatures: 263, 273, 283, 293, 313 and 333 K.

Self-diffusion coefficient

The diffusion coefficients of $[NTf_2]$ anion and cations ($[C_1C_4Im]^+$, $[C_1C_6Im]^+$ and $[Li]^+$) were obtained by, ^7Li, ^1H and ^{19}F NMR, respectively, from 353 to 278 K. Temperature and concentration dependences on the individual ions shown in Figure B3 and tables (table 3 and 4, Appendix II). In neat ILs, at 313 K, $D_{[C1C4Im]^+}$ and $D_{[NTf2]^-}$ in $[C_1C_4Im][NTf_2]$ were 5.8 and 4.4 x10^{-11} m^{2}s^{-1} and D_{C1C6Im^+} and D_{NTf2^-} in C_1C_6Im-NTf_2 were 4.1 and 3.7x10^{-11} m^{2}s^{-1}.

As reported in literature [9-12], diffusion coefficient of the cations (D_{C1CnIm^+}) decreases with n, *e.g.*.. $D_{[C1C4]^+}$ is always larger than $D_{[C1C6Im]^+}$ at any temperature. For the binary systems $[C_1C_4Im][Li][NTf_2]$ and $[C_1C_6Im][Li][NTf_2]$, $D_{[C1CnIm]^+}$ and $D_{[NTf2]^-}$ are lower than their values in neat IL in the same experimental conditions, and are decreasing with C_{Li} and increasing with

temperature. Moreover, same behavior was observed for Li^+ ions even though it have smaller molecular size, D_{Li}^+ is decreasing with C_{Li} and increasing with temperature. The Li^+ diffuses slower than the anion and the cation within each system probably due to the formation of lithium trap which is a similar trend for the increase in the viscosity [13-14].

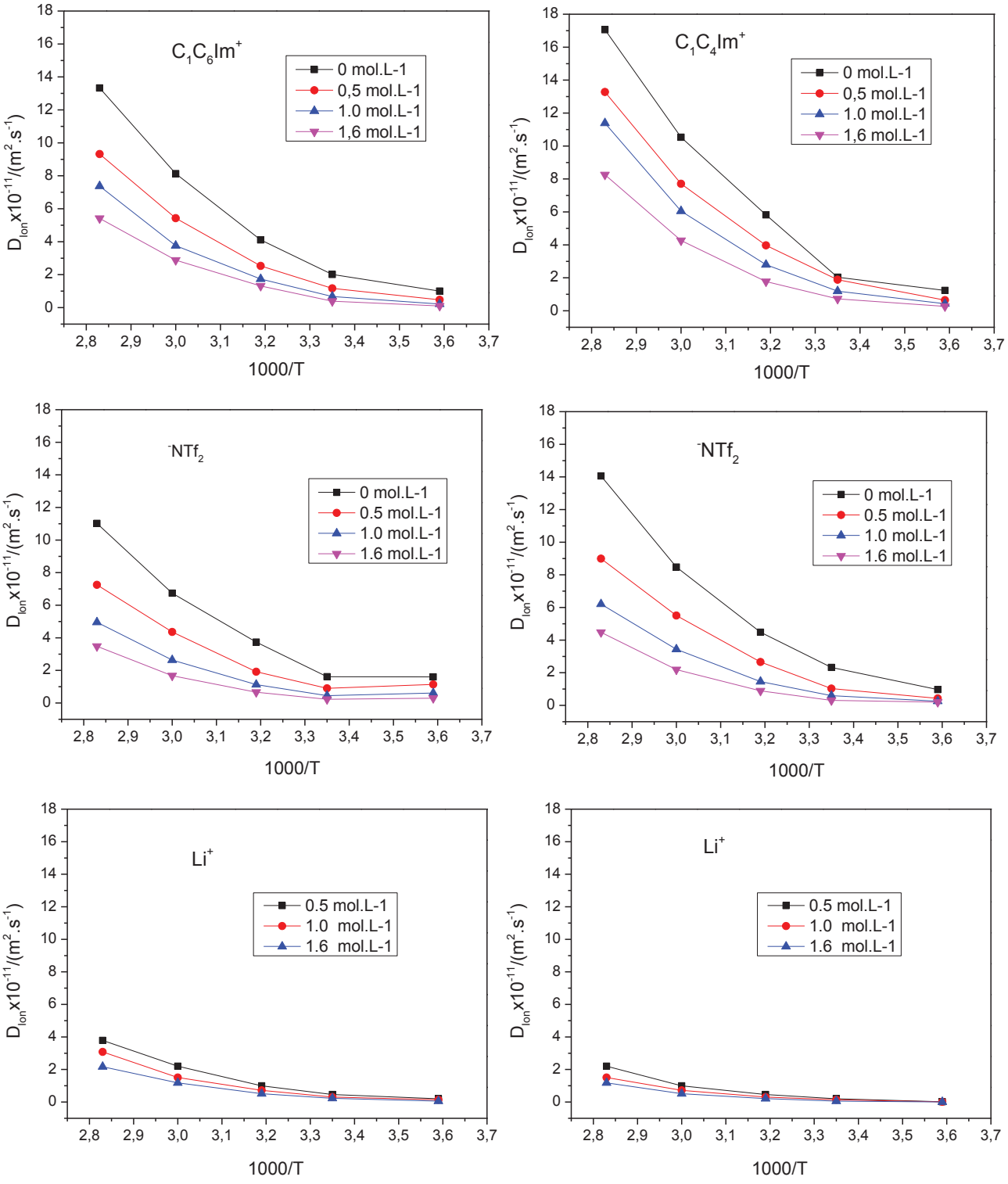

Figure B3: Arrhenius plots of the ion diffusion coefficients of the binary systems for $[C_1C_4Im][NTf_2]$ and $[C_1C_6Im][NTf_2]$ with 1.6 mol.L^{-1} $LiNTf_2$.

Electrochemical window

A general common feature of ILs is their inherent redox robustness of the cations and anions employed for their preparation. ILs generally exhibit wide electrochemical window which is very desirable property for applying the ILs as electrolytic solvents. Typical windows of 4.5-5 V have been reported [15-17] and even enlarged one was found up to 7V by Goncalves et al [18]. In fact, this potential window range is slightly wider than that observed for organic electrolytes. It has been shown that the oxidation of the anions and the reduction of the cations respectively are responsible for the anodic and the cathodic limits observed in ionic liquids [15-17]. The potential at which these processes start determine the accessible electrochemical window. However; an accurate comparison of the various electrochemical windows is very difficult. Firstly, the electrochemical window of ILs largely depends on their purity. Secondly, the nature of the material that is used for the working electrode may modify the decomposition potentials of the electrolyte.

The electrochemical stability was investigated by linear potential sweep technique. The values of the cathodic (Ec) and anodic (Ea) limits referenced to Li^+/Li, and the width of the electrochemical windows ($\Delta E=Ea-Ec$) of the ILs are summarized in tables B1 and B2.

Several cyclic voltammetries were carried in order to determine the influence of the lithium salt content. Figure B4 presents the potential data referenced to the redox potential of lithium experimentally established for neat $[C_1C_6Im][NTf_2]$ and its binary mixture at 1.6 mol.L^{-1} of $LiNTf_2$. Compared to the neat $[C_1C_6Im][NTf_2]$, the binary mixture $[C_1C_6Im][Li][NTf_2]$ exhibits a larger potential window (6.05V) and especially a good stability at highly anodic potentials up to 5.8 V vs Li^+/Li where the anion is supposed to be oxidized. Its cathodic limit is around -0.26V versus Li^+/Li. Consequently, as already reported [15-18], the addition of a lithium salt improves the apparent cathodic limit and the reduction occurring at more negative potential.

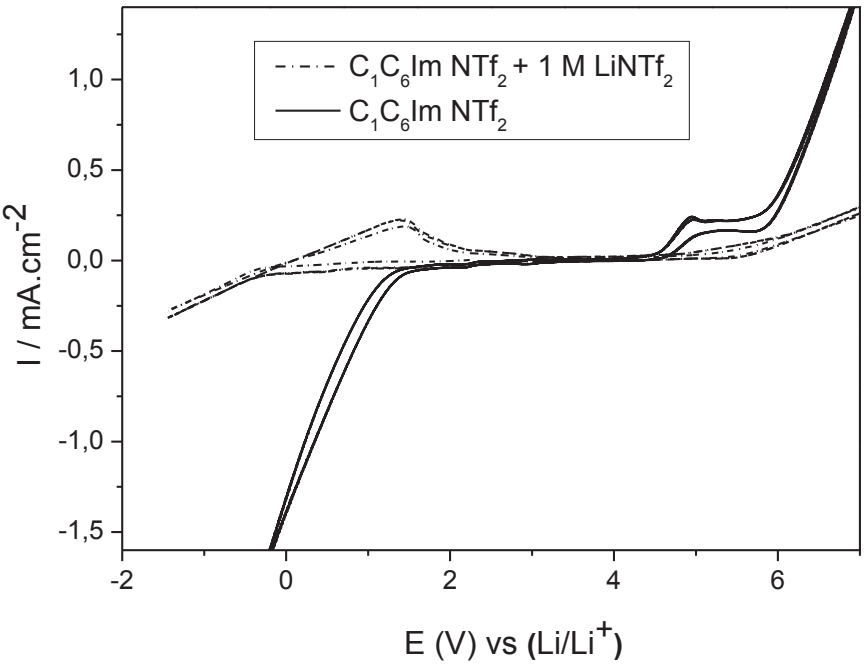

Figure B4: global electrochemical windows realized at 50 mV/s of neat $[C_1C_6Im][NTf_2]$ and their binary mixture at 1.6 mol.L^{-1} $LiNTf_2$: Pt working and counter electrodes and Ag/AgCl reference electrode at 303 K.

The electrochemical stability of $[C_1C_4Im][NTf_2]$ and $[C_1C_6Im][NTf_2]$ and their binary mixtures at 1.6 mol.L^{-1} of $[Li][NTf_2]$ at different temperatures are summarized in Tables B1 and B2. For pure ILs, no significant change in the EW is observed at different temperatures, proving the absence impurities and water [19].

Table B1. Electrochemical stability of $[C_1C_6Im][NTf_2]$ and its binary mixture at different concentration of $LiNTf_2$.

	$[C_1C_6Im][NTf_2]/C_{Li}$=0 mol/L			**$[C_1C_6Im][NTf_2]/C_{Li}$=0.5 mol/L**			**$[C_1C_6Im][NTf_2]/C_{Li}$=1 mol/L**			**$[C_1C_6Im]|NTf_2]/C_{Li}$=1.6 mol/L**		
T (K)	E_a (V)	E_c (V)	ΔE (V)	E_a (V)	E_c (V)	ΔE (V)	E_a	E_c (V)	ΔE (V)	E_a (V)	E_c (V)	ΔE (V)
303	5.73	0.64	5.09	5.74	-0.44	6.18	5.83	-0.28	6.11	5.79	-0.26	6.05
323	5.86	1.05	4.81	5.76	-0.50	6.26	5.71	-0.24	5.95	5.77	-0.22	5.99
343	5.77	1.21	4.56	5.68	-0.54	6.22	5.77	-0.22	5.99	5.70	-0.17	5.87
363	5.79	1.24	4.55	5.64	-0.36	6.00	5.77	-0.11	5.88	5.76	-0.13	5.89

Table B2. Electrochemical stability of $[C_1C_4Im][NTf_2]$ and its binary mixture at 1.6 mol.L^{-1} of $LiNTf_2$.

	$[C_1C_4Im][NTf_2]$ - C_{Li}=0 mol/L			$[C_1C_4Im][NTf_2]$ - C_{Li}=1 mol/L		
T (K)	E_a (V)	E_c (V)	ΔE (V)	E_a (V)	E_c (V)	ΔE (V)
303	5.58	0.90	4.68	5.22	-0.68	5.90
313	5.48	0.79	4.69	5.23	-0.67	5.90
333	5.50	0.93	4.57	5.22	-0.57	5.79
353	5.53	1.00	4.53	5.20	-0.41	5.61
373	5.47	0.98	4.49	5.10	-0.43	5.53

B2 Battery with $[C_1C_4Im][Li][NTf_2]$ and $[C_1C_6Im][Li][NTf_2]$

Our previous results on battery test (page 67, part B), showed that at 298 K the cell containing $[C_1C_6Im][Li][NTf_2]$ with C_{LiNTf2} = 1.6 mol.L^{-1} concentration displayed an initial capacity of about 120 mAh/g during the first 5 cycles and then slightly decreased to reach 80 mAh/g after 40 cycles (loss of capacity of about 0.7% per cycle up to 20) and 20 mAh/g after 75 cycles. These decreasing in performance probably maybe related to the high viscosity of this electrolyte. The viscosity could be reduced by using shorter alkyl chain i.e. four alkyl carbons instead of six. And decreasing the amount of dissolved $LiNTf_2$ i.e. 1.0 mol.L^{-1} instead of 1.6 mol.L^{-1} (Figure B1). The full cell configuration containing $[C_1C_4Im][Li][NTf_2]$ with C_{LiNTf2} = 1.0 mol.L^{-1} assembled with Cgr/LFP has been tested at 298 K and 333 K. Unexpectedly, no cycling was observed at 298 K while at elevated temperature (333 K), the coin cells show lower performances than with $[C_1C_6Im][Li][NTf_2]$ with C_{LiNTf2} = 1.6 mol.L^{-1} electrolyte (Figure B5).

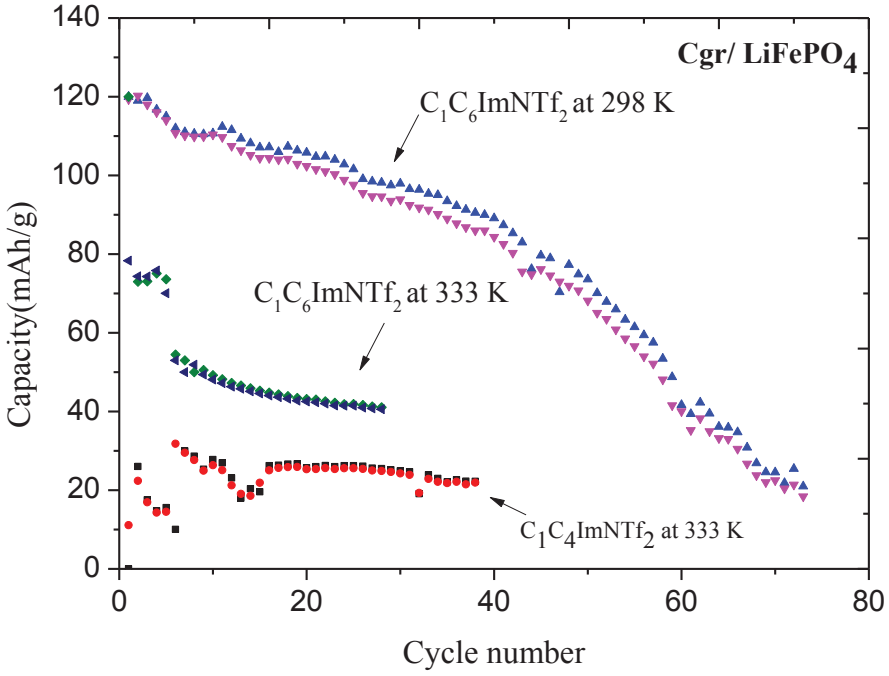

Figure B5. Cycle performance of Cgr/LFP cell with 1.6 mol.L^{-1} of $[C_1C_nIm][Li][NTf_2]$/ n= 4, 6 and 5%vol of VC at C/10 rate at 298 K and 333 K.

B3 Battery with $[C_1C_nIm][Li][NTf_2]$ and $[C_1C_1C_nIm][Li][NTf_2]$ as electrolyte

Although there have been a lot of research studies concerning ionic liquids that use imidazoium-based cations, they report a problem of stability limit in comparison to the redox potential of lithium metal, and there have been very few or no reports on rechargeable batteries that use lithium metal or Cgr as electrodes [20].

In order to show the impact of C_2-H on the battery performance, we introduced a donating group (CH_3) at position C_2 and we did a comparative study. Full cell configuration based on Cgr/LFP with ($[C_1C_4Im][NTf_2]$ and $[C_1C_1C_4Im][NTf_2]$) based on bis(trifluoromethanesulfonyl)imide ($[NTf_2]^-$) anion as the electrolyte media were tested at 60°C (Figure B6).

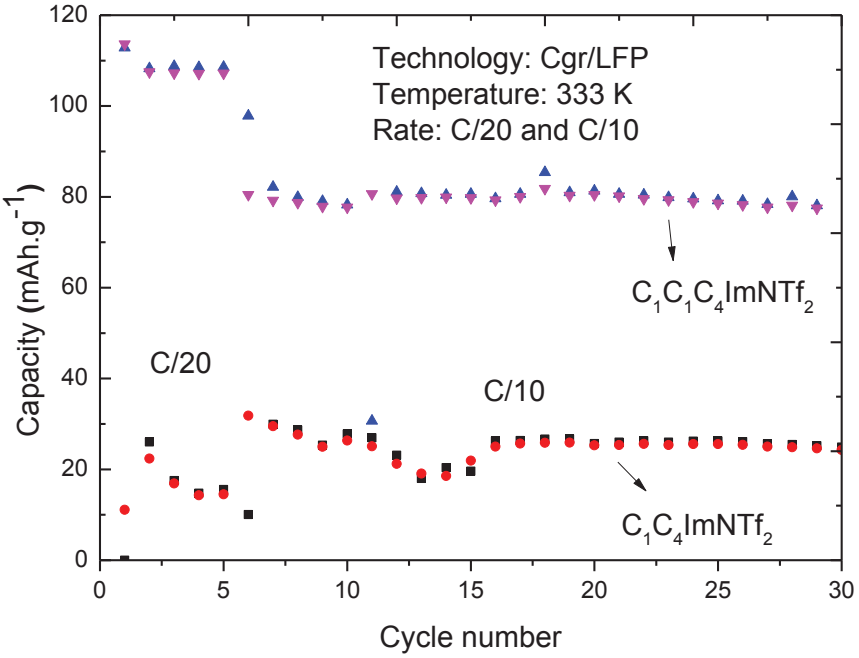

Figure B6: Cycle performance of Cgr/LFP cell with different electrolytes at 1.0 mol.L^{-1}: $[C_1C_4Im][Li][NTf_2]$ and $[C_1C_1C_4Im][Li][NTf_2]$ at 5%vol of VC and 333 K.

As clearly shown in Figure B6, substituting the chemically stable methyl group reduces the high reactivity and controls the side reaction with Cgr and LFP cathode under charge/discharge conditions. $[C_1C_1C_4Im][NTf_2]$ are able to exhibit almost the full capacity about 110 mAh/g obtained at C/20 (more than 90% of the expected capacity) for the first 5 cycles. Moreover, this behavior remains relevant at higher rate C/10 and the recovered capacity remains close to 80 mAh/g for a couple of cycles contrary to non-modified IL ($[C_1C_4Im][NTf_2]$) (Figure B6).

As we reported in Figure B5, at 333 K, the performance of $[C_1C_6Im][Li][NTf_2]$ electrolyte afforded best cycling test than $[C_1C_4Im][Li][NTf_2]$, in this part we have also compared $[C_1C_1C_nIm][Li][NTf_2]$ (n=4 and 6) as electrolytes.

As clearly shown in figure B7, the charge/discharge cycle performance of the battery have been improved with: the extension of the alkyl chain length of the imidazolium ring, and introducing a donating group (-CH_3) on the position two of the imidazolium ring ($C_{2\text{-H}}$ ----> $C_{2\text{-CH3}}$), the capacity value follow the order $[C_1C_1C_6Im][NTf_2]$> $[C_1C_1C_4Im][NTf_2]$> $[C_1C_6Im][NTf_2]$> $[C_1C_4Im][NTf_2]$ at

333 K (Figure B8). $[C_1C_1C_6Im][Li][NTf_2]$ electrolyte exhibits almost the full capacity with about 120 mAh/g obtained at C/20 (first 10 cycles) and C/10 (20 cycles) more than 90% of the expected capacity is recovered.

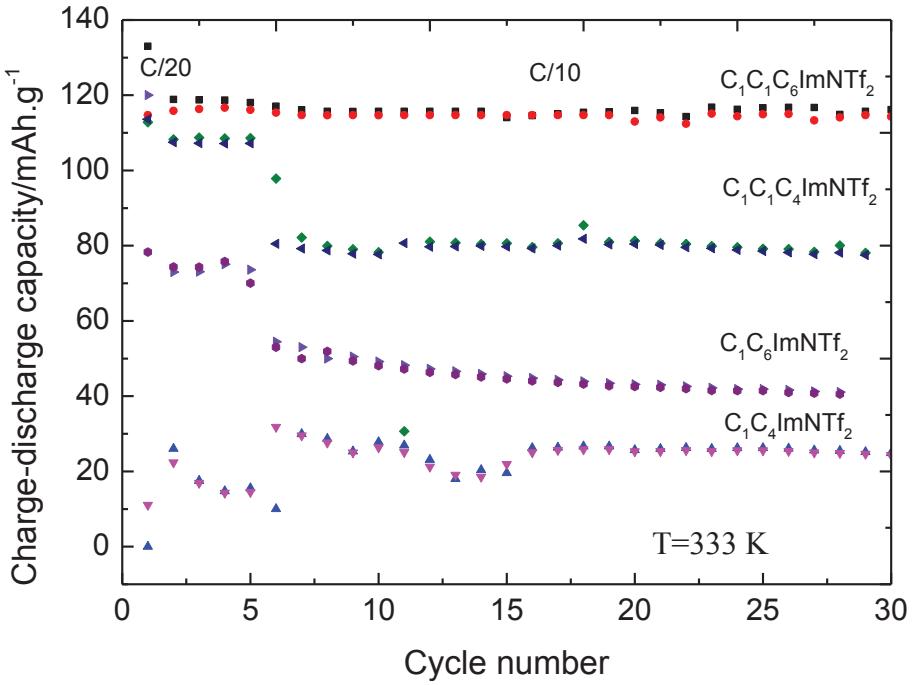

Figure B7: Tuned imidazoilum ILs with Cgr/LFP at 333 K.

Moreover, by comparing to the classical organic electrolyte. The performance of $[C_1C_1C_6Im][Li][NTf_2]$ remains relevant at higher rate C/20 and C/10 and the recovered capacity remains ~120 mAh/g over 100 cycles contrary to the organic electrolyte ($LiPF_6$:DMC:EC) (Figure B8).

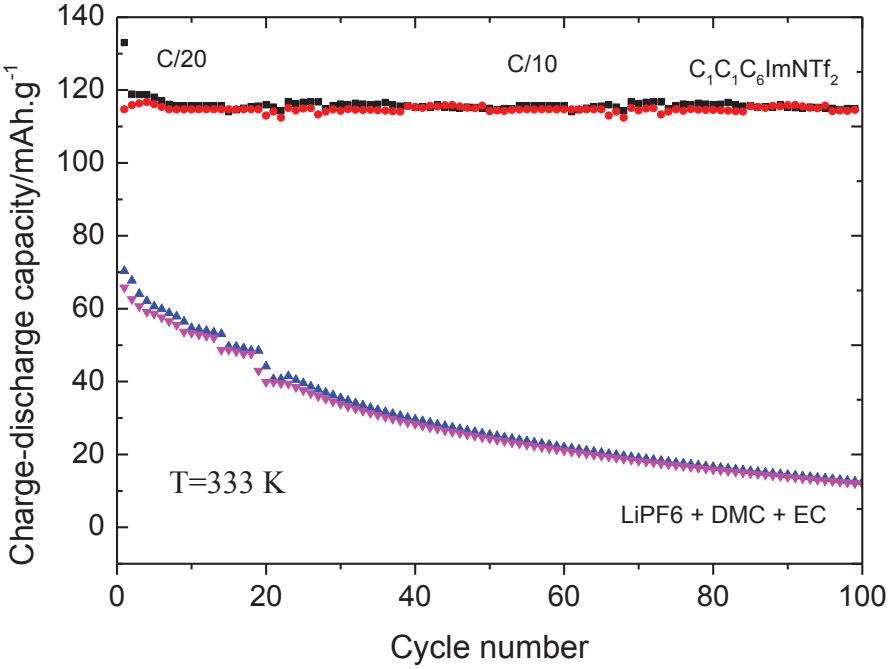

Figure B8: Cycle performance of Cgr/LFP cell with different electrolytes: $[C_1C_1C_6Im][Li][NTf_2]$ at 5%vol of VC and organic electrolyte at 333 K.

B4 Conclusions and discussion

In this part B, we have compared the cycling performances of $[C_1C_nIm][Li][NTf_2]$ n=2,6 with C_{Li}= 1.0, 1.6 mol.L^{-1} and $[C_1C_1C_nIm][Li][NTf_2]$ n=4, 6 C_{Li}= 1 mol.L^{-1} as electrolytes, at 298 K and 333 K in Li-ion cells based on Cgr/LFP electrodes.

For all these electrolytes as already reported in the literature, the cycling performances have been improved when,

i) The viscosity of the electrolyte was decreased either by increasing the temperature from 298 to 333 K (See part B1 page 69),or decreasing the C_{Li} from 1.6 to 1.0 mol.L^{-1} [21].

ii) The C_2 of the imidazolium ring was substituted by a donating group (-CH_3) [20].

iii) The alkyl chain of imidazolium ring was extended [22].

iv) For all electrolytes: $[C_1C_nIm][Li][NTf_2]$ n=2,6 with C_{Li}= 1.0, 1.6 mol.L^{-1} and $[C_1C_1C_nIm][Li][NTf_2]$ n=4, 6 CLi= 1.0 mol.L^{-1} cycling occurs only if VC is added. The role of VC has been linked to the formation of the SEI as demonstrated by SEM images part A page (66) [23].

However, when the cycling tests have been run with this electrolytes (with C_{Li}= 1 mol.L^{-1} at 333K) the performance of the Li-ion cell increased as followed: $[C_1C_1C_6Im][Li][NTf_2]$>

$[C_1C_1C_4Im][Li][NTf_2]$> $[C_1C_6Im][Li][NTf_2]$> $[C_1C_4Im][Li][NTf_2]$, inversely to the variation of viscosity and D_{Li^+} values.

As promising results, the addition of 5 vol% VC in $[C_1C_1C_6Im][Li][NTf_2]$ with 1.0 $mol.L^{-1}$ $LiNTf_2$ induces the best charge and discharge performances with a high reversible capacity (120 mAh/g) and good capacity retention at C/20 (first 10 cycles) and C/10 (20 cycles) more than 90% of the expected capacity is recovered at 333 K.

Consequently, to improve cycling performance of Li-ion cell based on Cgr/LFP electrodes, a delicate tuning between the physico-chemical properties of the electrolytes and the substitution of the imidazolium ring has to be found.

The impact of the length of the alkyl chain of imidazolium ring could be related to a possible interface/organization of them on Cgr surface. Molecular simulations concluded that the alkyl side chains tend to lie flat at the Cgr surface leading a stable interface [24-26].
Therefore, the ILs may exfoliate the graphite, and the process could be faster as with shorter alkyl chain ionic liquids (less steric hindrance) [27] and sensitive to polar or apolar surface as well as hydrophobic or hydrophilic IL components [28].

Understanding of this interface IL/Cgr should remove the technological barrier that is the use of VC as additive in Cgr/LFP devices with $[Im][Li][NTf_2]$ as electrolytes.

B5 References

1 H. Tokuda, K. Hayamizu, K. Ishii, M. A. H. Susan, M. Watanabe, *J. Phys. Chem B.*, **109** (2005) 6103-6110.

2 S. Tsuzuki, K. Hayamizu, S. Seki, *J. Phys. Chem. B*, **114** (2010) 16329-16336.

3 M. Diaw, A. Chagnes, B. Carré, P. Willmann, D. Lemordant, *J. Power Sources*, **146** (2005) 682-684.

4 H. Tokuda, K. Hayamizu, K. Ishii, Md. A. B. H. Susan, M. Watanabe, *J. Phys. Chem. B*, **109** (2005) 6103-6110.

5 A. Stoppa, O. Zech, W. Kunz, R. Buchner, *J. Chem. Eng. Data*, **55** (2010) 1768-1773.

6 B. Garcia, S. Lavallée, G. Perron, C. Michot, M. Armand, *Electrochimica Acta*, **49** (2004) 4583-4588.

7 A. I. Bhatt, A. S. Best, J. Huang, A. F. Hollenkamp, *J. Electrochem Soc*, **157** (2010) 66-74.

8 S. Seki, Y. Kobashashi, H. Miyashiro, A. Ohno, A. Usami, Y. Mita, N. Kihira, M. Watanabe, N. Terada, *J. Phys Chem B Lett*, **110** (2006) 10228-10230.

9 A. Noda, K. Hayamizu, M. Watanabe, *J. Phys. Chem B*, **105** (2001) 4603-4610.

10 S. Tsuzuki, W. Shinoda, H. Saito, M. Mikami, H. Tokuda, M. Watanabe, *J. Phys. Chem. B*, **113** (2009) 10641-10649.

11 F. Castiglione, M. Moreno, G. Raos, A. Famulari, A. Mele, G. B. Appetecchi, S. Passerini, *J. Phys. Chem. B*, **113** (2009) 10750-10759.

12 H. A. Every, A. G. Bishop, D. R. MacFarlane, G. Orädd, M. Forsyth, *Phys. Chem. Chem. Phys*., **6** (2004) 1758.

13 K. Hayamizu, S. Tsuzuki, S. Seki, K. Fujii, M. Suenaga, Y. Umebayashi, *J. Chem. Phys B*, **133** (2010) 194505-1-194505-13.

14 Y. Saito, T. Umecky, J. Niwa, T. Sakai, S. Maeda, *J. Phys. Chem. B.* **111**, (2007) 11794-11802.

15 P. Bonhôte, A.-P. Dias, N. Papageorgiou, K. Kalyanasundaram, M. Gratzël, *Inorg. Chem*. **35** (1996) 1168.

16 A. B. MacEwen, H. L. Ngo, K. LeCompte, J. L. Goldman, *J. Electrochem. Soc*., **146** (1999) 1687.

17 D. R. MacFarlane, P. Meakin, N. Amini, M. Forsyth, *J. Phys. Chem. B*, **103** (1999) 4164.

18 P. A. Z. Suarez, C. S. Consorti, R. F. de Souza, J; Dupont, R. S. J. Goncalves, *Braz. Chem. Soc* **13**. (2002) 106.

19 A. M. O'Mahony, D. S. Silvester, L. Aldous, C. Hardacre, R. G. Compton, *J. Chem. Eng. Data* **53** (2008) 2884–2891.

20 S. Seki, Y. Ohno, Y. Mita, N. Serizawa, K. Takei, H. Miyashiro, *ECS Electrochemistry Letters,* **1** (2012) A77-A79.

21 S. Seki, Y. Ohno, Y. Kobayashi, H. Miyashiro et al, *J. Electrochem Soc*, **154** (2007) A173-A177.

22 S. Seki, Y. Mita, H. Tokuda et al, *Electrochemical and Solid-State Letters*, **10** (2007) A237-A240.

23 M. Holzapfel, C. Jost, A. Prodi-Schwab, F. Krumeich, A. Wursig, H. Buqa, P. Novak, *Carbon*, **43** (2005)1488–1498.

24 S. Wang, S. Li, Z. Cao and T. Yan, *J. Phys. Chem. C* **114** (2010) 990–995.

25 Q. Dou, M. L. Sha, H. Y. Fu and G. Z. Wu, *J. Phys. Condens. Matter*, **23** (2011), 175001/175001-175001/175008.

26 M. Opallo and A. Lesniewski, *J. Electroanal. Chem.*, **656** (2011) 2-16.

27 X. Wang, P. F. Fulvio, G. A. Baker, G. M. Veith, R. R. Unocic, S. M. Mahurin, M. Chi and S. Dai, *Chem. Commun.*, **46** (2010) 4487-4489.

28 M. Acik, D. R. Dreyer, C. W. Bielawski, and Y. J. Chabal., *J. Phys. Chem., C* **116**, (2012) 7867−7873.

C. Battery performance: compatibility of $[C_1C_nIm][NTf_2]$ and $[C_1C_1C_nIm][NTf_2]$ (n=4,6) coupled with $Li_4Ti_5O_{12}$/$LiFePO_4$:

Our precedent investigations made with the use of electrolytes: $[C_1C_nIm][NTf_2]$ and $[C_1C_1C_nIm][NTf_2]$ in combination with Cgr electrode. We have found, in agreement with literature, the Cgr is not compatible with neat $[Im][Li][NTf_2]$ electrolytes due to the irreversible reduction of Im cations [1,2]. Consequently using Cgr electrode requires the use of organic additive, which is a drawback for the safety [3-8]. These two points could be crippling for the use of ILs as electrolytes. However, ILs are safer compared to organic electrolytes, and allow working at high temperature, thus opening a new domain of application for these batteries. Consequently, the development of full devices Li-ion batteries with ILs as electrolyte is still a scientific, environmental and economic challenge [9,10].

Our early investigations have done with the use of $[C_1C_6Im][Li][NTf_2]$ at 1.6 $mol.L^{-1}$ in combination with a graphite based electrode. We have found the key lock of this approach is the interphase if IL/Cgr. to may overcome this limitation, the use of alternative negative electordes, such as Ti-based oxides, e.g. $Li_4Ti_5O_{12}$ (LTO), have been tested. (LTO) has received significant attention as possible active materials to replace graphite. These materials have the disadvantage of reducing the energy density of conventional Li-ion cells because they operate at significantly higher potential (1.5-1.8 V *vs* Li^+/Li) compared to graphite (<0.1 V *vs* Li^+/Li). However, they do not require an electrolyte additive to form solid electrolyte interface (SEI) and the advantage of improved safety makes them particularly attractive materials [11-15].

We have Firstly evaluated the compatibility and the electrochemical performance of $[C_1C_6Im][Li][NTf_2]$ in full system configuration LTO/LFP. We have optimized the concentration of $LiNTf_2$ at 1.0 $mol.L^{-1}$ in order to keep the electrolyte viscosity not too high and we realized the cycling tests at 298 K and 333 K at various current rates.

C1 Cycling tests

Figures C1 to C4 display the charge-discharge capacity as a function of cycle number (galvanostatic cycling, capacity reported to the mass of LFP active material) and current rates obtained at 298 K and 333 K.

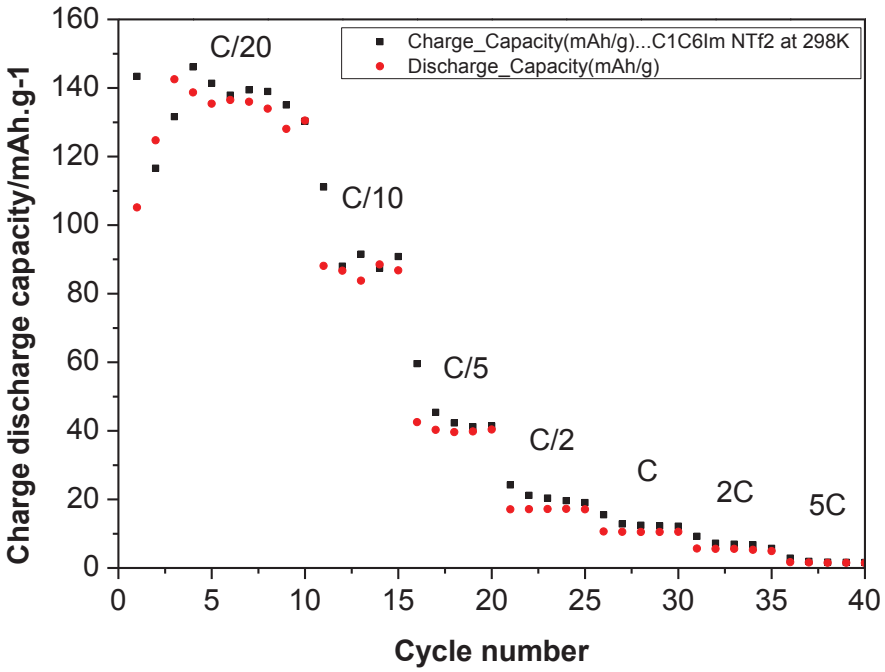

Figure C1: Charge discharge capacity of $[C_1C_6Im][NTf_2]$ and 1 mol.L^{-1} $LiNTf_2$ at 298 K of LTO/LFP at different currents rates.

At 298 K, as clearly shown in Figure C1, the LTO/LFP system is capable of storing and supplying energy at any current rate. At the low rate of C/20, the discharge capacity is about 140 mAh/g, which is comparable to the specific capacity of the LFP active material. At moderate rates like C/5 and C/2, the average value of the discharge capacity is 60 mA.h/g and 20 mA.h/g, respectively. At higher rates, it becomes inferior to 12 mAh/g.

Nevertheless, the cycling behaviour of the system appears unstable, with a very high loss of capacity decreasing from 150 mAh/g to 140 mAh/g at C/20 in less than 6 cycles. This tendency seems to be confirmed when the system is cycled at constant rate C/10 after a few cycles at C/20 as indicated in Figure C2. The capacity recovered exhibits fluctuating values with a general decrease of about 0.45% per cycle.

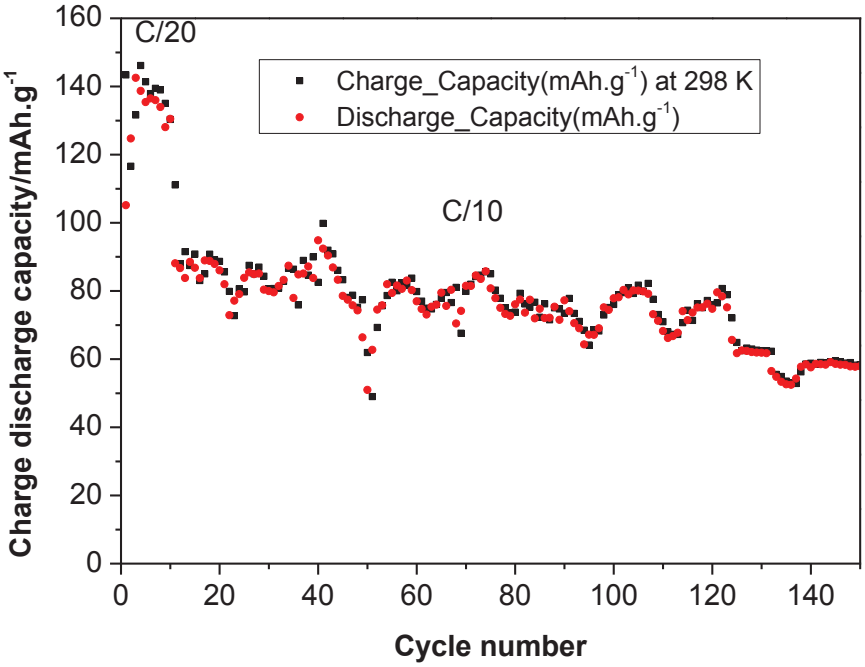

Figure C2: Charge discharge capacity of $[C_1C_6Im][NTf_2]$ and 1.0 mol.L^{-1} $LiNTf_2$ at 298 K of LTO/LFP at constant current rate C/10.

From earlier reports [16], the rate property depends on the charge transfer resistance on a cathode and an anode, which reflected the electrochemical kinetics on the $[Li^+]$ insertion /de-insertion process and Li-metal deposition/dissolution process, respectively. Short time charging-discharging process provided less than 40% of the theoretical capacity. In addition, unstable performance observed at C/10 is mainly due to the internal resistance of the cell, and the wettability of the electrode against the ILs also seems to be responsible [17].

It was the reason why tests are then performed at higher temperature, typically 333 K in similar conditions: they showed relevant behaviour (Figure C3).

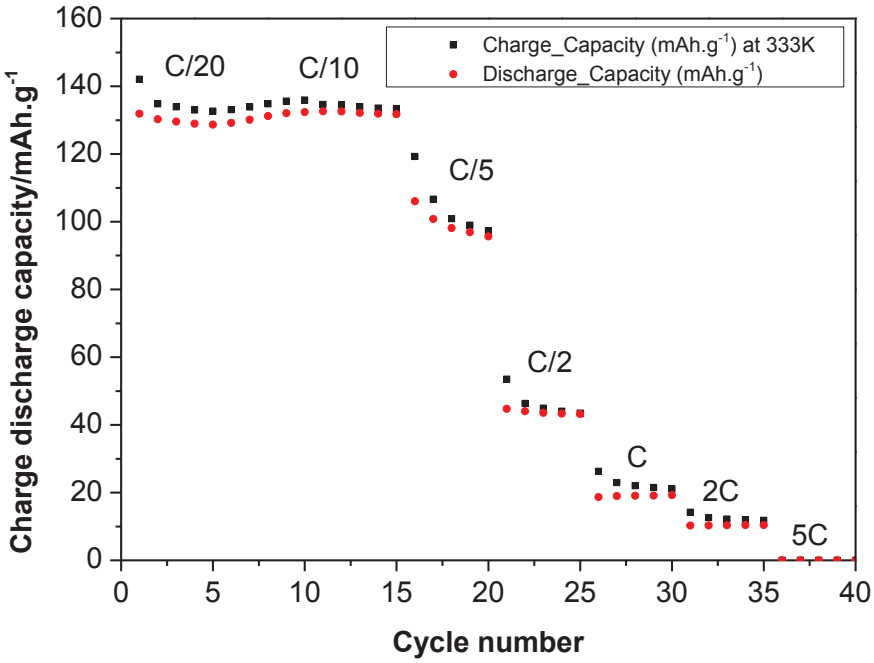

Figure C3: Charge discharge capacity of $[C_1C_6Im][NTf_2]$ at 298 K (left) and at 333 K (right) of LTO/LFP at different currents rates.

Figure C3 summarizes the delivered capacity at various current rates and showed that it exhibits higher and more stable values compared to the capacities recovered at 298 K. Thus, at low rate (typically C/10), an initial difference of capacity of at least 20 mAh/g between 333 K and 298 K may be observed. At higher rates, this difference remains similar, even rises: For instance the capacity of 100 mAh/g is recovered at C/5 at 333 K compared to the capacity of 60 mAh/g obtained at 298 K. Moreover, as confirmed in Figure C4, the system in cycling is more stable at 333 K. After a few cycles at C/20 rate, the same delivered discharge capacity of 130 mAh/g is obtained with a columbic efficiency of 98%, while at 298 K continuous decrease of the capacity is observed.

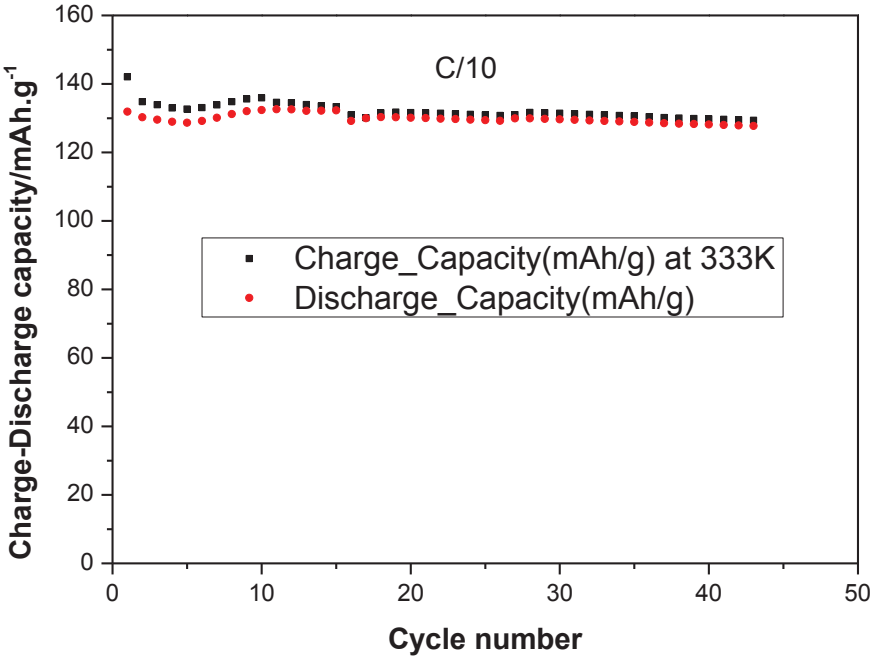

Figure C4: Charge discharge capacity of $[C_1C_6Im][Li][NTf_2]$ at 1.6 mol.L^{-1}at 333 K of LTO/LFP at constant current rate C/10.

These previous results allow highlighting some major influent parameters in the use of ILs as electrolytes: ILs/electrode interface and physico-chemical properties as viscosity and conductivity. Thus, in order to obtain lower viscosity and higher conductivy, the concentration of lithium salt were reduced from the starting electrolyte $[C_1C_6Im][Li][NTf_2]$ at 1.6 mol.L^{-1}. Indeed, Ohno et al [18], reported the best concentration in the range of 0.5-1.0 mol.L^{-1} of $LiNTf_2$. Moreover, as reducing the alkyl chain length or introducing a donating group ($-CH_3$) may have similar influence, it was investigated new designed ILs with 1 mol.L^{-1} of $LiNTf_2$ and $[C_1C_4Im]$ or $[C_1C_1C_nIm]$ based cation to lower these values [19].

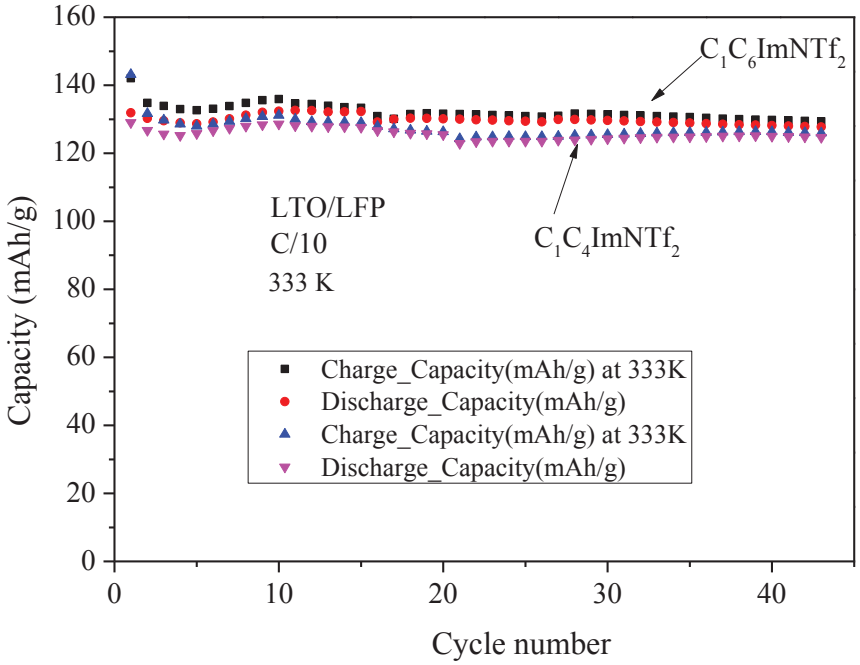

Figure C5: Charge-discharge capacity of LTO/LFP coupled with $[C_1C_nIm][NTf_2]$ (n=4,6) at 333 K constant current rate (C/10).

Figure C5 compares the rate capability of LTO/LFP full cell configuration coupled with $[C_1C_nIm][NTf_2]$ at 1.0 $mol.L^{-1}$ of $LiNTf_2$ and 333 K. The changes in the average charge-discharge capacity according to the cycle number were extremely low in case of $[C_1C_nIm][NTf_2]$ (n=4,6) electrolyte. The initial charge and discharge capacities were ~ 140 mAh/g which is relatively close to the theoretical capacity of LFP. The charge discharge capacity was maintained at 130 mAh/g for a couple of tenth of cycles. As in case of Cgr/LFP, the cycle performance of the battery was improved with the extension of the alkyl chain length.

We have also studied the performance of the lithium ion cell based on LTO/LFP using a substituting chemically stable methyl group is lower in case of with $[C_1C_1C_nIm][NTf_2]$ (n=4,6). The initial charge and discharge capacities were ~ 150 mAh/g and 130 mAh/g. With LTO/LFP electrodes, contrary to Cgr/LFP system, for the same alkyl chain (C_n) in $[C_1C_nIm][Li][NTf_2]$ electrolytes afford best performance than $[C_1C_1C_nIm][Li][NTf_2]$ (Figure C6). These results emphasize that LTO is compatible with imidazolium cation ring and has no problem with the reduction limit with graphite. With $[C_1C_1C_nIm][Li][NTf_2]/C_{Li}$=1.0 $mol.L^{-1}$ (n=4,6), the charge discharge capacity decreases as cycle number increases. For both for the first tenth of cycles sharp decrease in capacity is observed from 160 to 130 and 110 mAh/g for $[C_1C_1C_6Im][Li][NTf_2]$ and $[C_1C_1C_4Im][Li][NTf_2]$ respectively.

However, as for $[C_1C_nIm][Li][NTf_2]$ with $[C_1C_1C_nIm][Li][NTf_2]$ electrolytes, longer is the alkyl chain higher is the performance.

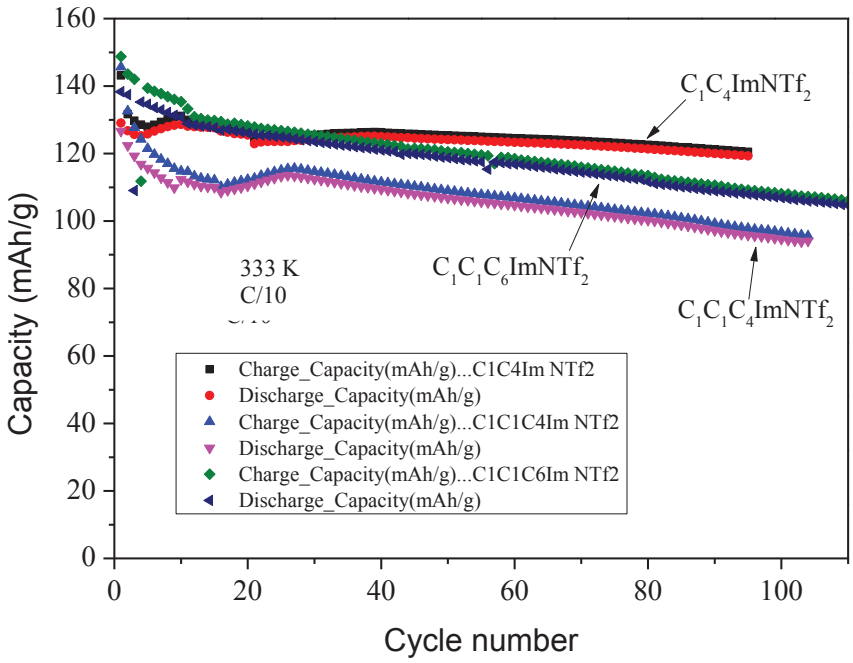

Figure C6: Charge-discharge capacity of LTO/LFP coupled with $[C_1C_1C_nIm][NTf_2]$ (n=4,6) at 333K at C/10 rate.

These previous results suggest that the LTO/LFP system, in presence of 1.0 $mol.L^{-1}$ $[C_1C_nIm][Li][NTf_2]$, could be considered as a first step towards safer and a more economical solution for the Li-ion technology.

C2 References

1 T.E. Sutto, T.T. Ducan, T.C. Wong, *Electrochim. Acta* **54** (2009) 5648.

2 E. Markevich, V. Baranchugov, G. Salitra, D. Aurbach, M.A. Schmidt, *J. Electrochem. Soc*. **155** (2008) 132.

3 M. Holzapfel, C. Jost, A. Prodi-Schwab, F. Krumeich, A. Wursig, H. Buqa and P. Novak, *Carbon*, **43** (2005) 1488-1498.

4 D. Aurbach, Y. Talyosef, B. Markovsky, E. Markevich, E. Zinigrad, L. Asraf, J. S. Gnanaraj, H.J Kim, *Electrochim. Acta* **50** (2004) 247–254.

5 D. Aurbach, K. Gamolsky, B. Markovsky, Y. Gofer, M. Schmidt, U. Heider, *Electrochim. Acta* **47** (2002) 1423–1439.

6 H. Srour, N. Giroud, H. Rouault and C. C. Santini, *ECS Trans*, **41** (2011) 23-28.

7 H. Srour, H. Rouault and C. Santini, *J. Electrochem. Soc*. **160** (2013) 66-69.

8 D. Aurbach, E. Zinigrad, Y. Cohen, H. Teller, *Solid State Ionics,* (2002), **148**, 405– 416.

9 J.-K. P*ark Principles and Applications of lithium secondar batteries*, Wiley –VCH, Weinheim (2012).

10 P. V. Braun, J. Cho, J. H. Pikul, W. P. King, H. Zhang, *Current Opinion in Solid State and Materials Science* **16** (2012) 186–198.

11 K. Zaghib, P. Charest, A. Guerfi, M. Dontigny, and K. Kinoshita; *ECS Trans*. **3** (2007) 89-93.

12 E. Ferg, R. J. Gummow, A. Dekock, and M. M. Thackeray, *J. Electrochem. Soc*. **141** (1994), 147.

13 N. Takami, H. Inagaki, T. Kishi, Y. Harada, Y. Fujita, and K. Hoshina, *J. Electrochem. Soc.* **156** (2009) 128.

14 B. Garcia, S. Lavallae, G. Perron, C. Michot and M. Armand, *Electrochim. Acta* **49** (2004) 4583-4588.

15 G.T. kim, M. Z. Xue, A. Balducci, M. Winter, S. Passerini, F. Alessandrini, G.B. Appetecchi, *J.Power Sources,* **199** (2012) 239-246.

16 H. Matsumoto, H. Sakaebe, K. Tatsumi, *J. Power Sources* **146** (2005) 45-50.

17 H. Ohno, *Electrochemical Aspects of Ionic liquids*, Second Edition, John Wiley & Sons, Inc., N.Y, (2011).

18 S.Seki, Y.Ohno, Y. Mita, N. Serizawa, K. Takei, *Electrochem Letters*, **1** (2012) 77-79.

19 H. Yoon, G. H. Lane, Y. Shekibi, P. C. Howlett, M. Forsyth, A. S. Best and D. R. MacFarlane, *Energy Environ. Sci*. **6** (2013) 979-986.

D Effect of Lithium Salts on the Transport and Electrochemical Properties of Nitrile-Functionalized Imidazolium-based Ionic Liquids.

As Lithium ion batteries are more and more present in consumer nomad devices and electric vehicles, the research are nowadays focused on the increase of their performance, and safety with simultaneous decrease of their cost and size (Moore low) [1].

Imidazolium-based ILs, the most thermally stable have been investigated as electrolyte components for Li-ion batteries [2], but their performance is lower compared with that of systems containing conventional electrolytes [3]. Several drawbacks have been identified namely linked to the use of graphite as a negative electrode [4]. To address this point, organic additives are often associated to the IL for use in graphite-based devices. Ethylene sulphite or acetonitrile vinylene carbonate have been proposed and show a certain stabilizing effect on graphite electrodes, due to the formation of a film evidenced by scanning electron microscopy [5].

Instead of using organic additives, that again render the lithium batteries less safe, the introduction of cyanomethyl or methylcarboxyl groups in the ILs (*i.e.* by functionalizing 1-ethyl-3-methyl imidazolium cations) have been considered as promising alternatives [6]. It has been reported that the incorporation of nitrile groups in imidazolium based ILs results in notable change in physicochemical, electrochemical, and conformational properties on the pure ILs [7]. Furthermore, it has been shown that for cyanoalkyl or carbonate-substituted pyrrolidinium-based ILs, the Li salt strongly coordinates with the functional groups [8]. The effect of the presence of these functional groups will surely have an effect on the properties of the IL as an electrolyte but, as far as the authors are aware of, no systematic study on this effect on the pure IL and on the mixtures IL/Li salt has been reported.

In order to address this question, we have selected two imidazolium-based ILs, one with an alkyl side chain – the 1-butyl-3-methylimidazolium bis(trifluoromethylsulphonyl) imide, $[C_1C_4Im][NTf_2]$ – and another with a nitrile functionalized alkyl side-chain–1-butylnitril-3-methylimidazolium bis(trifluoromethylsulphonyl)imide, $[C_1C_3CNIm][NTf_2]$. We have compared their physicochemical, electrochemical, and the evolution of their mass transport properties and cycling capacity when pure or when mixed with bis(trifluoromethylsulphonyl) imide lithium, $[Li][NTf_2]$, at the concentration of 1 $mol.L^{-1}$ corresponding to $[Li][NTf_2]$ mole fractions of 0.2262 and 0.2216 in $[C_1C_4Im][NTf_2]$ and $[C_1C_3CNIm][NTf_2]$, respectively.

D1 Self-diffusion coefficient

The pulse-field gradient spin echo DOSY NMR constitutes a tool to estimate the transport properties in these systems. The diffusion coefficients of the NTf_2 anion and of the cations ($[C_1C_4Im^+]$, $[C_1C_3CNIm^+]$ and $[Li^+]$) were measured by ^{19}F ^1H and ^7Li NMR respectively, from 278 to 353 K, in the pure ILs and in ILs mixed with $[Li][NTf_2]$. The results are presented in tables (D1 and D2).

Table D1: Self-diffusion coefficients of $[C_1C_4Im][NTf_2]$ and its binary mixture $[C_1C_4Im][Li][NTf_2]$ at 1 $mol.L^{-1}$ of $[Li][NTf_2]$.

	$[C_1C_4Im][NTf_2]$			$[C_1C_4Im][Li][NTf_2]$		
	$D_{Ion}x10^{-11}$ / $(m^2.s^{-1})$			$D_{Ion}x10^{-11}$ / $(m^2.s^{-1})$		
T (K)	$D_{[C1C4Im]^+}$	$D_{[NTf2]^-}$	$D_{[Li]^+}$ (V)	D_{C1C4Im^+}	D_{NTf2^-}	D_{Li^+}
298	2.04	2.32	-	1.19	0.59	0.33
313	5.82	4.48	-	2.79	1.46	0.79
333	10.53	8.47	-	6.05	3.44	1.69
353	17.06	14.06	-	11.39	6.21	3.11

Table D2: Self-diffusion coefficients of $[C_1C_3CNIm][NTf_2]$ and its binary mixture $[C_1C_3CNIm][Li][NTf_2]$ at 1 $mol.L^{-1}$ of $[Li][NTf_2]$.

	$[C_1C_3CNIm][NTf_2]$			$[C_1C_3CNIm][Li][NTf_2]$		
	$D_{Ion}x10^{-11}$ / $(m^2.s^{-1})$			$D_{Ion}x10^{-11}$ / $(m^2.s^{-1})$		
T (K)	$D_{[C1C3CNIm]^+}$	$D_{[NTf2]^-}$	$D_{[Li]^+}$ (V)	$D_{[C1C3CNIm]^+}$	$D_{[NTf2]^-}$	$D_{[Li]^+}$
298	0.6	0.62		0.17	0.15	0.15
313	1.59	1.57		0.47	0.41	0.42
333	3.5	3.51		1.42	1.18	1.11
353	6.33	6.49		3.21	2.86	2.44

All the diffusion coefficients increase with increasing temperature, following an Arrhenius law. In neat $[C_1C_4Im][NTf_2]$ at 313 K, $D_{[C1C4Im^+]}$ and $D_{[NTf2^-]}$ were found equal to 5.82 and 4.48 x 10^{-11} m^2s^{-1} respectively. These values agree with those reported in the literature to within the mutual experimental uncertainties [9]. For the pure $[C_1C_4Im][NTf_2]$ we have observed that the cation diffuses faster that the anion, also in agreement with the literature [9-11]. In $[C_1C_3CNIm][NTf_2]$ at 313K, the diffusion coefficients of the two ions are similar and lower than in the previous IL (1.59 and 1.57 x 10^{-11} m^2s^{-1} respectively), which can be attributed to its higher viscosity.

In both binary systems $[C_1C_4Im][Li][NTf_2]$ and $[C_1C_3CNIm][Li][NTf_2]$, the diffusion coefficients of ($[C_1C_4Im^+]$, $[C_1C_3CNIm^+]$ and $[NTf_2^-]$ are lower than in the pure ILs, which is coherent with the

increase in viscosity. In $[C_1C_4Im][Li][NTf_2]$, the relative order of the diffusivities is $D_{[C1C4Im^+]} > D_{[NTf2^-]} > D_{[Li+]}$. Molecular dynamics simulations [12] and experimental studies [113-16] have proved that the lower value of $D_{[Li+]}$ can be explained by a coordination between $[Li^+]$ and $[NTf_2^-]$ leading to aggregates typically formed by clusters of one $[Li^+]$ and $2x[NTf_2^-]$. In $[C_1C_3CNIm][Li][NTf_2]$, the diffusion coefficients of the three ions are much smaller and very similar, particularly at low temperatures.

The plots of D versus the fluidity (η^{-1}) for both pure ILs and lithium mixtures show an excellent linearity suggesting that the Stokes – Einstein relationship is followed (Figure E1a and E1b). The comparison of the decrease of the slope of the curve D vs $1/\eta$ between pure IL $[C_1C_4Im][NTf_2]$ and their mixture with $[C_1C_4Im][Li][NTf_2]$ confirm that a higher drop for $D_{[NTf2]}$ than for $D_{[C1C4Im]}$ in agreement with a higher interaction/solvation of $[NTf_2^-]$ with $[Li^+]$[12, 17-19] (Figure D1a). Contrarily, in $[C_1C_3CNIm][NTf_2]$ and its binary mixture $[C_1C_3CNIm][Li][NTf_2]$ the slope for all ions are similar (Figure D1b), leading to the same decrease of the value of the slope of the curve D as a function of the fluidity $1/\eta$. This evolution could mean that both $[C_1C_3CNIm^+]$ and $[NTf_2^-]$ are in interaction with $[Li^+]$.

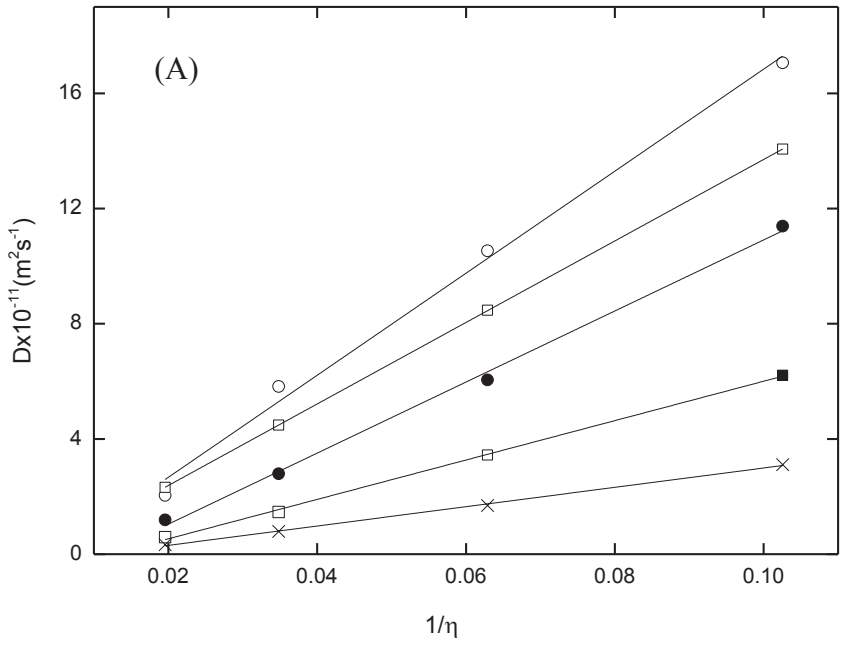

*η has been determined by P. Husson, submitted manuscript (publications: page 159).

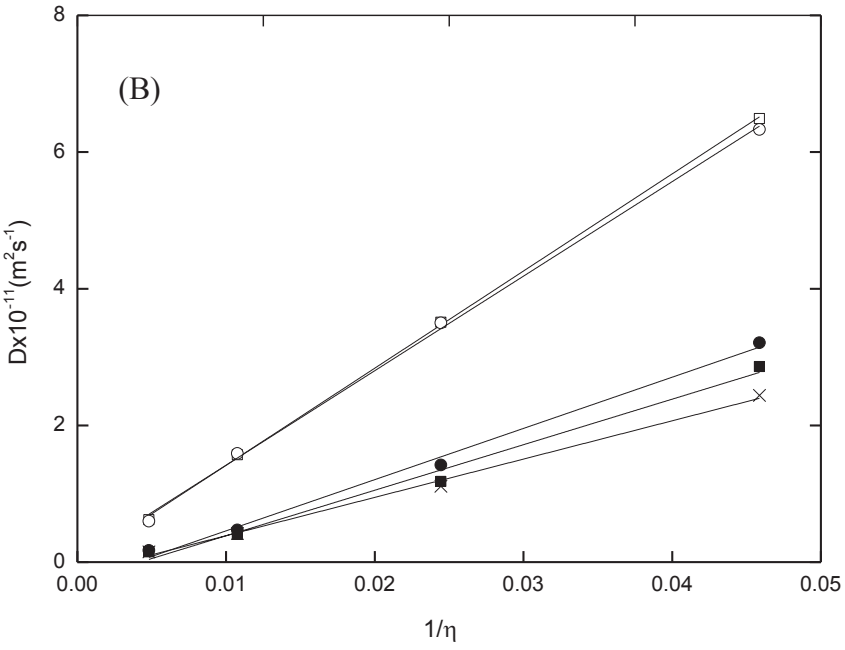

Figure D1: Diffusion coefficients plotted as a function of 1/η for all the ions.
(A) in $[C_1C_4Im][NTf_2]$ and $[C_1C_4Im][Li][NTf_2]$. ○, $C_1C_4Im^+$ in $[C_1C_4Im][NTf_2]$; ●, $C_1C_4Im^+$ in $[C_1C_4Im][Li][NTf_2]$; □, NTf_2^- in $[C_1C_4Im][NTf_2]$; ■, NTf_2^- in $[C_1C_4Im][Li][NTf_2]$; ×, Li^+ in $[C_1C_4Im][Li][NTf_2]$.
(B) in $[C_1C_3CNIm][NTf_2]$ and $[C_1C_3CNIm][Li]NTf_2]$. ○, $C_1C_3CNIm^+$ in $[C_1C_3CNIm][NTf_2]$; ●, $C_1C_3CNIm^+$ in $[C_1C_3CNIm][Li][NTf_2]$; □, NTf_2^- in $[C_1C_3CNIm][NTf_2]$; ■, NTf_2^- in $[C_1C_3CNIm][Li][NTf_2]$; ×, Li^+ in $[C_1C_3CNIm][Li][NTf_2]$.

D2 IR and NMR study

Few information are available on the nature of the coordination sphere of the $[Li]^+$ ion dissolved in functionalized ILs. It has been shown that the Li salt strongly coordinates the cyano group of cyanoalkyl chain of pyrrolidinium-based ILs [7]. To further investigate this fact, ^1H, ^7Li, ^{13}C and ^{15}N NMR spectra (Figures 2 to 7 Appendix II) and IR characterization of $[C_1C_3CNIm][NTf_2]$ and $[C_1C_3CNIm][Li][NTf_2]$ have been realized. The IR spectra of pure IL shows one band at 2248 cm^{-1} assigned to the vibration ν(C≡N). Yet, three bands at 2276, 2248 and 2171 cm^{-1} are observed in IR spectra of $[C_1C_3CNIm][Li][NTf_2]$ as can be seen on (Figure D2).

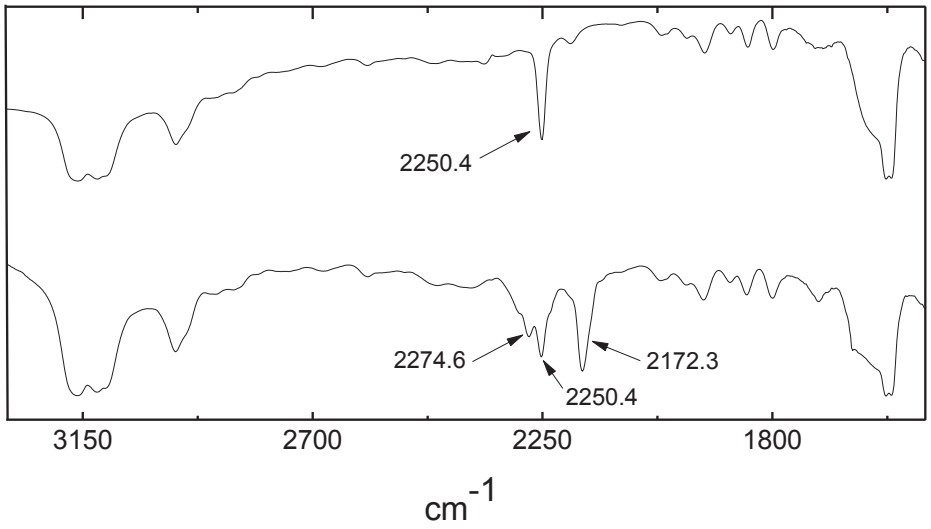

Figure D2: Infrared spectra of (A) the neat $[C_1C_3CNIm][NTf_2]$ and of (B) the mixture $[C_1C_3CNIm][Li][NTf_2]$.

The new band at 2276 cm^{-1} is assigned to the ν(C≡N) stretch mode of the solvent coordinated to $[Li^+]$, which causes a shift, towards higher wavenumbers, of 23 cm^{-1} [21]. The shifting of the ν(C≡N) vibration from 2248 cm^{-1} to 2171 cm^{-1} indicates a coordination between the π electrons of C≡N bond and $[Li^+]$ [22].

These intermolecular interactions must induce a modification of the electronic environment of the nitrogen atoms. The ^{15}N NMR spectra of $[C_1C_3CNIm][NTf_2]$ and $[C_1C_3CNIm][Li][NTf_2]$ (figure E3), which directly reflect the electronic changes on the N atoms, were analyzed. In the ^{15}N spectrum of $[C_1C_3CNIm][NTf_2]$ the resonance at 139 ppm/NH_3 (i.e.-242.6 ppm/CD_3NO_2) as assigned to the nitrogen atom of $[NTf_2]^-$ anion, while the other 3 chemical shift δN-C1, δN-C3CN and δC≡N at 171.68, 179.48, and 245.74 ppm/NH_3 (i.e. -209.9, 202.12 and -135.86 ppm/CD_3NO_2) respectively were assigned to the nitrogen atom of the imidazolium cation [23].

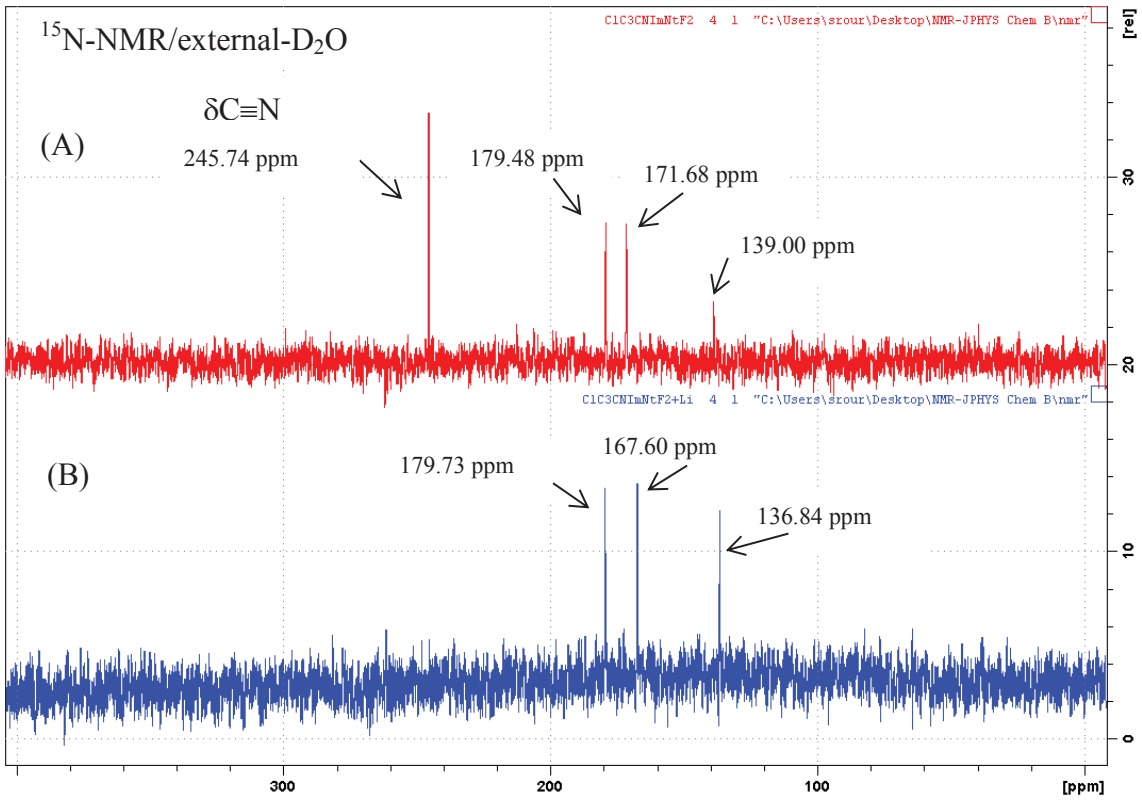

Figure D3: ^{15}N NMR spectra of (A) $[C_1C_3CNIm][NTf_2]$ and (B) $[C_1C_3CNIm][Li][NTf_2]$ recorded at RT and using $NH_{3(liq)}$ as external standard.

In the ^{15}N spectrum $[C_1C_3CNIm][Li][NTf_2]$ $\delta N\text{-}C_1$ is unchanged (179.73 ppm/NH_3 i.e. -202.12 ppm/CD_3NO_2). However, $\delta N\text{-}C_3CN$ is deshielded (167.60 vs 171.68 ppm/NH_3 i.e -214 vs -209.92 ppm/CD_3NO_2), indicating a change in negative charge on the nitrogen atoms.

No resonance of CN is observed, probably reflecting a dynamic process between free and coordinated population of the CN with the lithium salt. In the ^{13}C NMR spectra (Figure 5, appendix II) the chemical shift of -$\boldsymbol{C}H_2CN$ was shielded of $\Delta\delta$= 0.115 ppm, no other significant changes were observed. The NMR and IR results confirm that $[C_1C_3CNIm^+]$ and $[Li^+]$ are interconnected mainly through a π-cation interaction between $[Li^+]$ and the C≡N function as represented in Scheme D1. This hypothesis of coordination of the lithium ion by the functionalized IL is also compatible with the evolution of the diffusion coefficients of D versus 1/viscosity (η^{-1}), as explained above (Figure D1). The ^{15}N and ^{13}CNMR spectra of $[C_1C_4Im][NTf_2]$ and $[C_1C_4Im][Li][NTf_2]$ show no difference (Figures 2 and 7, Appendix II) confirming that only $[NTf_2]^-$ anions [2 to 4] are surrounding around the $[Li^+]$ ion [15-16, 21-22].

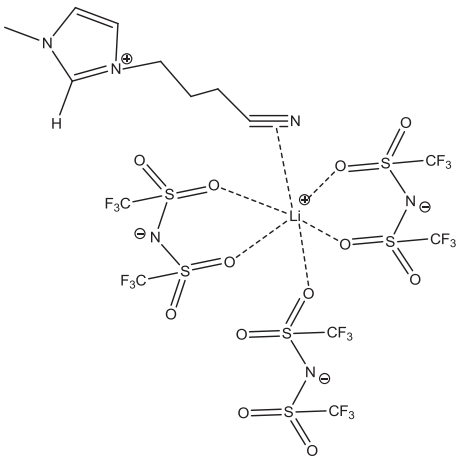

Scheme D1: Lithium coordination sphere.

D3 Electrochemical stability

The electrochemical stability of ILs is estimated on the basis of the electrochemical window (EW), which is another important factor that governs such aspects of lithium ion battery performance as the out voltage and the charge-discharge cycling property. The values of the cathodic ($E_{cathodic}$) and anodic (E_{anodic}) limits, and electrochemical windows ($\Delta E=E_{anodic}-E_{cathodic}$) of these ILs and their binary mixtures at 1 mol.L^{-1} of [Li][NTf_2] at different temperatures are summarized in Tables (6 and 7 Appendix II). For pure ILs, no significant change in the EW is observed. For both ILs, EW is constant at different temperatures, proving the absence of water impurities [24].

The presence of Li salt shifted the reduction potential (E_c) affording a wider EW than in the pure ILs, as has been generally reported [19-22]. The anodic stability is roughly the same, but the cathodic stability is higher of ≈ 1.5 V for [C_1C_4Im][Li][NTf_2] and of ≈ 0.7 V for [C_1C_3CNIm][Li][NTf_2].

D4 Battery tests

The electrochemical performance of the negative Cgr or LTO and positive LFP electrodes was tested at 333 K in full cell lithium ion configurations using an IL-based electrolyte among [C_1C_3CNIm][Li][NTf_2] and [C_1C_4Im][Li][NTf_2] at 1.0 mol.L^{-1} of [Li][NTf_2] without any electrolyte additive. The objective was to observe the effect of nitrile group on the cycling results through its influence on the formation of the Solid Electrolyte Interphase (SEI) on the graphite based electrode [1,5].The cycling experiments were undertaken with the use of an Arbin multi-channel potentiostat/galvanostat between 2.6 V and 3.7 V for the Cgr/LFP technology, respectively 1 V and 2.8 V for the LTO/LFP one.

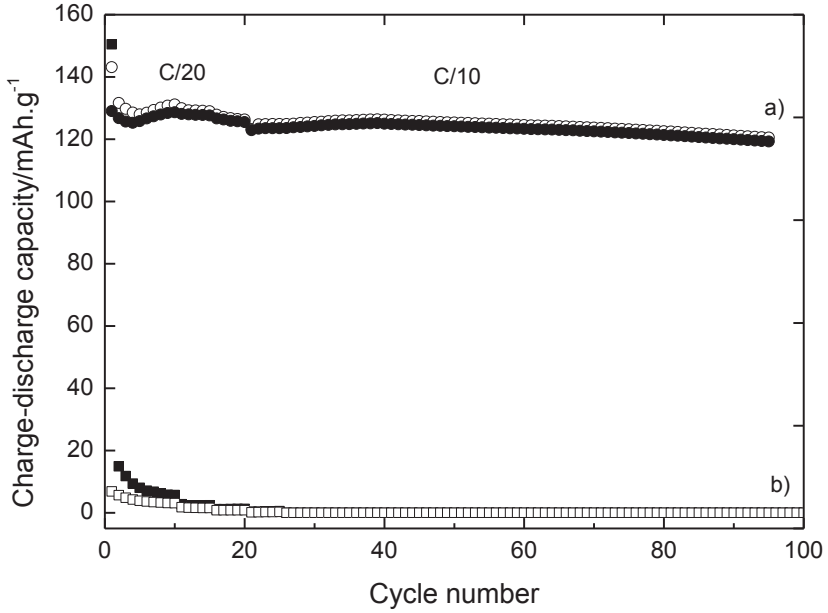

Figure D8: Cycling performance of $[C_1C_4Im][NTf_2]$ and $[C_1C_3Im][NTf_2]$ at 1 mol.L^{-1} of $LiNTf_2$ with LTO/LFP full systems at 333 K.

Figure D8 shows the cycling performance of $[C_1C_4Im][NTf_2]$ and $[C_1C_3CNIm][NTf_2]$ at 1 mol.L^{-1} of $[Li][NTf_2]$ with LTO/LFP full systems at 333 K at the same rate of charge and discharge : first at C/20 (corresponding to a current for a complete charge or discharge in 20 hours), then at C/10 (complete charge or discharge in 10 hours) on several tens of cycles. The same protocol was applied on the complete system (Cgr/LFP).

At the first step of charge at C/20 the lithium ion cell based on $[C_1C_3CNIm][Li][NTf_2]$ displayed an initial capacity of about 150 mAh.g^{-1} with the typical charge curve of the LTO/LFP system. Then the recovered capacity in discharge is reduced at less than 20 mAh.$g^{-1}$and decreases continuously up to 0 mAh/g after 20 cycles. Contrarily, the lithium ion cell based on $[C_1C_4Im][Li][NTf_2]$ exhibits an initial capacity of about 140 mAh/g close to the expected one and reaching 130 mAh/g yet after 90 cycles (more than 95 % efficiency).

As observed on Figure D9, with $[C_1C_4Im][Li][NTf_2]$ the profile of the discharge curve remains regular with the typical plateau of the LTO/LFP system, during the first step of charge/discharge.[1] With $[C_1C_3CNIm][Li][NTf_2]$ as a blocking interface resulting probably from interactions between LTO electrode and $[C_1C_3CNIm][Li][NTf_2]$ was built during the first charge (Figure D10). As $[Li][C_1C_3CNIm][NTf_2]$ and $[Li][C_1C_4Im][NTf_2]$ have a similar Ec value, this result could also be due

to the reduction of the [C_1C_3CNIm] cation. Further electrochemical characterizations are so in progress with the objective to determine the nature and the formation reactions of such film.

With both electrolytes vinylene carbonate has to be added to improve cycling performances, (Figure 8- Appendix II) [5-6]. Acetonitrile used as additive with ILs based electrolyte has already proved its positive effect on the performances of Cgr based lithium-ion cells. However, the nitrile group grafted to the imidazolium cation in [C_1C_3CNIm][Li][NTf_2] appears to be not so effective. Indeed, in the case of [C_1C_3CNIm][Li][NTf_2] the complex structuration of the electrolytic media characterized by higher density, higher viscosity than [C_1C_4Im][Li][NTf_2] reduces, even prevents any cycling behaviour due probably to the coordination and solvation of the lithium ions, *vide supra*. The substitution of a nitrile functional group does not contribute to the surface film formation, as claimed but mainly coordinate the Li salt.

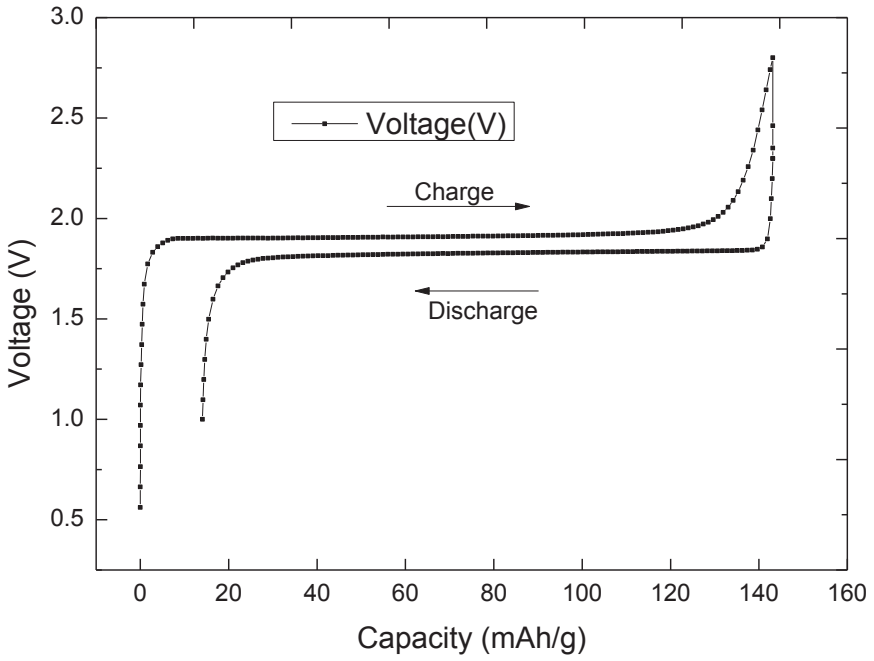

Figure D9: Charge-Discharge Capacity of [C_1C_4Im][NTf_2] at 1 mol.L^{-1} of $LiNTf_2$ with LTO/LFP C/20 and 333 K.

In [C_1C_3CNIm][NTf_2], at the first step of charge at 0.05 C the lithium ion cell displayed an initial capacity of about 150 mAh.g^{-1} with the typical charge curve of the LTO / LFP system, as shown in Figure D10. The intercalation of [Li^+] ions occurred during the first charge. Then the recovered capacity in discharge is reduced at less than 20 mAh/g and decreases continuously up to 0 mAh/g after 20 cycles.

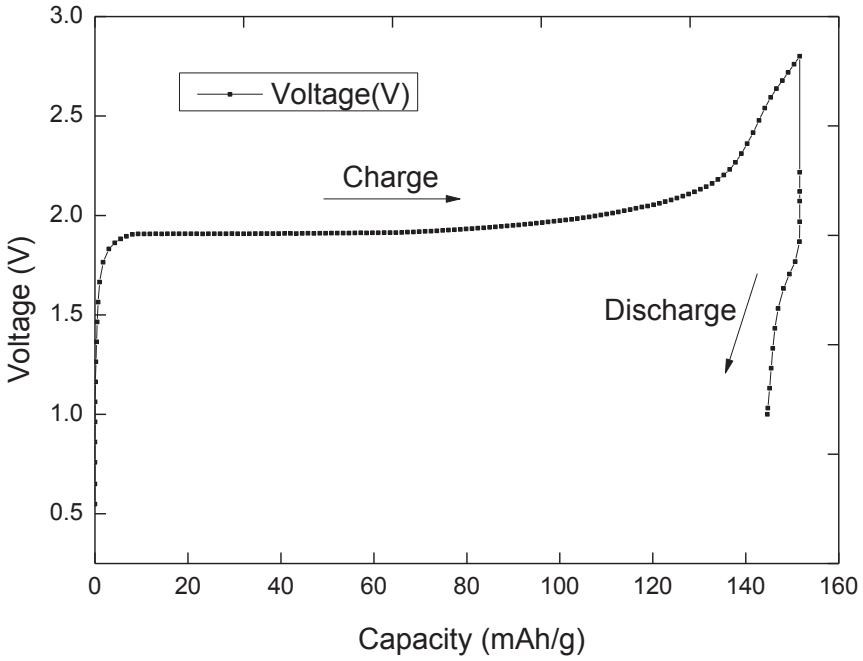

Figure D10: Charge-Discharge Capacity of $[C_1C_3CNIm][NTf_2]$ at 1 mol.L^{-1} of $LiNTf_2$ with LTO/LFP C/20 and 333 K.

A blocking interface resulting from interactions between the LTO electrode and the $[C_1C_3CNIm][Li][NTf_2]$ seems to be built during the first charge. Further electrochemical and physico-chemical characterizations are so in progress with the objective to determine the nature and the formation reactions of such film.

D5 Conclusions

In order to estimate the potential of ILs to be used as electrolytes in lithium batteries, the effect of the presence of lithium salts and of a nitrile functionalization of an imidazolium IL was studied on the transport and electrochemical properties of these components. Both the presence of nitrile group and the addition of $[Li][NTf_2]$ increase the viscosity of the liquid. In the mixtures $[C_1C_3CNIm][Li][NTf_2]$, the lithium ion has strong interactions with both anion and cation of the IL contrarily to the lithium in the $[C_1C_4Im][NTf_2]$ mixtures in which it is only surrounded by the anion.

The presence of nitrile functional group in $[C_1C_3CNIm][Li][NTf_2]$ appears to be not effective to the building of the SEI on the graphite based electrode. Consequently no improvement of the behaviour in cycling for the Cgr/LFP full system may be expected from so functionalized IL. The same conclusion about this IL electrolyte may be drawn for the LTO/LFP system: it reduces, even prevents any cycling behaviour due probably to the coordination and solvation of the lithium ions.

D6 References

1 Park, J.-K.; Principles and Applications of lithium secondary batteries, *Wiley –VCH, Weinheim.* (2012).

2 Wasserscheid, P.; Welton, T.; Ionic liquids in synthesis, *Wiley-VCH, Weinheim*. (2008), Maton. C, De. V. N, Stevens. C. V, *Chem. Soc. Rev.*, **42** (2013) 5963-5977.

3 Lewandowski, A.; Swiderska-Mocek, A. *J. Power Sources.* **171** (2007), 938.; Armand, M.; Endres, F.; MacFarlane, D. R.; Ohno, H.; Scrosati, B. *Nature Mater*. **9** (2009), 621; Kim, J.-K.; Matic, A.; Ahn, J.-H.; Jacobsson, P. *J. Power Sources*. **195** (2010) 7639; Srour, H.; Giroud, N.; Rouault, H.; Santini, C. C. *ECS Trans*. **41** (2012) 23. and *J. Electrochem. Soc*. **160** (2013), A1.

4 Seki, S.; Kobayashi, Y.; Miyashiro, H.; Ohno, Y.; Usami, A.; Mita, Y.; Kihira, N.; Watanabe, M.; Terada, N. *J. Phys. Chem. B*., **110** (2006) 10228.

5 Holzapfel, M.; Jost, C.; Novak, P. *Chem. Commun*. (2004), 2098; Holzapfel, M.; Jost, C.; Prodi-Schwab, A.; Krimeich, F.; Würsig, A.; Buqa, H.; Novak, P. *Carbon* **43** (2005) 1488; Balducci, A.; Jeong, S. S.; Kim, G. T.; Passerini, S.; Winter, M.; Schmuck, M.; Appetecchi, G. B.; Marcilla, R.; Mecerreyes, D.; Barsukov, V.; Khomenko, V.; Cantero, I.; De, M. I.; Holzapfel, M.; Tran. N, *J. Power Sources.* **196** (2011) 9719.; Egashira, M.; Tanaka, T.; Yoshimoto N.; and Morita, M.; *Solid State Ionics*, **219** (2012) 29.

6 Egashira, M.; Okada, S.; Yamaki, J.-i.; Dri, D. A.; Bonadies, F.; Scrosati, B.; *J. Power Sources*. **138** (2004) 240; Egashira, M.; Nakagawa, M.; Watanabe, I.; Okada, S.; Yamaki, J.-i. *J. Power Sources.* **146** (2005) 685; Egashira, M.; Tanaka, T.; Yoshimoto, N.; Morita, M. *Solid State Ionics.* **219** (2012) 29.

7 Zhang, Q.; Li, Z.; Zhang, J.; Zhang, S.; Zhu, L.; Yang, J.; Zhang, X.; Deng, Y. *J. Phys. Chem. B.* **111** (2007) 2864.

8 Baek, B.; Lee, S.; Jung, C.; Int. *J. Electrochem. Sci.,* **6** (2011) 6220; Nguyen, D. Q.; Oh, J. H.; Kim, C. S.; Kim, S. W.; Kim, H.; Lee, H.; Kim, H. S. *Bull. Korean Chem. Soc*. **28** (2007) 2299.

9 Tokuda, H.; Tsuzuki, S.; Susan, M. A. B. H.; Hayamizu, K.; Watanabe, M. *J. Phys. Chem. B.* **110(39)** (2006) 19593.

10 Podgorsek, A.; Salas, G.; Campbell, P.S.; Santini, C.C.; Padua, A.A.H; Costa Gomes, M.F.; Fenet, B.; Chauvin, Y. *J. Phys. Chem. B*. **115** (2011) 12150.

11 Castiglione, F.; Moreno, M.; Raos, G.; Famulari, A.; Mele, A.; Appetecchi, G. B.; Passerini, *S. J. Phys. Chem. B.* **113** (2009) 10750.

12 Borodin, O.; Smith, G.D.; Henderson, W. *J. Phys. Chem. B.* **110** (2006) 16879.

13 Castiglione, F.; Ragg, E.; Mele, A.; Appetecchi, G.B.; Montanino, M. Passerini, S. *J. Phys. Chem. Letters.* **2** (2011) 153.

14 Lassègues, J.C.; Grondin, J.; Talaga, D. *Phys. Chem. Chem. Phys*. **8** (2006) 5629.

15 Umebayashi, Y.; Mori, S.; Fujii, K.; Tsuzuki, S.; Seki, S.; Hayamizu, K.; Ishiguro, S. *J. Phys. Chem. B* **114** (2010) 6513.

17 Duluard, S.; Grondin, J.; Bruneel, J.L.; Pianet, I. ; Grélard, A.; Campet, G.; Delville, M.H.; Lassègues, J.C. *J. Raman Spectrosc*. **39** (2008) 627.

18 Troncoso, J.; Cerdeirina, C. A.; Sanmamed, Y. A.; Romani, L.; Rebelo, L. P. N. *J. Chem. Eng. Data*. **51** (2006) 1856.

19 Tsuzuki, S.; Hayamizu, K.; Seki, S. *J. Phys. Chem. B.* **114** (2010) 16329.

20 Nicotera, I.; Oliviero, C.; Henderson, W.A.; Appetecchi, G.B.; Passerini, S. *J. Phys. Chem. B.* **109** (2005) 22814.

21 Hayamizu, K.; Tsuzuki, S.; Seki, S.; Fujii, K.; Suenaga, M.; Umebayashi, Y. *J. Chem. Phys*. **133** (2010) 194505.

22 Xuan, X.; Zhang, H.; Wang, J.; Wang, H.; J. Phys. Chem. A. **108** (2004) 7513.

23 Siriwardana, A. I.;Torriero, A. A. J.;Reyna-Gonzalez, J. M.; Burgar, I. M.; Dunlop, N. F; Bond, A. M.; Deacon G. B.; MacFarlane, D. R.; *J. Org. Chem.* **75** (2010) 8376.

24 Lycka, A.; Dolecek, R.;. Simunek, P.; Machacek, V.; *Magn. Reson. Chem.* **44** (2006) 521.

25 M. Hayyan,M.; Mjalli, F. S.; Hashim, M. A.; Al, N. I. M.; Mei, T. X. *J. Ind. Eng. Chem.* **19** (2013) 106.

Chapter 3
Conclusions and Perspectives

1. Conclusions

Among all the existing batteries, lithium ion batteries are the most used for nomad devices 63% and its global market is blossoming due to their use in electric cars. So the price of lithium-ion batteries has dropped by 20-50% during the last few years. The ILs which is safer than organic carbonates will be potential substitute if their cost and efficiency are improved.

The aim of my PhD was to design new synthetic routes reducing wastes and cost, and novel ILs to tune their physical-chemical and electrochemical properties to improve their performances as electrolytes in Li-ion cell based on Cgr /LFP and LTO/LFP as electrodes.

For the common ILs, an alternative synthetic silver and water free route for the metathesis reaction which is run at the temperature of the melting point of the amine halide salts, playing the role of solvent, in the presence of Na or Li salt of the chosen anion A. Therefore, imidazolium, phosphonium pyrrolidinium based ILs and anions associated with different anions such as dicyanamide, thiocyanate, tetrafluoroborate and Bis(trifluoromethylsulfonyl)imide were obtained in high purity ($\geq$ 99.5%) and high yields. This route is very well adapted for water miscible ILs preparation (Scheme 1).

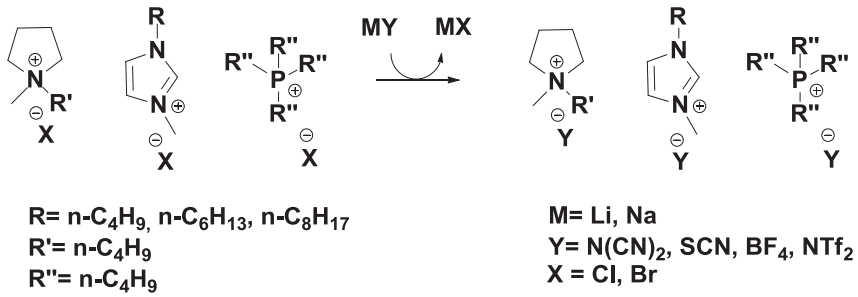

Scheme 1: water free metathesis reaction.

Then cycling performances of $[C_1C_nIm][Li][NTf_2]$ n=2,6 with C_{Li}= 1.0, 1.6 mol.L^{-1} and $[C_1C_1C_nIm][Li][NTf_2]$ n=4, 6 C_{Li}= 1.0 mol.L^{-1} as electrolytes, at 298 and 333K in Li-ion cells based on Cgr/LFP and LTO/LFP electrodes have been studied. The influence of the substitution of imidazolium ring on the cyclic performance in different experimental conditions (temperature concentration of lithium salt, organic additives) have been evaluated.

For Li-ion cell based on LTO/LFP, with all electrolytes, in absence of additive, a high cyclic efficiency was observed (Figure 1).

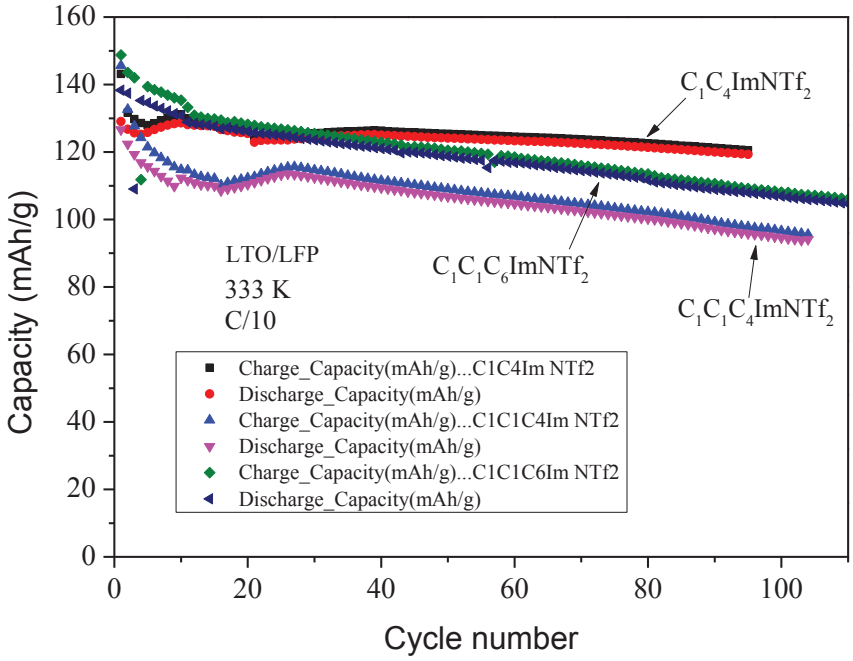

Figure 1: Charge-discharge capacity of LTO/LFP coupled with $[C_1C_1C_nIm][NTf_2]$ (n=4,6) at 333K at C/10 rate.

While, for Li-ion cell based on Cgr/LFP, the cyclic efficiency was dependent of the presence additive and strongly influenced by the nature of imidazolium ring.

For Li-ion cell based on Cgr/LFP with all chosen electrolytes cycling performances have been improved by i) reducing the viscosity of the electrolyte (increase of the temperature and decrease the C_{Li}; ii) replacing H atom of the $C_{2\text{-}H}$ by alkyl group (CH_3-) iii) extending alkyl side chain of imidazolium ring.

The cycling performances run with these electrolytes (with C_{Li}= 1 $mol.L^{-1}$ at 333K) increased inversely to the variation of viscosity and D_{Li}^{+} values: $[C_1C_1C_6Im][Li][NTf_2]$> $[C_1C_1C_4Im][Li][NTf_2]$> $[C_1C_6Im][Li][NTf_2]$> $[C_1C_4Im][Li][NTf_2]$.

With 5 vol% VC in $[C_1C_1C_6Im][Li][NTf_2]$ C_{Li}= 1 $mol.L^{-1}$ a high reversible capacity (120 mAh/g) and good capacity retention at C/20 (first 10 cycles) and C/10 (20 cycles) more than 90% of the expected capacity has been recovered at 333 K. The capacity remains ~120 mAh/g over 100 cycles contrary to the organic electrolyte ($LiPF_6$:DMC:EC) (Figure 2).

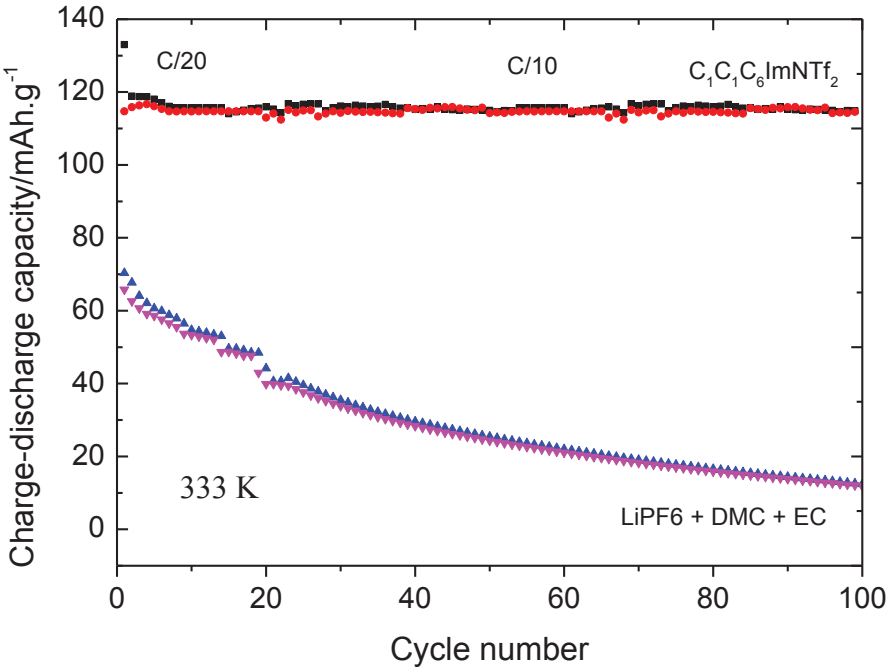

Figure 2: Cycle performance of Cgr/LFP cell with different electrolytes: $[C_1C_1C_6Im][Li][NTf_2]$ at 5%vol of VC and organic electrolyte at 333 K.

The formation of an interface/organization of alkyl side chain parallel to the Cgr surface affording a stable interface (SEI) could explain this unexpected result. Understanding of this interface IL/Cgr should remove the technological barrier that is the use of VC as additive in Cgr/LFP devices with $[Im][Li][NTf_2]$ as electrolytes. Further investigations in the identification of interface IL/Cgr are currently under study in our team.

The goal of my research theme is to replace flammable organic solvents by safer ILs. The use of mixture of ILs and organic additive to improve the performance in batteries invalidate the safety issue. Thus the use of functionalized alkyl side chain of imidazolium ring was done. With $[C_1C_3CNIm][Li][NTf_2]$ the complex structuration of the electrolytic media characterized by high viscosity reduces, even prevents any cycling behaviour in Cgr/LFP devices, due to the coordination and solvation of the lithium ions (Scheme 2).

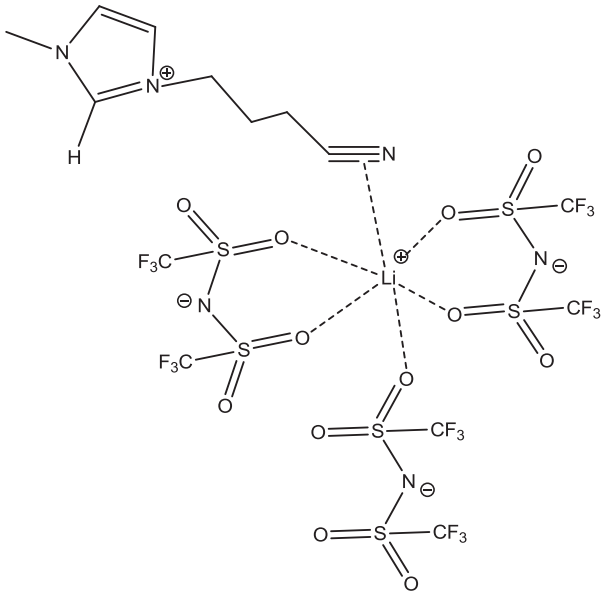

Scheme 2: Lithium coordination sphere.

Moreover, with LTO/LFP devices, a blocking interface resulting from interactions between the LTO electrode and the $[C_1C_3CNIm][Li][NTf_2]$ was built during the first charge (Figure 3).

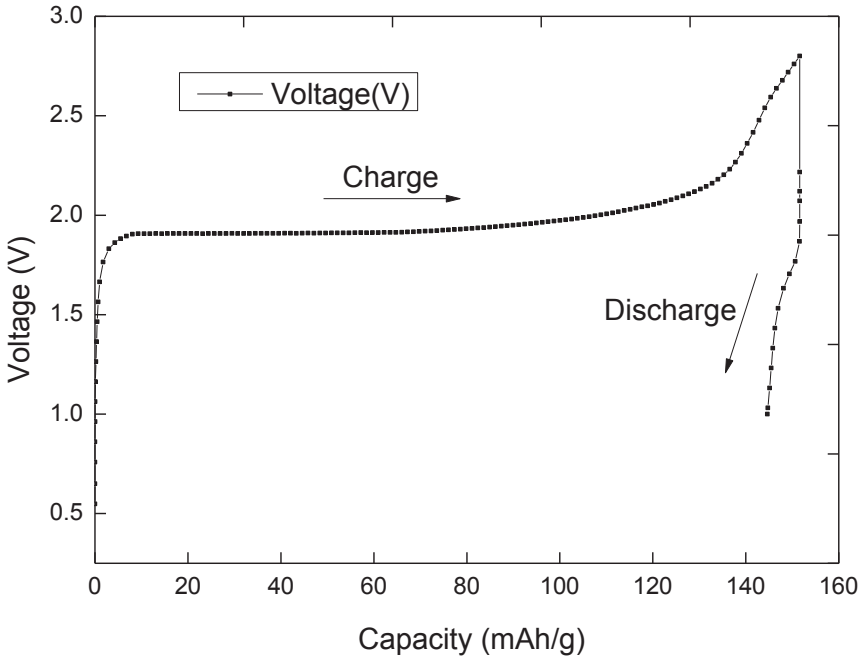

Figure 3: Charge-discharge capacity of $[C_1C_3CNIm][NTf_2]$ at 1 mol.L^{-1} of $LiNTf_2$ with LTO/LFP at C/20 and 333 K.

2. Perspectives

Further improvement in cycling with [Im][Li][NTf_2] as electrolytes could be divided in three main direction:

1. Improvement of our knowledge on the interface IL/Cgr. Current investigations in the identification by several surface techniques of the nature of this interface IL/Cgr on post mortem cells are under study in our team.

2 For all ILs based on NTf_2 anion, the Li-ion cells show low performance at 278 K due to high viscosity. Other anions such as dicyanamide, lowering the viscosity should be considered.

3. Substitution of the flammable additive by safer functionalized ILs

Others and us report that alkyl carbonate VC, is required in Li-ion cell based on Cgr to obtain SEI. One possible route should be ILs functionalized by carbonate, (Scheme 3).

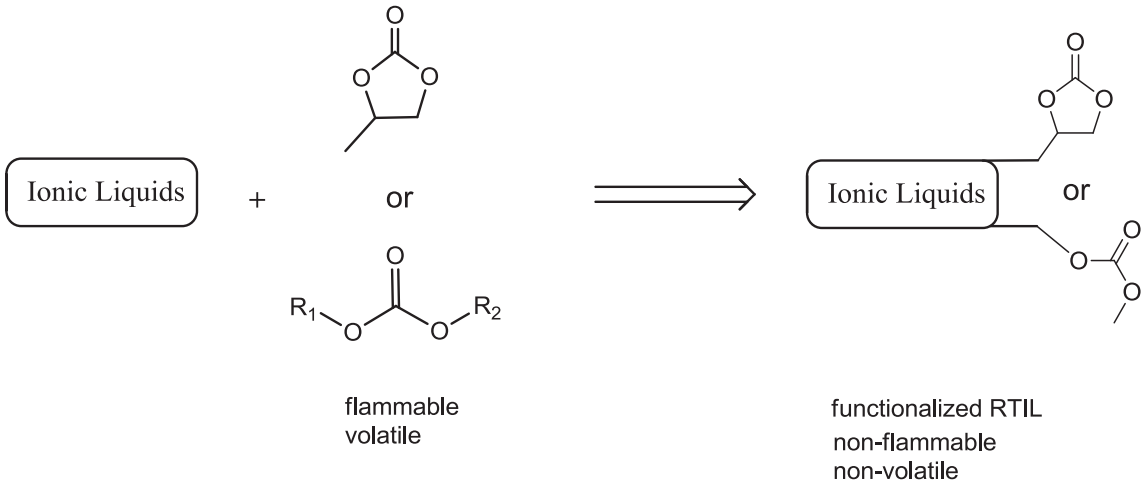

Scheme 3: RTILs attached to carbonate functional group.

But carbonate derivate ILs could not be obtained by classical metathesis route, due to LiCl coordination by this function (Scheme 4) [1].

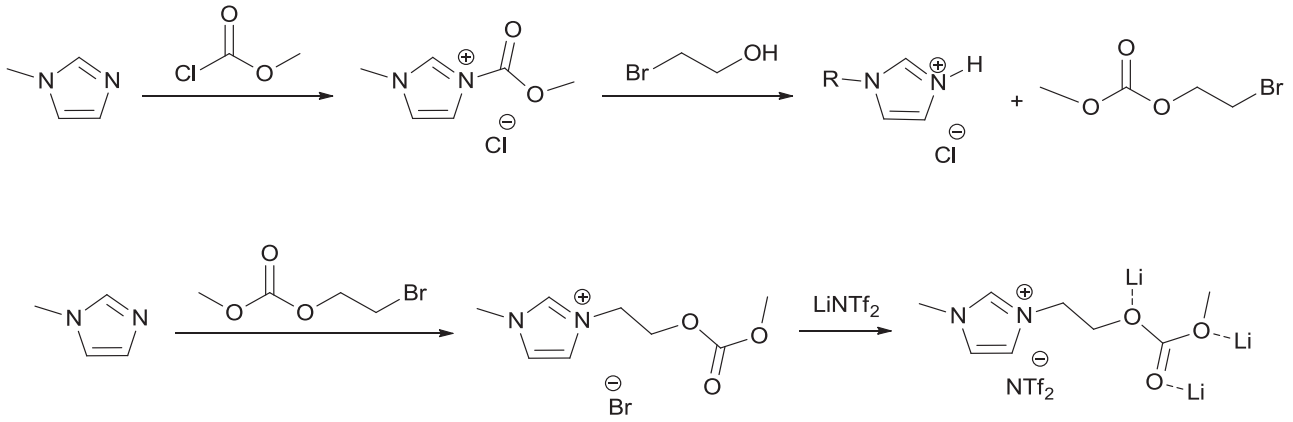

Scheme 4: Synthetic route of ILs containing an alkyl carbonate group [1].

We are currently developping a lithium free novel, and selective synthesis of carbonate-functionalized ionic liquids [2]. The condensation of methylchloroformate on 3-methyl,1-ethanolimidazoliumbis(trifluoromethane)sulfonimide in the presence of .1-methylimidazole as an acid scavenging, affords 1-[2-(methoxycarbonyloxy)ethyl]-3-methylimidazolium-bis(trifluoromethane)sulfonimide (Scheme 5, see experimental part Appendix III page 155).

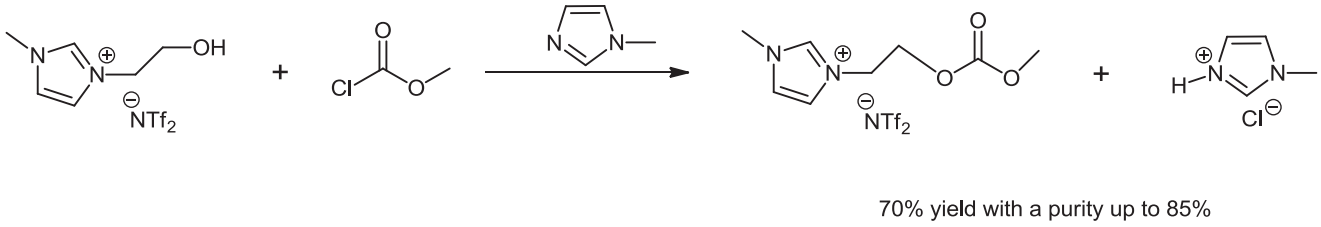

Scheme 5: Reaction scheme for the synthesis of carbonate functionalized ILs**.**

The expected advantage of these IL-carbonates is that:

- they would favor the SEI formation on Cgr surface,
- In their mixture with $LiNTf_2$, the carbonate group coordinates the Li^+ cation.

  A possible formation of $[Li(carbonate)][NTf_2]^+$ instead of $[Li(NTf_2)_2]^-$ would improve the Li^+ diffusion.

References

1. Nguyen, D.Q., J.H. Oh, C.S. Kim, S.W. Kim, H. Kim, H. Lee, H.S. Kim, *Bull. Korean Chem. Soc*. **28** (2007) 2299-2302.
2. H. Srour, H. Rouault, C. C. Santini, *FR-Pat,* (2013) n°13 51205

Experimental part
Appendix I, II and III

Appendix I

1-Experimental Part

Metathesis reaction: General synthetic method

1-butyl-3-methyl-imidazolium chloride heated gently at 70°C. The salt of lithium or sodium of each anion were added to the melt under argon and stirred for 24 h. The resultant product was dissolved in CH_2Cl_2 (THF is used for dicyanamide anion) and stirred for 20 min to precipitate the resulting halide salt (NaCl or LiCl) which was filtered off (0.2 μm filter). The resulting filtrate was placed in the fridge (-5°C) for one night for complete precipitation of the halide salt, in case of salt precipitation another filtration was performed and the resulting filtrate evaporated to dryness.

Note that for N-butyl-N-metylpyrrolidinium chloride and tetrabutylphosphonium bromide melting arournd ~120°C, the exchange reactions were performed at this temperature. ILs were kept under high vacuum (10^{-5} mbar) at room temperature for 24 h then stocked under argon in glove box. Their water content was lower than 100 ppm, as assessed by Karl Fisher titration. The chloride content was lower than 0.1% as shown by high resolution mass spectra (MS QTOF).

Synthesis and characterization

1-butyl-3-methylimidazolium dicyanamide: $[C_1C_4Im][N(CN)_2]$

$[Na][N(CN)_2]$ (1.12 g, 12.63 mmol) was added with a Bush tube into melt $[C_1C_4Im][Cl]$ (2 g; 11.49 mmol) at ~ 70°C and kept under stirring for 24 h. After cooling down at 25°C, THF (20 mL) was added. The white precipitate of NaCl was filtered, and the filtrate was kept at -5°C overnight to complete the precipitation of NaCl which was filtered off; this work up was repeated until no more NaCl precipitate observed. Evaporation of THF afforded $[C_1C_4Im][N(CN)_2]$ as a slightly yellow oil; (yield. 85%). ^{1}H-NMR (300 MHz, d6-DMSO): δ (ppm) : 9.10 (s, 1H, C2*H*) ; 7.74 (d, 1H, C4*H*) ; 7.67 (d, 1H, C5*H*) ; 4.16 (t, 2H, NCH_2) ; 3.85 (s, 3H, NCH_3) ; 1.75 (qt, 2H, $CH_2CH_2CH_2$) ; 1.23 (st, 2H, $CH_2CH_2CH_3$) ; 0.85 (t, 3H, CH_2CH_3) ; ^{13}C$^{[84]}$-NMR (300MHz, d6-DMSO) : δ (ppm) : 135.3 (C2H) ;123.5 (*C*4H) ; 122.2 (*C*5H) ; 119.74 (N*C*N); 49.81 (N*C*H_2) ; 35.8 (N*C*H_3) ; 31.5 ($CH_2CH_2CH_2$) ; 18.9 ($CH_2CH_2CH_3$) ; 12.8 (CH_2CH_3). Electrospray, MS (+ve): m/z 139 (100% - $C_1C_4Im^+$), MS (-ve): m/z 66 (100% dca^-).

1-butyl-3-methylimidazolium thiocyanate: $[C_1C_4Im][SCN]$

Slightly yellow clear oil, 90% yield. ^{1}H-NMR (300 MHz, CD_2Cl_2):δ (ppm) : 9.15 (s, 1H, C2*H*) ; 7.55 (d, 1H, C4*H*) ; 7.53 (d, 1H, C5*H*) ; 4.31 (t, 2H, NCH_2) ; 4.04 (s, 3H, NCH_3) ; 1.90 (qt, 2H, $CH_2CH_2CH_2$) ; 1.38 (st, 2H, $CH_2CH_2CH_3$) ; 0.92 (t, 3H, CH_2CH_3) ; ^{13}C$^{[84]}$-NMR (300 MHz, CD_2Cl_2)

: δ (ppm) : 136.48 (S*C*N); 131.58 (*C*2H) ;123.80 (*C*4H) ; 122.38 (*C*5H) ; 49.54 (N*C*H_2) ; 36.54 (N*C*H_3) ; 32.01 (CH_2*C*H_2CH_2) ; 19.8 (CH_2*C*H_2CH_3) ; 13.6 (CH_2*C*H_3). Electrospray, MS (+ve): m/z 139 (100% - $C_1C_4Im^+$), MS (-ve): m/z 58 (100% $^-$SCN).

1-butyl-3-methylimidazoliumtetrafluoroborate:[C_1C_4Im][BF_4]

Slightly yellow clear oil, 90% yield. ^{1}H-NMR (300 MHz, CD_2Cl_2):δ (ppm) : 8.87 (s, 1H, C2*H*) ; 7.43 (d, 1H, C4*H*) ; 7.42 (d, 1H, C5*H*) ; 4.15 (t, 2H, NC*H*$_2$) ; 3.92 (s, 3H, NC*H*$_3$) ; 1.85 (qt, 2H, CH_2C*H*$_2$$CH_2$) ; 1.32 (st, 2H, CH_2C*H*$_2$$CH_3$) ; 0.91 (t, 3H, CH_2C*H*$_3$) ; ^{13}C$^{[84]}$-NMR (300 MHz, CD_2Cl_2) : δ (ppm) : 136.28 (C2H) ;123.66 (*C*4H) ; 122.25 (*C*5H) ; 49.69 (N*C*H_2) ; 36.10 (N*C*H_3) ; 31.84 (CH_2*C*H_2CH_2) ; 19.27 (CH_2*C*H_2CH_3) ; 13.05 (CH_2*C*H_3). ^{19}F-NMR (300 MHz, CD_2Cl_2); δ (ppm): -150.7 (s, BF_4). ^{11}B-NMR (300 MHz, CD_2Cl_2): δ (ppm): -0.96 (s, BF_4). Electrospray, MS (+ve): m/z 139 (100% - $C_1C_4Im^+$), MS (-ve): m/z 87 (100% $^-$$BF_4$).

1-butyl-3-methylimidazolium Bis (trifluoromethane)-sulfonimide: [C_1C_4Im][NTf_2]

Slightly yellow clear oil, 90% yield. ^{1}H-NMR (CD_2Cl_2): δ (ppm) : 8.73 (s, 1H, C2*H*) ; 7.28 (d, 1H, C4*H*) ; 7.24 (d, 1H, C5*H*) ; 4.15 (t, 2H, NC*H*$_2$) ; 3.90 (s, 3H, NC*H*$_3$) ; 1.83 (qt, 2H, CH_2C*H*$_2$$CH_2$) ; 1.32 (st, 2H, CH_2C*H*$_2$$CH_3$) ; 0.94 (t, 3H, CH_2C*H*$_3$) ; ^{13}C$^{[84]}$-NMR (CD_2Cl_2) : δ (ppm) : 134.3 (*C*2H) ; 124.3 (*C*4H) ; 122.4 (*C*5H) ; 118.2 (*C*F_3) ; 50.3 (N*C*H_2) ; 37.1 (N*C*H_3) ; 33.2 (CH_2*C*H_2CH_2) ; 19.8 (CH_2*C*H_2CH_3) ; 13.5 (CH_2*C*H_3). Electrospray, MS (+ve): m/z 139 (100% - $C_1C_4Im^+$), MS (-ve): m/z 280 (100% NTf_2^-).

1-hexyl-3-methylimidazolium dicyanamide: [C_1C_6Im][$N(CN)_2$]

Slightly yellow clear oil, >90% yield. ^{1}H-NMR (300 MHz, d6-DMSO): δ (ppm) : 8.68 (s, 1H, C2*H*) ; 7.45 (d, 1H, C4*H*) ; 7.41 (d, 1H, C5*H*) ; 4.16 (t, 2H, NC*H*$_2$) ; 3.86 (s, 3H, NC*H*$_3$) ; 1.84 (qt, 6H,CH_2C*H*$_2$C*H*$_2$C*H*$_2$$CH_2$) ; 1.27 (st, 2H, CH_2C*H*$_2$$CH_3$); 0.81 (t, 3H, CH_2C*H*$_3$) ; ^{13}C$^{[84]}$-NMR (300 MHz, d6-DMSO) : δ (ppm) :135.82 (*C*2H) ;123.62 (C4H) ; 122.28 (*C*5H) ; 119.74 (N*C*N), 49.68 (N*C*H_2) ; 35.73 (N*C*H_3) ; 30.56 (CH_2*C*$H_2CH_2CH_2CH_2$) ; 29.37 (CH_2CH_2*C*H_2CH_2); 25.21 (CH_2*C*H_2CH_2); 21.96(CH_2*C*H_2CH_3); 13.40 (CH_2*C*H_3). Electrospray, MS (+ve): m/z 167 (100% - $C_1C_6Im^+$), MS (-ve): m/z 66 (100% dca^-).

1-hexyl-3-methylimidazolium thiocyanate: [C_1C_6Im][SCN]

Slightly yellow clear oil, 90% yield. ^{1}H-NMR (300 MHz, CD_2Cl_2): δ (ppm) : 9.32 (s, 1H, C2*H*) ; 7.51 (d, 1H, C4*H*) ; 7.46 (d, 1H, C5*H*) ; 4.29 (t, 2H, NC*H*$_2$) ; 4.07 (s, 3H, NC*H*$_3$) ; 1.92 (qt, 6H,CH_2C*H*$_2$C*H*$_2$C*H*$_2$$CH_2$) ; 1.33 (st, 2H, CH_2C*H*$_2$$CH_3$); 0.88 (t, 3H, CH_2C*H*$_3$) ; ^{13}C$^{[84]}$-NMR (300 MHz, CD_2Cl_2) : δ (ppm) : 136.75 (SCN); 131.12 (*C*2H) ;123.69 (*C*4H) ; 122.26 (*C*5H) ; 50.57 (N*C*H_2) ; 36.57 (N*C*H_3) ; 31.03 (CH_2*C*$H_2CH_2CH_2CH_2$) ; 30.08 (CH_2CH_2*C*H_2CH_2); 25.81

($CH_2CH_2CH_2$); 22.36 ($CH_2CH_2CH_3$); 13.70 (CH_2CH_3). Electrospray, MS (+ve): m/z 167 (100% - $C_1C_6Im^+$), MS (-ve): m/z 58 (100% $^-$SCN).

1-hexyl-3-methylimidazoliumtetrafluoroborate:[C_1C_6Im][BF_4]

Slightly yellow clear oil, 90% yield. ^{1}H-NMR (300 MHz, CD_2Cl_2): δ (ppm) : 8.78 (s, 1H, C2*H*) ; 7.39 (d, 1H, C4*H*) ; 7.36 (d, 1H, C5*H*) ; 4.18 (t, 2H, NC*H*$_2$) ; 3.95 (s, 3H, NC*H*$_3$) ; 1.89 (qt, 6H,$CH_2CH_2CH_2CH_2CH_2$) ; 1.34 (st, 2H, $CH_2CH_2CH_3$); 0.90 (t, 3H, CH_2CH_3) ; ^{13}C$^{[84]}$-NMR (CD_2Cl_2) : δ (ppm) : 136.20 (*C*2H) ;123.67 (*C*4H) ; 122.18 (*C*5H) ; 50.07 (N*C*H$_2$) ; 36.17 (N*C*H$_3$) ; 30.98 ($CH_2CH_2CH_2CH_2CH_2$) ; 29.91 ($CH_2CH_2CH_2CH_2$); 25.72 ($CH_2CH_2CH_2$); 22.31 ($CH_2CH_2CH_3$); 13.64 (CH_2CH_3). ^{19}F-NMR (300 MHz, CD_2Cl_2); δ (ppm): -151.16 (s, BF_4). ^{11}B-NMR (300 MHz, CD_2Cl_2): δ (ppm): -1.02 (s, BF_4). Electrospray, MS (+ve): m/z 167 (100% - $C_1C_6Im^+$), MS (-ve): m/z 87 (100% $^-BF_4$).

1-octyl-3-methylimidazolium dicyanamide: [C_1C_8Im][$N(CN)_2$]

Slightly yellow clear oil, 90% yield. ^{1}H-NMR (300 MHz, d6-DMSO): δ (ppm) : 8.68 (s, 1H, C2*H*) ; 7.41 (d, 1H, C4*H*) ; 7.39 (d, 1H, C5*H*) ; 4.11 (t, 2H, NC*H*$_2$) ; 3.83 (s, 3H, NC*H*$_3$) ; 1.79 (qt, 6H,$CH_2CH_2CH_2CH_2CH_2$) ; 1.20 (st, 2H, $CH_2CH_2CH_3$); 0.75 (t, 3H, CH_2CH_3) ; ^{13}C$^{[84]}$-NMR (300 MHz, d6-DMSO) : δ (ppm) : 135.87 (*C*2H) ;123.72 (*C*4H) ; 122.13 (*C*5H) ; 119.65 (N*C*N); 49.62 (N*C*H$_2$) ; 35.78 (N*C*H$_3$) ; 31.55 ($CH_2CH_2CH_2CH_2CH_2CH_2CH_2$) ; 29.68 ($CH_2CH_2CH_2CH_2CH_2CH_2$); 28.82 ($CH_2CH_2CH_2CH_2CH_2$); 28.82 ($CH_2CH_2CH_2CH_2$); 25.89 ($CH_2CH_2CH_2$) ; 22.42 ($CH_2CH_2CH_3$); 13.73 ($CH_2CH_3$). Electrospray, MS (+ve): m/z 195 (100% - $C_1C_8Im^+$), MS (-ve): m/z 66 (100% dca^-).

1-octyl-3-methylimidazolium tetrafluoroborate: [C_1C_8Im][BF_4]

Slightly yellow clear oil, 90% yield. ^{1}H-NMR (300 MHz, CD_2Cl_2): δ (ppm) : 9.42 (s, 1H, C2*H*) ; 7.45 (d, 1H, C4*H*) ; 7.39 (d, 1H, C5*H*) ; 4.22 (t, 2H, NC*H*$_2$) ; 3.99 (s, 3H, NC*H*$_3$) ; 1.88 (m, 12H,$CH_2CH_2CH_2CH_2CH_2$ CH_2CH_3) ; 1.29 (st, 2H, $CH_2CH_2CH_3$); 0.87 (t, 3H, CH_2CH_3) ; ^{13}C$^{[84]}$-NMR (300 MHz, CD_2Cl_2): δ (ppm) : 136.82 (*C*2H) ;123.59 (*C*4H) ; 122.06 (*C*5H) ; 49.98 (N*C*H$_2$) ; 36.17 (N*C*H$_3$) ; 31.64 ($CH_2CH_2CH_2CH_2CH_2CH_2$) ; 29.68 ($CH_2CH_2CH_2CH_2CH_2$); 28.98 ($CH_2CH_2CH_2CH_2$); 28.86 ($CH_2CH_2CH_2$); 26.11 (CH_2CH_2); 22.55 ($CH_2CH_2CH_3$); 13.80 (CH_2CH_3). ^{19}F-NMR (300 MHz, CD_2Cl_2); δ (ppm): -150.96 (s, BF_4). ^{11}B-NMR (300 MHz, CD_2Cl_2): δ (ppm): -1.05 (s, BF_4). Electrospray, MS (+ve): m/z 195 (100% - $C_1C_8Im^+$), MS (-ve): m/z 87 (100% $^-BF_4$).

N- butyl- N- metylpyrrolidinium dicyanamide: [Py_{14}][$N(CN)_2$]

Slightly yellow clear oil, 90% yield. ^{1}H NMR (300 MHz, d6-DMSO): δ (ppm): 3.45 (m, 4H, C2*H*, C5*H*), 3.24 (t, NC*H*$_2$), 2.98 (s, C*H*$_3$), 2.08 (m, 4H, C3*H*, C4*H*), 1.68 (m, $CH_2CH_2CH_2$), 1.31 (m,

$CH_2CH_2CH_3$), d 0.93 (t, CH_2CH_3). ^{13}C NMR (300 MHz d6-DMSO): δ (ppm): 119.56 (N*C*N); 63.93 (*C*2H); 63.89 (*C*5H); 63.85 (*C*3H); 63.39 (*C*4H); 47.96 (NCH_3); 25.39 (NCH_2); 21.56 ($CH_2CH_2CH_2$); 19.78 ($CH_2CH_2CH_3$); 13.92 (CH_2CH_3). Electrospray, MS (+ve): m/z 142.1 (100% - P_{14}^+), MS (-ve): m/z 66.0 (100% - $^-N(CN)_2$).

N-butyl-N-metylpyrrolidinium bis(trifluoromethanesulfonyl)amide: [Py_{14}][NTf_2]

Colourless oil, 90% yield. ^1H NMR (300 MHz, d6-DMSO): δ (ppm): 3.45 (m, 4H, C2*H*, C5*H*), 3.24 (t, NCH_2), 2.98 (s, CH_3), 2.08 (m, 4H, C3*H*, C4*H*), 1.68 (m, $CH_2CH_2CH_2$), 1.31 (m, $CH_2CH_2CH_3$), d 0.93 (t, CH_2CH_3). ^{13}C NMR (300 MHz d6-DMSO): δ (ppm): 119.56 (N*C*N); 63.93 (*C*2H); 63.89 (*C*5H); 63.85 (*C*3H); 63.39 (*C*4H); 47.96 (NCH_3); 25.39 (NCH_2); 21.56 ($CH_2CH_2CH_2$); 19.78 ($CH_2CH_2CH_3$); 13.92 (CH_2CH_3).^{13}C NMR (300 MHz d6-DMSO): δ (ppm): 119.56 (N*C*N); Electrospray, MS(+ve): m/z 142.1 (P_{14}^+), MS (-ve): m/z 279.9 ($^-NTf_2$).

Tetrabutylphosphonium bis(trifluoromethanesulfonyl)amide: [P_{4444}][NTf_2]

white solid; (yield 90%). ^{31}P NMR (300 MHz CD_2Cl_2): δ (ppm): 33.18. MS (+ve): m/z 259 ($^+P_{4444}$), MS (-ve): m/z 280 (NTf_2^-).

Tetrabutylphosphonium tetrafluoroborate: [P_{4444}][BF_4]

white solid; (yield 90%). ^{31}P NMR (300 MHz CD_2Cl_2): δ (ppm): 33.18. MS (+ve): m/z 259 ($^+P_{4444}$), MS (-ve): m/z 280 (BF_4^-).

2-NMR and mass spectra

1-butyl-3-methylImidazolium tetrafluoroborate: $[C_1C_4Im][BF_4]$

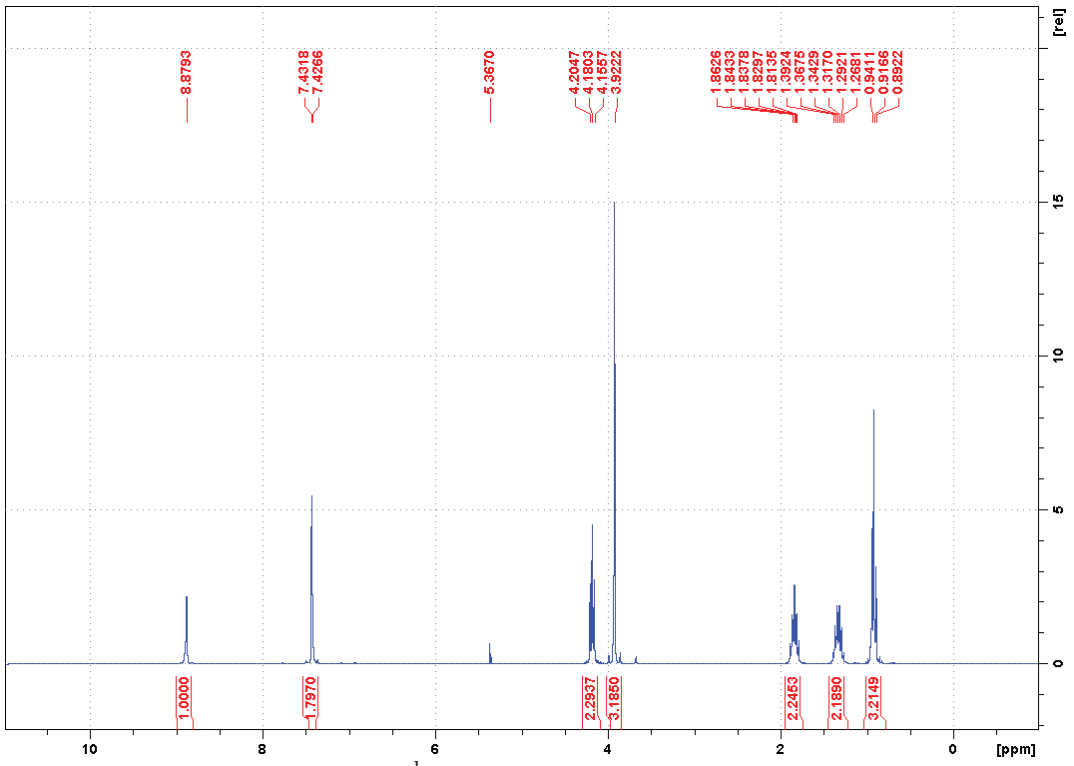

^1H NMR in CD_2Cl_2

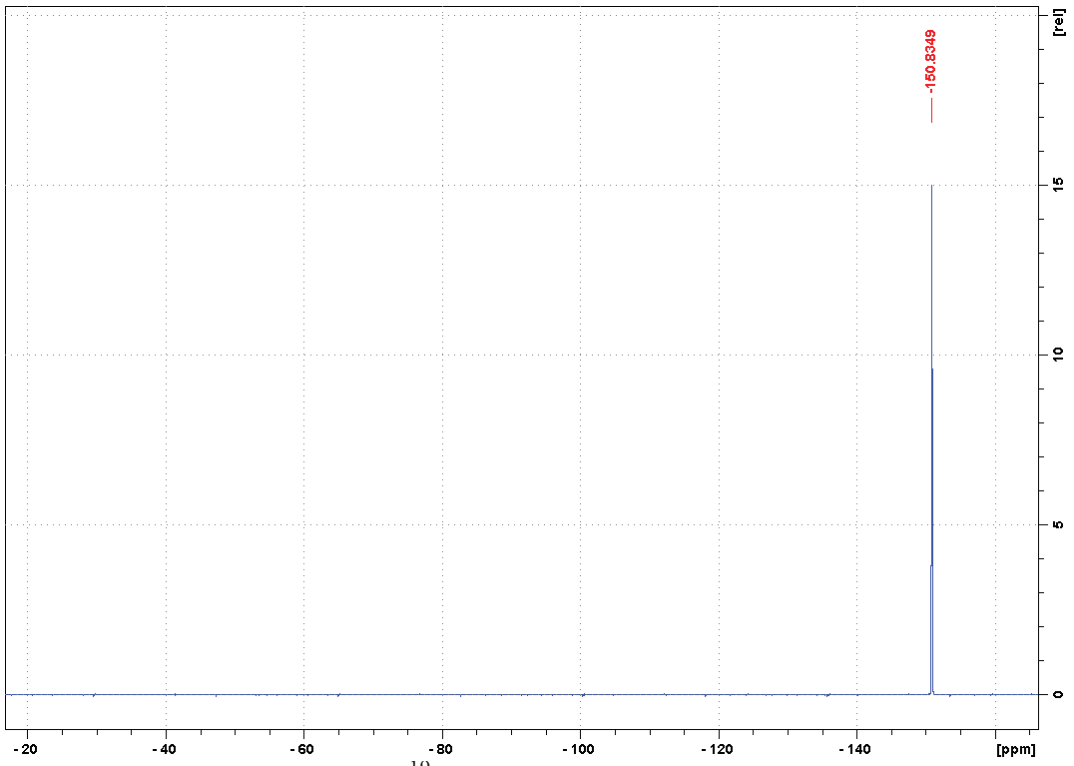

^{19}F NMR in CD_2Cl_2

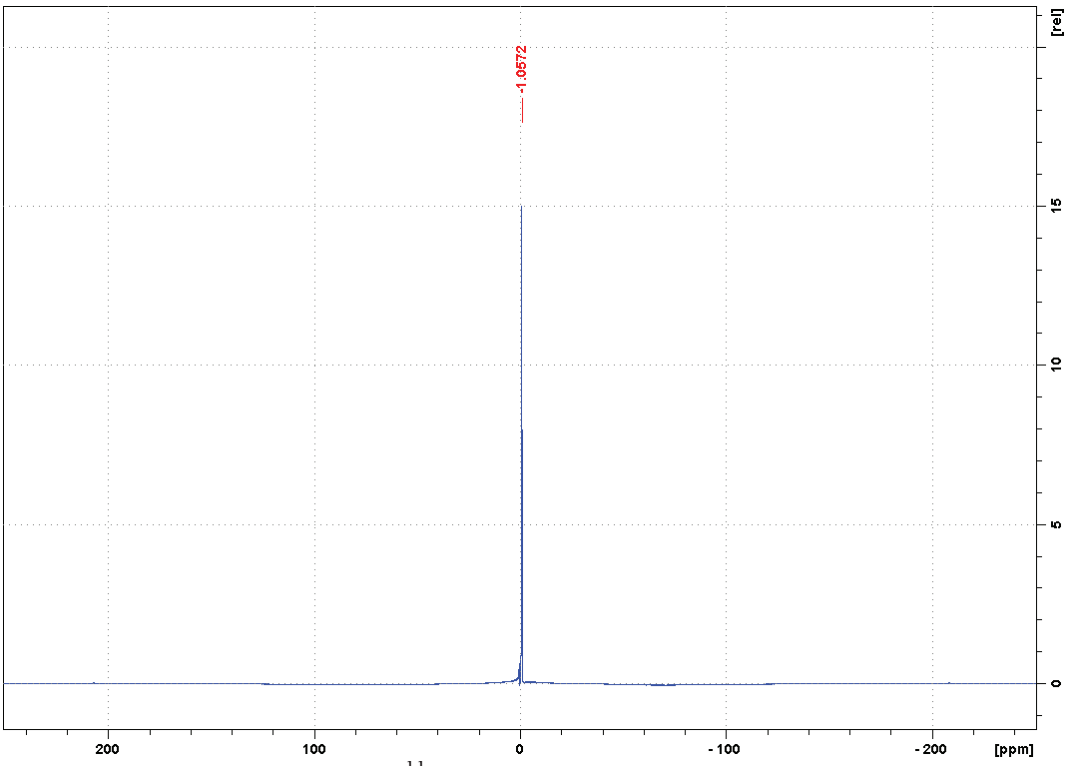

^{11}B NMR in CD_2Cl_2

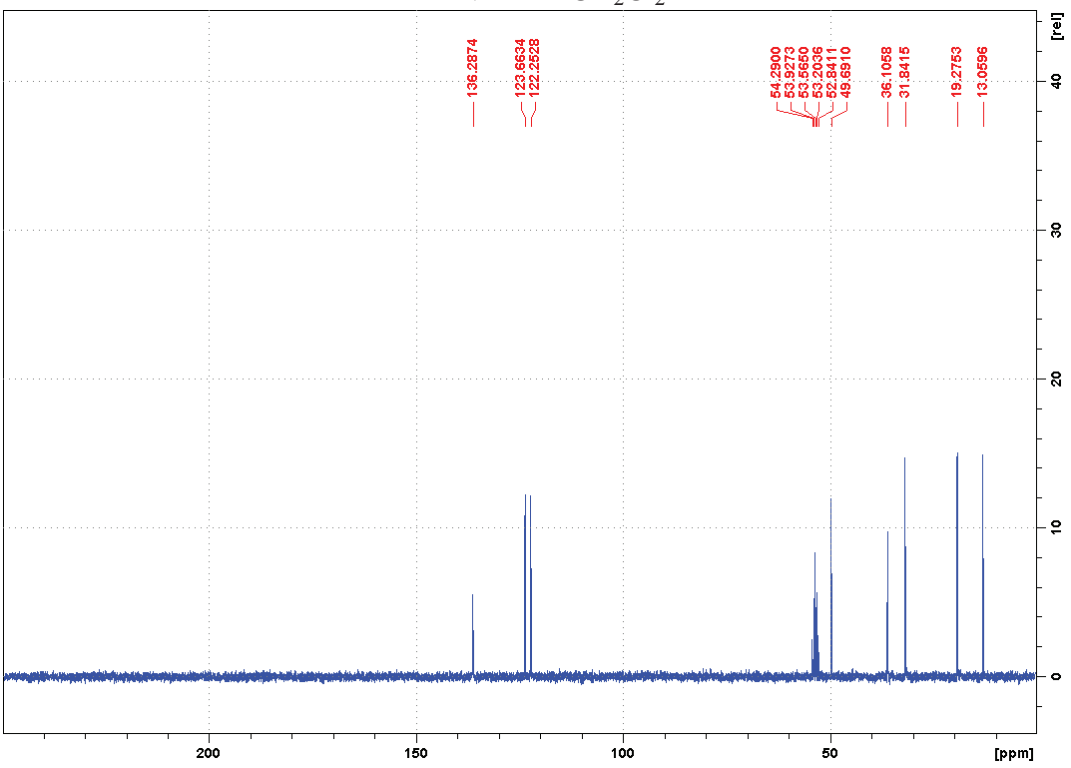

^{13}C NMR in CD_2Cl_2

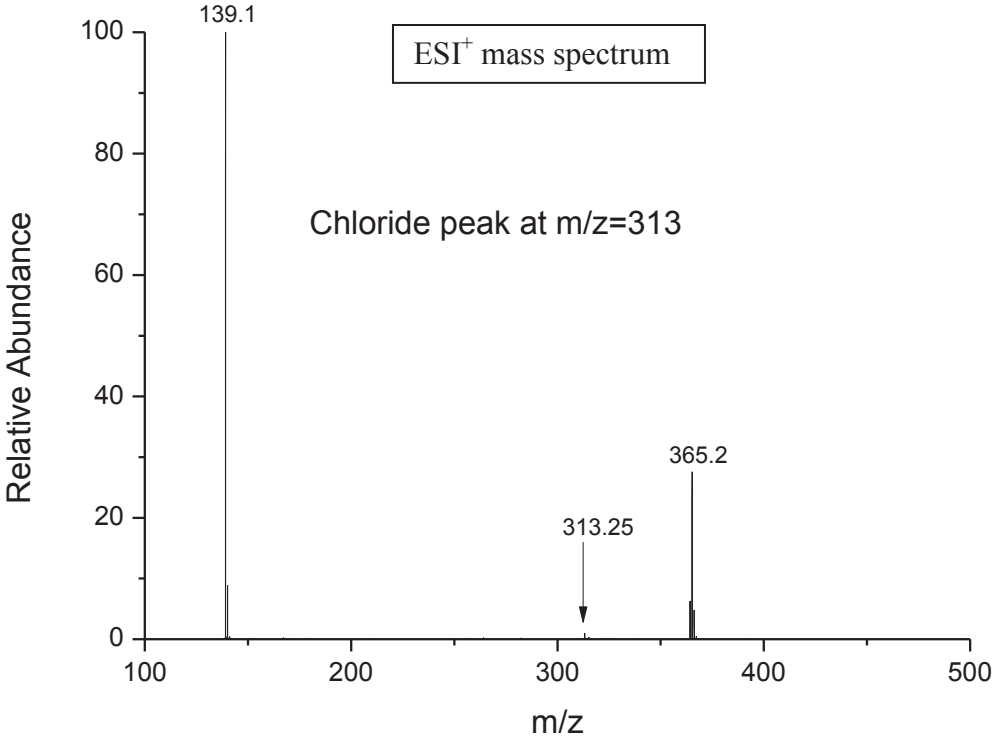

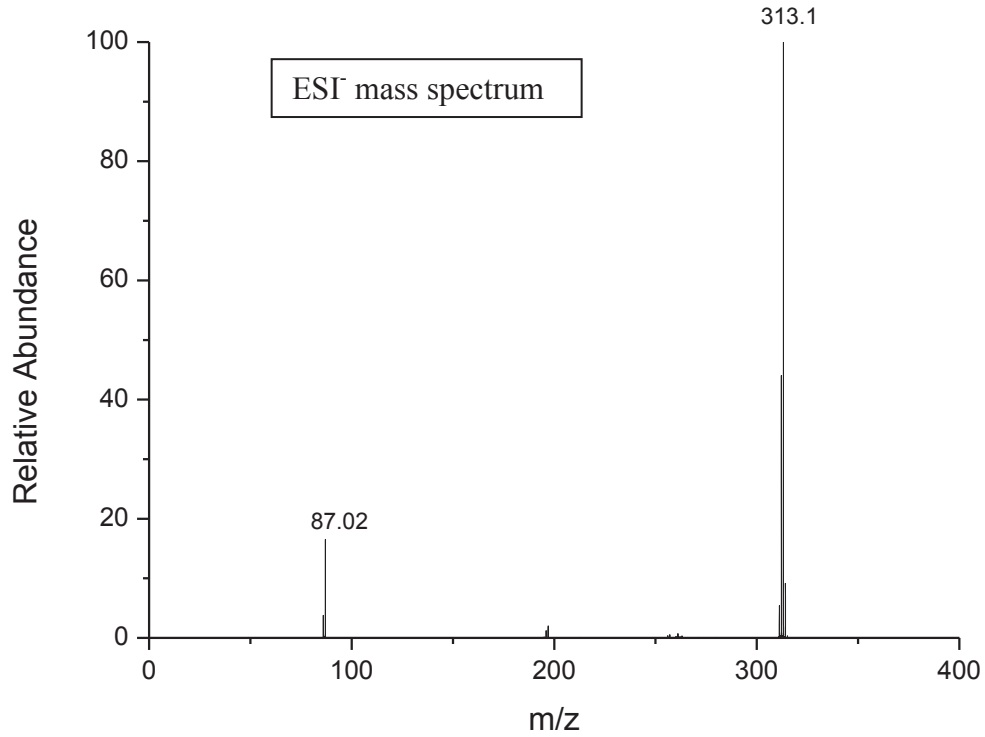

	Entire	Cation	Anion
Mass calculated	226.1	139.1	87.0

1-butyl-3-methylImidazolium thiocyanate : $[C_1C_4Im][SCN]$

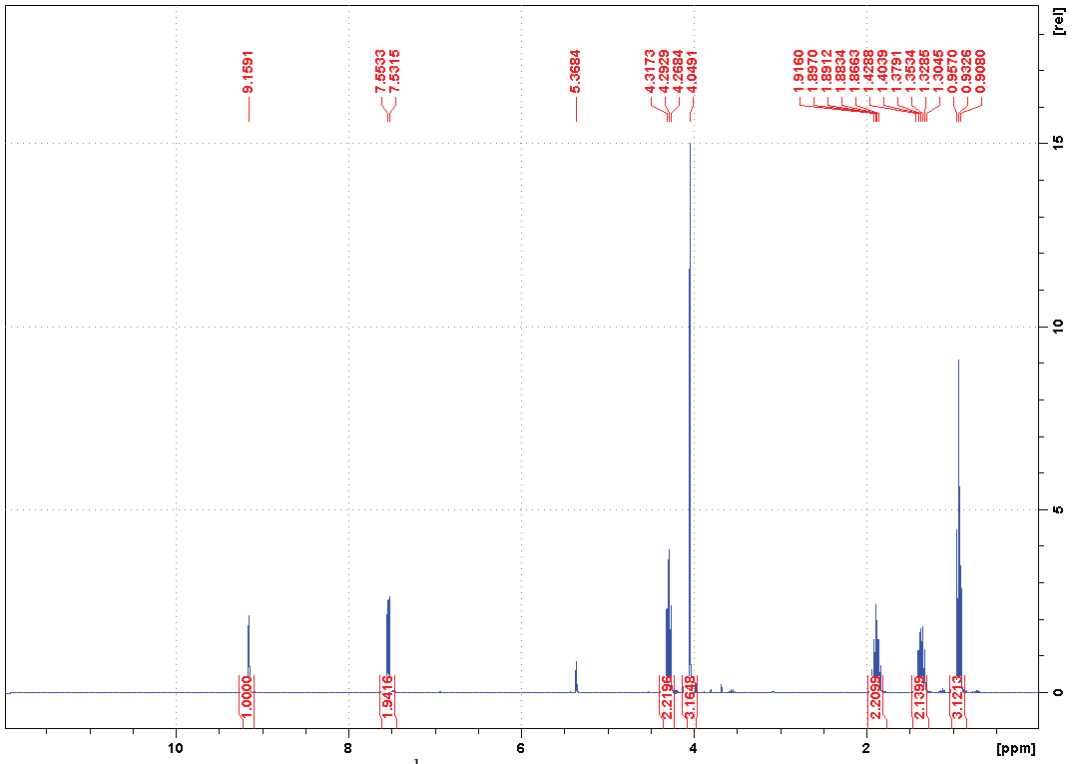

^{1}H NMR in CD_2Cl_2

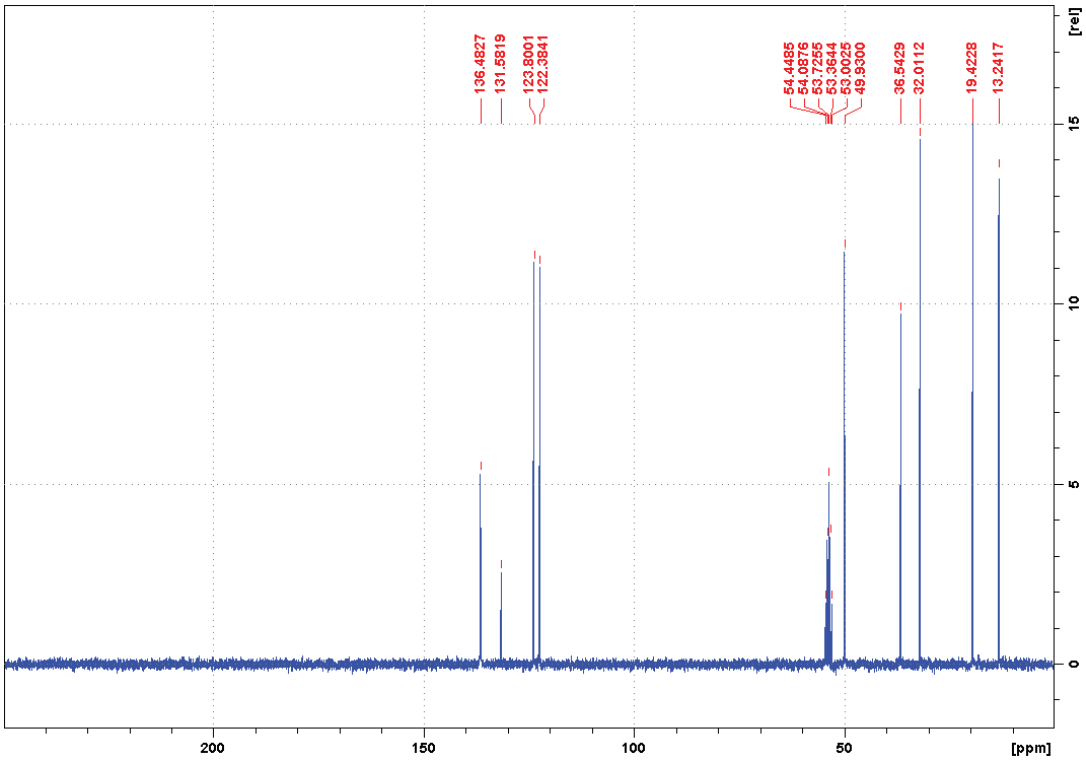

^{13}C NMR in CD_2Cl_2

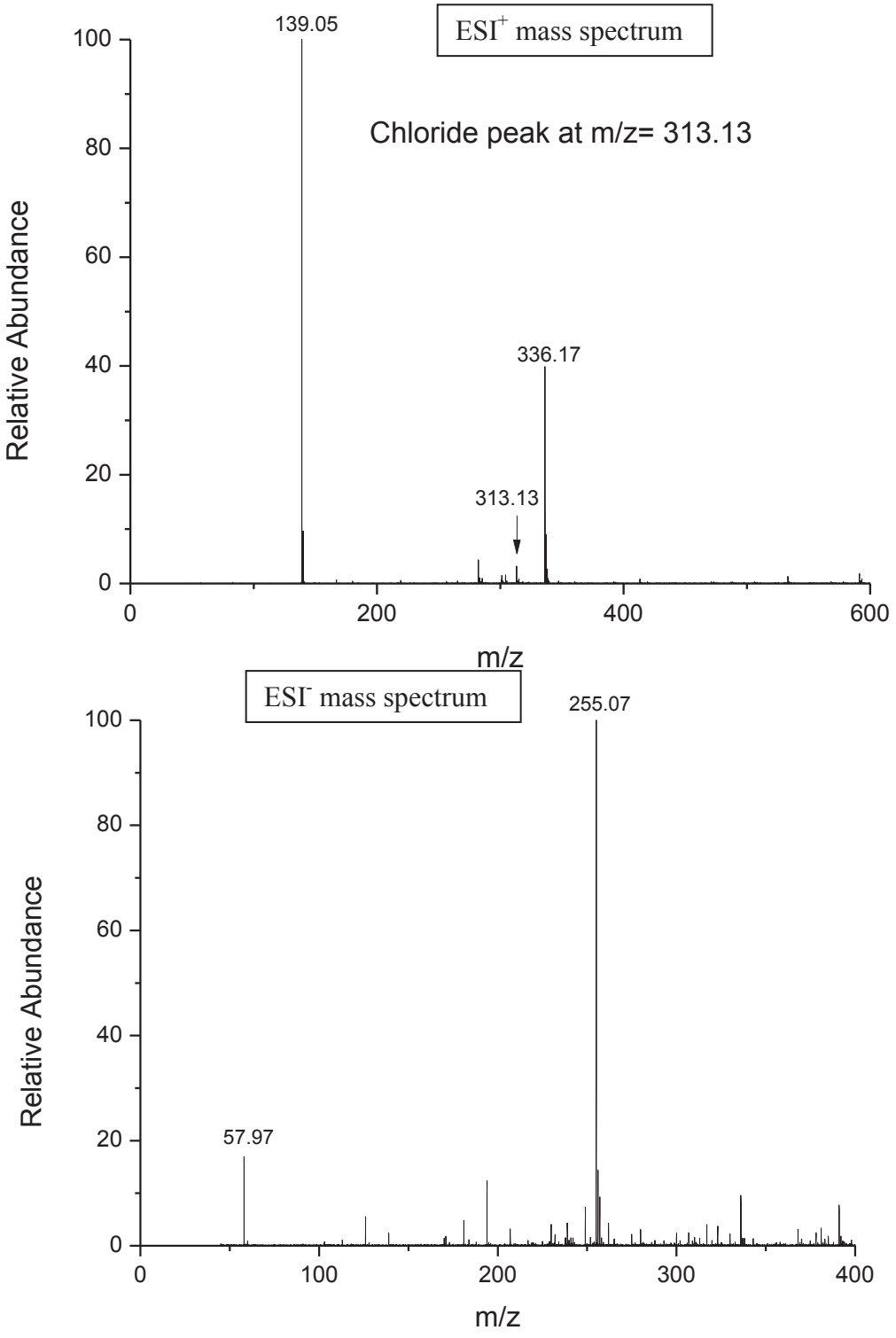

	Entire	Cation	Anion
Mass calculated	197.1	139.1	57.9

1-butyl-3-methylImidazolium bis(trifluoromethylsulfonyl)imide: $[C_1C_4Im][NTf_2]$

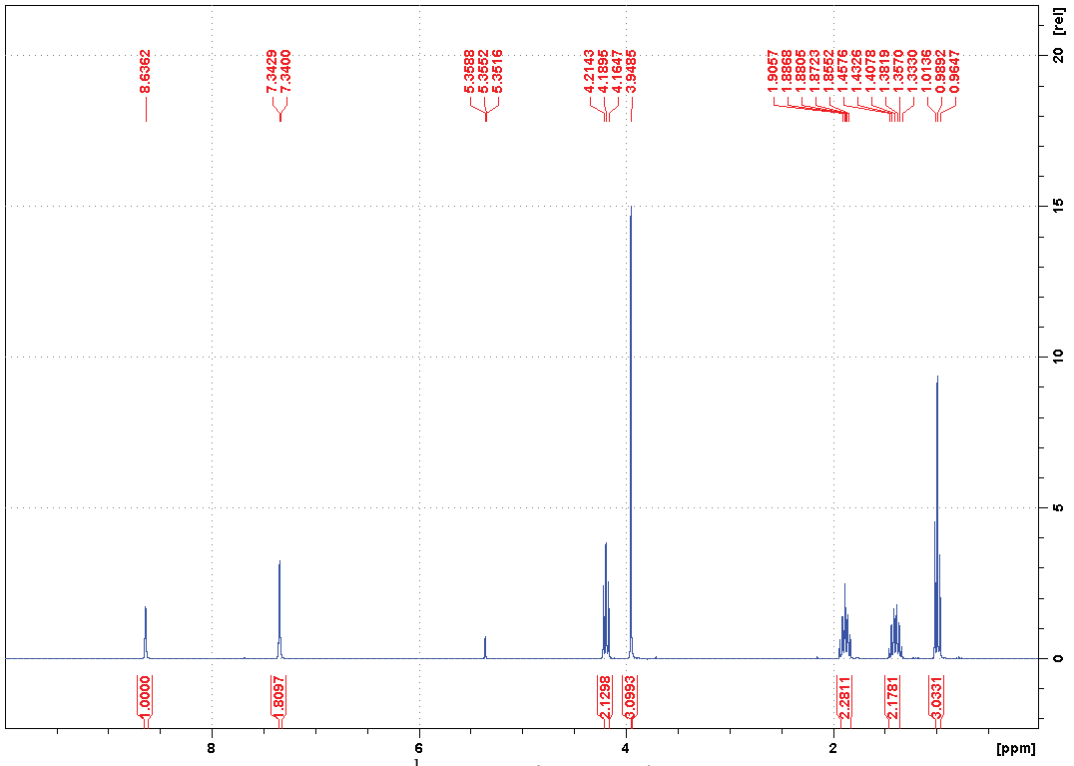

^{1}H NMR in CD_2Cl_2

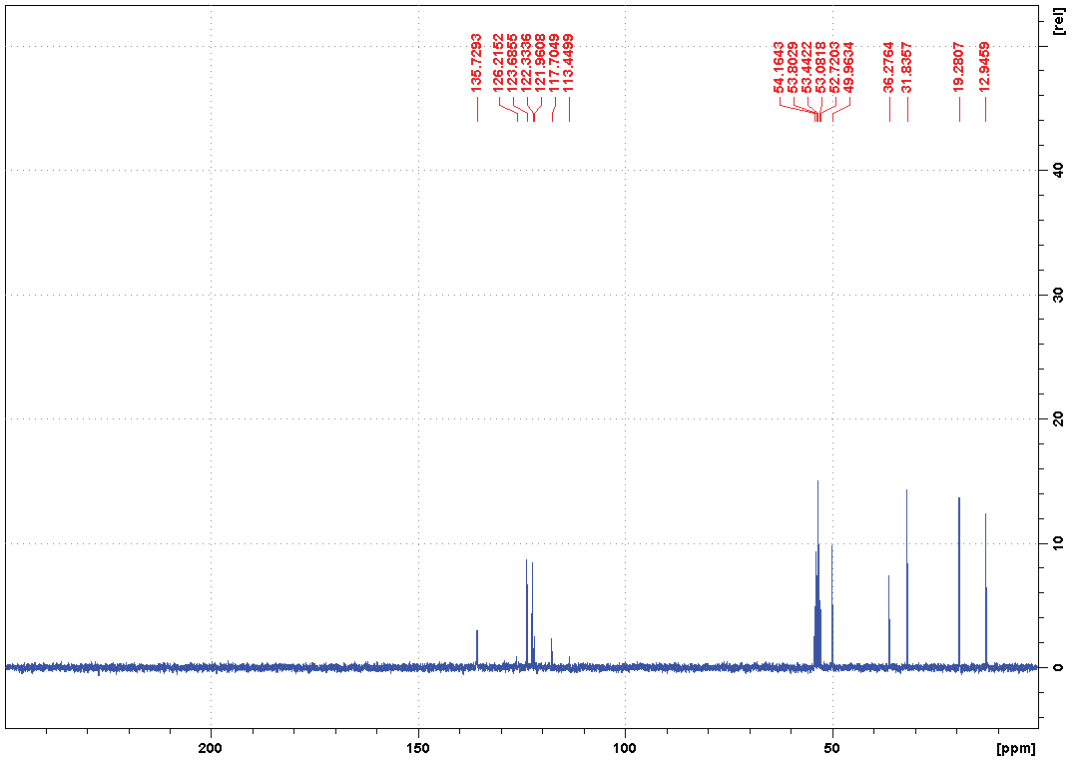

^{13}C NMR in CD_2Cl_2

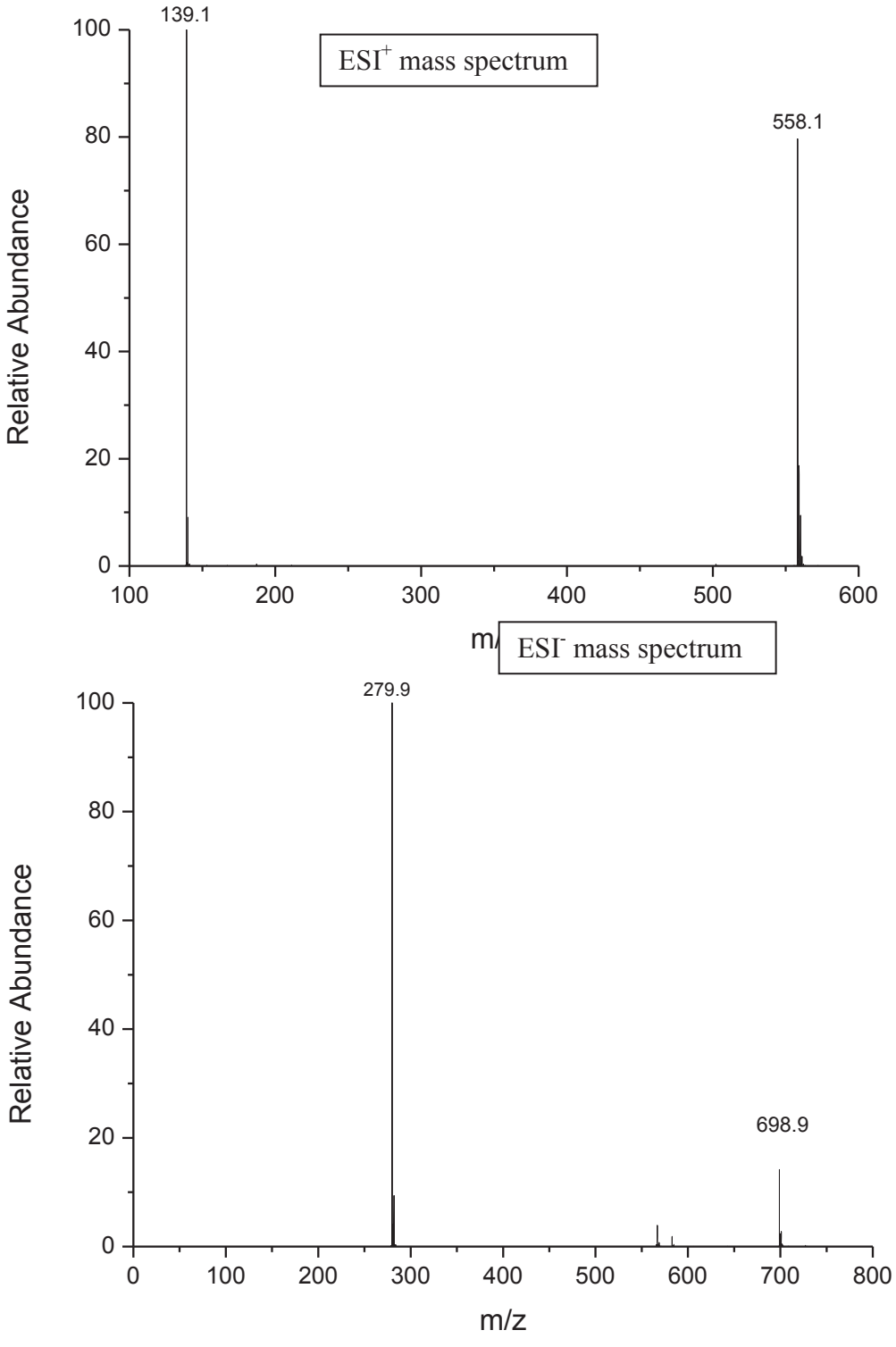

	Entire	Cation	Anion
Mass calculated	419.0	139.1	279.9

1-butyl-3-methylImidazolium dicyanamide: $[C_1C_4Im][N(CN)_2]$

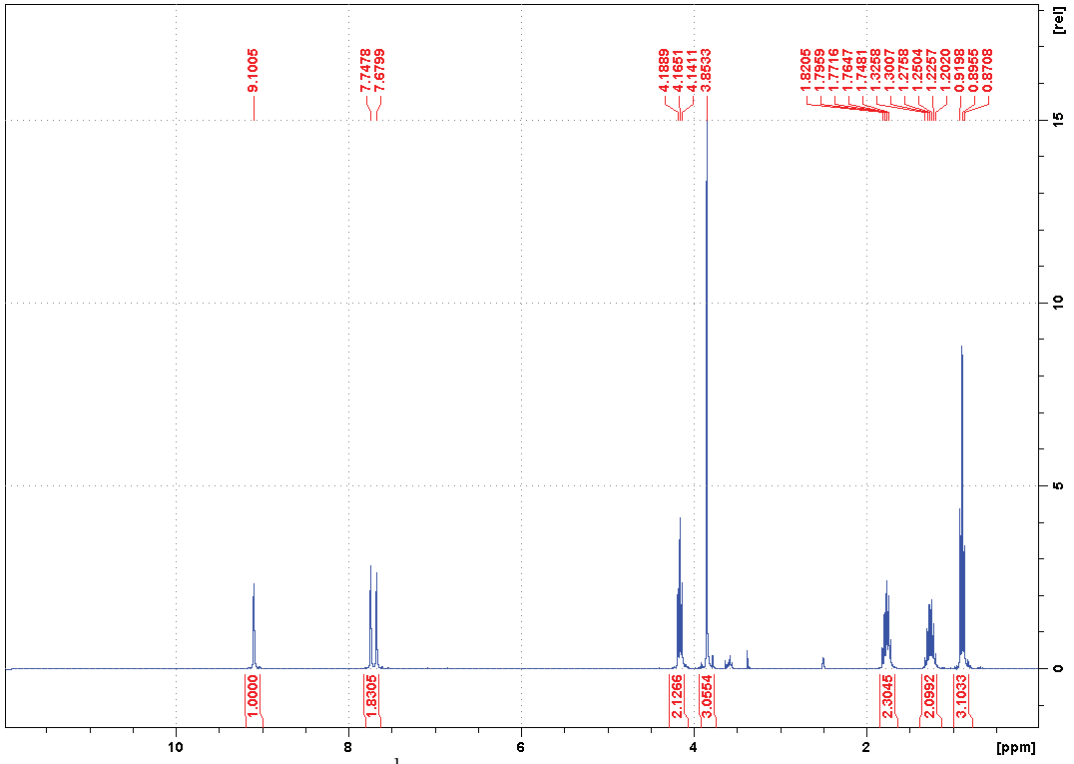

^{1}H NMR in d6-DMSO

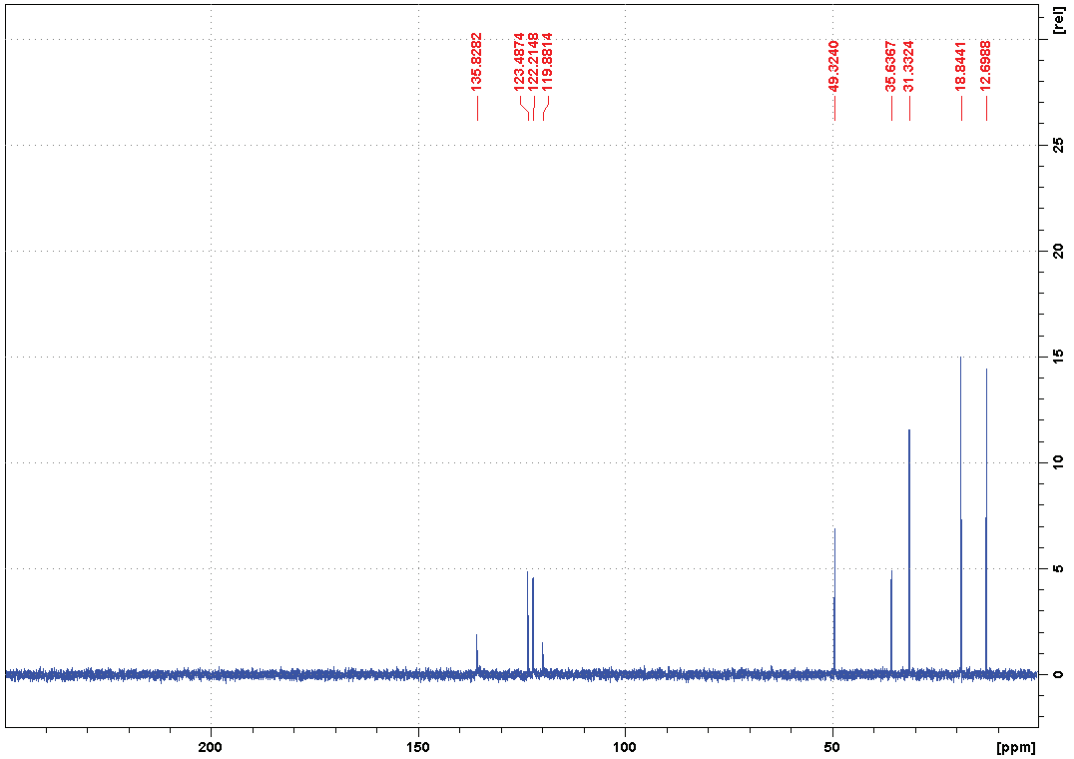

^{13}C NMR in d6-DMSO

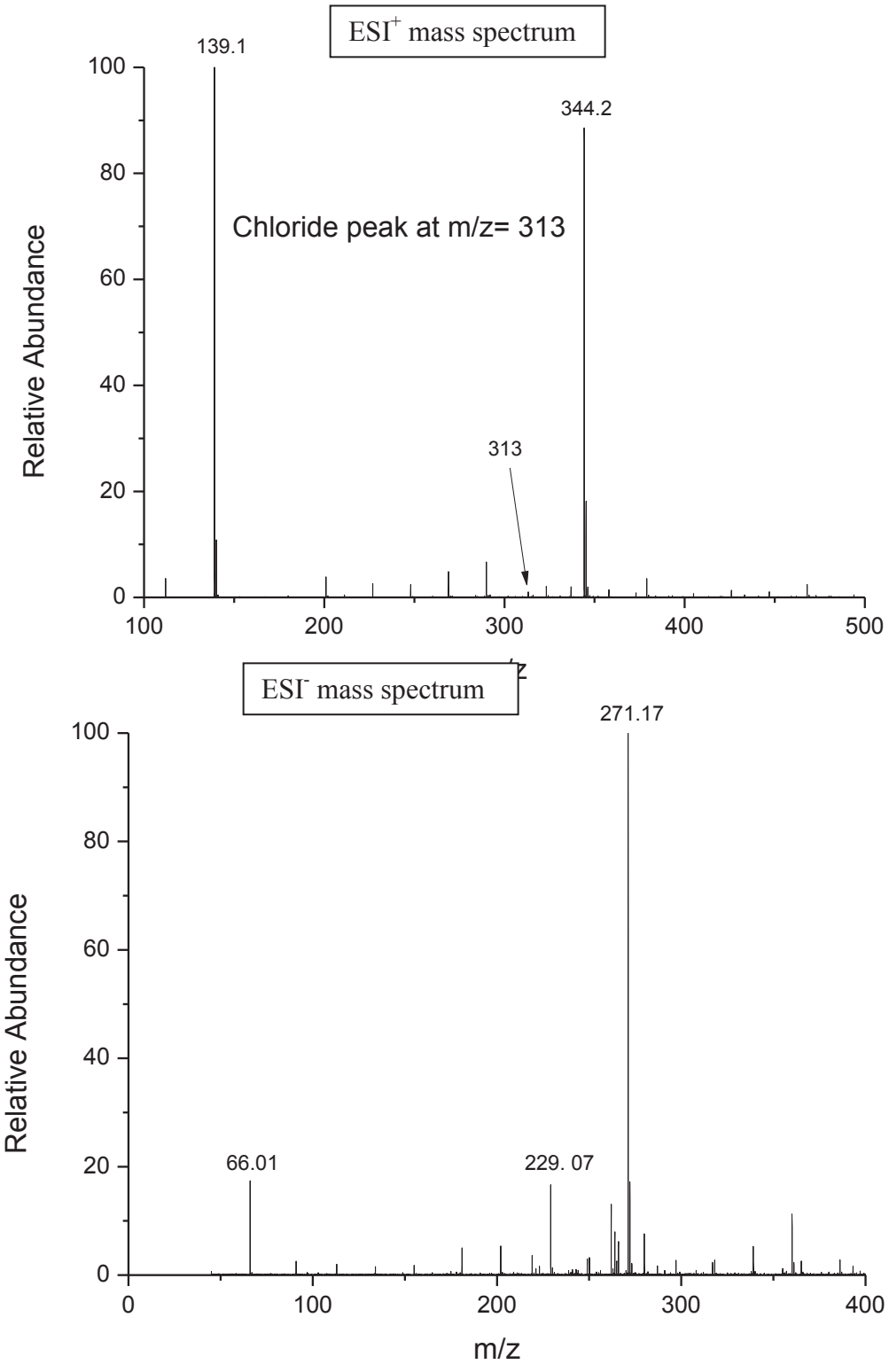

	Entire	Cation	Anion
Mass calculated	205.1	139.1	66.0

1-hexyl-3-methylimidazolium tetrafluoroborate: $[C_1C_6Im][BF_4]$

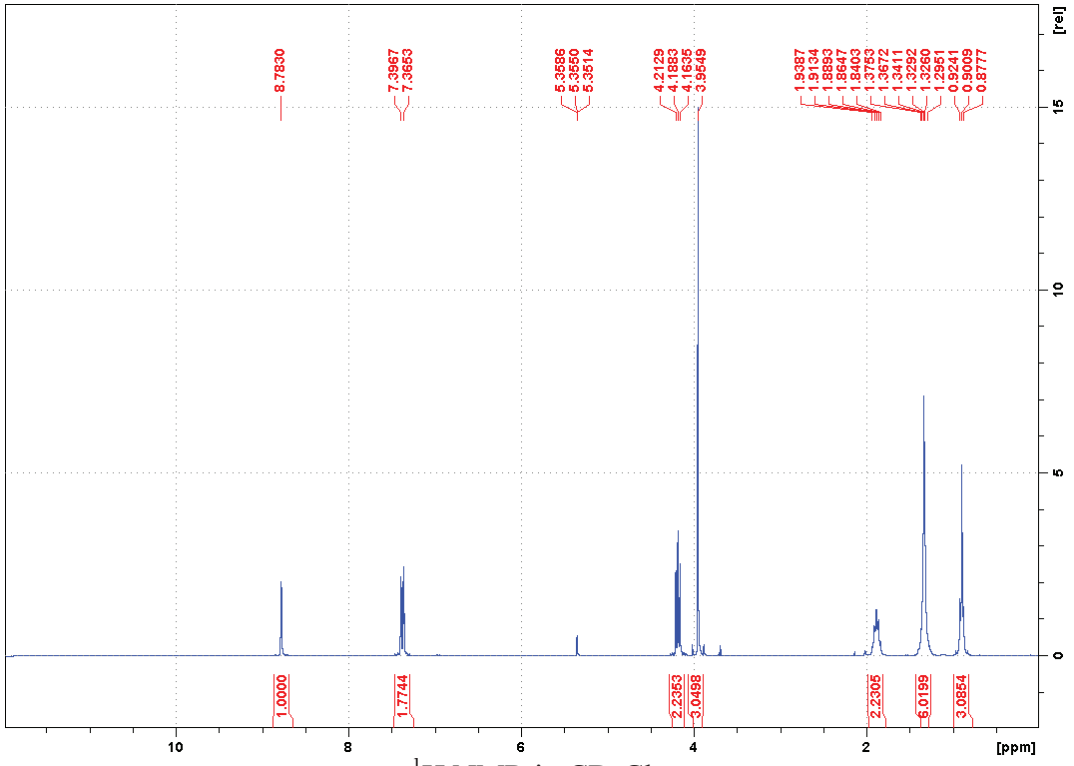

^{1}H NMR in CD_2Cl_2

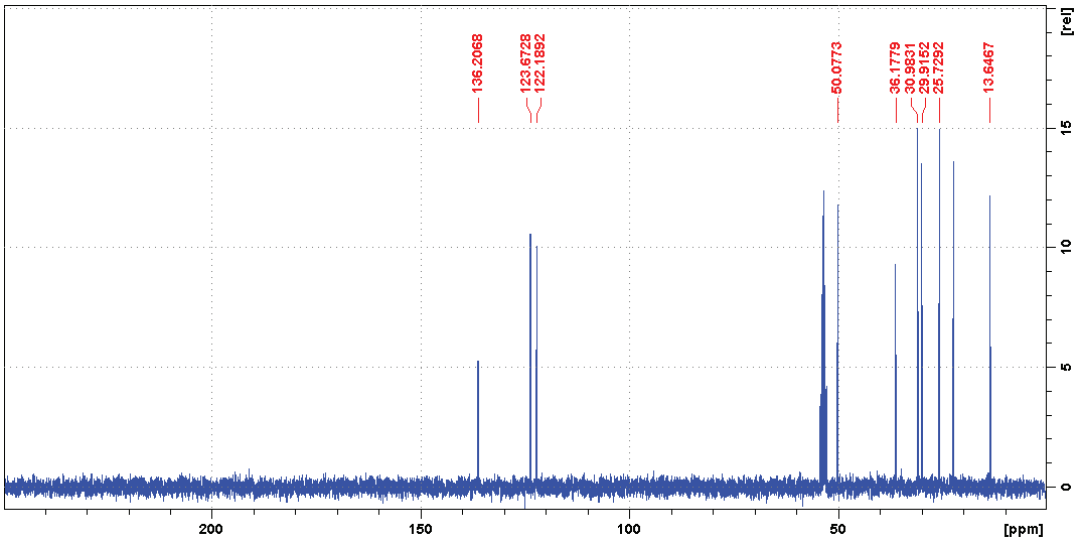

^{13}C NMR in CD_2Cl_2

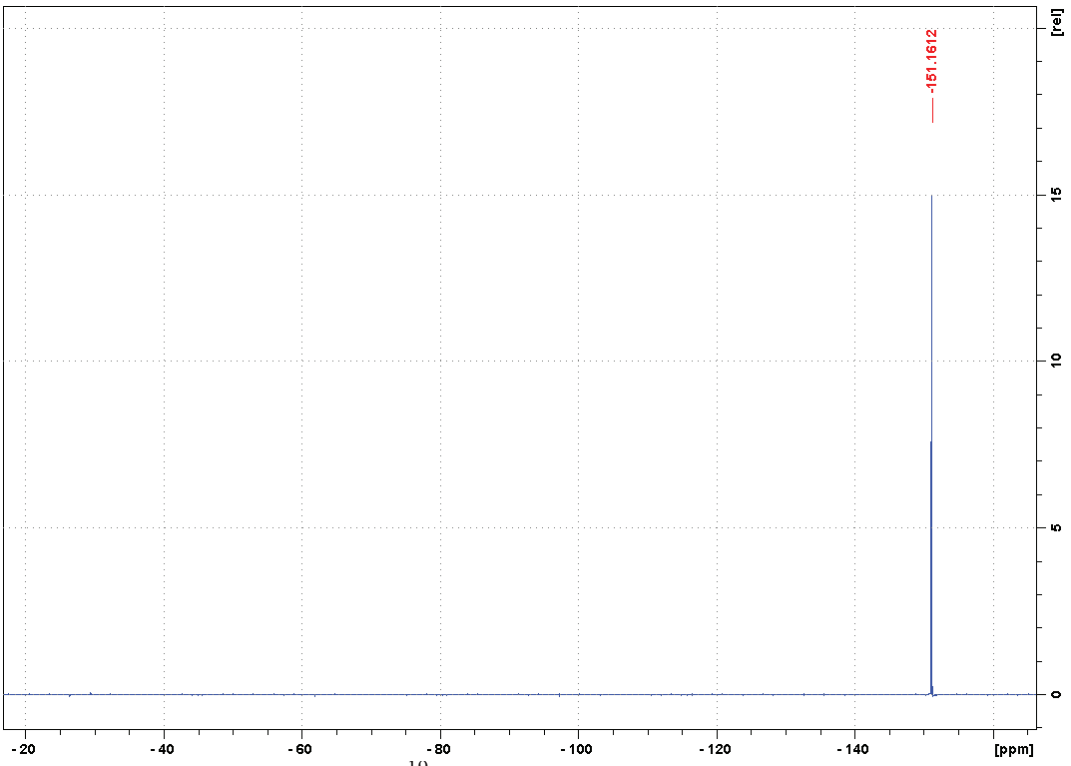

^{19}F NMR in CD_2Cl_2

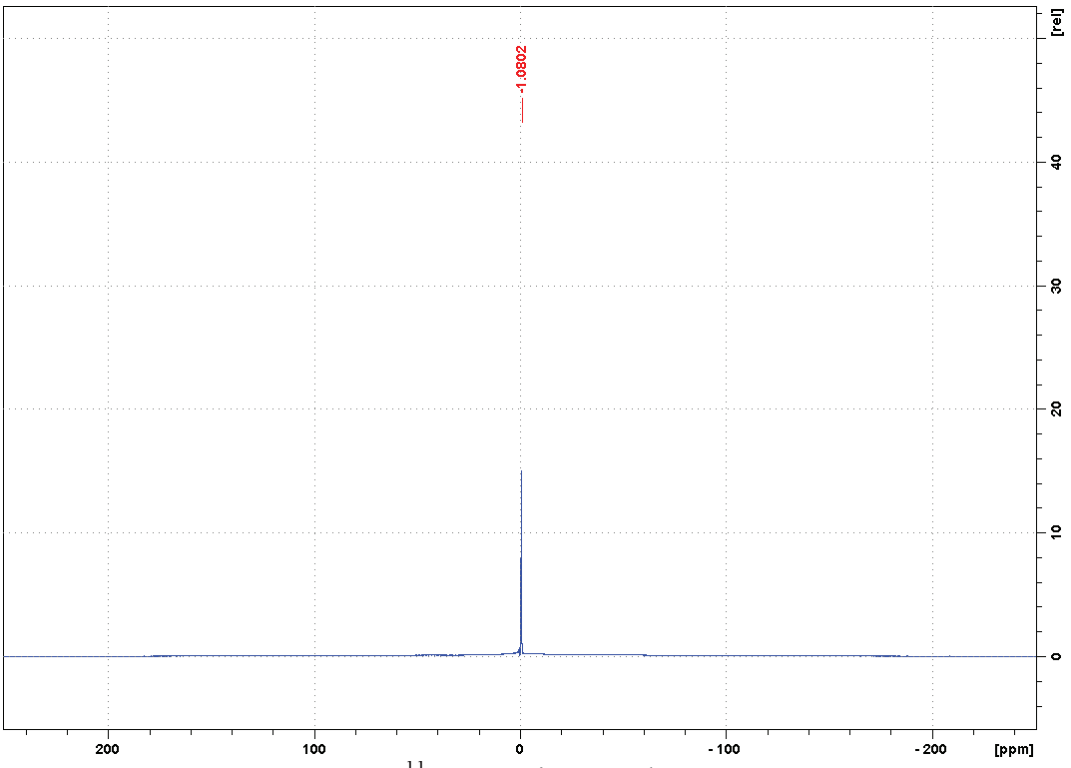

^{11}B NMR in CD_2Cl_2

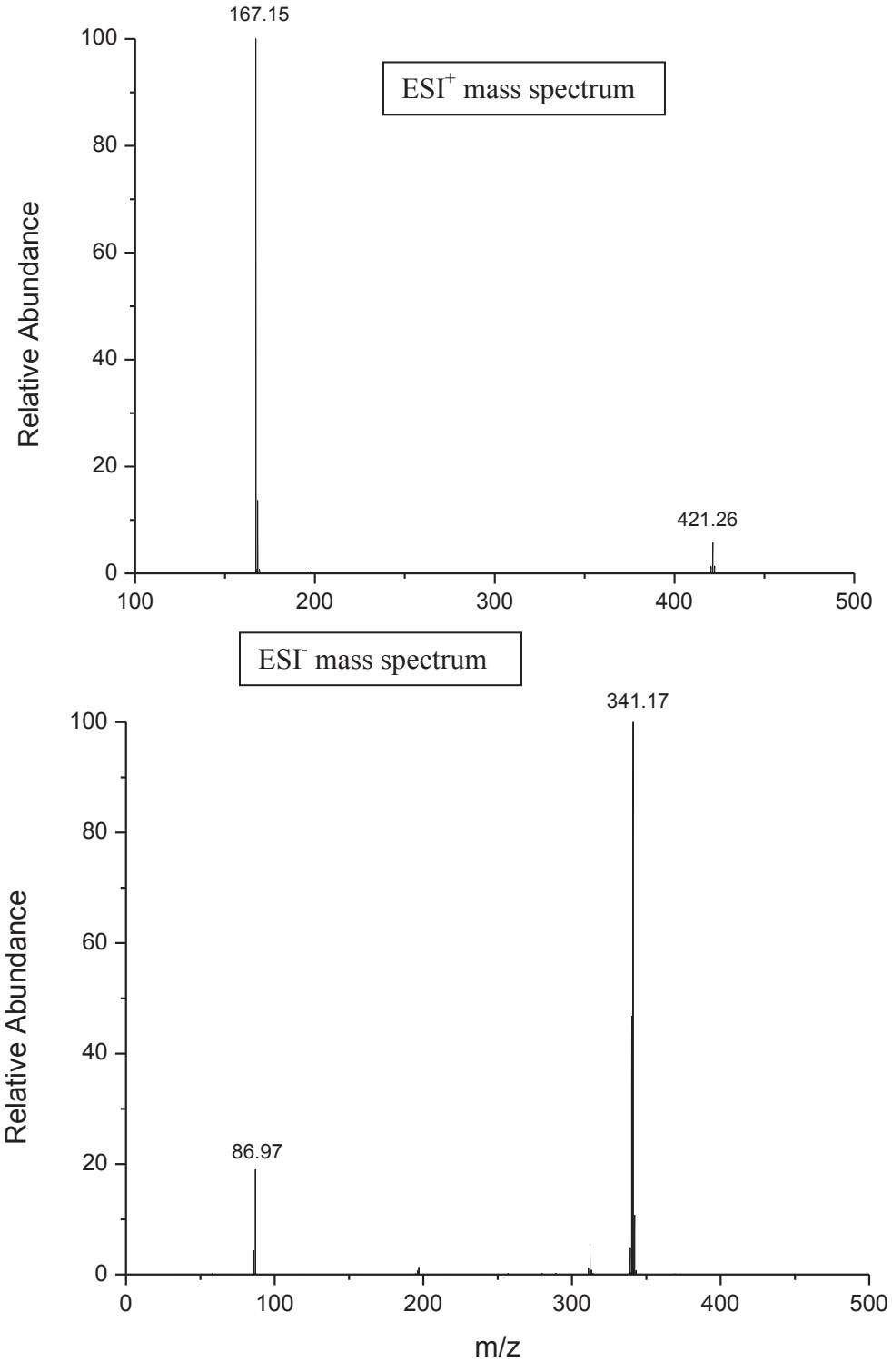

	Entire	Cation	Anion
Mass calculated	254.1	167.1	87

1-hexyl-3-methylimidazolium thiocyanate : $[C_1C_6Im][SCN]$

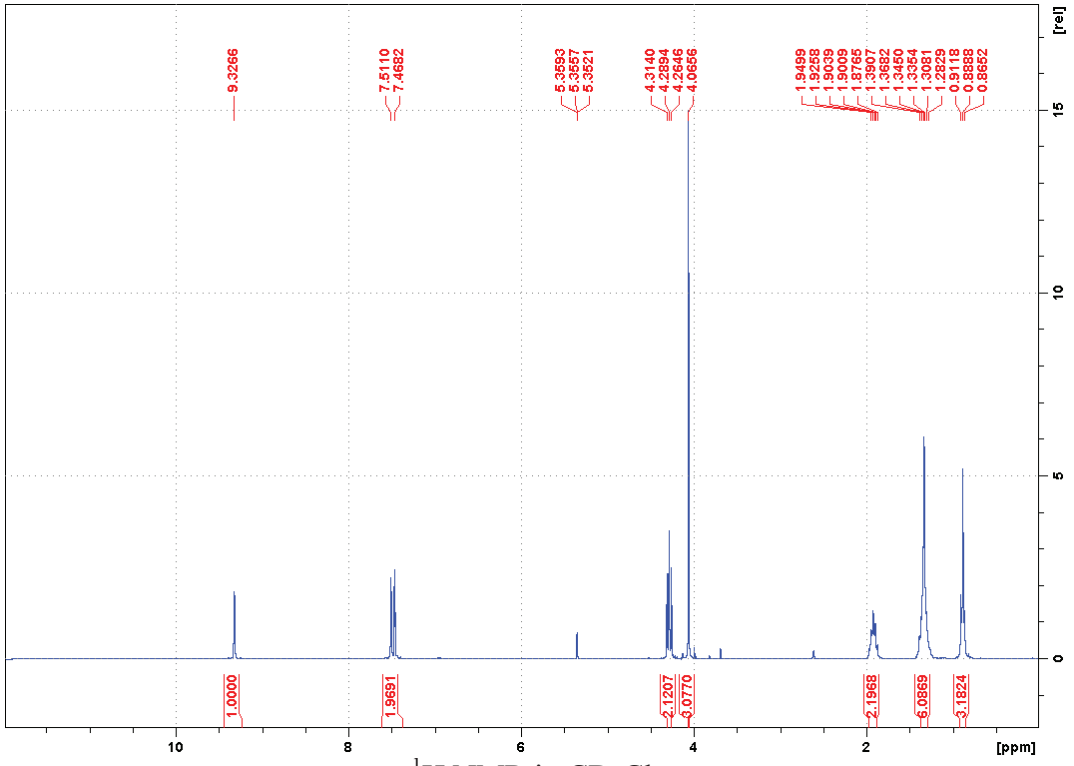

^1H NMR in CD_2Cl_2

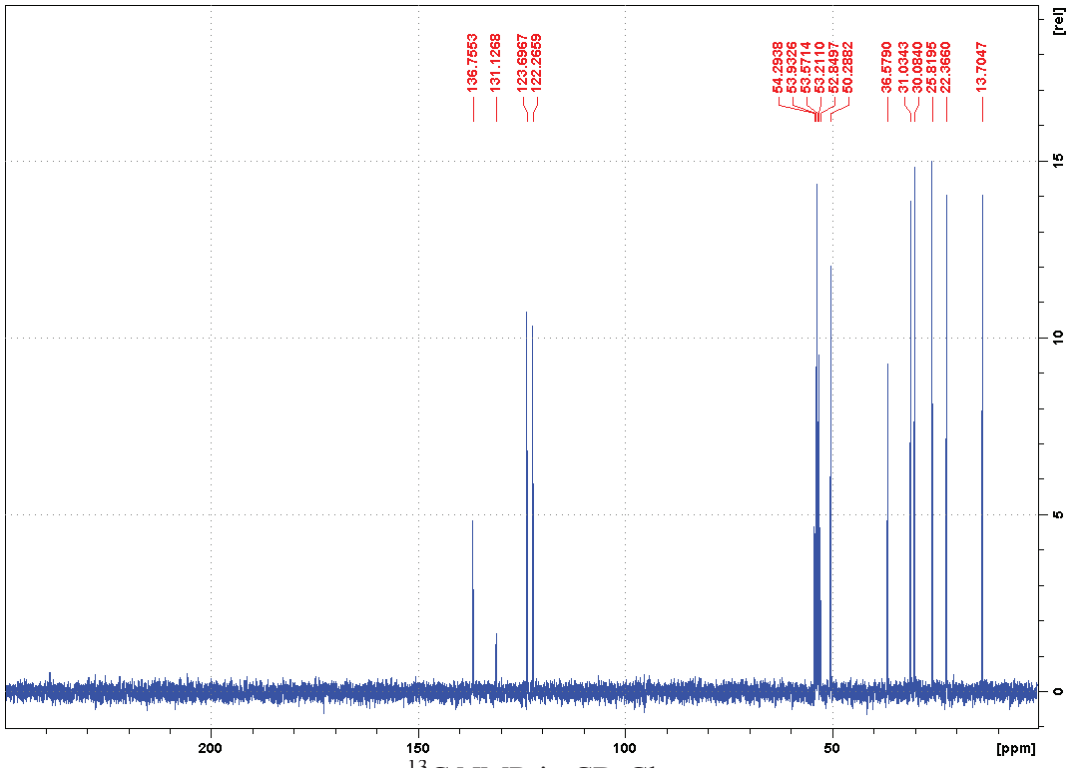

^{13}C NMR in CD_2Cl_2

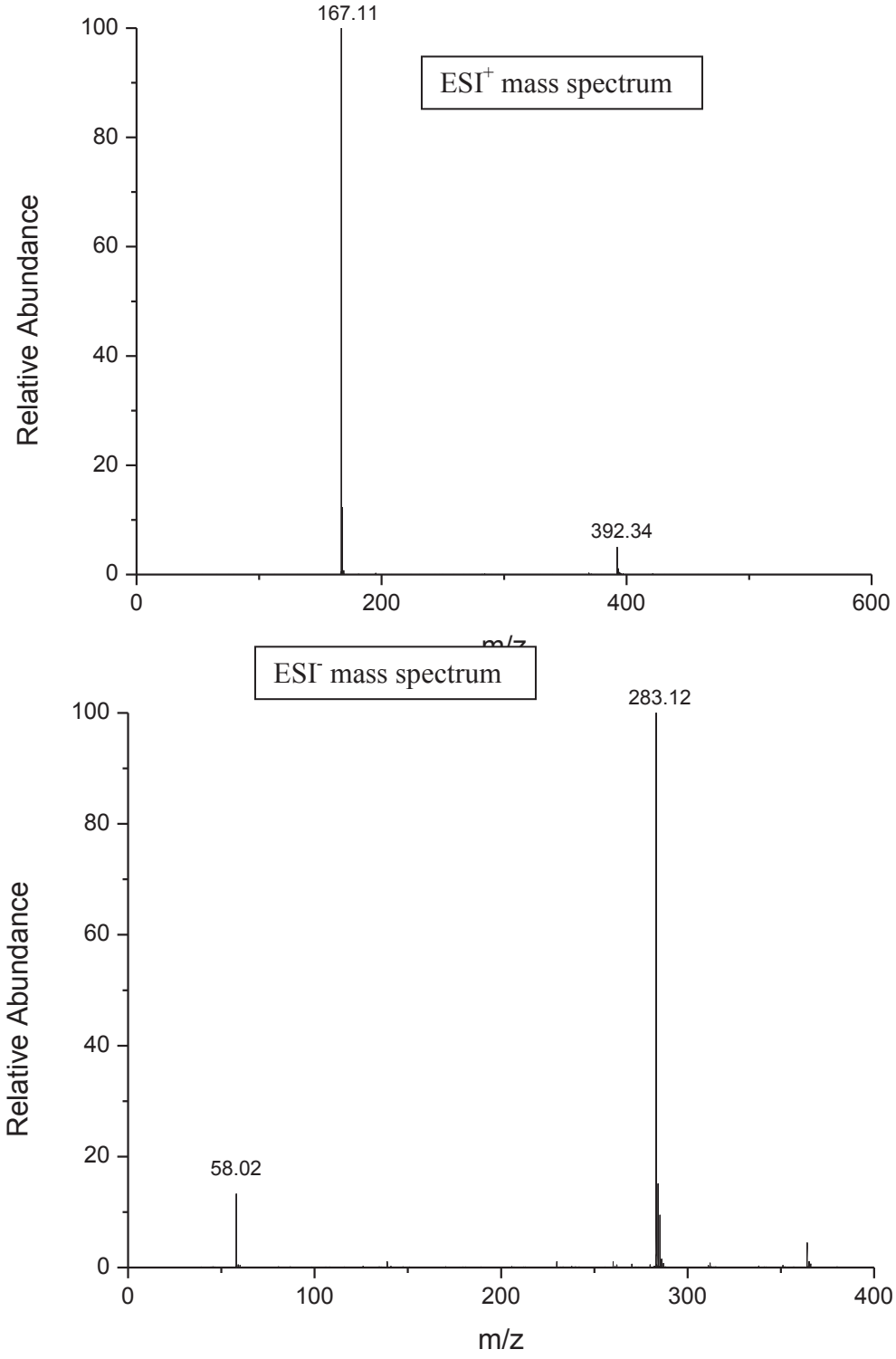

	Entire	Cation	Anion
Mass calculated	225.1	167.1	57.9

1-hexyl-3-methylimidazolium dicyanamide: $[C_1C_6Im][N(CN)_2]$

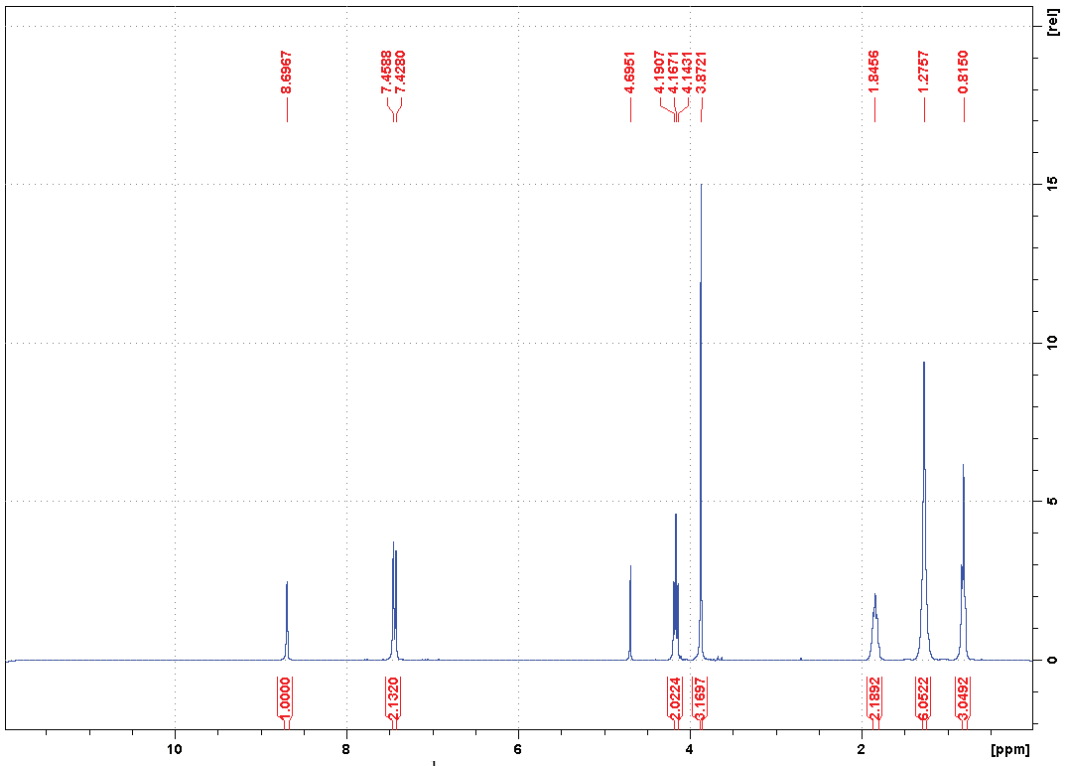

^{1}H NMR in D_2O

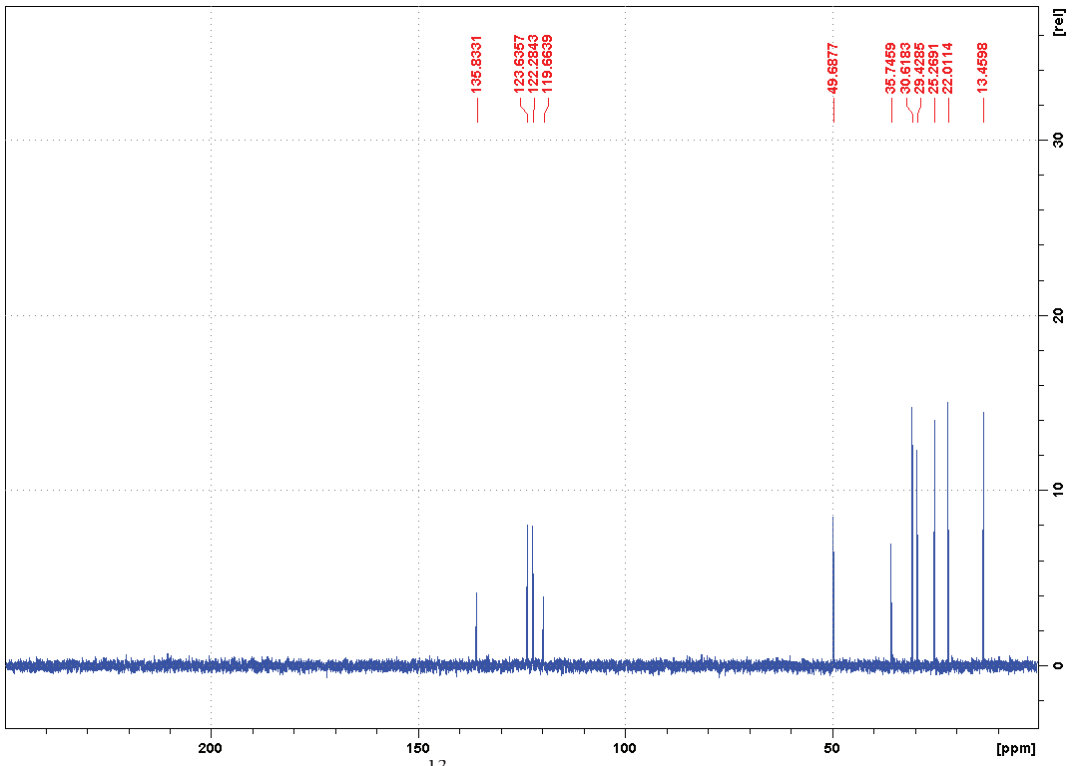

^{13}C NMR in D_2O

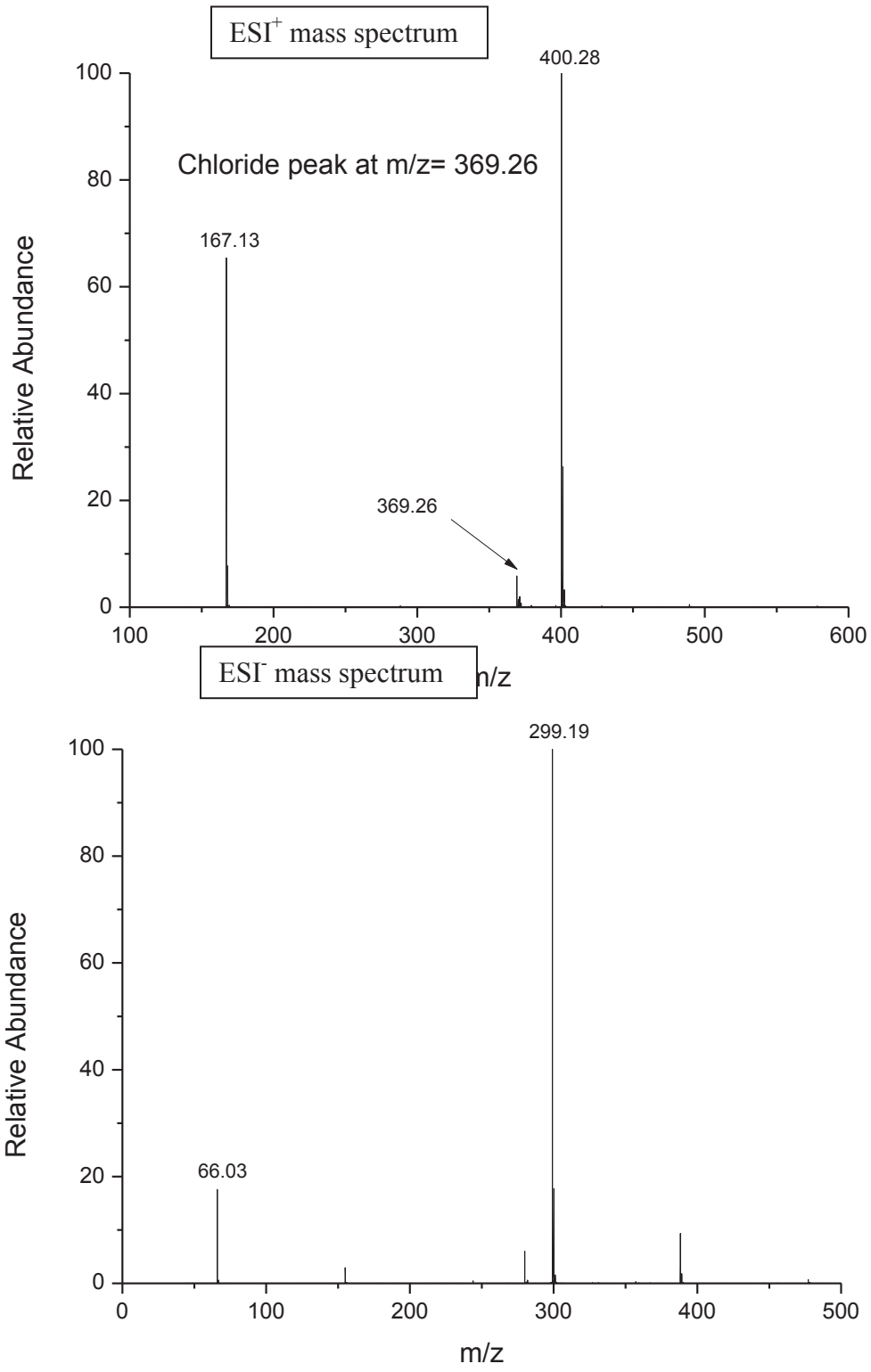

	Entire	Cation	Anion
Mass calculated	233.1	167.1	66.0

1-octyl-3-methylimidazolium tetrafluoroborate: $[C_1C_8Im][BF_4]$

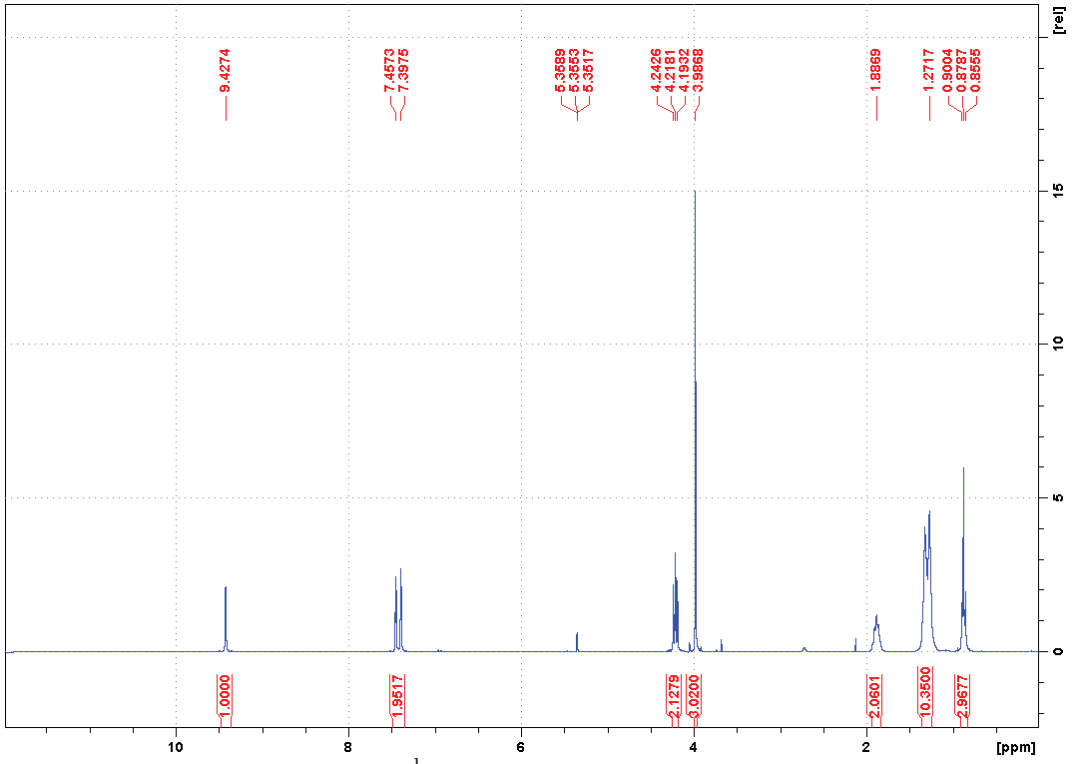

^{1}H NMR in CD_2Cl_2

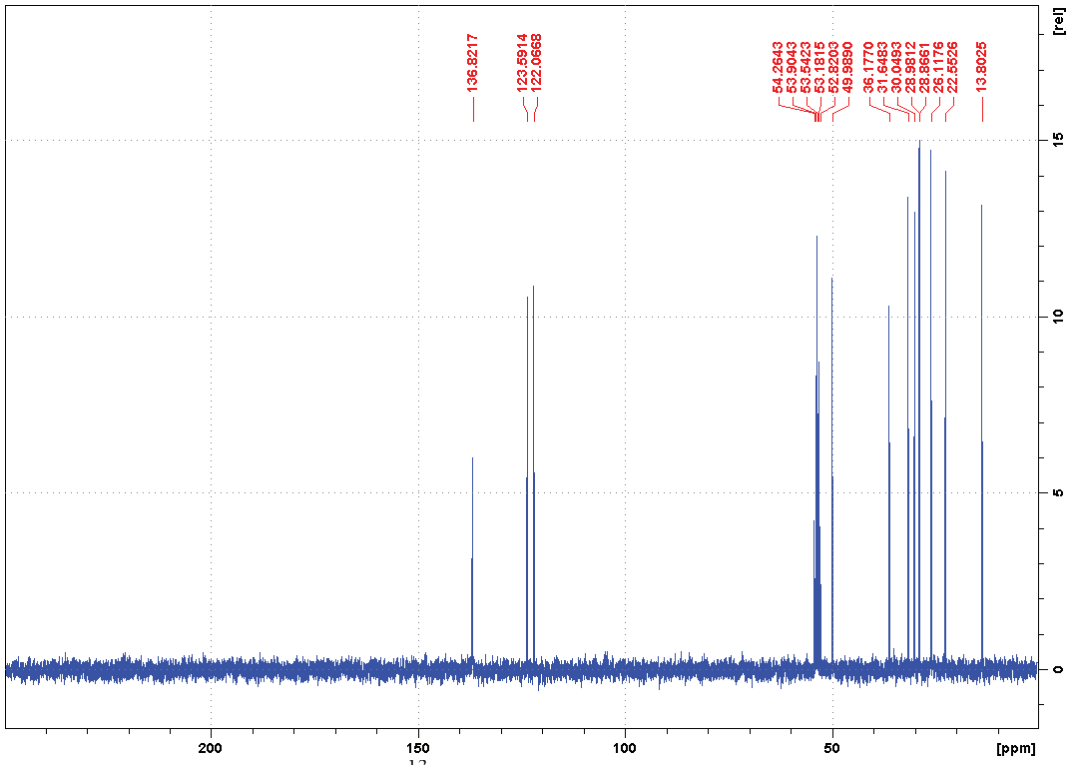

^{13}C NMR in CD_2Cl_2

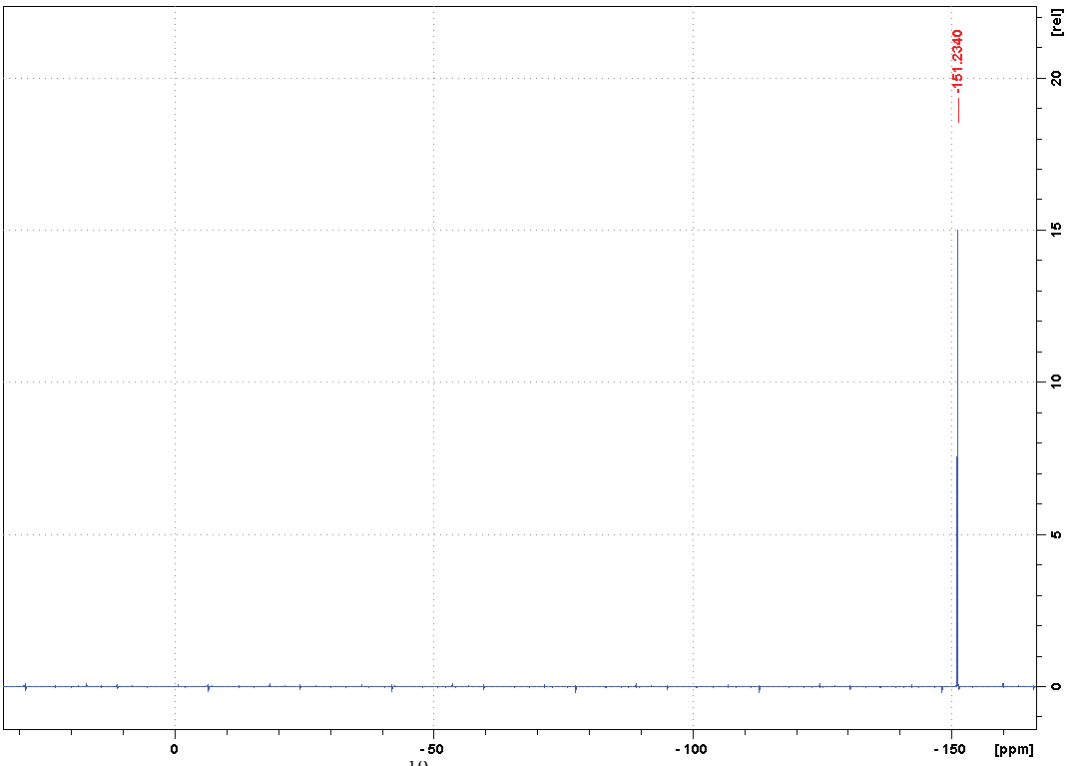

^{19}F NMR in CD_2Cl_2

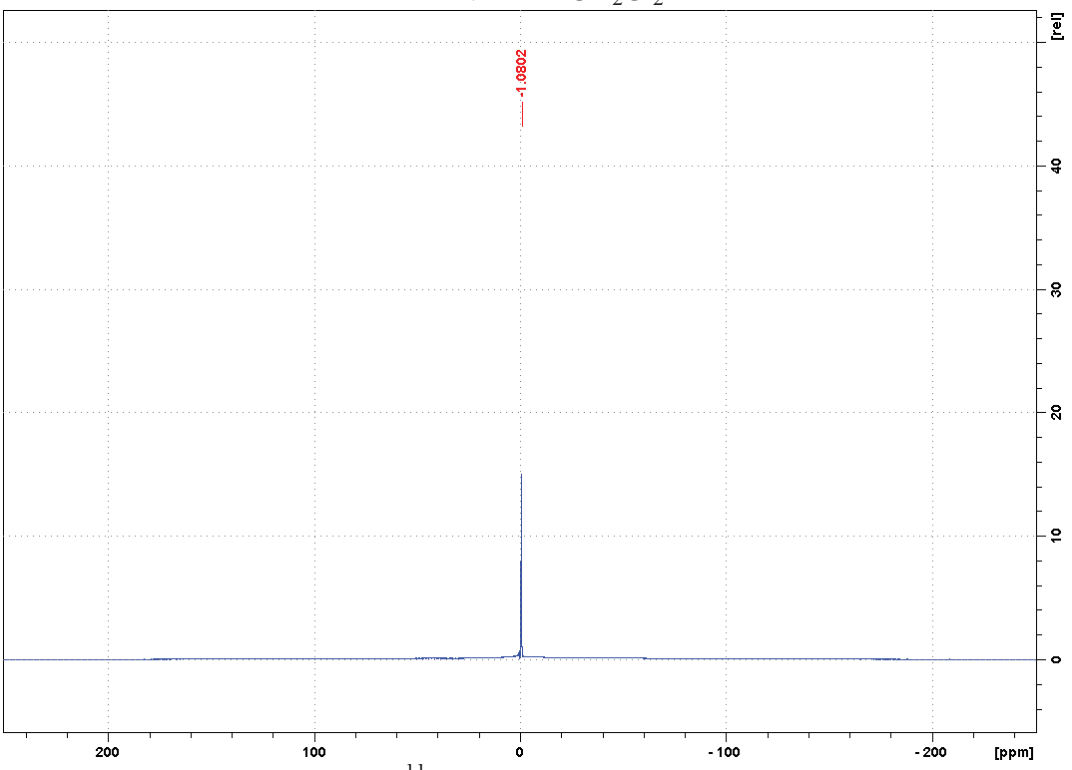

^{11}B NMR in CD_2Cl_2

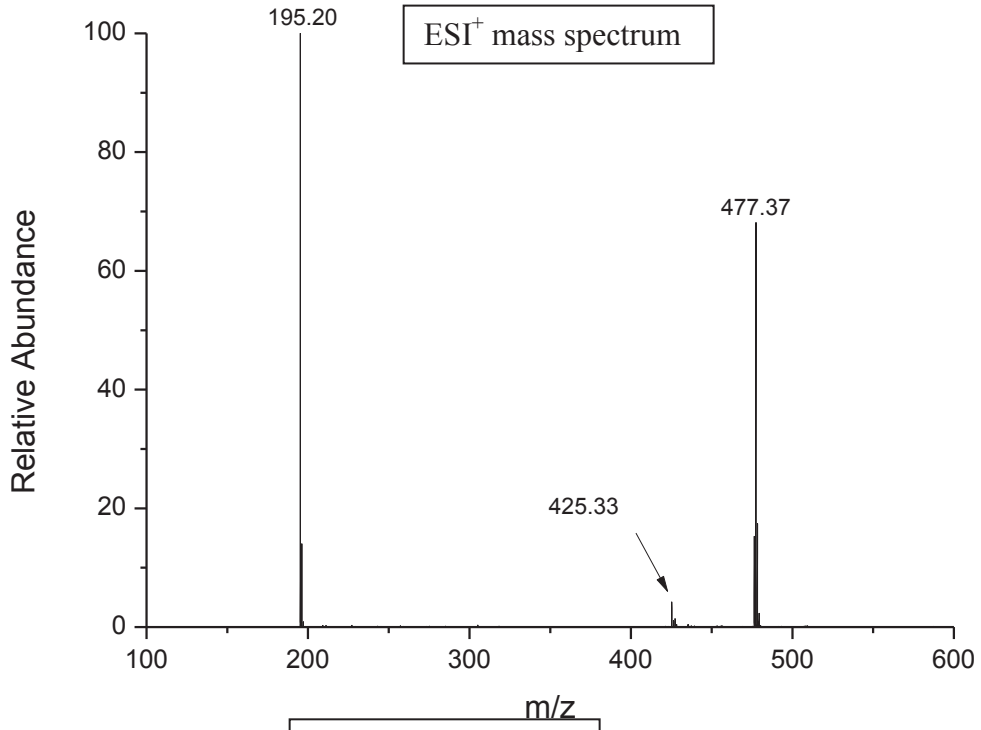

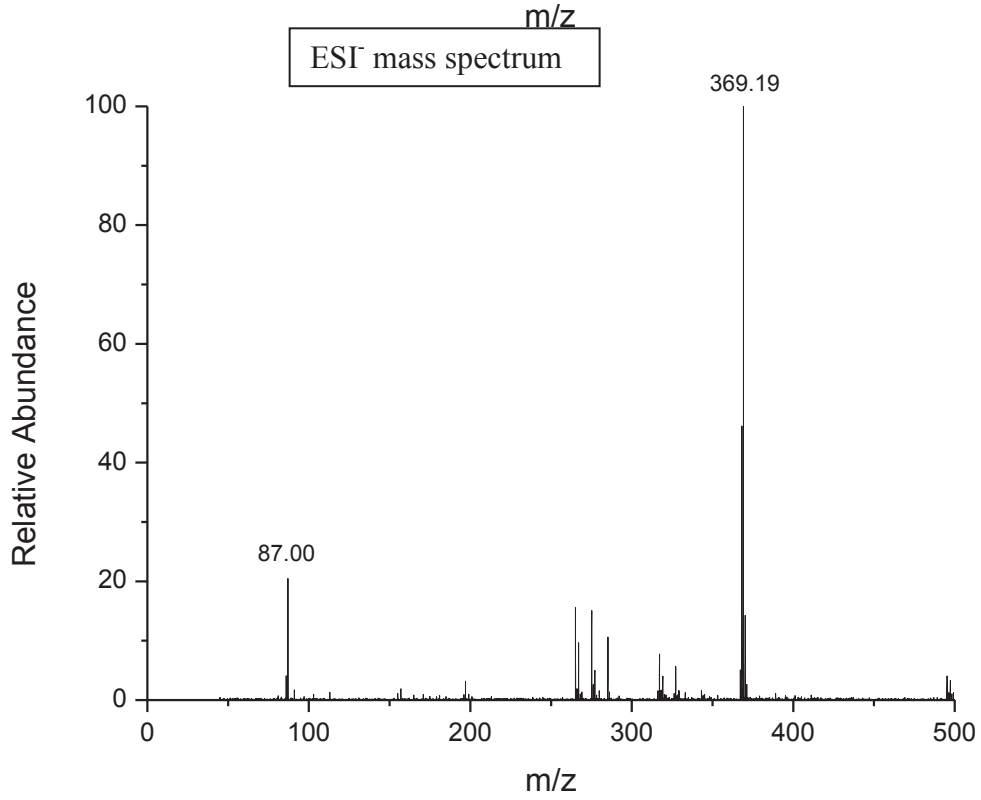

	Entire	Cation	Anion
Mass calculated	282.1	195.1	87.0

1-octyl-3-methylimidazolium dicyanamide: $[C_1C_8Im][N(CN)_2]$

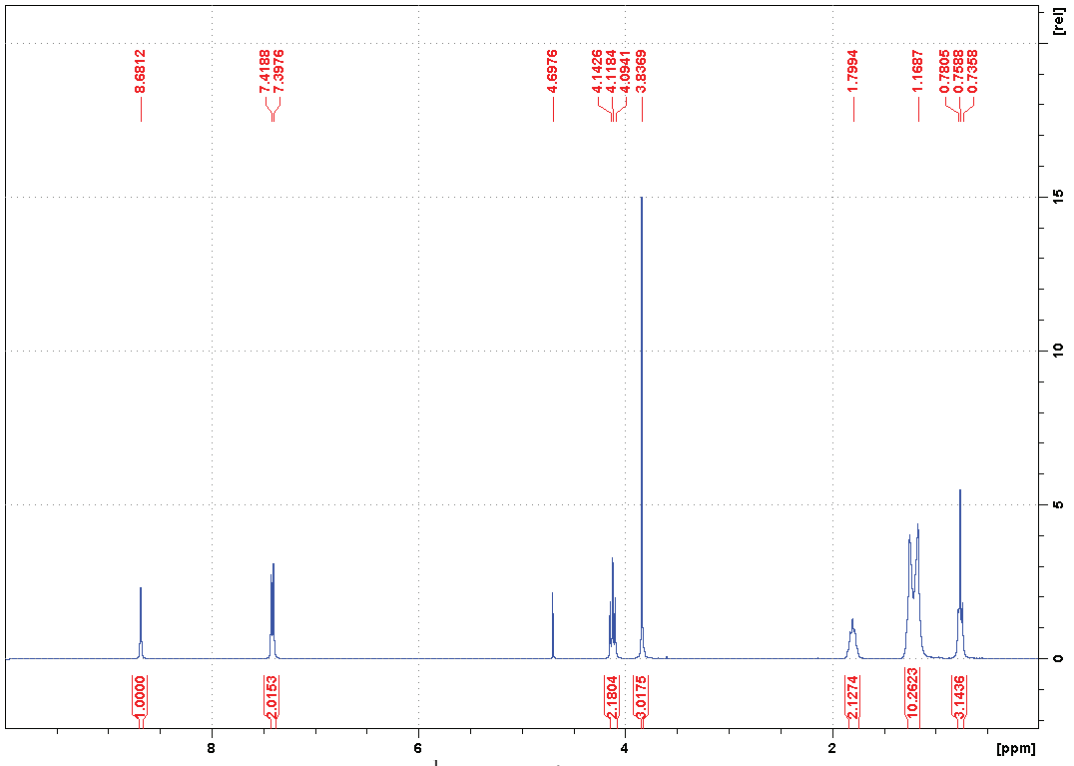

^{1}H NMR in D_2O

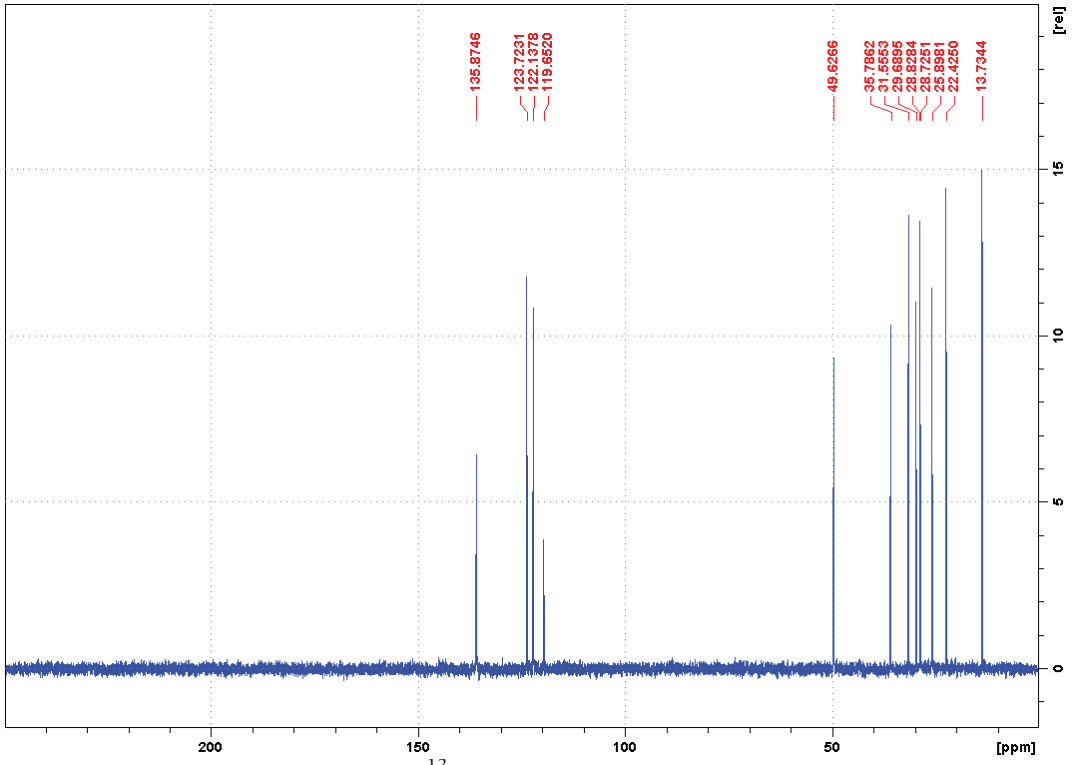

^{13}C NMR in D_2O

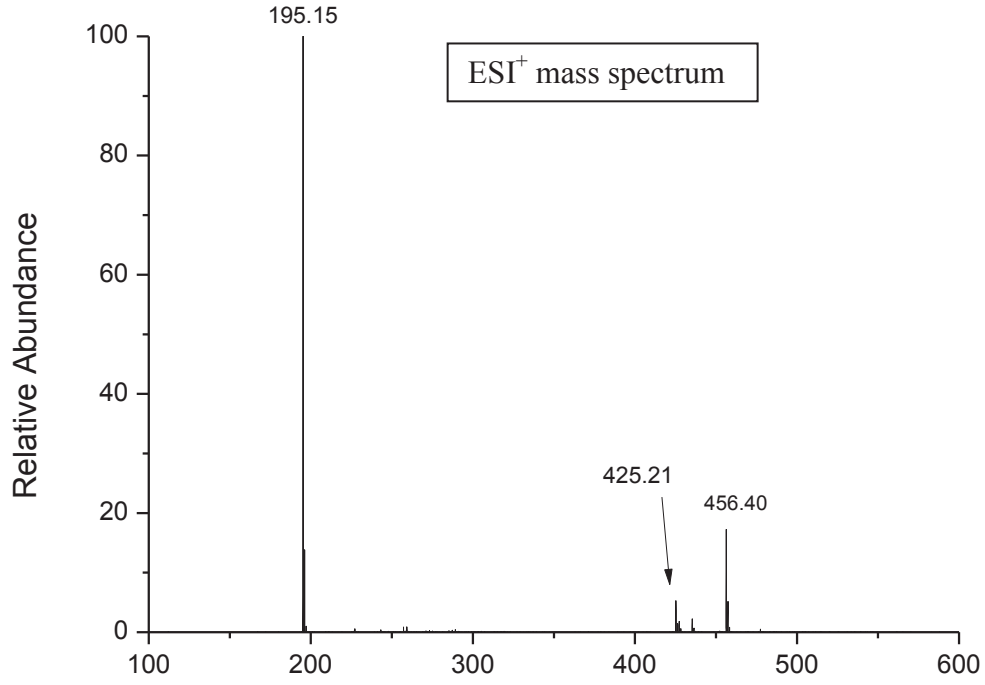

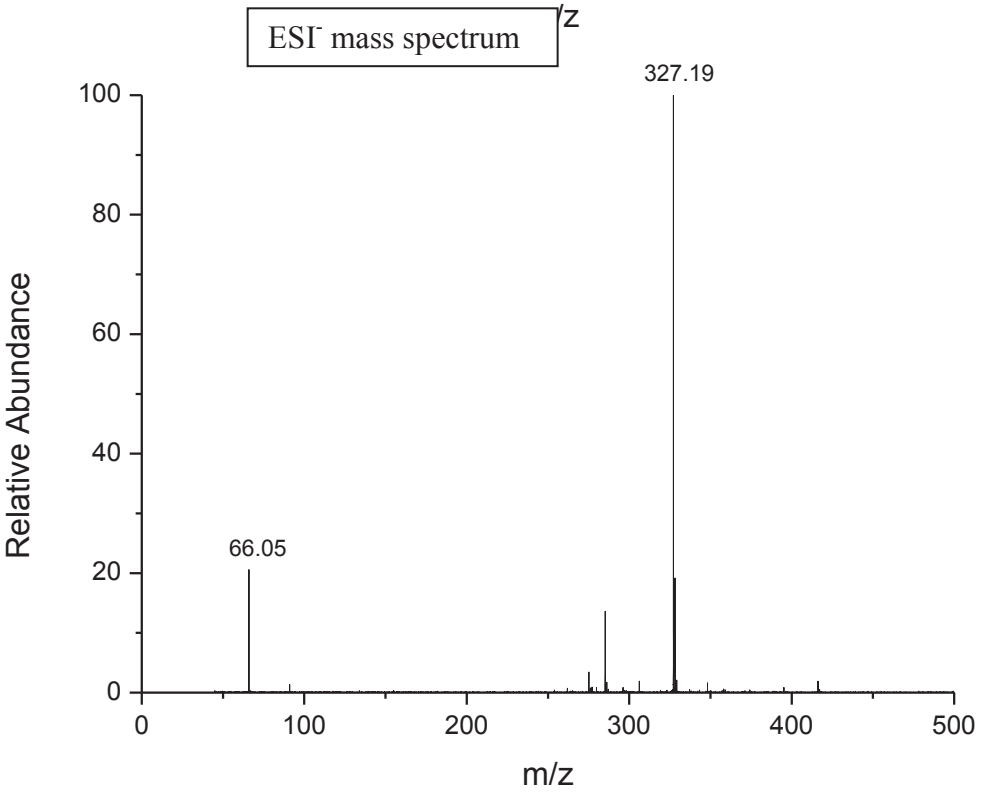

	Entire	Cation	Anion
Mass calculated	261.2	195.1	66.0

N-butyl-N-methylpyrrolidinium dicyanamide: $[P_{14}][N(CN)_2]$

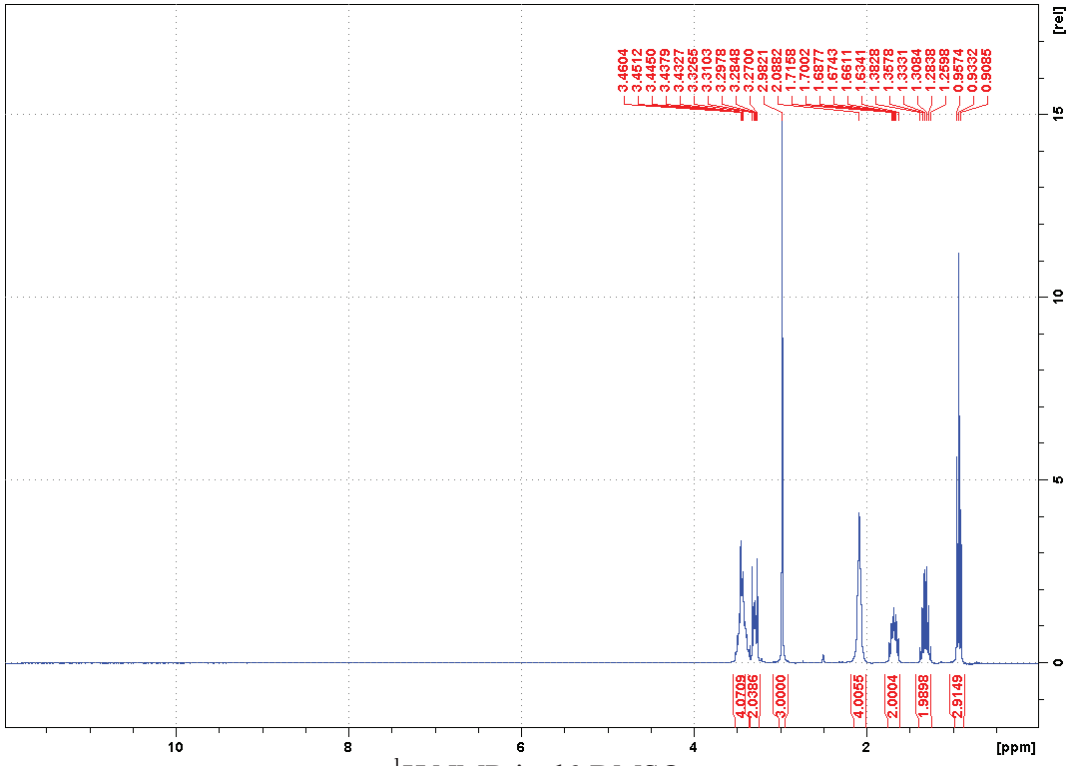

^{1}H NMR in d6-DMSO

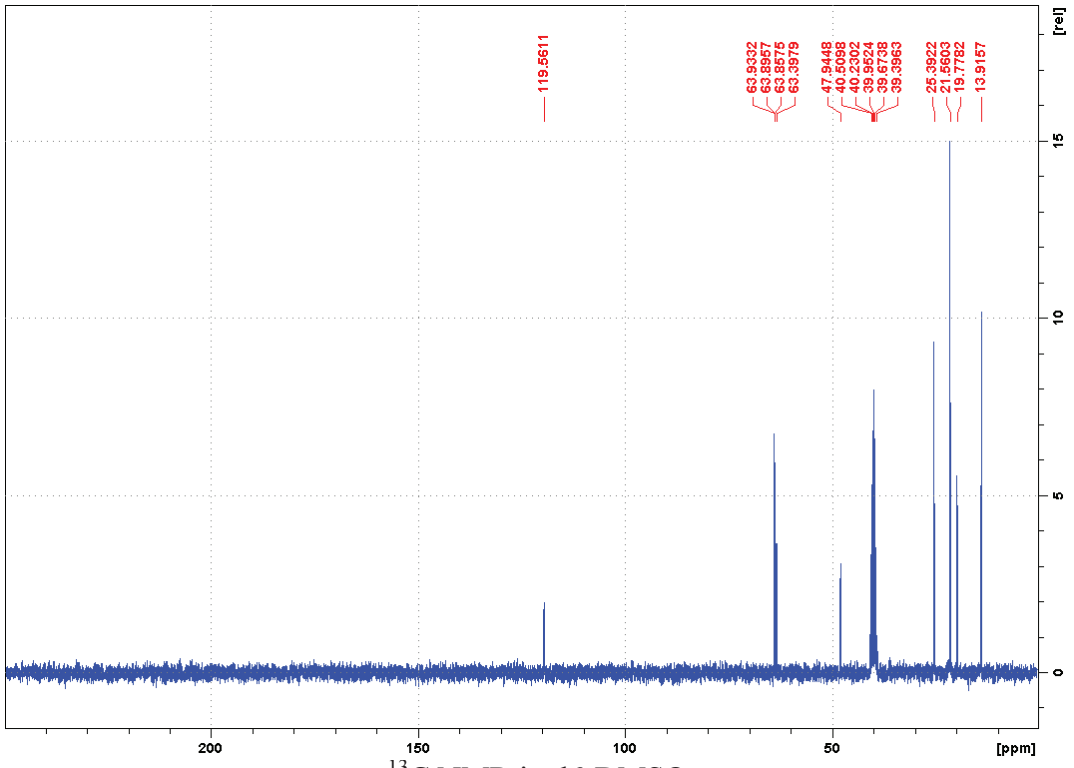

^{13}C NMR in d6-DMSO

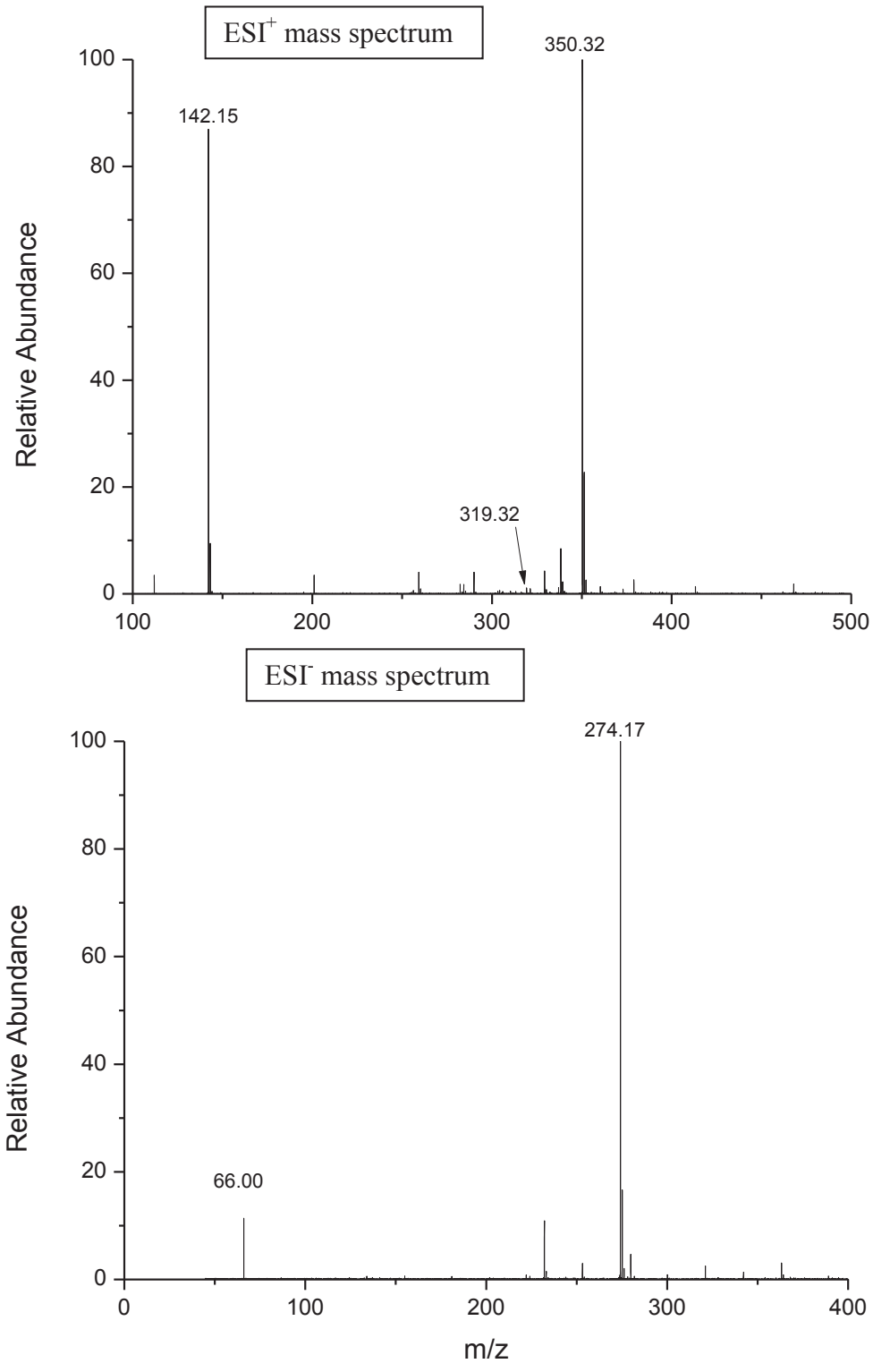

	Entire	Cation	Anion
Mass calculated	208.1	142.1	66.0

N-butyl-N-methylpyrrolidinium bis(trifluoromethylsulfonyl)imide: $[P_{14}][NTf_2]$

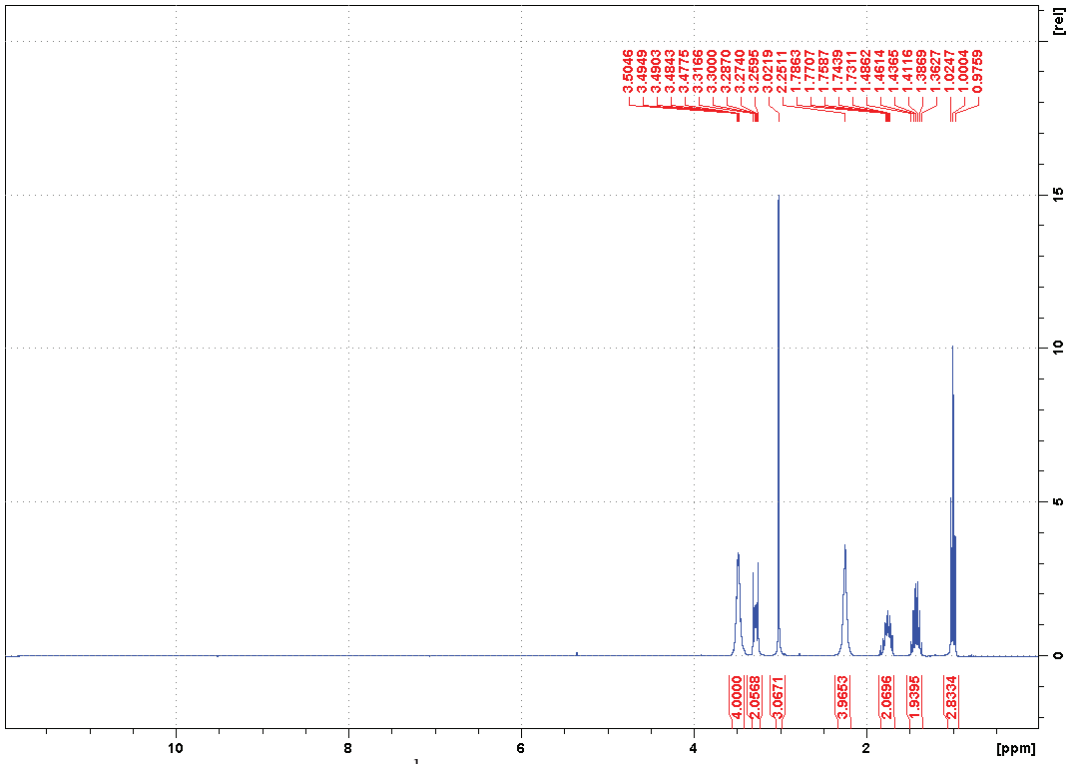

^{1}H NMR in CD_2Cl_2

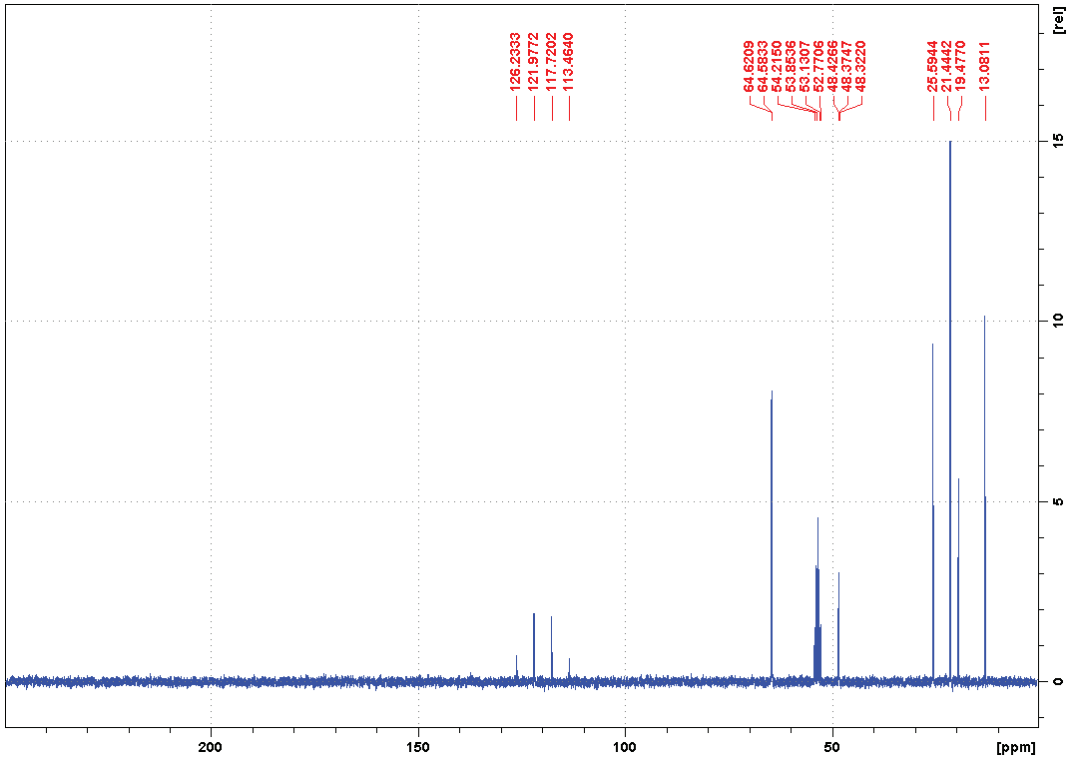

^{13}C NMR in CD_2Cl_2

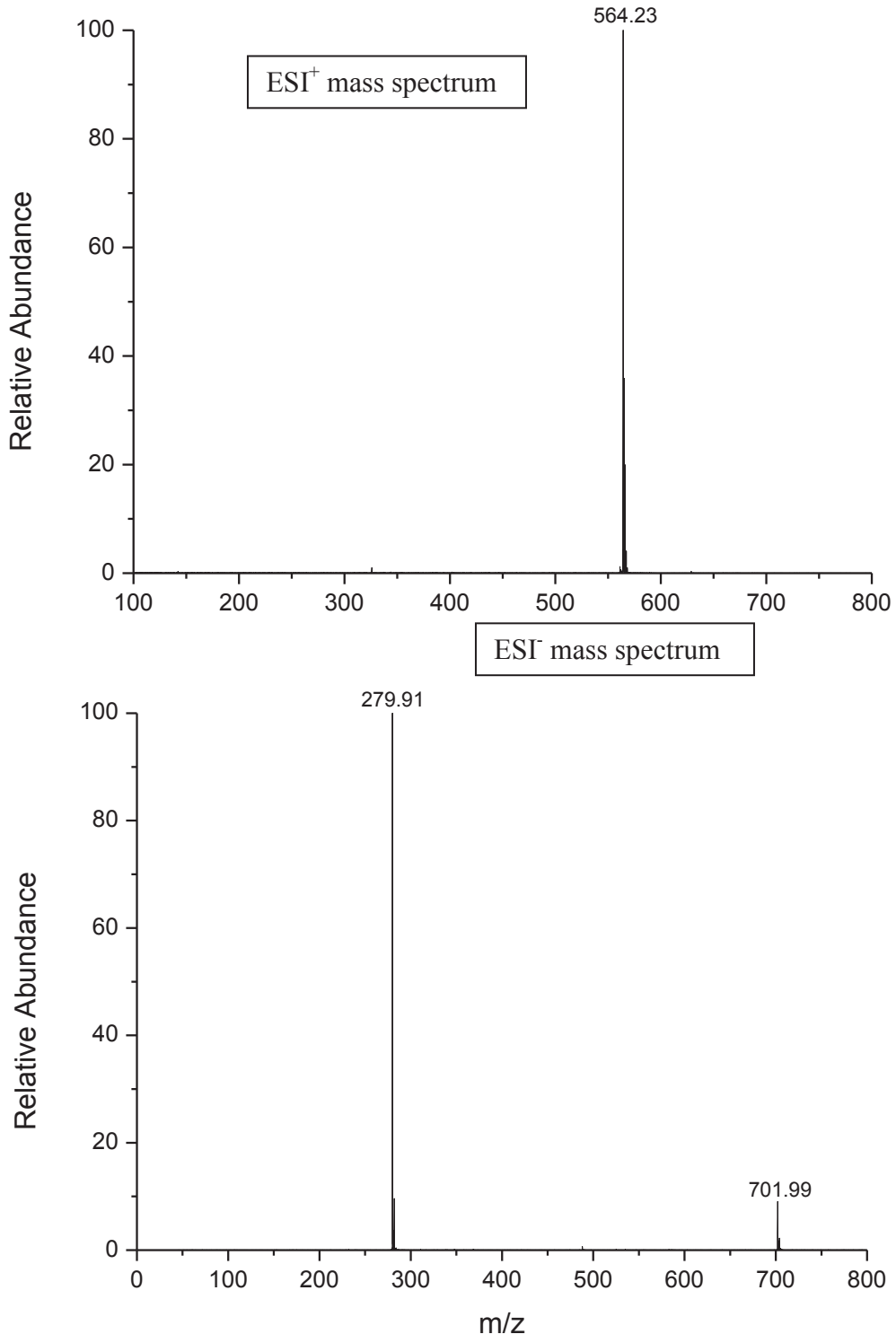

	Entire	Cation	Anion
Mass calculated	422.0	142.1	279.9

Tetrabutylphosphonium bis(trifluoromethylsulfonyl)imide: $[P_{4444}][NTf_2]$

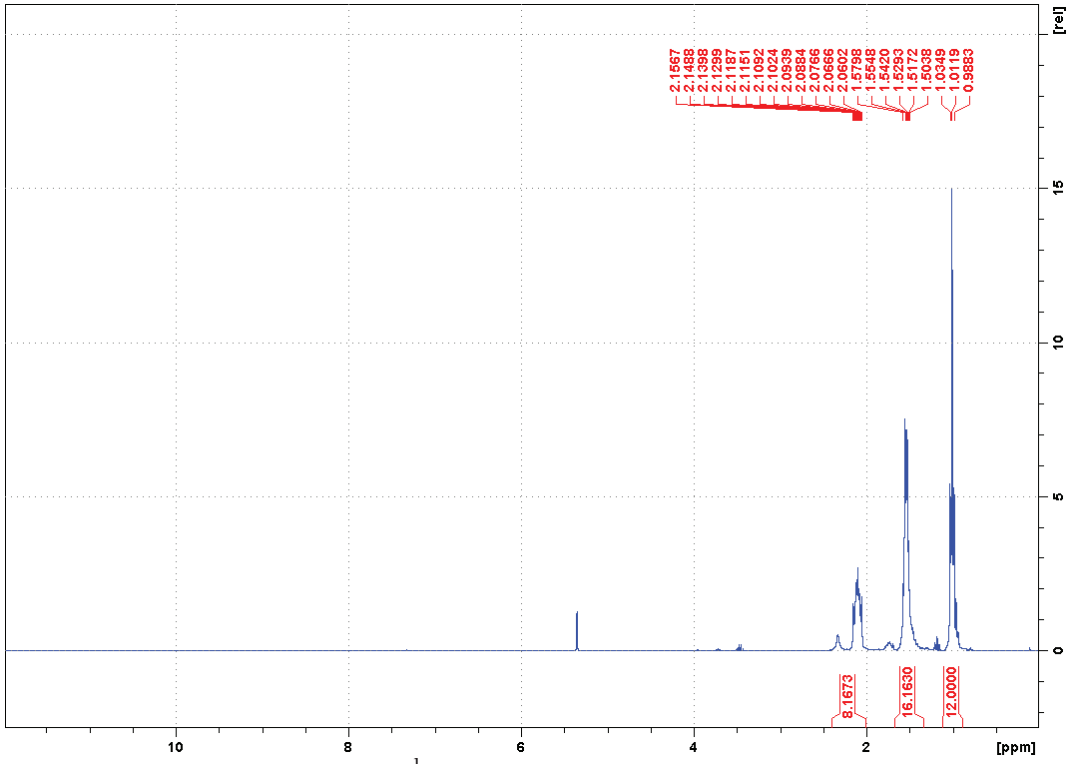

^{1}H NMR in CD_2Cl_2

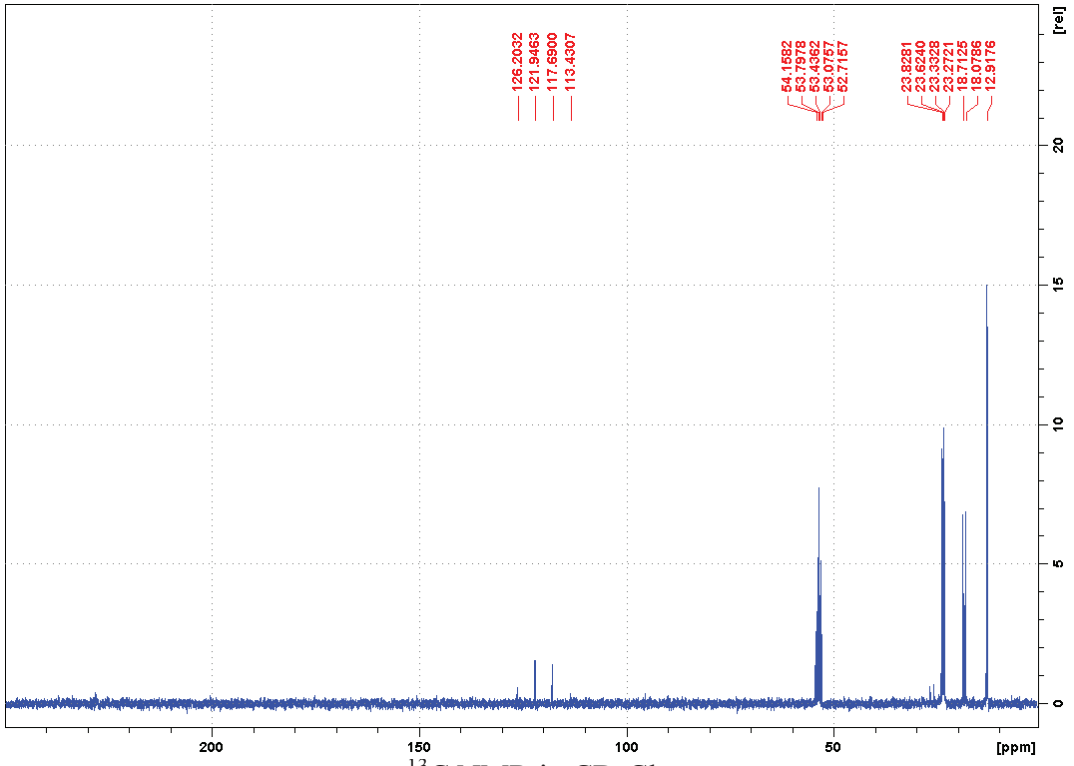

^{13}C NMR in CD_2Cl_2

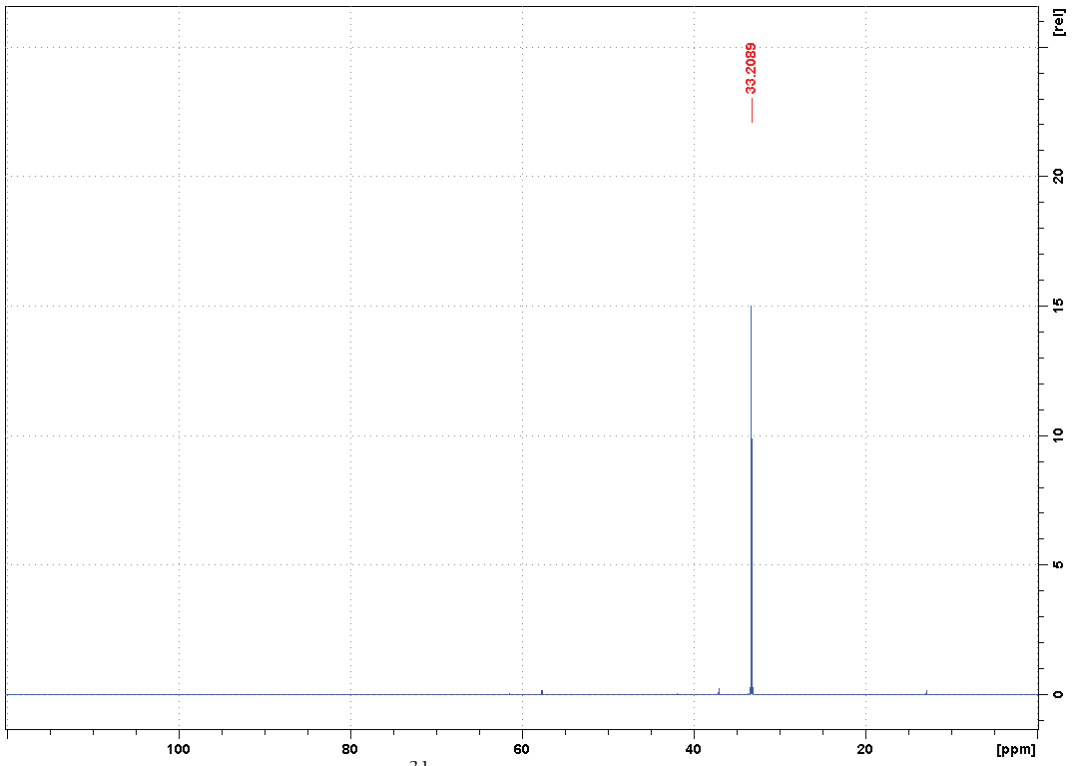

^{31}P NMR in CD_2Cl_2

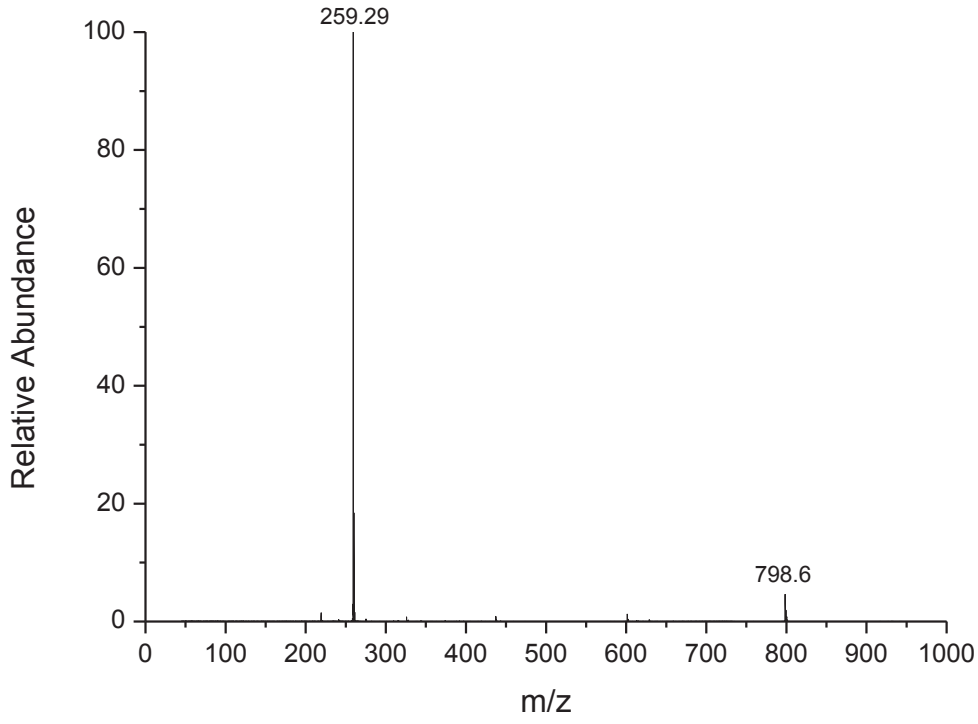

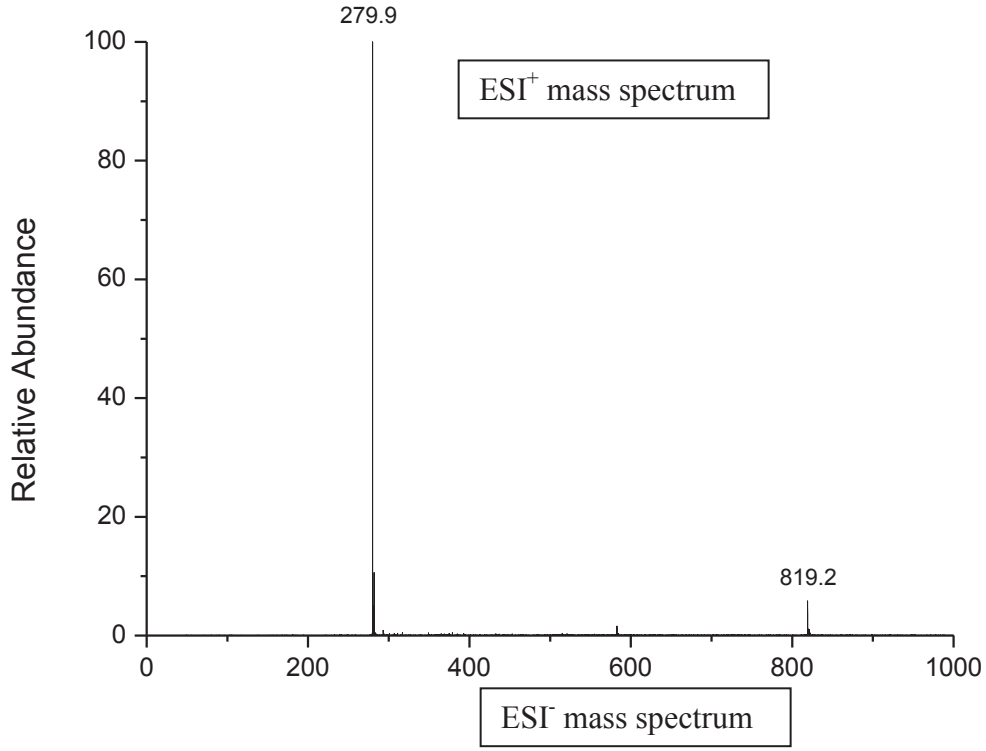

	Entire	Cation	Anion
Mass calculated	539.1	259.2	279.9

Tetrabutylphosphonium tetrafluoroborate: $[P_{4444}][BF_4]$

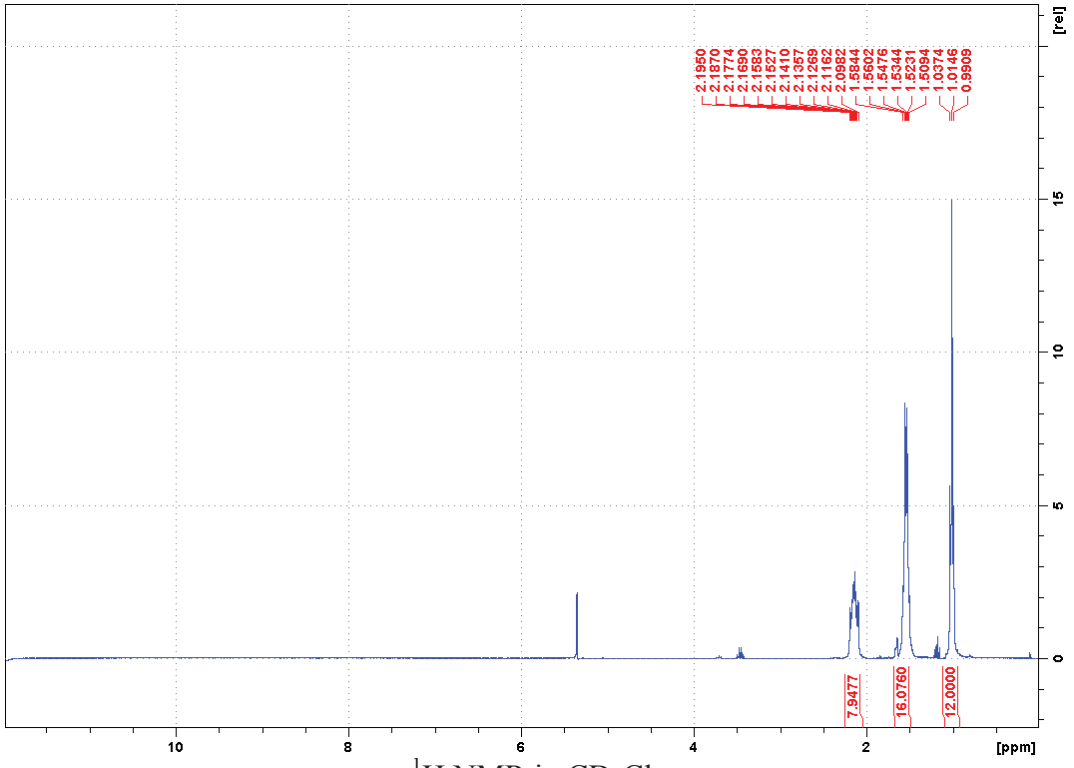

^{1}H NMR in CD_2Cl_2

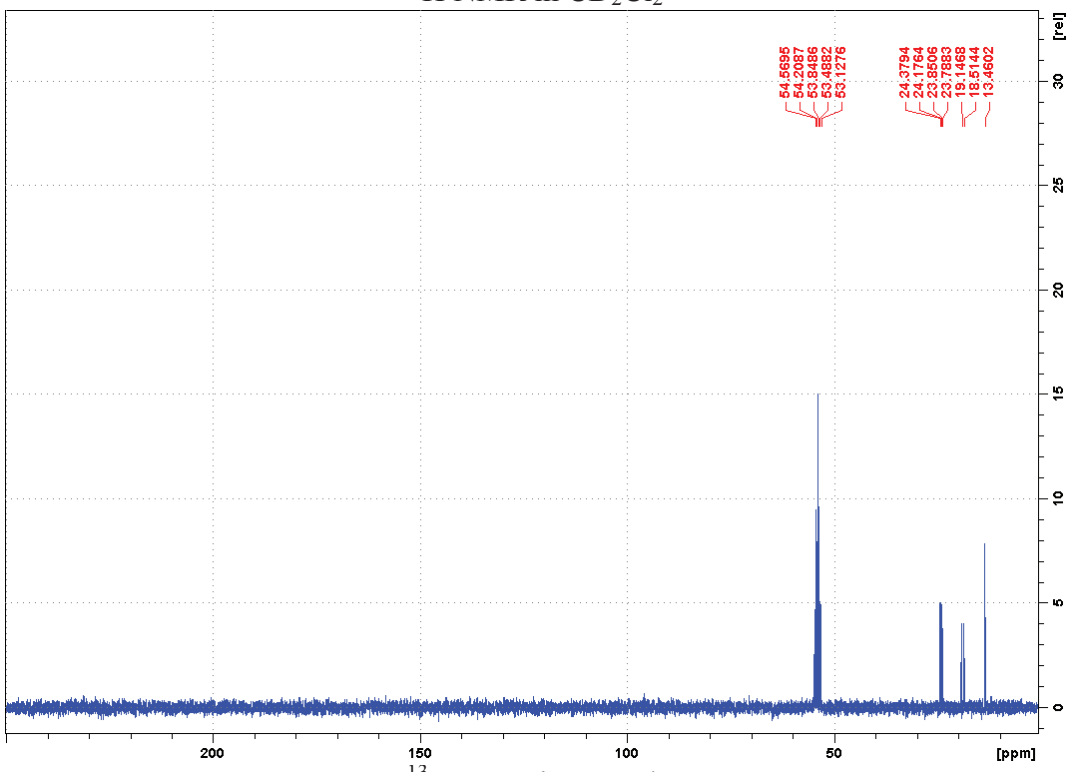

^{13}C NMR in CD_2Cl_2

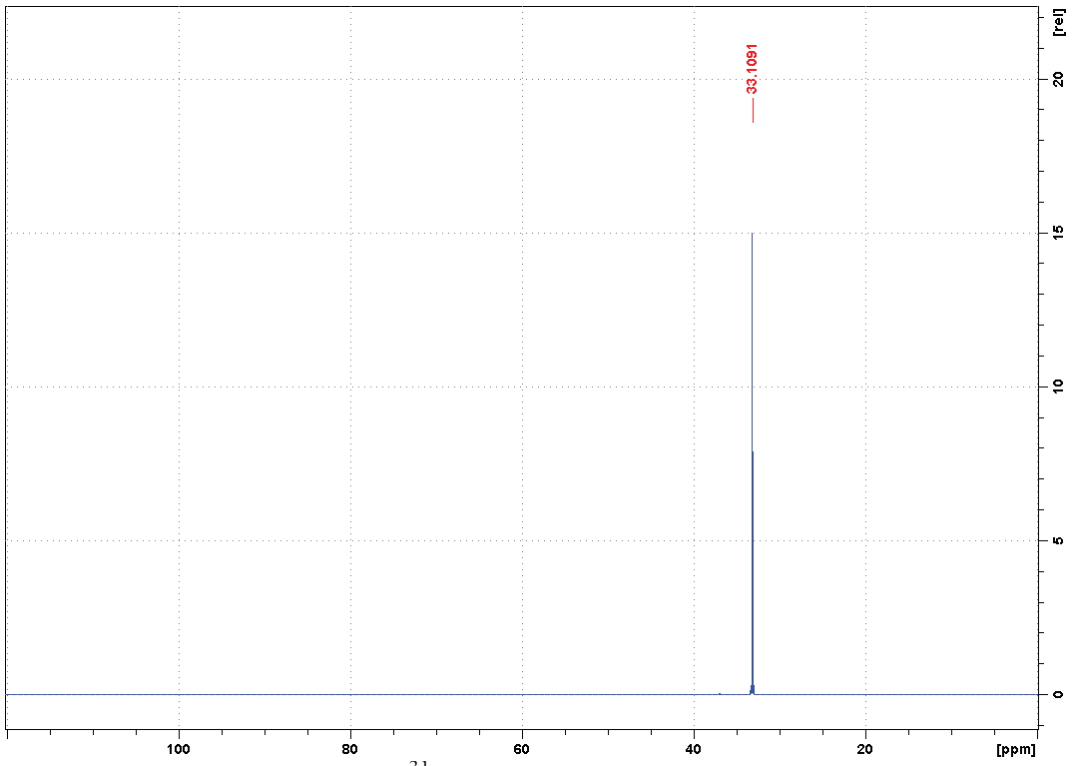

^{31}P NMR in CD_2Cl_2

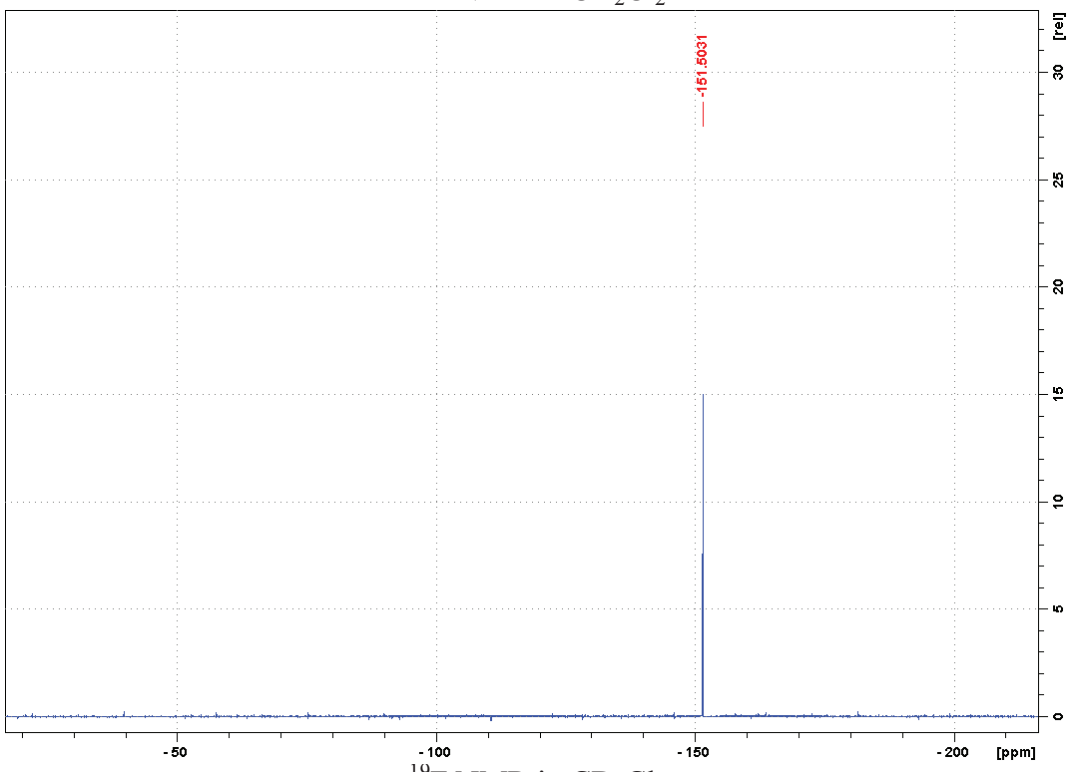

^{19}F NMR in CD_2Cl_2

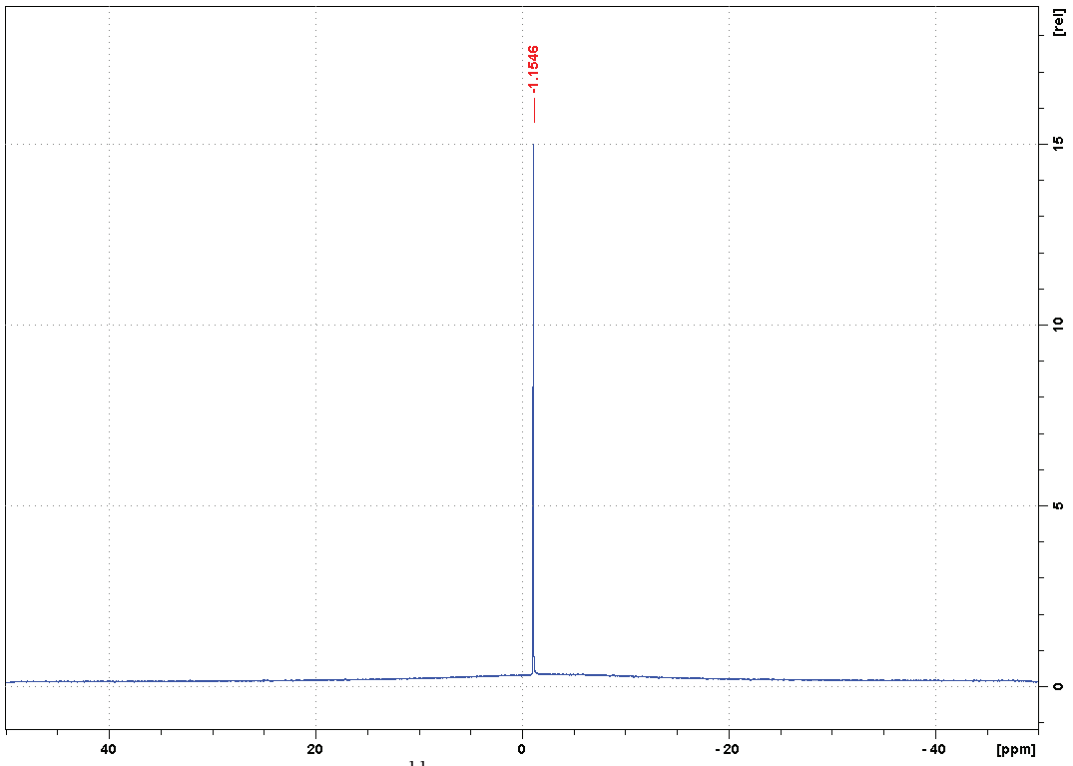

^{11}B NMR in CD_2Cl_2

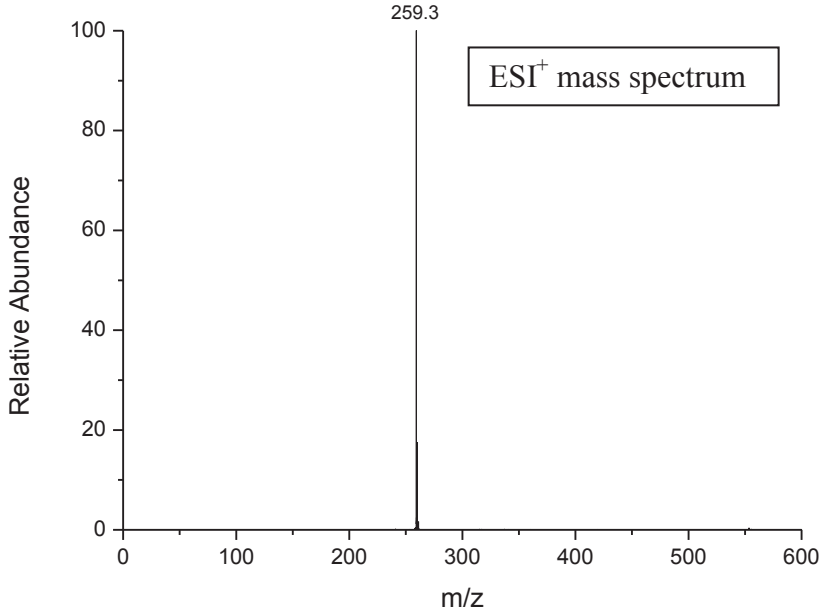

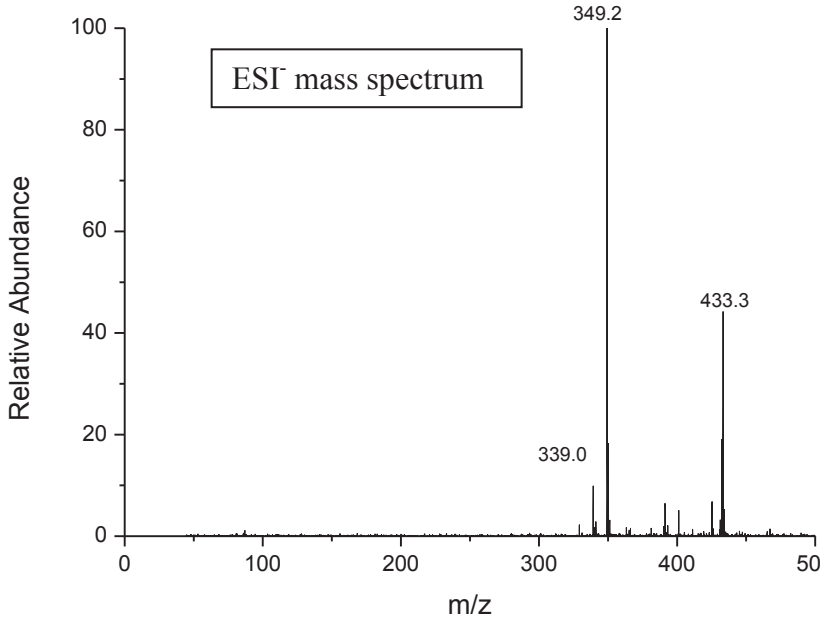

	Entire	Cation	Anion
Mass calculated	346.2	259.2	87.0

Appendix II

Synthesis of $[C_1C_4Im][Cl]$ and $[C_1C_4Im][NTf_2]$

$[C_1C_4Im][Cl]$ 1-chlorobutane (106 mL, 1.01 mol) was added to freshly distilled 1-methylimidazole (50 mL, 0.63 mol). The mixture was stirred for 48 h at 65°C. The hot solution was then transferred drop wise via a cannula into toluene (200mL) at 0°C under vigorous mechanical stirring. The white precipitate formed was then filtered and washed repeatedly with toluene (3×200 mL) and dried overnight *in vacuo* giving a white powder (95.6 g, 87 %).^{1}H-NMR (CD_2Cl_2): δ (ppm) : 11.05 (s, 1H, C_2H) ; 7.33 (d, 1H, C_4H) ; 7.28 (d, 1H, C_5H) ; 4.31 (t, 2H, NCH_2) ; 4.07 (s, 3H, NCH_3) ; 1.90 (qt, 2H, $CH_2CH_2CH_2$) ; 1.41 (st, 2H, $CH_2CH_2CH_3$) ; 0.96 (t, 3H, CH_2CH_3) ; $^{13}C\{^1H\}$-NMR (CD_2Cl_2) : δ (ppm) : 138.3 (C_2H) ; 122.3 (C_4H) ; 119.8 (C_5H) ; 50.1 (NCH_2) ; 36.8 (NCH_3) ; 32.5 ($CH_2CH_2CH_2$) ; 19.8 ($CH_2CH_2CH_3$) ; 13.6 (CH_2CH_3).

$[C_1C_4Im][NTf_2]$ A solution of $[LiNTf_2]$ (50 g, 0.17 mol) in water (50 mL) was added to a solution of C_1C_4ImCl (30.4 g, 0.17 mol) in water (100 mL). The solution was stirred for 2 h at room temperature, then dichloromethane (50 mL) was added and the mixture transferred to a separating funnel. The lower phase was collected and washed repeatedly with water (8 × 100 mL) until no chloride traces remained in the washings (tested with silver nitrate solution). The ionic liquid in dichloromethane was purified through a short alumina column and the solvent removed *in vacuo* giving a colourless viscous liquid. ^{1}H-NMR (CD_2Cl_2): δ (ppm) : 8.73 (s, 1H, C_2H) ; 7.28 (d, 1H, C_4H) ; 7.24 (d, 1H, C_5H) ; 4.15 (t, 2H, NCH_2) ; 3.90 (s, 3H, NCH_3) ; 1.83 (qt, 2H, $CH_2CH_2CH_2$) ; 1.32 (st, 2H, $CH_2CH_2CH_3$) ; 0.94 (t, 3H, CH_2CH_3) ; $^{13}C\{^1H\}$-NMR (CD_2Cl_2) : δ (ppm) : 134.3 (C_2H) ; 124.3 (C_4H) ; 122.4 (C_5H) ; 118.2 (CF_3) ; 50.3 (NCH_2) ; 37.1 (NCH_3) ; 33.2 ($CH_2CH_2CH_2$) ; 19.8 ($CH_2CH_2CH_3$) ; 13.5 (CH_2CH_3).

NMR measurements

NMR spectra were recorded on BRUKER AVANCE 300 spectrometer (^{1}H: 300.1 MHz, ^{13}C: 75.4) and on BRUKER AVANCE III 500 spectrometer operating at 500.13MHz for ^{1}H, 470.55MHz for ^{19}F, 194.369MHz for ^{7}Li and 50.67MHz for ^{15}N. Deuterated solvent (CD_2Cl_2,) was used as external standard. The chemical shift are noted in parts per million (ppm), the coupling constant in Hz.

The pulsed-field gradient spin-echo NMR technique was used to measure the self-diffusion coefficients of both the cation and anion species by observing ^{1}H, ^{19}F and ^{7}Li nuclei. NMR measurements were made on a BRUKER AVANCE III 500 spectrometer operating at 500.13MHz for ^{1}H, 470.55MHz for ^{19}F and 194.369MHz for ^{7}Li with a 5 mm pulsed-field gradient BBFO probe.

The sample temperature was controlled within ± 0.1 K by a variable temperature control unit BVT3200 using a nitrogen gas flow (527 $L.h^{-1}$). In view to minimize convection effects at high temperature, the IL was introduced in **a sealed 3mm tube centered in a 5 mm tube filled** with the locking solvent DMSO-d_6 and we used the standard Bruker dstebpgp3s sequence. For each sample and temperature, the probe was carefully tuned, and the 90 pulse evaluated.

For each DOSY experiment, we optimized the pulse gradients lengths and diffusion time to get a signal attenuation of at least 90% with the contradictory constrains: i) set minimum diffusion time to minimize convection, ii) keep minimum gradient pulse length to obtain sufficient attenuation, iii) avoid heating effect of the gradients coil and iv) keep the ratio Δ/δ the highest. The interval between two gradient pulses, Δ, was set between 100 and 400 ms, and the duration of the field gradient, δ, was varied from 3.5 to 8 ms depending on the temperature. The signals were accumulated 16 times for a linear set of 32 different gradient values distributed from 3 to 47.5 G/cm. The relaxation delay was set to 5s and 16 dummy scans where programmed prior to acquisition. The determination of self-diffusion coefficients used the BRUKER T1/T2 module for each peak. For the imidazolium cation, we took the average of the different available peaks.

Electrode preparation and cycling test

$LiFePO_4$ composite electrodes were prepared from a paste constituted of $LiFePO_4$ (Pulead), acetylene black (Showa Denko) and PolyVinylydene difluoride PVdF (Solvay) with a weight ratio 90:2:2:6 mixed in n-Methyl 2 Pyrrolidone, coated onto aluminium foil, then dried and compressed using a roll-press machine to improve the electrode conductivity (two different loadings: 1.0 mAh/cm^2 when coupled with $Li_4Ti_5O_{12}$ (LTO) and 2.4 mAh/cm^2 with Cgr negative electrodes).

LTO composite electrode was prepared by coating the aqueous-based slurry on an aluminium foil. The slurry was composed of LTO with acetylene black (Showa Denko) carboxymethylcellulose (CMC) and styrene butadiene rubber (SBR), then dried and compressed (electrode thickness after pressing: 60µm, 1.1 mAh/cm^2).

A graphite composite electrode was prepared from natural graphite, carboxymethylcellulose (CMC) and styrene butadiene rubber (SBR) in a weight ratio 96:2:2, deposited onto a copper collector with a loading of 2.6 mAh/cm^2.

The cycling experiments were undertaken with the use of an Arbin multi-channel potentiostat/galvanostat at 0.1C rate at 333 K between the cut off voltages of [2.6V - 3.7V] for the Cgr/LFP and of [2.6V – 2.8V] for the LTO/LFP.

Electrochemical window

The electrochemical behavior of ILs and their binary mixtures were investigated using cyclic voltammetry in a three electrodes cell: a platinum working electrode, Ag/AgCl (3M KCl) reference electrode and a platinum counter electrode. Cyclic voltammetries measurements were carried out with Autolab PGStat 301Z potentiostat. The voltammograms were obtained at various temperatures (303 K up to 373 K) between -5 to 5 V at a scan rate 50 $mV.s^{-1}$. The values of electrochemical windows (EW = Ea – Ec) proposed have been converted versus Li^+/Li.

Table 1: Electrochemical stability of $[C_1C_3CNIm][NTf_2]$ and $[C_1C_3CNIm][Li][NTf_2]$ at different temperatures, cathodic (E_c) and anodic (E_a) limits related to Li^+/Li.

	$[C_1C_3CNIm][NTf_2]$			$[C_1C_3CNIm][Li][NTf_2]$		
T (K)	E_a (V)	E_c (V)	ΔE (V)	E_a (V)	E_c (V)	ΔE (V)
303	5.8	1.1	4.7	5.4	-0.4	5.0
313	5.8	1.1	4.7	5.4	-0.4	5.0
333	5.8	1.2	4.6	5.4	-0.4	5.0
353	5.8	1.2	4.6	5.4	-0.5	4.9
373	5.8	1.2	4.6	5.4	-0.5	4.9

Table 2: Electrochemical stability of $[C_1C_4Im][NTf_2]$ and $[C_1C_4Im][Li][NTf_2]$ at different temperatures, cathodic (E_c) and anodic (E_a) limits related to Li^+/Li.

	$[C_1C_4Im][NTf_2]$			$[C_1C_4Im][Li][NTf_2]$		
T (K)	E_a (V)	E_c (V)	ΔE (V)	E_a (V)	E_c (V)	ΔE (V)
303	5.6	0.9	4.7	5.2	-0.7	5.9
313	5.5	0.8	4.7	5.2	-0.7	5.9
333	5.5	0.9	4.6	5.2	-0.6	5.8
353	5.5	1.0	4.5	5.2	-0.4	5.6
373	5.5	1.0	4.5	5.1	-0.4	5.5

Figure 1: High resolution mass spectrometry of $[C_1C_4Im][NTf_2]$.

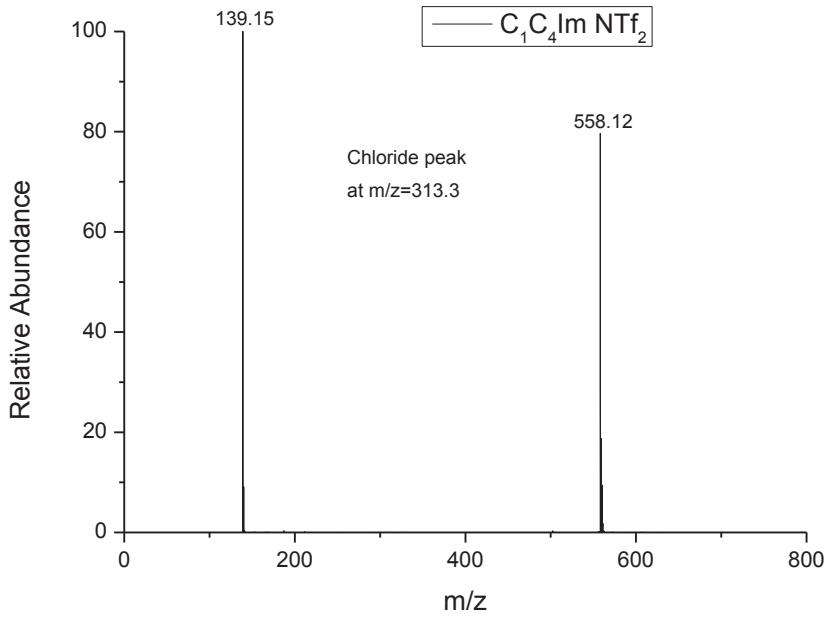

Figure 1: High resolution mass spectrometry of $[C_1C_4Im][NTf_2]$.

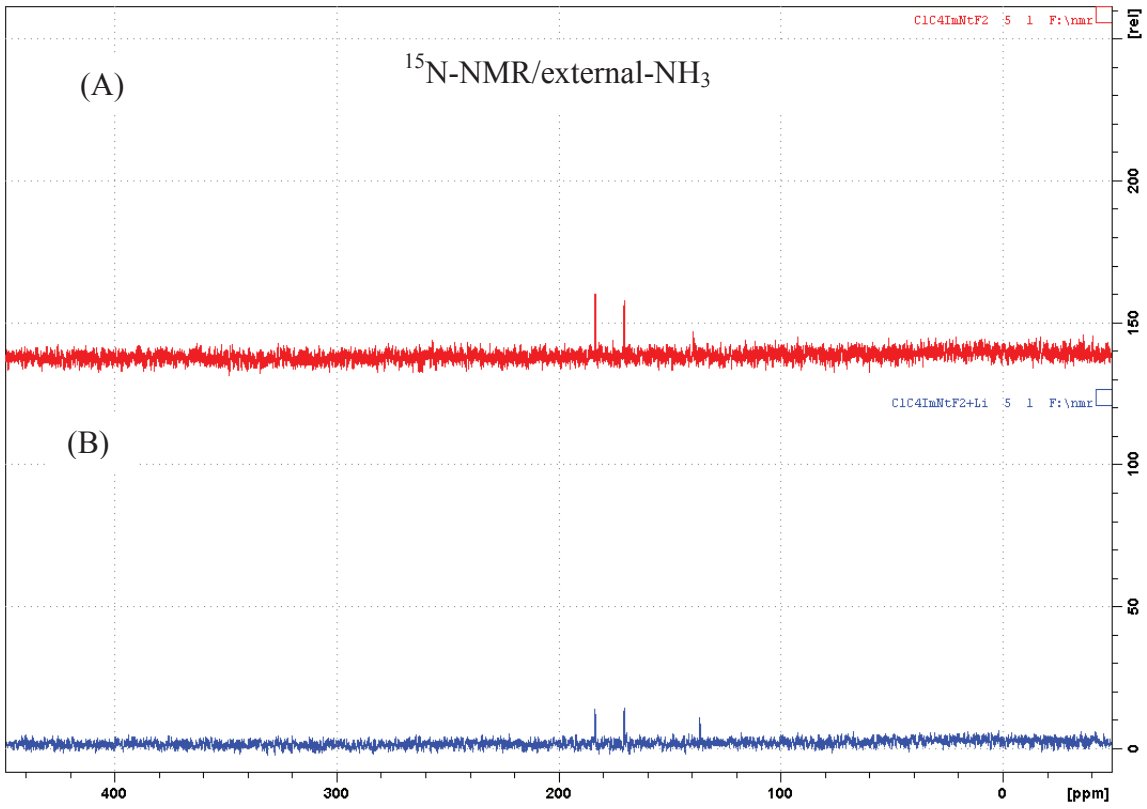

Figure 2: ^{15}N-NMR spectra of (A) $[C_1C_4Im][NTf_2]$ and (B) $[C_1C_4Im][Li][NTf_2]$ recorded at room temperature.

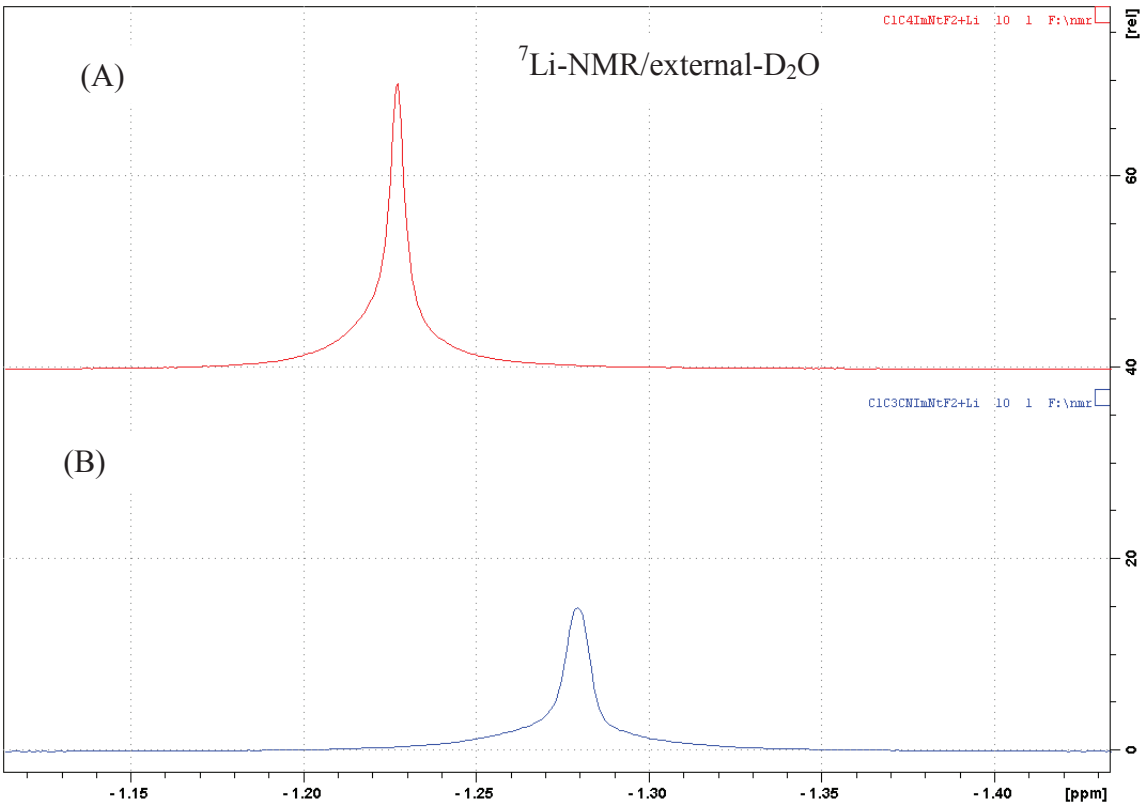

Figure 3: ^{7}Li-NMR spectra of (A) [C_1C_4Im][Li][NTf_2] and (B) [C_1C_3CNIm][Li][NTf_2] recorded at room temperature.

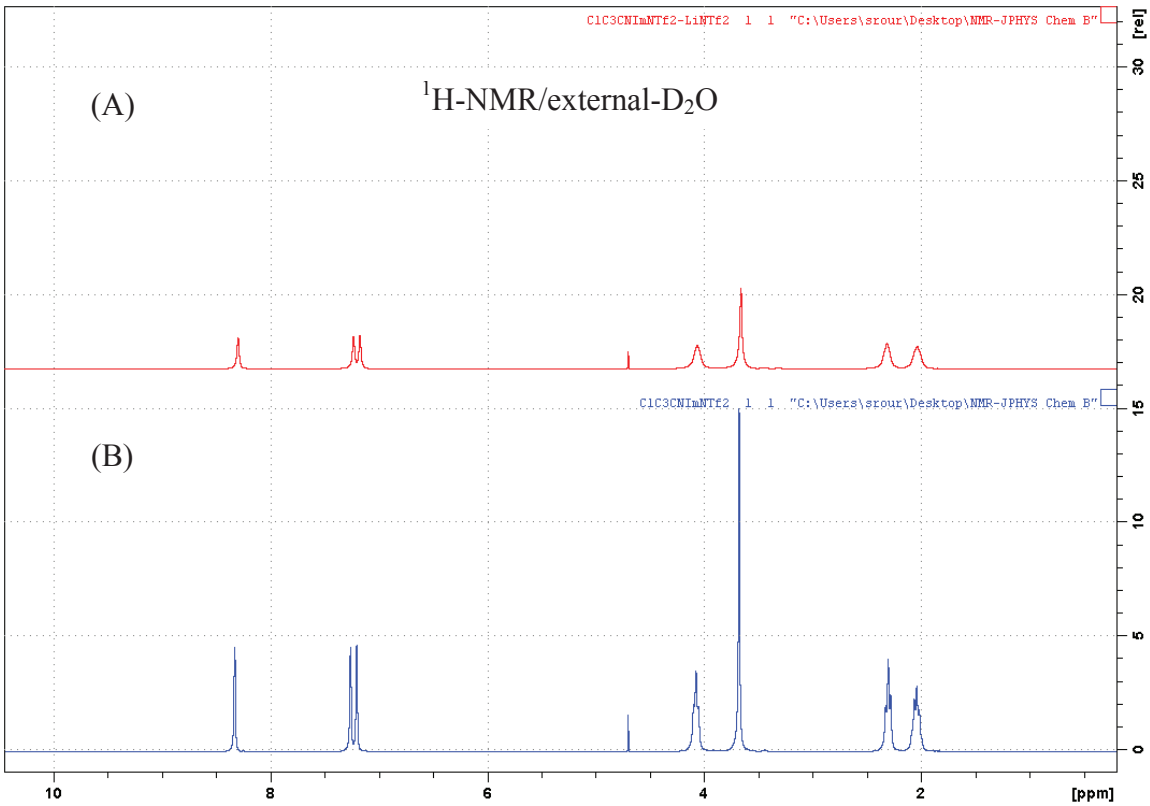

Figure 4: ^{1}H-NMR spectra of (A) [C_1C_3CNIm][NTf_2] and (B) [C_1C_3CNIm][Li][NTf_2] recorded at room temperature

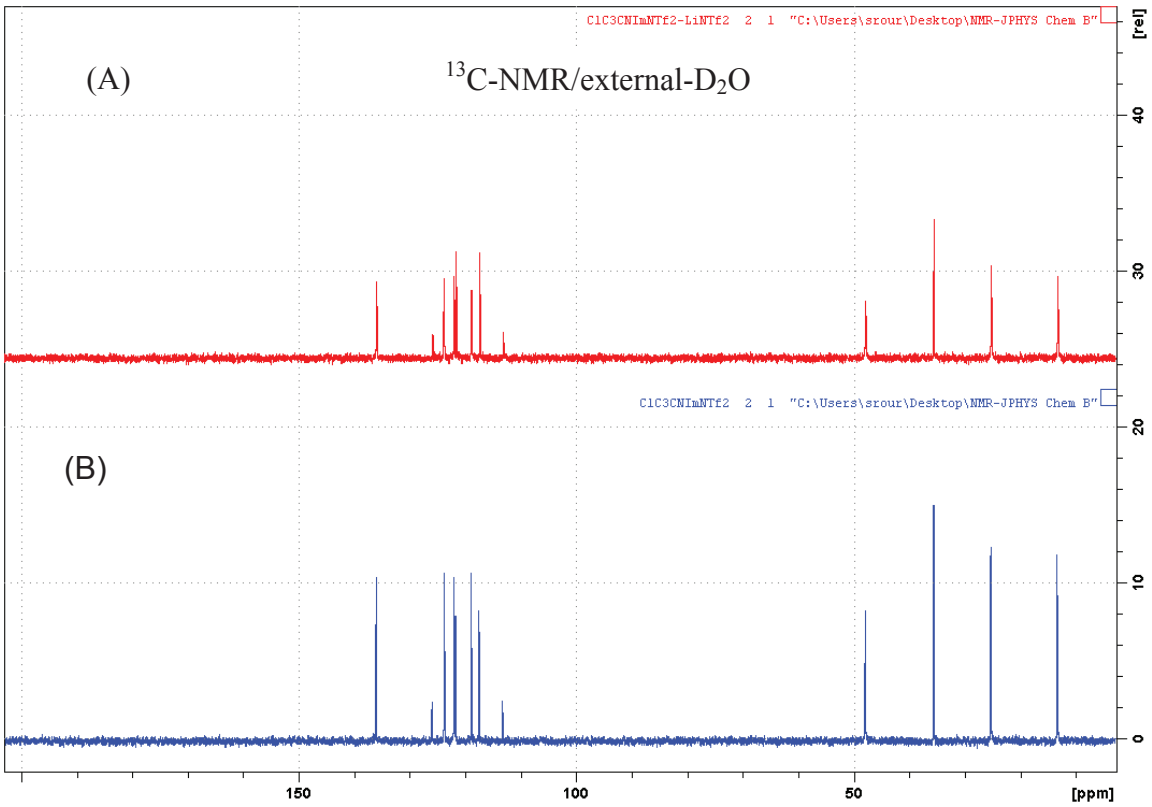

Figure 5: ^{13}C-NMR spectra of (A) [C_1C_3CNIm][NTf_2] and (B) [C_1C_3CNIm][Li][NTf_2] recorded at room temperature.

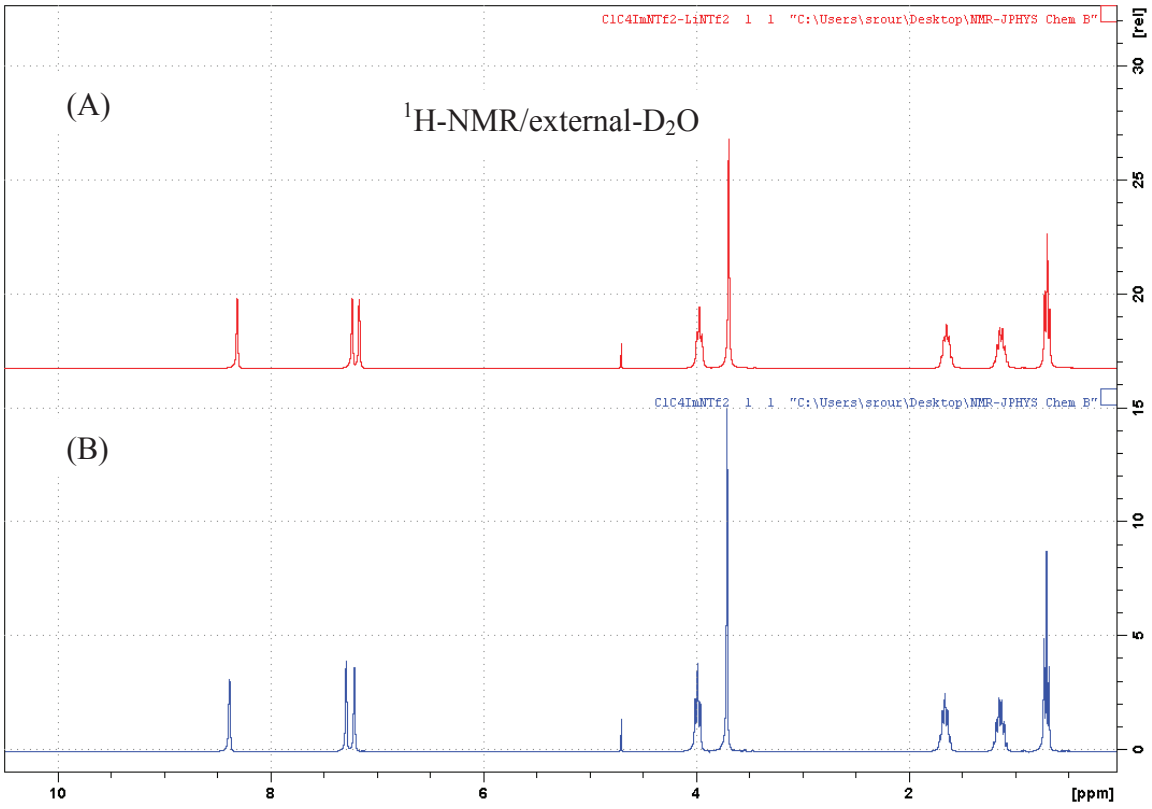

Figure 6: ^{1}H-NMR spectra of (A) [C_1C_4Im][NTf_2] and (B) [C_1C_4Im][Li][NTf_2] recorded at room temperature.

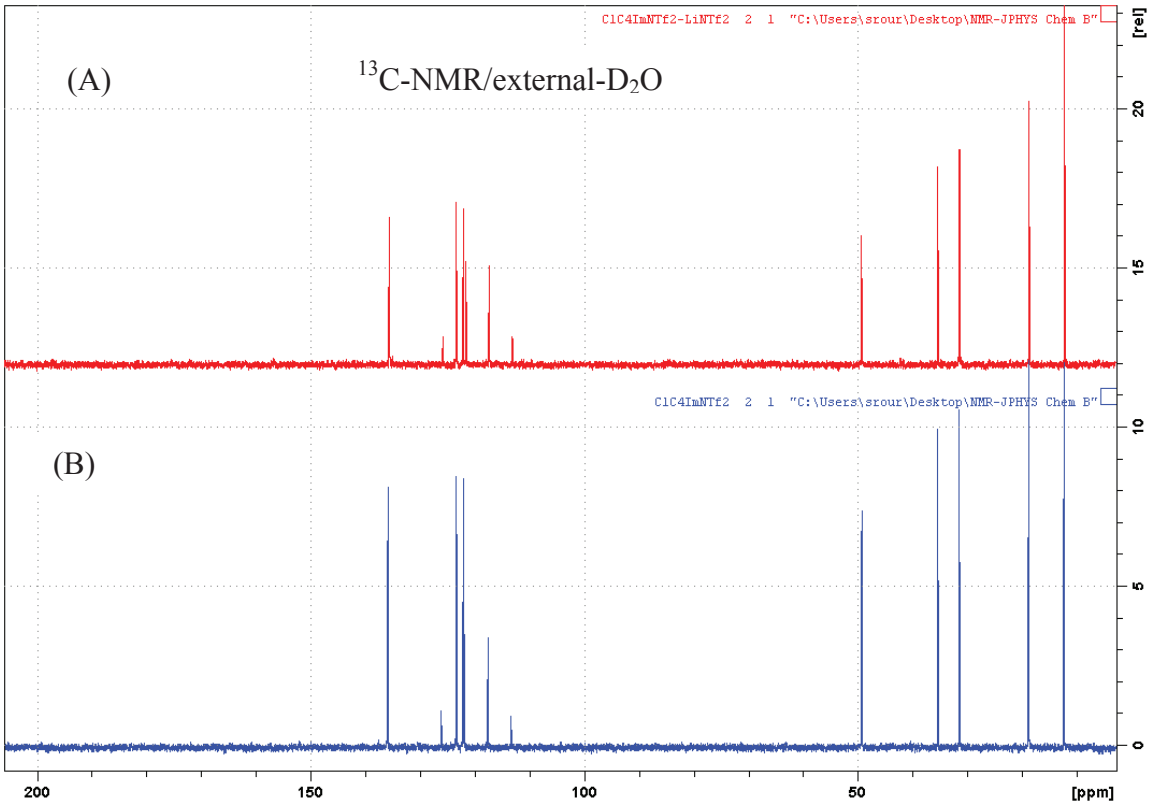

Figure 7: ^{13}C-NMR spectra of (A) $[C_1C_4Im][NTf_2]$ and (B) $[C_1C_4Im][Li][NTf_2]$ recorded at room temperature.

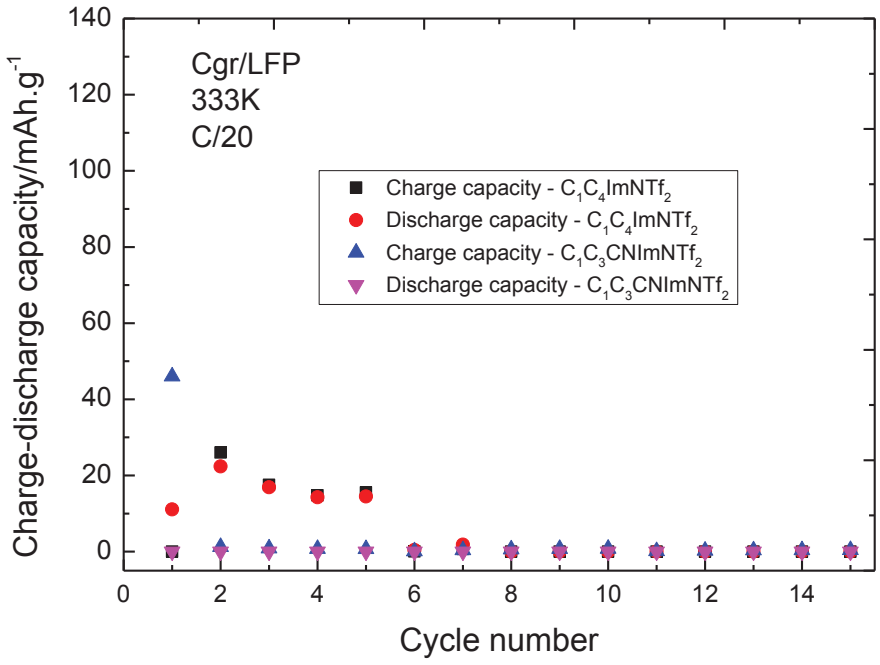

Figure 8: Cycling performance of $[C_1C_4Im][NTf_2]$ and $[C_1C_3Im][NTf_2]$ at 1 mol.L^{-1} of $[Li][NTf_2]$ with Gr/LFP full systems at 333 K.

Appendix III

Experimental Part

General synthetic method

1-[2-(Methoxycarbonyloxy)ethyl]-3-methylimidazolium bis(trifluoromethane)sulfonimide

3-methyl-1-ethanolimidazolium bis(trifluoromethane)sulfonimide (10.0 g, 24.57 mmol) was added into a 100 mL two-neck flask at 0°C. Methyl chloroformate (2.54 g, 27.02 mmol) was added drop wise with a vigorous stirring followed by the slow addition of 1-methylimidazole (2.21 g, 26.93 mmol). The flask was then heated to 50°C and reacted for overnight. After the reaction, the flask was cooled down to room temperature and ethyl acetate was added to the reaction mixture and kept in the fridge in order to precipitate the resulting imidazolium chloride. The resulting product was extract by dichloromethane several times to remove the dissolved imidazolium chloride and then dried under vacuum at 50°C to give 1-[2-(methoxycarbonyloxy) ethyl]-3-methylimidazolium trifluoromethanesulfonimide [EMCMIm][NTf_2] as a slightly yellowish liquid in 70% yield with a purity up to 85% proved by ^{1}H NMR and HRMS analyses (Figure 1 and 2). In the high resolution mass analysis (MS QTOF) of the resulting product beside the the peak at m/z 185.0 coresonding to 1-[2-(methoxycarbonyloxy) ethyl]-3-methylimidazolium cation thepeak at 405.11 corresponds to $[C_1C_2OHIm]_2[Cl]^+$.

^{1}H NMR (300 MHz, acetone-d6, 25°C): δ (ppm) = 9.12 (s, 1H, CHIm), 7.81 (d, J = 13.5 Hz, 3H, CH-Im), 4.76 (t, J = 4.5 Hz, 2H, OCH2), 4.63 (t, J = 4.5 Hz, 2H, NCH2), 4.13 (s, 3H, CH3), 3.78 (s, 3H, CH3). ^{13}C-NMR (75.4 MHz, CDCl3, 25 oC): δ (ppm) = 155.14 (OCOO), 136.52 (CH-Im), 124.16 (CH-Im), 199.94 (q, J = 1277 Hz, CF3), 123.23 (CH-Im), 65.53 (CH2O), 55.39 (OCH3), 48.82 (NCH2), 36.46 (NCH3).

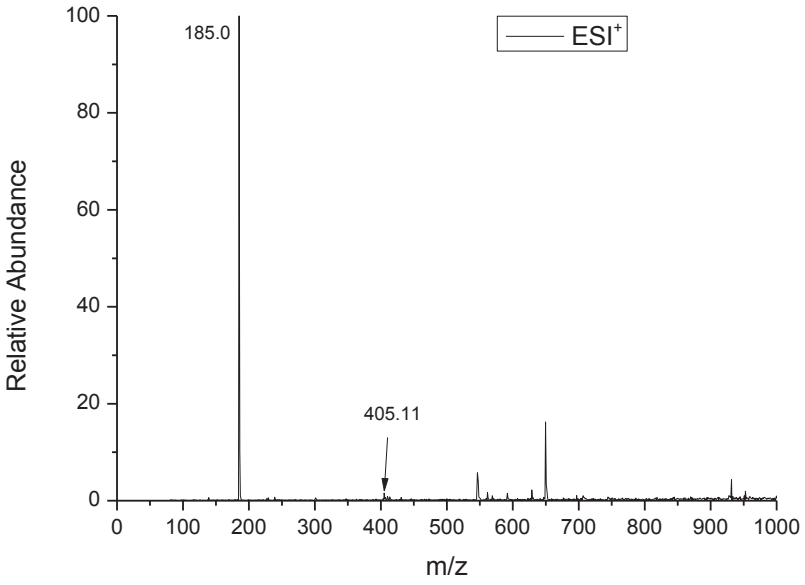

Figure 1: High resolution mass spectra of 1-hexyl-3-methylimidazolium dicyanamide synthesised in our lab.

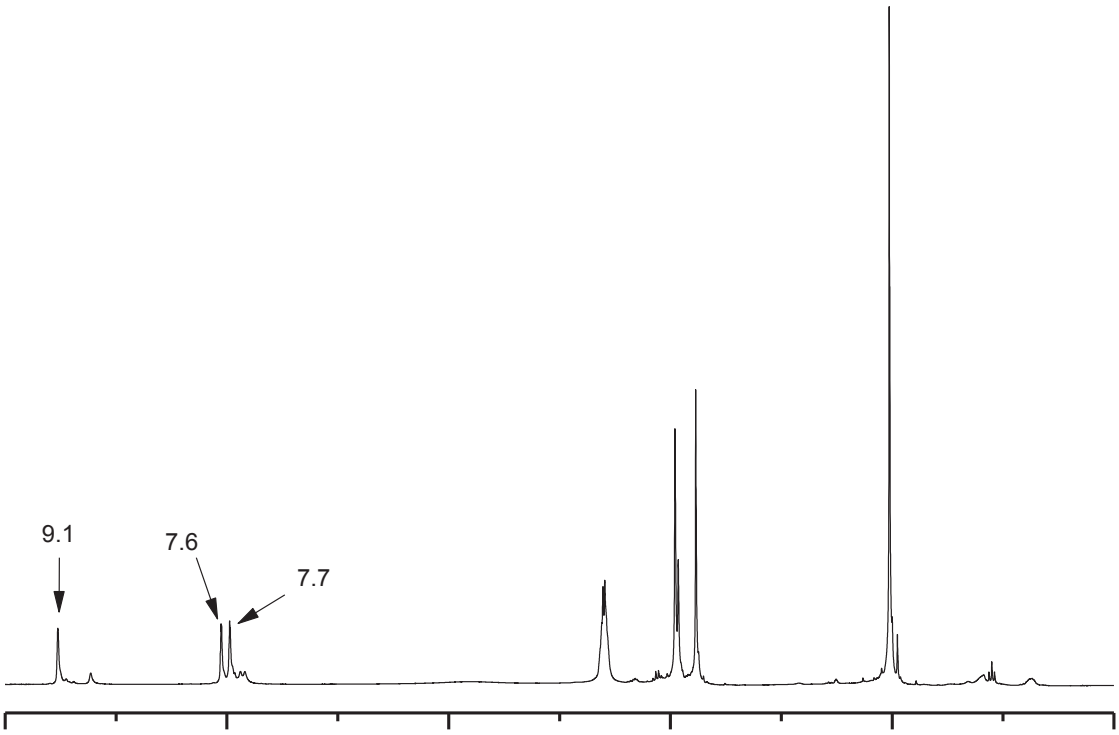

Figure 2: ^{1}H NMR spectra of $[C_1C_2OHIm][NTf_2]$.

Publications

List of papers and oral presentations

List of patents

Patent 1: Hassan Srour, Leila Moura, Hélène Rouault, and Catherine C. Santini, Pat *WO*, 2013037923 (**2013**).

Patent 2: Hassan Srour, Hélène Rouault, Catherine C. Santini, *FR-Pat,* EN n°13 51205 **2013**.

List of papers

Paper 1: *A silver and water free metathesis reaction: a route to ionic liquids;* Hassan Srour, Hélène Rouault, Catherine C. Santini and Yves Chauvin, *Green Chem* 2013, **15**, 1341-1347.

Paper 2*: Imidazolium Based Ionic Liquid Electrolytes for Li-Ion Secondary Batteries Based on Graphite and $LiFePO_4$;* Hassan Srour, Hélène Rouault, and Catherine Santini, *J. Electrochem. Soc,* 2013, **160**(1) A66-A69.

Paper 3: *Study on Cycling Performance and Electrochemical Stability of 1-Hexyl-3-methylimidazolium Bis(trifluoromethanesulfonyl)imide Assembled with $Li_4Ti_5O_{12}$ and $LiFePO_4$ at 333 K;* Hassan Srour, Hélène Rouault, and Catherine Santini, *J. Electrochem. Soc,* 2013, **160**(6) A781-A785.

Paper 4: *Ionic liquids: Potential electrolytes for lithium ion batteries;* Hassan Srour, Nelly Giroud, Hélène Rouault, and Catherine Santini, *ECS Trans*, 2012, **41**(41) 23-28.

Paper 5: *Novel IL Based Electrolytes for Secondary Lithium Ion Batteries;* Hassan Srour, Hélène Rouault, and Catherine Santini, *ECS Trans,* 2013, **50** (26) 15-24.

Paper 6: *Physicochemical and electrochemical properties of imidazolium ionic liquids: Cycling performance of low cost lithium ion batteries with $LiFePO_4$ cathode;* Hassan. Srour, Helene. Rouault and Catherine C. Santini, *MRS Proceedings* 2013, 1575, 684.

Paper 7: *Towards new battery electrolyte;* Hassan Srour, Hélène Rouault, and Catherine Santini, *ECS Trans,* 2013, **53** (36) 33-39.

Paper 8: *Effect of Lithium Salts on the Transport and Electrochemical Properties of Nitrile-Functionalized Imidazolium-based Ionic Liquids;* Hassan Srour, Margarid F. Costa Gomes, Bernard Fenet, Hélène Rouault, Mounir Traikia, Pascale Husson, Catherine C. Santini, *Ind. Eng. Chem. Res. 2013*, **Accepted**.

Paper 9: Tuned imidazolium based ionic liquids for energy storage; Hassan Srour, Hélène Rouault, and Catherine Santini, *J. Power Sources*, **In preparation.**

Résumé:Développement d'un électrolyte à base de liquide ionique pour accumulateurs au lithium

Dans les accumulateurs au lithium, l'électrolyte joue un rôle important car ses propriétés physico-chimiques et électrochimiques conditionnent l'efficacité du générateur électrochimique. Actuellement, les électrolytes organiques utilisés induisent des difficultés pour la mise en œuvre et l'utilisation de la batterie (composants volatils et inflammables). De nouveaux électrolytes à base de sels fondus à température ambiante, dit liquides ioniques, sont des candidats potentiels plus sécuritaires (faible inflammabilité, basse pression de vapeur saturante, point éclair élevé), qui présentent en outre une large fenêtre électrochimique. Dans un premier temps, le travail de thèse a été de concevoir de nouvelles voies de synthèses plus économes, tenant compte des exigences environnementales (limitation des déchets, pas de solvant) et proposant des liquides ioniques de haute pureté >99.5% compatibles avec une production industrielle. De nouveaux liquides ioniques dérivés du cation imidazolium ont alors été conçus afin de moduler leurs propriétés physico-chimiques et optimiser leurs performances dans les batteries. Ils ont été évalués dans diverses technologies de batteries (Graphite/$LiFePO_4$) et ($Li_4Ti_5O_{12}$/$LiFePO_4$) dans différentes conditions expérimentales, à 298 K et 333 K, cette dernière température étant proscrite pour les batteries conventionnelles. Ce travail de thèse a permis d'identifier les modifications chimiques pour conduire aux électrolytes les plus prometteurs et à mis en exergue l'importance de l'étude de la compréhension des phénomènes d'interphase liquides ioniques/ électrodes.

Abstract: Development of an electrolyte based on ionic liquid for lithium ion batteries

In lithium ion batteries, the electrolyte plays an important role because its physicochemical and electrochemical properties determine their efficiency. Currently, the used organic electrolytes induce difficulties in the manufacturing and the use of the battery (volatile and flammable components). New electrolytes based on molten salts at room temperature, called ionic liquids, are safer potential candidates (low flammability, low vapor pressure, high flash point) with a wide electrochemical window. The first stage of this PhD was to design new and more efficient synthetic routes, taking into account the environmental requirements (waste minimization, no solvent) and allowing the elaboration of ionic liquids with high purity> 99.5%, compatible with an industrial production. New ionic liquids derived from imidazolium cation were then designed in order to modulate their physicochemical properties, and to optimize their performance in batteries. They were evaluated in various battery technologies (Graphite/$LiFePO_4$) and ($Li_4Ti_5O_{12}$/$LiFePO_4$) under different experimental conditions, 298 K and 333 K, when the conventional lithium ion batteries (organic electrolyte) are used only under 313 K. This PhD work has identified the chemical modifications to yield the most promising electrolytes, and highlighted the importance of the study on the understanding of ionic liquid/electrode interphase phenomena.